Targeted Neurotherapeutics for Chronic Inflammatory Pain

A thesis submitted for degee of Ph.D

By

Hui Ma, B.Sc., M.Sc.

November, 2013

Based on research carried out at

School of Biotechnology

and

International Centre for Neurotherapeutics

Dublin City University,

Ireland,

Under the supervision of Professor Richard O'Kennedy

Declaration

I hereby certify that this material, which I now submit for assessment on the programme of study leading to the award of Doctor of Philosophy is entirely my own work, that I have exercised reasonable care to ensure that the work is original, and does not to the best of my knowledge breach any law of copyright, and has not been taken from the work of others save and to the extent that such work has been cited and acknowledged within the text of my work.

Signed: _____

(Candidate) ID No.: _ 58121412 ___

Date: _____

This thesis is dedicated to God, my saviour and my life, even it will never be good enough for Him.

Acknowledgements

To me, this 4 years PhD is more like a journey of faith. In this journey, I have gotten to know myself better as I know and trust God more during both the unhappy and happy times of my research.

'Whatever you do, work at it with all your heart, as working for the Lord, not for men (Colossians 3:23)'. This is God's word, and I find it is so real, as my relationship with my supervisor Professor Richard O'Kennedy always reminding me the relationship with God.

Richard is a supervisor with gentle and kind heart, even sometimes is harsh as well. Interesting enough, God is in great and mysterious balance of both love and righteousness. I would especially like to thank him for the extra guidance and help at the start of my research by meeting me once a week no matter how busy he was (lot of work for a vice-president of Learning Innovation). Then I meditated God's work on me: *'what is man that you are mindful of him, the son of man that you care for him (Hebrews 2:6)'.* Some times I was still anxious and frustrated even already got assurance from Richard, this lack of faith remind me that I actually so often lack of faith to mighty God, even knowing he understand every situation of me and will provide all good things, which may hard to be understood or accepted. God's power is just way much than my weakness.

'Do not be anxious about anything, but in every situation, by prayer and petition, with thanksgiving, present your requests to God. And the peace of God, which transcends all understanding, will guard your hearts and your minds in Christ Jesus (Philippians 4:6-7)'.

Thank Professor Oliver Dolly for your intelligential suggestion in my work related to toxin, which is very helpful and speed my project progress.

I appreciate all the help, support, trust, comfort and hug in the last four years from lab mates. In my lowest point, even a smile can keep me move on for a long time ^___^. Thank you Stephen Hearty, Paul Conroy and Barry Byrne for

amazed me and leads me to the understanding of real trust, submission and success to death. Then I realize the trouble in experiment which is surely less than death can also be overcome by faith, and it has been proved by so many times when I already gave up after repeating so many time without success (e.g. rabbit scFv selection, BoNT-scFv fusion purification), God always bringing positive result to me.

Pray for you, my beloved parents and brother. Thank you for all your honest love and anxiety to me. My PhD journey will be finish but journey of faith will move on. I love you, and may we can be family in heaven as well.

'And God shall wipe away all tears from their eyes; and there shall be no more death, neither sorrow, nor crying, neither shall there be any more pain: for the former things are passed away (Revelation 21:4)'.

Table of contents

xiii

Abbreviations

AA: amino acid

Ab: antibody

Abs: absorbance

ATP: adenosine-5'-triphosphate

BCA: bicinchoninic acid

BM: bone marrow

BoNT: Botulinum toxin serotype A

BoNT/A/B/C/D/E/F/G: Botulinum toxin serotype A/B/C/D/E/F/G

BSA: bovine serum albumin

bTg: bovin thyroglobulin

cDNA: complementary deoxyribonucleic acid

CDR: complementarity determining region

CD4/8: cluster of differentiation 4/8

Cfu: colony forming units

CGRP: Calcitonin gene-related peptide

C_H: constant heavy chain of antibody

C_L: constant light chain of antibody

CRP: C-reactive protein

CS: core streptavidin

CS5: LC-H_N/A-core streptavidin

dH_2O: distilled water

DIV: days *in vitro*

DMSO: dimethyl sulfoxide

DNA: deoxyribonucleic acid

dNTP: deoxyribonucleotide triphosphate

DRG: dorsal root ganglion

DTT: dithiothreitol

EDTA: ethylenediaminetetraacetic acid

EIA: enzyme immunoassay

ELISA: enzyme-linked immunosorbent assay

Fab: antigen-binding region

FBS: fetal bovine serum

FCA: Freund's complete adjuvant

FICA: Freund's incomplete adjuvant

HA: haemagglutinin

HBS: Hepes buffered saline

HBSS: Hank's balanced salt solution

His: histidine

HRP: horse radish peroxidase

IC_{50}: half maximal inhibitory concentration

IgA/D/E/M/G/Y: immunoglobulin A/D/E/M/G/Y

IL: interleukin

IMAC: immobilised metal affinity chromatography

IMS: industrial methylated spirits

IPTG: isopropyl-β-D-1-thiogalactopyranoside

κ: kappa light chain of antibody

λ: lambda light chain of antibody

kDa: dissociation constant (units = M)

LC: BoNT light chain

H_N: BoNT heavy chain translocation domain

H_{CN}: BoNT heavy chain binding domain

KLH: keyhole limpet haemocyamin

LDS: lithium dodecyl sulfate

LOD: limit of detection

mAb: monoclonal antibody

MHC: major histocompatibility complex

MPBST: phosphate buffered saline with 1% (w/v) milk and 0.05% (v/v) Tween

MPO: myeloperoxidase

MWCO: molecular weight 'cut-off'

N/A: not applicable

NGF: nerve growth factor

O/N: overnight

OD: optical density

pAb: polyclonal antibody

PAGE: polyacrylamide gel electrophoresis

PBS: phosphate buffered saline

PBSM: phosphate buffered saline with milk

PBST: phosphate buffered saline with 0.05% (v/v) Tween

PBSTM: phosphate buffered saline with 0.05% (v/v) Tween and milk

PCR: polymerase chain reaction

PEG: polyethylene glycol

Pfu: phage forming units

pI: isolectric point

P/S: penicillin/streptomycin solution

$P2X_3$: P2X purinoceptor 3

RNA: ribonucleic acid

rpm: revolutions per minute

RT: reverse transcriptase

SA: streptavidin

SB: super broth

scFv: single-chain variable fragment

SDS: sodium dodecyl sulfate

SDS-PAGE: sodium dodecyl sulphate polyacrylamide gel electrophoresis

SNAP-25: Synaptosomal-associated protein 25

SNARE: soluble N-ethylmaleimide-sensitive factor attachment protein receptor

SOC: super optimal catabolite

SOE: splice-overlap-extension

SP: substance P

TAE: Tris-acetate-EDTA

TBS: Tris-buffered saline

TBSM: Tris-buffered saline with milk

TBST: Tris-buffered saline with 0.05% (v/v) Tween

TBSTM: Tris-buffered saline with 0.05% (v/v) Tween and milk

TMB: tetramethylbenzidine dihydrochloride

TRI: trizol

VAMP: Vesicle-associated membrane protein

V_H: variable heavy chain of antibody

V_κ: variable kappa light chain of antibody

V_λ: variable lambda light chain of antibody

V_L: variable light chain of antibody

Publications and Presentations

Paper – Ma H., Meng J.H., Wang J.F., Stephen Hearty, Dolly J.O. and O'Kennedy R. (2013). Recombinant anti-P2X$_3$ scFv antibody targeted delivers BoNT/A for inflammatory pain therapy [in preparation for the Federation of European Biochemical Societies (FEBS) Journal].

Poster – Ma H., Meng J.H., Wang J.F., Dolly J.O. and O'Kennedy R. (2011). Targeted neurotherapeutics for persistent inflammatory pain. (Bio)pharmaceutical & Pharmacological Sciences Research Day, Dublin City University, Dublin, Ireland, 11th, January.

Poster – Ma H., Meng J.H., Wang J.F., Dolly J.O. and O'Kennedy R. (2012). Recombinant anti-P2X$_3$ scFv antibody targeted to sensory neurons. School of Biotechnology Research Day, Dublin, Ireland, 27th, January.

Poster – Ma H., Meng J.H., Wang J.F., Dolly J.O. and O'Kennedy R. (2012). Recombinant anti-P2X$_3$ scFv antibody targeted to sensory neurons. Antibodies 2012 meeting, Dublin, Ireland, 8th-9th, May.

Abstract

The P2X purinoceptor 3 (P2X$_3$) plays a crucial role in signalling leading to chronic inflammatory pain and, thus, the P2X$_3$ receptor provides a proven target for its treatment. Botulinum toxin type A (BoNT/A) is a potentially promising candidate drug for use in this situation. Long-acting botulinum neurotoxin type D (BoNT/D) inhibits inflammatory pain peptide release from cultured sensory neurons evoked by K$^+$, bradykinin or capsaicin. The purpose of this project is to develop single-chain antibody variable fragments (scFv) recognising extracellular domains of P2X$_3$, for use as a targeting agent to deliver protease and translocation domains of BoNT/A and BoNT/D (LC-H$_N$/A and LC-H$_N$/D) to pain-signalling neurons.

A rabbit scFv library was generated, and phage display was applied for anti-P2X$_3$ scFv recombinant antibody selection. After five rounds of bio-panning, followed by polyclonal phage ELISA, monoclonal ELISA, cross reactivity analysis, competitive ELISA, western blotting and immunofluorescence staining, anti-P2X$_3$-257 scFv clones with high specificity and affinity were successfully selected. The scFv gene was fused to BoNT/A and BoNT/D and expressed as a fusion protein in *E. coli*. After purification, this protein was shown to enter sensory neurons and to cleave its neuronal target, VAMP2.

The efficacy of this therapeutic will be further evaluated using established capsaicin-induced or formalin-induced rat inflammatory pain models.

Chapter 1

General Introduction

1.1 Inflammatory pain

1.1.1 What is inflammatory pain?

Inflammatory pain results from the activation of inflammatory cascades (which transport and develop the inflammatory response involving the local vascular system, the immune system and different cells at the injured location) and chemoreceptors (sensory receptors that transduce a chemical signal into an action potential) (Kidd and Urban, 2001). Many situations can lead to inflammatory pain, for instance, arthritis, extreme cold, penetration wounds, fractures, burns, vasoconstriction, infections and excessive stretching. It is a major challenge for health providers to address this issue as suffers represent approximately 20% of the adult population (Breivik *et al.*, 2006). There remains an unmet need for its effective treatment, as traditionally used non-steroidal anti-inflammatory drugs, are short-acting and can cause serious side effects.

Soluble N-ethylmaleimide-sensitive factor attachment protein receptor (SNARE) is a large protein superfamily which mediates vesicle fusion in yeast and mammalian cells. Three SNAREs were found to be important in inflammatory pain signalling pathways. They are synaptosomal-associated protein 25 (SNAP-25) located in the cell membrane, vesicle-associated membrane protein (VAMP, also known as synaptobrevin) in vesicular membrane and syntaxin 1 also in vesicular membranes. SNAP-25, VAMP and syntaxin 1 cause the release of peptides which mediate inflammatory pain, for instance, calcitonin gene-related peptide (CGRP) and substance P (SP) (Kidd and Urban, 2001; Meng *et al.* 2007). Both CGRP and SP play crucial roles in the transmission of pain (Datar *et al.*, 2004).

1.1.2 Therapy for inflammatory pain

1.1.2.1 The role of P2X$_3$ in inflammatory pain

The P2X receptor functions as an ionotropic (Na$^+$, K$^+$ and Ca^{2+}) ligand-gated cationic channel (Radford *et al.*, 1997). It is activated by extracellular ATP and mediates fast synaptic transmission (a process of releasing signalling molecules by the neuron which then binds to the receptors of another neuron for activation). The P2X receptor is made up of a number of P2X subunits, P2X$_{1-7}$. The P2X subunits form hetero-oligomers which assemble to form the P2X ion channel. It was previously demonstrated by many researchers that all the P2X subunits especially the subunit P2X$_3$ plays a crucial role in inflammatory pain signalling (Jarvis *et al.*, 2002; Xu and Huang, 2002).

ATP can be released and produces pain in humans by stimulating the nociceptors after tissue injury or visceral distension (Burnstock, 1996; Burnstock, 2000). It was reported that in several experimental models the responses to ATP are enhanced during inflammation (Kidd and Urban, 2001; Burnstock, 2009). P2X$_3$ was proven to be involved in pain signalling through ATP released by inflamed tissues. Hence, it could be used as a molecular target for pain treatment (North, 2003).

P2X$_3$ is selectively expressed in certain pain-propagating neurons (i.e. dorsal root ganglion neurons and trigenminal ganglion neurons). Souslova *et al.* (2000) demonstrated that after deletion of the P2X$_3$ gene, dorsal root ganglion neurons lost rapidly desensitizing ATP-gated cation currents, thus suggesting a role for ATP acting through P2X$_3$ in inflammatory pain processing. P2X$_3$ receptors expressed by dorsal root ganglion neurons play also a crucial regulatory role in inflammatory pain. Furthermore, Honore *et al.* (2002) reported that chronic inflammation-induced thermal hyperalgesia decreased, with reduction of the expression level of P2X$_3$, by repeating administration of antisense oligouncleotides into the intrathecal space of rats. Jarvis *et al.* (2002) proved that a potent and selective blocker (A-317491) of P2X$_3$ can reduce chronic inflammatory pain induced by Freund's adjuvant. Cockayne *et al.* (2000) demonstrated that P2X$_3$ is a proven target for drugs to treat inflammatory

3

diseases and associated pain because behavioural testing of P2X$_3$ knock-out mice demonstrated its pivotal role in signalling leading to chronic inflammatory pain. Kaan *et al.* (2010) also reported that much less bone cancer pain behaviour was observed in a rat bone cancer pain model after the blocking of P2X$_3$ receptors on peripheral and central terminals of nociceptors.

1.1.2.2 Dorsal root ganglion neurons (DRGs)

Dorsal root ganglion neurons are cell bodies of neurons in the dorsal root ganglion (DRG), the nodule on the dorsal root of spinal nerve. DRGs were chosen as an *in vitro* model for therapy of inflammatory pain, as DRGs are among the most common and major sensory neurons in vertebrates. It is reported that during inflammatory pain DRG neurons were sensitized by a majority of identified signalling cascades (Kallenborn-Gerhardt and Schmidtko, 2011). A high percentage of DRGs express P2X$_3$ receptor (Table 1.1), i.e. on postnatal day seven, $72.6 \pm 3.4\%$ of DRG cells could be identified as P2X$_3$ receptor-positive cells (Ruan *et al.*, 2004).

Table 1.1 Expression of P2X$_3$ receptor immunoreactivity in dorsal root ganglions (DGRs) in embryonic and postnatal development.

	E16	E18	P1	P7	P14	Adult
P2X$_3$ immunopositive DRGs (%)	100	97.2 ± 1.5	92.5 ± 2.2	$72.6 \pm 3.4*$	$47.5 \pm 2.8*$	$44.3 \pm 3.5*$

*$P<0.001$

Note: statistical significance indicated by asterisks relates to embryonic days E16 and E18, as compared with postnatal ages P7, P14 and adult (This table is modified from Ruan *et al.*, 2004).

1.1.2.3 Pain relief by botulinum neurotoxins (BoNTs)

Botulinum neurotoxins (BoNTs), which are produced by *Clostridium botulinum*, are known to be highly potent. BoNTs contain three domains (Fig. 1.1 and table 1.2), a binding domain (H_C), a translocation moiety (H_N) and a Zn^{2+}-dependent light chain (LC) (Lacy *et al.*, 1998; Jin *et al.*, 2006). BoNTs were proven to be effective for inflammatory pain treatment by inhibiting the release of pain-related peptides (i.e. CGRP or SP) by cleaving their specific intracellular SNAREs (i.e. SNAP-25 or VAMP) (Fig. 1.2 and Table 1.3). There are seven serotypes of BoNTs, BoNT/A-G. BoNT/A/C/E cleaves synaptosomal-associated protein 25 (SNAP-25), while BoNT/B/D/F/G cleaves vesicle-associated membrane protein (VAMP).

Many researchers have suggested that BoNT is a promising candidate for treatment of pain. For instance, Mahowald *et al.* (2009) reported that intra-articular injection of BoNT/A into joints was effective in treating chronic inflammatory pain with no serious adverse effects. Kaufman and Karceski (2009) found that the injection of BoNT/A into both feet up to the ankle or mid-shin skin can relieve neuropathic pain in individuals with diabetes. BoNT/D was proved to be a strong candidate for inflammatory pain therapy by cleaving all VAMP isoforms I, II and III, and then inhibiting release of CGRP, one of the main mediators of inflammatory pain (Meng *et al.*, 2007). It was also found that a re-targeted botulinum toxin type E (BoNT/E) is very effective in blocking the release of the pain-peptide, CGRP, from sensory neurons and attenuating pain signalling in brain (Meng *et al.*, 2009). Moreover, another more advanced long-acting variant of BoNT/E has proved to be very potent and versatile as an inhibitor of CGRP release in an inflammatory pain model (Wang *et al.*, 2009).

Cleavage site

COOH   NH₂   COOH   NH₂

448 | 449

LC — S — S — Hₙ   LC — S — S — Hₙ

NH₂   H_CN   NH₂   H_CN

H_CC   H_CC

COOH   COOH

Single chain (SC)   **Di-chain (DC)**
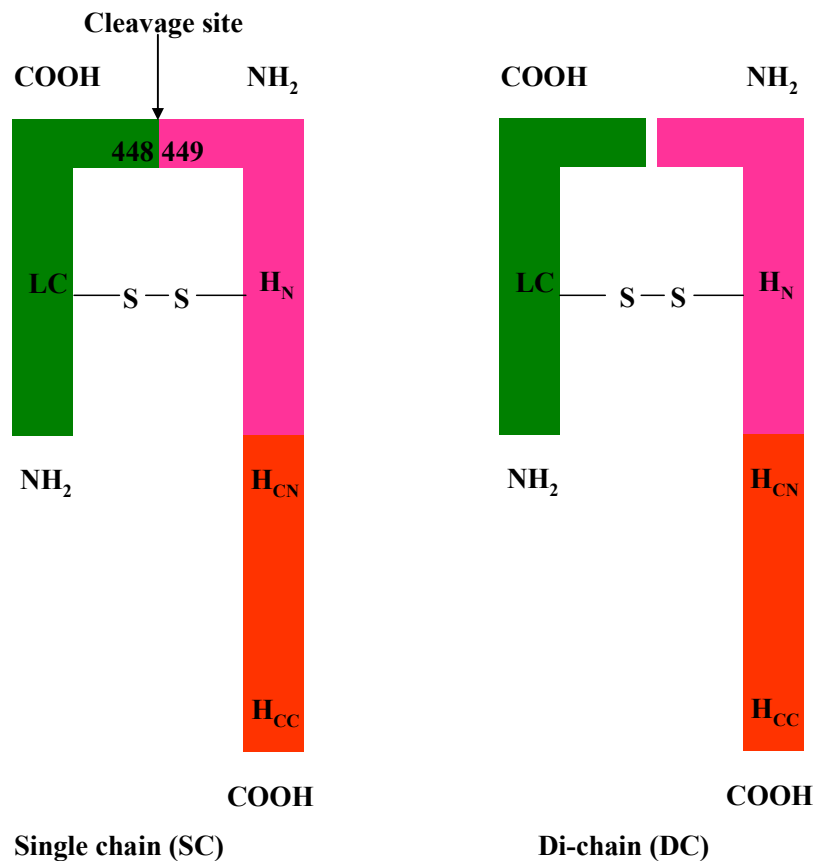
Fig. 1.1 Structure of botulinum neurotoxin. The botulinum neurotoxin consists of one light chain and one heavy chain which are connected by a disulfide bond. In the form of single chain (SC), toxins have relatively little potency as neurotoxins. Botulinum neurotoxin activation requires cleavage between amino acids 448 and 449 to form an active di-chain (DC), which is one light chain (L-chain, amino acids 1-448, 50 kDa) and one heavy chain (H-chain, amino acids 449-1295, 100 kDa) mutually connected by a disulfide bond. LC = light chain of botulinum toxin; H_N = translocation domain of botulinum toxin; H_{CN} = N-terminal binding domain of botulinum toxin; H_{CC} = C-terminal binding domain of botulinum toxin; SC = single chain of botulinum toxin before separate light chain and heavy chain; DC = di-chain of botulinum toxin before separate light chain and heavy chain; MW = molecular weight markers and -S-S- = disulfide bond.
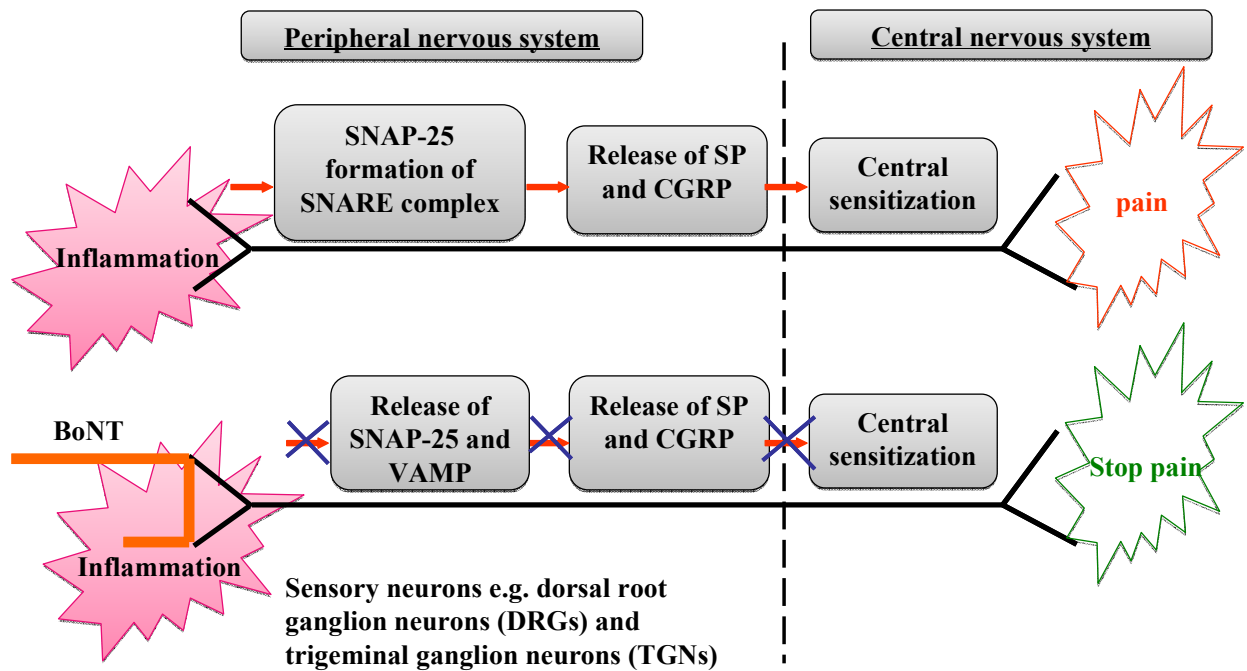
Fig. 1.2 Mechanism of BoNTs inhibition of inflammatory pain. Inflammatory pain involves both peripheral and central sensitization. BoNTs relieve inflammatory pain (central sensitization) by inhibiting the release of pain-related peptides, CGRP and SP by cleaving their specific intracellular SNAREs, SNAP-25 and VAMP during peripheral sensitization.

Table 1.2 Function of each domain of BoNT.

Individual domains of BoNT	Function
Heavy chain binding domain (H_C, 100 kDa): C terminal binding domain (H_{CC}, 50 kDa) & N terminal binding domain (H_{CN}, 50 kDa)	Bind to gangliosides and high-affinity protein acceptors on cholinergic nerve terminals.
Heavy chain translocation domain (H_N, 50 kDa)	Internalization and translocation of catalytic light chain across membranes.
Light chain (LC, 50 kDa)	Mediates toxic activity. Works as a Zinc-dependent endopeptidase for selective proteolysis and digestion of SNAREs.

Table 1.3 Target SNAREs cleaved, pain-peptide inhibited and function for different serotypes of BoNT (this table is modified from Dolly *et al.*, 2011).

BoNT serotype	Target SNAREs cleaved	Pain-peptide inhibited	Function
BoNT/A	SNAP-25	CGRP	Stop the transmission of pain
BoNT/B	VAMP I, II and III	SP	Stop the transmission of pain
BoNT/C	SNAP-25 and syntaxin	CGRP	Stop the transmission of pain
BoNT/D	VAMP I, II and III	SP	Stop the transmission of pain
BoNT/E	SNAP-25	CGRP	Stop the transmission of pain
BoNT/F	VAMP I, II and III	SP	Stop the transmission of pain
BoNT/G	VAMP I, II and III	SP	Stop the transmission of pain

1.2 The immune system

1.2.1 Basic components of the immune system

Throughout evolution the mammalian immune system has developed two arms of defence, the innate and the adaptive immune systems. Both systems function to defend against pathogen invasion and are linked. The immune system consists of organs, which were classified into central immune organs (i.e. thymus, bone marrow and Bursa of Fabricius) and peripheral immune organs (i.e. spleen and lymph nodes). The immune system utilizes immune cells, for example, lymphocytes, monocytes, macrophages, dendritic cells, neutrophils, eosinophils, basophils and mast cells, all of which work in concert for the

production of an immune response which is mediated by immune-related molecules, such as complement, immunoglobulins (Ig), interferons (IFNs), interleukins (IL), chemokines and cytokines (Table 1.4).

Table 1.4 Cellular and molecular components of the immune system (this table is modified from Merk, 2012).

Compound	Type	Main Source	Major function
Antigen-Presenting Cells (APCs)	B cells; Monocytes; Macrophages; Dendritic cells	Skin, lymph nodes, and tissues throughout the body	Present antigen-derived peptides in conjunction with the major histocompatibility complex (MHC) molecules for T cell–dependent acquired immune responses.
Polymorphonuclear (PMN) Leukocytes	Neutrophils; Eosinophils; Basophils; Mast cells	Whole blood	Digest and kill pathogenic bacteria.
Cytotoxic Leukocytes	Natural killer (NK) cells; Lymphokine-activated killers (LAK)	Peripheral blood	Induce apoptosis, in infected or abnormal cells, killing a wide spectrum of tumor target cells and abnormal lymphocytes.
Lymphocytes	B cells (which mature in bone marrow); T cells (which mature in the thymus)	Bone marrow and thymus	Recognise specific antigen by antigen-specific surface receptors (i.e. antibodies) and clusters of differentiation.
Antibodies	IgM; IgG (Ig Y);	Spleen, bone	Recognise antigen on

	IgA; IgD; IgE	marrow, blood	the surface of B cells and then responded to antigen.
Acute Phase Reactants	C-reactive protein and mannose-binding lectin (which fix complement and act as opsonins); the transport protein α_1-acid glycoprotein, and serum amyloid P component	Liver	Limit tissue injury; enhance host resistance to infection, and promote tissue repair and resolution of inflammation.
Cytokines	TNFs (TNF-α, lymphotoxin-α, lymphotoxin-β); Interleukins; Chemokines; Transforming growth factors (TGFs); Hematopoietic colony-stimulating factors (CSFs)	Immune cells	Bridge innate and acquired immunity and generally influence the magnitude of inflammatory or immune responses.

1.2.2 The genetics of recombinant antibody production

Immunoglobulins (Ig), also known as antibodies are produced by B lymphocytes in response to foreign molecules. Antibody diversity and increased affinity is generated through a process known as somatic hypermutation. During this process different gene segments rearrange resulting in different combinations of heavy and light chains. All antibodies are composed of two heavy chains and two light chains which are connected through disulfide bridges (Fig. 1.1). The antibody light chain is encoded by

three gene segments: constant segment (C), variable segment (V), diversity segment (D) and joining segment (J); while the heavy chain is encoded by four gene segments: constant segment (C), variable segment (V), diversity segment (D) and joining segment (J). In humans, there are seven families of functional heavy chain germline sequences, thirty variable lambda (λ) and forty variable kappa (κ) light chain germline sequences, one constant lambda and multiple constant kappa light chain genes. The ratio of κ:λ is 3:2. For rabbits, there are more than twenty functional heavy chain germline genes, two constant kappa light chain genes and several variable lambda light chain genes. The κ:λ ratio is 10-20:1. The chicken library is the most simple to create as it consists of only one variable heavy chain and one variable lambda light chain germline sequence (Barbas *et al.*, 2001).

1.2.3 Generation of an immune response

The generation of the immune response involves the recognition of foreign antigens such as viruses, bacteria, fungi, parasites and self-reactive molecules by a host of immune receptors present both in and on immunocompetent cells. Following recognition, the immune cells are activated leading to the up-regulation of the immune system, cell proliferation, differentiation or apoptosis. The three main phases of an immune response are antigen-recognition, lymphocyte-activation and antigen-elimination.

1.2.3.1 Innate immune response

The innate immune response is a non-specific response and is the first line of defence in the immune system. The level of innate response can be very significant (i.e. on exposure to microbes), but does not lead to immunological memory (Hussain *et al.*, 2006).

There are four ways in which the immune system functions. Firstly, by inhibiting the invasion and reproduction of pathogens by the presence of immune barriers, for instance, hairs, skin, blood brain barrier, blood-embryo barrier and the blood-thymus barrier. Secondly, pathogens will be killed

directly by complement molecules and lysozymes which are induced by the inflammatory response. Thirdly, immune cells discriminate between pathogen and host molecules using specific germline-encoded receptors known as pattern recognition receptors (PRRs), causing enhanced phagocytosis by phagocytes and natural killer (NK) cells at inflammatory sites. The immune cells ingest and subsequently destroy the pathogen by means of the phagolysosome. These three reactions are very general and function against most pathogens. However, the fourth mechanism involves a specific response to a particular pathogen and leads to an adoptive response, which is a specific immune response by presenting antigen through dendritic cells to active T and B cells.

1.2.3.2 Adaptive immune response

1.2.3.2.1 Structure and function of major histocompatibility complex (MHC)

The adaptive immune response generates specific defences against disease-associated pathogens or antigens (e.g. proteins) that can be invoked during subsequent infections. In adaptive immune responses, disease-associated proteins will be proteolytically digested by the cells (e.g. cytotoxic T cells, natural killer cells and macrophages) and then the disease-associated peptides will be transported to the cell surface and be bound by the major histocompatibility complex (MHC). MHC proteins, which found in all kinds of vertebrates, can transport internal or external antigens to the T cells for distinguishing self from non-self molecules. Without the transporting function of MHC, adoptive immune response cannot occur.

The MHC is a large group of genes located on the short arm of chromosome 6. The MHC gene group consists of four million base pairs of DNA, 128 genes and 96 non-functional gene remnants (Spector, 2003). The MHC is divided into three regions, class I, II and III regions. These three regions are composed of a group of genes with specific functions which play vital roles in the immune system (Table 1.5).

MHC proteins expressed by MHC class I region (found on all nucleated cell surfaces) have the ability to present antigens to cytotoxic T lymphocytes (CTLs). MHC proteins expressed by MHC class II region (found only on B lymphocytes, macrophages, and other cells present antigens to T cells) present peptides which have been digested from external sources. This function is crucial to T-cell communication with B-cells and macrophages.

Table 1.5 Function and location of proteins expressed by MHC class I, II and III regions.

MHC region	Function	Location
MHC class I region	Present fragments of proteins that are synthesised inside cells. i.e. present antigens to cytotoxic T lymphocytes (Rodenko *et al.*, 2009).	On surfaces of all nucleated cells.
MHC class II region	Present peptides which are needed for T-cell communication with B-cells and macrophages (Kimura *et al.*, 2005).	B lymphocytes, macrophages, and other cells that present antigens to T cells.
MHC class III region	Encode several components, i.e. complement proteins which are involved in the antibody response; the inflammatory cytokines; tumor necrosis factor-α and -β (TNF-α and -β) and two heat shock proteins which help cells deal with heat, stress and viral infection (Milner and Campbell, 2001).	Peripheral blood

1.2.3.2.2 Function of cluster of differentiation 4 and 8 (CD4 and CD8)

Cluster of differentiation 4 (CD4) T cell is a glycoprotein which expressed on the surface of monocytes, T helper cells, dendritic cells and macrophages, and cluster of differentiation 8 (CD8) T cell is a transmembrane glycoprotein function as a co-receptor for the T cell receptor. Both CD4 and CD8 T cells mediate cell-mediated adoptive immune response. CD4 plays a role as a co-receptor helps the T cell receptor with an antigen-presenting cell for activation of the T cell. It is achieved by either amplifying the signal generated by the T cell receptor using its intracellular domain or interacting directly with the MHC class II molecules on the surface of the antigen-presenting cell using its extracellular domain (Wu, 2009). CD8 specifically binds to class I MHC protein which causes the T cell receptor of the cytotoxic T cell and its target cell to bind tightly together during antigen-specific activation (Devine *et al.*, 1999).

1.2.3.2.3 Process of adaptive immune response

The first exposure to pathogenic antigens leads to immunological memory which takes from two days to two weeks to establish, and an enhancement of the immune response will be achieved by future exposures. Immunological memory ensures quick and efficient immune response to later exposures. The adaptive immune response is also classified as humoral or cell-mediated immune responses. The humoral immune response is mediated through B cells by producing immunoglobulins which are specific to foreign antigens. There are five isotypes of immunoglobulins, IgM, IgD, IgE, IgA and IgG (which is called Ig Y in birds). The antigen-specific immunoglobulins then move from primary lymphoid organs (i.e. bone marrow, thymus and fetal liver) to secondary lymphoid organs, for instance, spleen, lymph nodes and small masses of lymph tissue.

Mature circulating B cells secrete for one type of immunoglobulin on their surface. Upon a second or subsequent encounter with their specific antigen the B cell rapidly proliferates and transforms into antibody-secreting plasma cells.

Cell-mediated immune response is mediated by T cells. The body's cells that are infected with bacteria, parasites or viruses are recognised by CD4 and CD8 T cell. T cells proliferate and become activated T cells, which are also called effector T cells. Effector T cells kill antigen directly or through a synergistic killing effect with secreted cytokines when the same antigen is encountered in invade the body for a second time (Gao and Jakobsen, 2000; Hoebe *et al.*, 2004).

1.2.4 Hosts for antibody production

Rabbits, mice and chickens are three of the most common host animals chosen for the generation of human therapeutic antibodies. Both rabbits and chickens can generate large amounts of polyclonal antibodies with high specificity, and all animals may generate recombinant antibodies with good specificity and affinity. After animal immunisation, the antigen specific antibodies in a B-cell pool are enriched through clonal expansion and repeated exposure to antigen. Usually at least two animals per antigen is recommended, as in some cases there maybe little or no response to the target antigen. This often occurs as each animal has a unique immune system and therefore immune response is highly variable. Further comparisons between human, rabbit, mouse and chicken antibodies are shown in Table 1.6.

Table 1.6 Comparison of human, rabbit, mouse and chicken antibodies.

Key characters	Human	Rabbit	Mouse	Chicken
Structure	IgM/G/A/D/E	IgM/G/A/D/E	IgM/G/A/D/E	IgY/A/M
Primarily used antibody	IgG	IgG	IgG	IgY
Molecular weight	~150 kDa	~150 kDa	~150 kDa	~180 kDa
Main source and Concentration	Serum (~10 mg/mL)	Serum (7-15 mg/mL)	Serum (7-10 mg/mL)	Egg yolk (15-25 mg/mL); serum (~5 mg/mL)
Generation	--	Slow	Moderate	Fast
Genetic diversity	Light and heavy chain/ high	Light chain/ high	Light and heavy chain/ high	Heavy chain/low
Antibody avidity to human antigens	--	Moderate	Moderate	High
Cross reacting to human antigens	--	Moderate	Moderate	Low

The generation of antibodies using a rabbit as the host for immunisation offers a number of advantages. It is a medium sized animal and is easier and cheaper to maintain than large animals (e.g. goats, sheep and donkeys). A rabbit is able to produce a large amount of polyclonal antibodies in serum with an antibody concentration of 7-15 mg/mL (~5 mL serum per week). Young adult female rabbits are preferred because young rabbits have better antibody response than old ones, and female rabbits are more docile and less aggressive in social interaction than males (Hendriksen and Hau, 2003). However, there are more than twenty functional heavy chain germline genes in the rabbit immune system, two constant kappa light chain (Cκ) genes and multiple variable kappa

light chain (Vκ) genes. The κ:λ ratio is 10-20:1 (Barbas *et al.*, 2001). Enormous diversity is generated by re-arrangement of the V (variable), D (diversity) and J (joining) gene segments.

Bachmann *et al.* (1994) reported that in the mouse, approximately 1,000 to 10,000 specific B-cells are produced in response to a complex antigen. In the murine immune system, there are 300 to 1,000 V_H gene segments, 13 D_H gene segments, four J_H gene segments, nearly 300 Vκ gene segments, five Jκ gene segments, one Cκ gene segment, two Vλ gene segments, three Jλ gene segments and three Cλ gene segments (Early *et al.*, 1980). Murine complementarity determining regions 1 and 2 (CDR1 and CDR2) of heavy and light chains of are determined by V gene segments, while CDR3 is produced by inaccurate joining of V, D and J gene segments ensuring great structural antibody diversity (Selsing *et al.*, 1996).

In general, the larger the phylogenetic distance between the immunised animal (e.g. chicken) and the antigen host (e.g. human), the greater the antibody response will be. Thus, chickens, which are phylogenetically more distant from humans than rabbits and mice, are more likely to achieve better immune responses to human proteins (Zhang *et al.*, 2003). Female chickens (hens) are favoured for producing large amounts of IgY, which is the 180 kDa homolog of mammal IgG as this can be harvested from egg yolk. This process is more convenient than producing antibodies from blood and other organs, for instance, spleen and bone marrow. The immunoglobulin locus of chickens consists of only one functional copy of the V and J segment for both the heavy and light chains of the antibody (Ratcliffe, 2006). The production of an antibody repertoire in the chicken immune system is derived by re-arrangement of the V and J segments, which makes the diversity of antibodies extremely limited. However, this makes the generation of chicken recombinant antibody libraries easier (only two sets of primers for the amplification of variable chains are required) than generation of rabbit or mouse recombinant antibody libraries.

1.3 Production and amplification of antibodies

1.3.1 The antibody: structure and function

Antibodies, also known as immunoglobulins (Igs), possess antigen binding specificity. They are produced by B-cell-derived plasma cells. Antibodies mainly exist in serum, as well as in interstitial fluids and exocrine secretions. Antibodies can effectively identify, kill or neutralize invading bacteria, parasites, toxins, viruses and destroy other foreign compounds.

1.3.2 Structure of mammalian antibody

Mammalian antibodies are classified into five isotypes IgM, IgD, IgG, IgE and IgA based on five different heavy polypeptide chains μ, δ, γ, ε and α, respectively. The heavy polypeptide chains μ and ε consist of about 550 amino acids and about 450 amino acids comprise the heavy polypeptide chains α and γ (Janeway, 2001; Strome *et al.*, 2007).

There are two types of light chains for mammal antibodies, namely, lambda (λ) and kappa (κ). However, each antibody consists of only one of these. κ and λ light chains are about 211 to 217 amino acids in length (Diaz and Casali, 2002).

Both heavy and light chains contain two regions: namely, the variable (V) region at the N-terminal end and the constant (C) region at the C-terminal end. The amino acid sequence of the variable regions is responsible for the specificity of the antibody, and it is this region that is used for antigen-specific binding. For each isotype, the constant domain remains the same with the same amino acid consensus sequence.

The synonymous "Y" shape associated with a basic immunoglobulin unit (Ig) monomer (or subunit) (Fig. 1.3) consists of two light and two heavy chains, which are connected by disulfide bonds (Woof and Burton, 2004). All five isotypes, IgM, IgD, IgG, IgE and IgA, are composed of this Ig monomer. IgD, IgE and IgG are monomers, while IgA is a dimer and IgM is a pentamer (Carey Hanly *et al.*, 1973).

The single chain variable fragment (scFv) consists of variable (binding) regions of antibody heavy chain (V_H) and light chain (V_L), which are linked by a short peptide chain. The popularity achieved by the scFv fragment is due to its short generation time, capacity to be expressed in *Escherichia coli* (*E. coli*) and high antigen affinity and structural stability (Townsend *et al.*, 2006).

The fragment antigen-binding (Fab) region consists of the full antibody light chain, connected to a second antibody domain comprised of V_H and C_H1 regions by disulphide bonding. Thus, each heavy and light chain has one constant and one variable domain. The two variable domains play a role in specific binding of defined antigens (Barbas *et al.*, 2001).
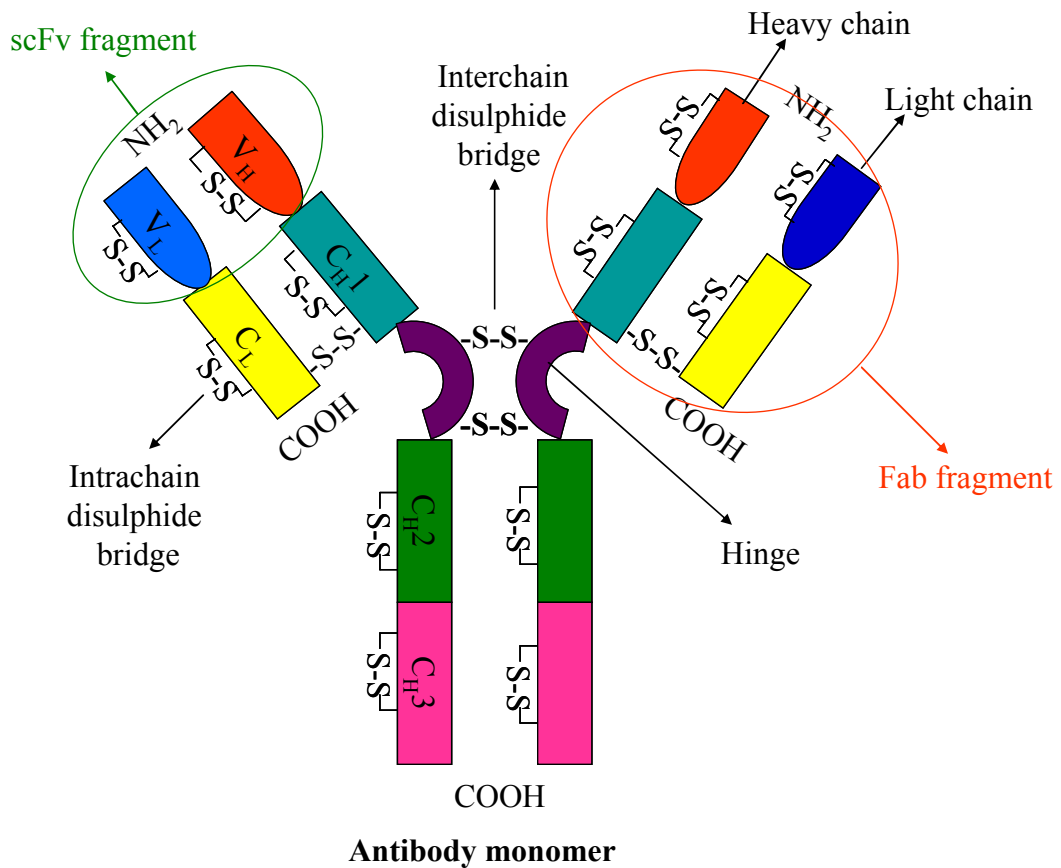
Antibody monomer

Fig. 1.3 Structure of a basic IgG antibody. The basic antibody monomer consists of two light chains and two heavy chains which are connected by disulfide bonds.

1.3.3 Antibody types and production

1.3.3.1 Polyclonal antibodies

Antibodies that are derived from multiple B cell clones are called polyclonal antibodies and they recognise multiple epitopes. The production of polyclonal antibodies is usually conducted by carrying out several rounds of antigen immunisation into the host animal, for example, rabbits, mice, chicken, horses or goats. Specific antibodies are then generated by B lymphocytes. Finally, polyclonal antibodies are extracted from the serum of mammalian animals, whereas for chickens, polyclonal antibodies can also be extracted from egg yolks. Polyclonal serum offers the advantage of broad reactivity. However, polyclonal antibodies also display variability in specificity, avidity, relative percentage generated and are produced in limited quantities. It may also be difficult to reproduce these characteristics in new batches.

1.3.3.2 Monoclonal antibodies

Unlike polyclonal antibodies, monoclonal antibodies are generated from a single B cell and react with a single antigenic epitope. For monoclonal antibody production, antibody-generating spleen cells are initially fused to myeloma cells and the specific hybrids with the required antibody specificity selected. Compared to polyclonal antibodies, monoclonal antibodies are homogeneous in specificity, and unlimited quantities can be produced, but take more time to generate.

1.3.3.3 Recombinant antibodies

A recombinant antibody does not exist naturally but is assembled from recombinant DNA by combining antibody heavy chain and light chain gene sequences (Jeremy *et al.*, 2007). First, the specific antibody genes are amplified using specifically designed primers and are assembled to form the recombinant antibody gene. These genes are cloned into a phage display vector (i.e.

pComb3H or pComb3X). The recombinant gene is then transformed into electrocompetent bacteria (i.e. XL1-Blue and ER2537) to produce the antibody phage library. Each bacterium from this library will express a single individual recombinant antibody on the surface of the phage particle. Finally, the extraction and selection of highly specific antibody is performed generally using phage display technology with several rounds of bio-panning. The most widely applied formats for recombinant antibodies are scFv and Fabs (Fig. 1.2 A and B).

Over the last twenty years, antibody genes have been cloned, genetically manipulated and expressed in *E. coli* to produce antigen binding proteins. Antibody expression in *E. coli* has several advantages i.e. large quantities, can be produced quickly and at low cost. Furthermore, recombinant antibody technology offers the possibility of production of anti-human antibodies with both high specificity and affinity for human disease diagnosis and therapy (de Lalla *et al.*, 1996). Recombinant technology was proved to be a promising method for producing antibodies for diagnosis and therapy.

1.4 Application of different types of recombinant antibodies

Recombinant antibodies play a crucial role in biomedical research and are used as clinical therapeutic reagents. ScFv and Fab are the most popular recombinant antibody formats used for diagnosis and therapy. They are also important because of their high specificity for target antigens, their small size, and the lower negative response that they generate when exposed to the human immune system. Using molecular biological approaches it is possible to generate a recombinant chimeric antibody (a promising candidate in the treatment of many human diseases), which consists of mouse antibody variable region sequences with human antibody constant region sequences and then this chimeric gene can be largely expressed in either myeloma cells or *E. coli*. (Xiong *et al.*, 2006).

It is reported that over 151 recombinant therapeutics have been approved by the FDA or by the European Medicines Agency for different clinical indications (Huang *et al.*, 2012). In addition to scFv and Fab, bispecific

antibodies [i.e. Fab-scFv fusion antibody, F(ab')$_2$ and ic scFvs] are also used as possible therapeutic agents for cancer treatment and have been developed since the mid-1980s because of their improved efficacy and stability (Table 1.7; Fig. 1.4; Conroy *et al.*, 2009; Thakur and Lum, 2010).

Table 1.7 Types of recombinant antibodies.

Types of recombinant antibodies	Abbreviation	Molecular mass
scFv	Single-chain variable fragment	25 kDa
Fab	Fragment antigen-binding region	50 kDa
sc(Fv)$_2$	Bivalant single-chain variable fragment	50 kDa
F(ab')$_2$	Bivalant fragment antigen-binding region	100 kDa
Fab-scFv	Single-chain variable fragment and fragment antigen-binding fusion	75 kDa
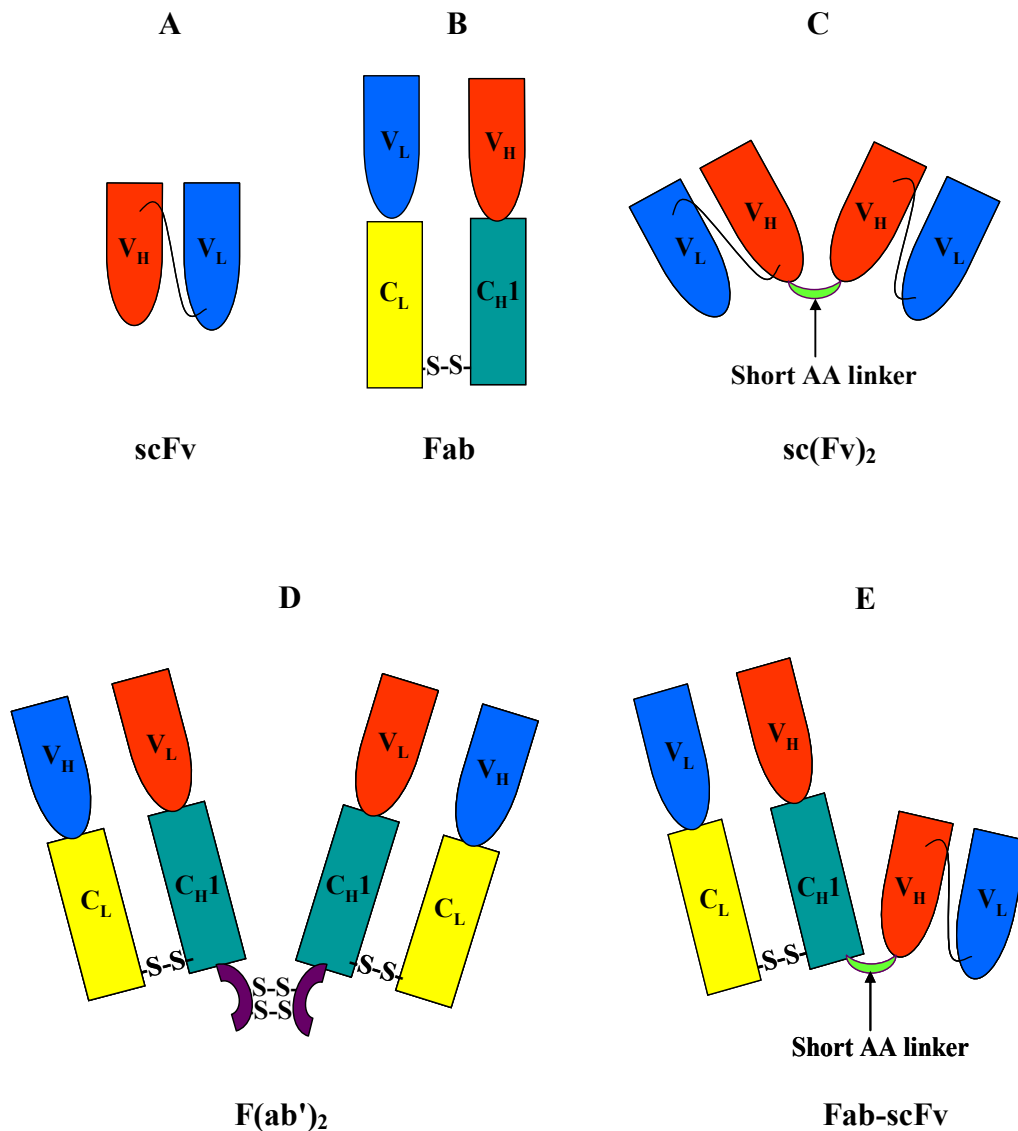
Fig. 1.4 Structures of a scFv (A), a Fab fragment (B), a (scFv)$_2$ (C), a F(ab')$_2$ (D) and a Fab-scFv (E). (A) The scFv fragment is composed of one variable region of a light chain (V$_L$) and one variable region of a heavy chain (V$_H$), with a flexible linker joining [i.e. (GGGGS)$_3$ linker] the terminal ends of either the V$_H$ to V$_L$ (or V$_L$ to V$_H$). (B) The Fab fragment is formed by one variable and one constant domain of both light and heavy chain linked with a disulphide bond. (C) A ic scFv, (scFv)$_2$, is generated by linking two scFvs with a short amino acid (AA) linker. (D) F(ab')$_2$ involves linking the two Fabs by disulphide bonds. F(ab')$_2$ can also be produced by proteolytic cleavage of an IgG molecule. (E) A Fab-scFv can be generated by linking Fab and scFv via a short amino acid (AA) linker.

1.4.1 Single-chain variable fragment (scFv)

The scFv (Fig. 1.4A) contains variable regions of antibody heavy (V_H) and light chains (V_L). In most cases, the scFv recombinant antibody fragment was used for targeted therapy through fusing to different proteins or genes. Chen *et al.* (2010) developed a stable anti-human CD44v6 scFv by selecting from a human phage-displayed scFv library. It can effectively and specifically target CD44v6-expressing cancer cells. Therefore, anti-CD44v6 scFvs may have significant value for cancer therapy. Ayyar *et al.* (2010) successfully generated anti- heart-type fatty acid binding protein (hFABP, a promising cardiac biomarker) scFv with high affinity and specificity and low limit of quantitation (1.9 ng/mL) for immunodiagnosis of cardiovascular diseases. He *et al.* (2010) reported that a prostate tumor-targeting scFv (UA20) internalizes in prostate tumor cells rapidly and specifically *in vitro*, and also accumulates in prostate tumor xenografts *in vivo*. It indicates the potential of UA20 for targeted therapy for prostate cancer. Furthermore, MacDonald *et al.* (2009) demonstrated that VB4-845, a scFv-Pseudomonas exotoxin A fusion construct that targets epithelial cell adhesion molecule (EpCAM), can provide a safe and feasible therapy for squamous cell carcinoma of the head and neck (SCCHN).

1.4.2 Fragment antigen-binding (Fab) fragment

The Fab fragment, which is double the size of the scFv, consists of the full antibody light chain, connected to a second antibody domain comprised of V_H and C_H1 regions by disulphide bonding (Fig. 1.4B). Recombinant antibody fragment Fabs have been used in therapy for various diseases (e.g. digitalis poisoning, human neuroblastoma, heart disease, severe preeclampsia, severe North American pit viper envenomation and heart disease). There are many medicines, which have been derived from Fabs and that are now approved by the FDA. For example, Abciximab (ReoPro), a monoclonal Fab (c7E3 Fab) for the treatment of cardiac ischemic complications, was approved by the FDA in 1994 (Faulds and Sorkin, 1994). Ranibizumab (Lucentis), a monoclonal Fab with therapeutic efficacy of macular degeneration, was approved by the FDA

in 2006. ReoPro (Fab/chimeric) targeted to GpIIb/gpIIa for treatment of cardiovascular disease was approved by the FDA in 1994 (Holliger and Hudson, 2005).

Recent research indicated more potential therapeutic applications of Fab. Mao *et al.* (2012) demonstrated that a novel Fab antibody fragment which targeted latent membrane protein 1 (a latent gene which was expressed when nasopharyngeal carcinoma occurs) has the ability to significantly inhibit nasopharyngeal carcinoma xenograft tumor growth *in vivo* (in nasopharyngeal carcinoma xenograft nude mice) after combining with mitomycin C. Hamatake *et al.* (2010) produced a CD4-reactive Fab of an IgM clone which limited the replication of HIV from a healthy HIV-seronegative individual. This Fab against CD4 may provide an efficacious therapy for HIV/AIDS.

1.4.3 Bivalent and trivalent scFvs

Bivalent or trivalent scFvs can be generated by linking two or three scFvs with a short amino acid linker (Fig. 1.4C). Heitner *et al.* (2006) selected a therapeutic ic scFv candidate (AT-19) using live cell (the human prostate carcinoma cell line PC-3) panning against native tomoregulin (a cell surface protein which provides potential prostate cancer target). Monomeric scFv can not bind the native receptor expressed by cells, while ic scFv AT-19 binds with nanomolar affinity. Wittel *et al.* (2005) reported that scFv dimer, $sc(Fv)_2$, and tetramers, $[(scFv)_2]_2$, are stable *in vivo* and have significant potential for diagnostic and therapeutic applications. Pavlinkova *et al.* (1999) generated a stable noncovalent dimer of CC49 scFv by joining the V_L and V_H variable region genes together using a 25-amino acid helical linker (205C). The rapid clearance from the blood, higher tumor uptake and longer retention of the stable dimer CC49 scFv make it an important agent for potential imaging and therapeutic applications. Based on the variable regions of the monoclonal antibody (MAb) CC49, Beresford *et al.* (1999) generated a unique divalent single-chain Fv protein [$sc(Fv)_2$]. This $sc(Fv)_2$ is different from other ic single-chain fragments as a linker sequence (L) is inserted between the repeated V_L and V_H domains [V_L-L-V_H-L-V_L-L-V_H]. This soluble construct

was expressed in *E. coli*, followed by purification by ion-exchange and gel-filtration chromatography. This ic scFv of MAb CC49 was proved to be a competitive candidate for imaging and therapeutic applications.

1.4.4 Fab dimer

A F(ab')$_2$ fragment contains two Fab fragments. It can be obtained by cleaving whole immunoglobulins using the enzyme pepsin below the hinge region (Fig. 1.4D). A novel F(ab')$_2$ fragment, 125I-F(ab')$_2$, from the chimeric monoclonal antibody U36 (cMAb U36) recognizes the CD44v6 antigen (expressed by xenograft tumors) was proved by Sandström *et al.* (2012) to have better tumor-to-blood ratio and tumor penetration than cMAb U36 to the monovalent Fab fragment. This test was performed in nude mice with CD44v6-expressing xenograft tumors. Herrmann *et al.* (2008) constructed optimized bispecific antibodies, anti-CD3 F(ab')$_2$ fragments, for selective activation of the death receptor CD95. Monoclonal anti-CD3 F(ab')$_2$ fragments were generated by digestion with pepsin for 17 hr at 37°C in acetic acid, pH 4.0. The reaction was quenched with 2 M Tris and dialysed against PBS overnight at 2–8°C. F(ab')$_2$ fragments were finally purified by size-exclusion chromatography. Leavenworth *et al.* (2010) reported that anti-NKG2A F(ab')$_2$ treatment in experimental autoimmune encephalomyelitis (EAE) induced mice had no detectable effect on the numbers or activity of T and B lymphocytes and NK cells in peripheral lymphoid tissues. This anti-NKG2A-based approach may offer a secure and efficient therapy for CNS disorders. Anti-NKG2A 20d5 F(ab')$_2$ antibodies were produced from a 20d5 rat IgG$_{2a}$ antibody using a F(ab')$_2$ preparation kit (Pierce).

1.4.5 Fab-scFv fusion

The Fab-scFv fusion antibody which is known as a kind of bispecific antibody (BsAb), has been proven to be an efficient approach in developing novel therapies for many diseases (Fig. 1.4E). Fab-scFv BsAb can be made by C-terminal fusion of scFv molecules to the light chain or heavy chain of a Fab.

This gave rise to disulphide stabilized Fab-scFv of intermediate molecular size (Schoonjans *et al.*, 2000). Fab-scFv can bind to two different sites of the same or different antigens, e.g. one part of the BsAb targets a molecule or cell specifically for targeting; while the other part is directed towards an enzyme, toxin, virus or effector cell for therapy (Schoonjans *et al.*, 2001; Lu *et al.*, 2002).

Schoonooghe *et al.* (2009) developed an anti-MUC1 Fab-scFv antibody with better penetration in the tumor compared with a full-size monoclonal antibody for better anti-cancer therapeutics. MUC1 (a tumor-associated antigen on the surface of tumor cells) has been used as a specific antibody target for immunotherapy of human malignancies. Based on the anti-MUC1 PH1 Fab, they also developed bivalent PH1 bibodies and trivalent PH1 tribodies of intermediate molecular mass by addition of PH1 scFvs to the C-terminus of the Fab chains using flexible peptide linkers.

1.5 Production and selection of recombinant antibodies

1.5.1 Production and selection of recombinant antibodies through phage display

Phage, a kind of virus that infects bacteria, can adopt foreign genes into its non-crucial regions of genome. In phage display technology, foreign DNA (i.e. gene of scFv or Fab), is inserted into phage gene III, the gene encodes one of the phage coat proteins, and is expressed as a fusion protein. After infecting gram-negative bacteria (i.e. Top-10, XL1-blue *E. coli*) the phage starts the replication of coat protein genes, including gene III and foreign DNA fusion. This fusion is then expressed as a fusion protein and is displayed on the surface of phage (Smith, 1985).

The phage-expressed (i.e. M13, T4, T7 and λ phage) antibodies are then screened via biopanning for antibodies which are specific to the target molecule. Usually, several cycles of biopanning are needed for enrichment of specific antibodies, as more rounds of biopanning are more likely to result in higher enrichment of specific antibodies (McCafferty *et al.*, 1990).

Each cycle of biopanning includes three basic steps. Firstly, selection of specific phage which bind to the target molecules. At this step, the prepared phage clones are added to a tube or mircrowell which is coated with a defined amount of the target antigen. The coating antigen concentration usually decreases with each round of biopanning. Secondly, removal of non-specific phage by washing 5-10 times using PBST and PBS. The unbound (non-specific) phage are washed away from the solid surface normally by washing several times with PBST followed by PBS. The number of washings is usually increased with each round of biopanning. Finally, specific phage are collected by eluting phage remaining bound to the antigen using freshly made trypsin. The eluted phage can be kept at 4°C for long-term storage (de Kruif *et al.*, 1996) and are analysed initially for specificity by polyclonal phage ELISA. If specific binding to the target antigen is detected, monoclonal phage ELISA will then be performed for selection of single colonies which express specific antibodies. However, if no specific binding is detected, the eluted phage will be infected into bacteria and the next round of biopanning is performed. The typical biopanning cycle is illustrated in figure 1.5.
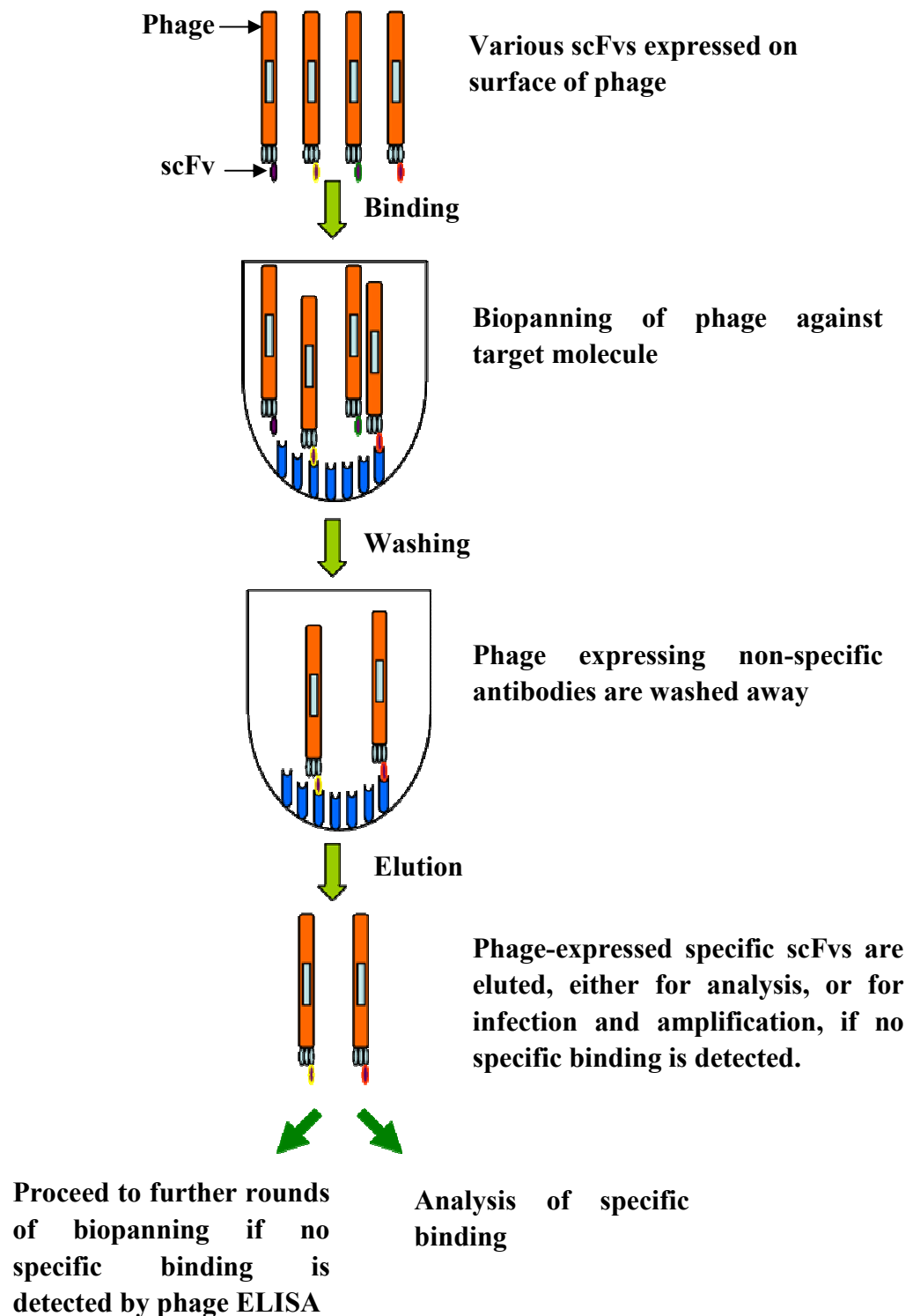
Fig. 1.5 Illustration of biopanning cycle. A typical cycle of biopanning of specific phage binding. Removal of non-specific phage by washing and specific phage elution.

1.5.2 Production of soluble recombinant antibodies in *E. coli*

The functional antibody fragments are transported to an oxidising environment to ensure that the required disulfide bonds are generated with attendant protein folding, by attaching the bacterial leader peptide sequences to the N terminus of the antibody (Rapoport, 1992). The antibody chains are usually transported to the periplasmic space which contains proteins (i.e. DsbA, PDI, DsbC, SKp and FkpA) that are crucial for the formation of disulfide bonds, folding and assembly of recombinant proteins (Bothmann and Pluckthun, 2000). However, the expression levels of functional antibodies are usually very low (Chen *et al.*, 2004). Therefore, cytoplasmic expression with higher protein expression level may be more productive. Intra-molecular disulfide bonds, which are crucial for antibody function, cannot be formed correctly in the cytoplasm, resulting in insoluble and inactive antibodies (Biocca *et al.*, 1995).

1.6 Aims of project

The overall aim of this project was to generate single-chain antibody variable fragments (scFvs) which recognise extracellular domains of $P2X_3$. The anti-$P2X_3$ scFv will then be used as a targeting agent to deliver BoNT/A and BoNT/D to pain-signalling neurons for the treatment of inflammatory pain.
There are four aims in this project:
Firstly, generation of scFv libraries, using spleen and bone marrow cDNA from $P2X_3$-BSA/KLH immunised animals, and selection of anti-$P2X_3$ scFvs from scFv libraries using phage display. Various animals (rabbits, mice and chickens) will be immunised with two extracellular domains of $P2X_3$ ($P2X_3$-60 and $P2X_3$-257). Large $P2X_3$-specific scFv libraries will be constructed using these animal immune models. Phage display technology will be applied for screening for anti-$P2X_3$ scFv recombinant antibodies, followed by polyclonal phage ELISA, monoclonal ELISA, cross reactivity analysis, competitive ELISA, Western blotting and immunofluorescence stain technologies, in order to select highly-specific anti-$P2X_3$ scFvs.

Secondly, BoNT/A(or/D) and anti-P2X$_3$ scFv fusion proteins will be expressed and purified. The neuron-acceptor binding domain gene in the long-acting BoNT/A or BoNT/D protease and the DNA sequence encoding the anti-P2X$_3$ scFv will be joined using a non-structural linker, (GGGGS)$_3$. This resultant molecule will be inserted in a pET29a plasmid vector and expressed in *E.coli*, followed by IMAC affinity purification.

Thirdly, the specificity of this new therapeutic will be investigated *in vitro* on DRGs (major sensory neurons). Their susceptibility to toxins will be investigated based on differential ability of the BoNT-scFv fusion protein to cleave specific SNAREs and inhibit release of pain transmitters.

Finally, the specificity of this new therapeutic will be investigated *in vivo* in the rat. A capsaicin-induced or formalin-induced model for pain in rats will be used to investigate the anti-nociceptive behaviour of this new generation of therapeutics, and to elucidate how they perturb the propagation of pain signals.

Chapter 2

Materials and Methods

2.1 Materials and equipment

2.1.1 Equipment

This section describes equipment used and there relevant suppliers.

Table 2.1 List of equipment

Equipment	Suppliers
Biometra $T_{GRADIENT}$ PCR machine	LABREPCO, 101 Witmer Road, Suite 700, Horsham, PA19044, USA.
Nanodrop™ ND-1000	NanoDrop Technologies, Inc., 3411 Silverside Rd 100BC, Wilmington, DE19810-4803, USA.
Gene Pulser Xcell ™ electroporation system	Bio-Rad Laboratories, Inc., 2000 Alfred Nobel Drive, Hercules, California 94547, USA.
Roller mixer SRT1	Sciencelab, Inc., 14025 Smith Rd., Houston, Texas 77396, USA.
Safire 2 plate reader	Tecan Group Ltd., Seestrasse 103, CH-8708 Männedorf, Switzerland.
Vibra Cell™ sonicator	Sonics and Materials Inc., 53 Church Hill Road, Newtown, CT 06470-1614, USA.
UV-Vis Spectrophotometers (UV-160A)	Shimadzu Scientific Instruments (SSI), 7102 Riverwood Drive, Columbia, MD 21046, USA.
IX71 inverted microscope	Olympus America Inc., 3500 Corporate Parkway, P.O. Box 610, Center Valley, PA 18034-0610.
CO_2 incubator (IG 150)	Jouna, 10 Rue Duguay Trouin, 44807 St-Herblain, France.

G:BOX Gel & Blot Imaging Series	Syngene international Ltd, 5108 Pegasus Court Suite M. Frederick, MD. 21704, USA.

2.1.2 Consumables

This section describes the disposable labware used and the associated suppliers.

Table 2.2 List of consumables

Consumables	Suppliers
Plastic labware, i.e. centrifuge tubes, pipettes tips, pipettes and tissue culture plates	Sarstedt, Sinnottstown, Drinagh, Co. Wexford.
Maxisorb 96-well plates	Nunc, Kamstrup DK, Roskilde, Denmark.
BIAcore CM5 sensor chips	GE Healthcare Bio-Sciences AB, SE-751 84 Uppsala, Sweden.
NuPAGE Bis-Tris Gel	Invitrogen, 5791 Van Allen Way, Carlsbad, CA 92008, USA.
Sealing membrane	Sarstedt AG & Co., Sarstedtstraße, Postfach 1220, 51582 Nümbrecht, Germany.
Filters	Sarstedt AG & Co., Sarstedtstraße, Postfach 1220, 51582 Nümbrecht, Germany.
Microscope slide	Fisher Thermo Scientific, 47341 Bayside Pkwy., Fremont, CA 94538, USA.
Cover glass	VWR International, LLC 1310 Goshen Parkway, West Chester, PA 19380, USA.
$10 \times$ TAE buffer (#T9650)	Sigma Aldrich, 3050 Spruce Street, St. Louis, MO 63103, USA.

2.1.3 Microbial cells and plasmids

2.1.3.1 Bacterial cells for cloning and expression

Table 2.3 List of bacterial cells

Bacterial cells	Genotypes
E. coli TOP10 F	Strain: {*lac*I^q, Tn*10*(Tet^R)} *mcr*A Δ (*mrr-hsd*RMS-*mcr*BC) ϕ80*lac*ZΔM15 Δ *lac*X74 *rec*A1 *ara*D139 Δ(*ara-leu*)7697 *gal*U *gal*K *rps*L (Str^R) *end*A1 *nup*G
E. coli XL1-Blue strain	recA1 endA1 gyrA96 thi-1 hsdR17 supE44 relA1 lac *[F'* proAB lacI^{q}ZΔM15 Tn10 *(Tet^R)]*
BL21(DE3)	F– *omp*T *hsd*SB(rB–, mB–) *gal dcm* (DE3)
Origami 2(DE3)	*Δ(ara-leu)7697 ΔlacX74 ΔphoA Pvu*II *phoR araD139 ahpC galE galK rpsL* F'[*lac$^+$ lacI^q pro*] (DE3) *gor522*::Tn*10 trxB* (Str^R, Tet^R)

2.1.3.2 Plasmids used as expression vector

A genetic map of the pComb3XSS vector used in the generation and expression of scFv antibodies is shown in Fig. 2.1a. ScFv expression is directed using a single *lac* promoter and an ompA leader sequence. The amber codon enables soluble expression, and the *SfiI* restriction sites enable directional insert cloning. Hemagglutinin (HA) and His tags make it is possible to detect and purify the scFv antibody (Berry *et al.*, 2003). Thus, the pComb3XSS vector provides a good choice for soluble scFv expression, detection, purification and phage selection.

A map of the pET-29a (+) vector used in the generation and expression of BoNT-scFv fusion is shown in Fig. 2.1b. The pET-29a (+) vector contains an N-terminal thrombin restriction enzyme site which enables directional insert cloning and includes an ampicillin resistance marker for specific selection. The His-tag allows affinity purification by NTA–Ni affinity column and immunodetection using an anti-His tag antibody (Guo *et al.*, 2006).
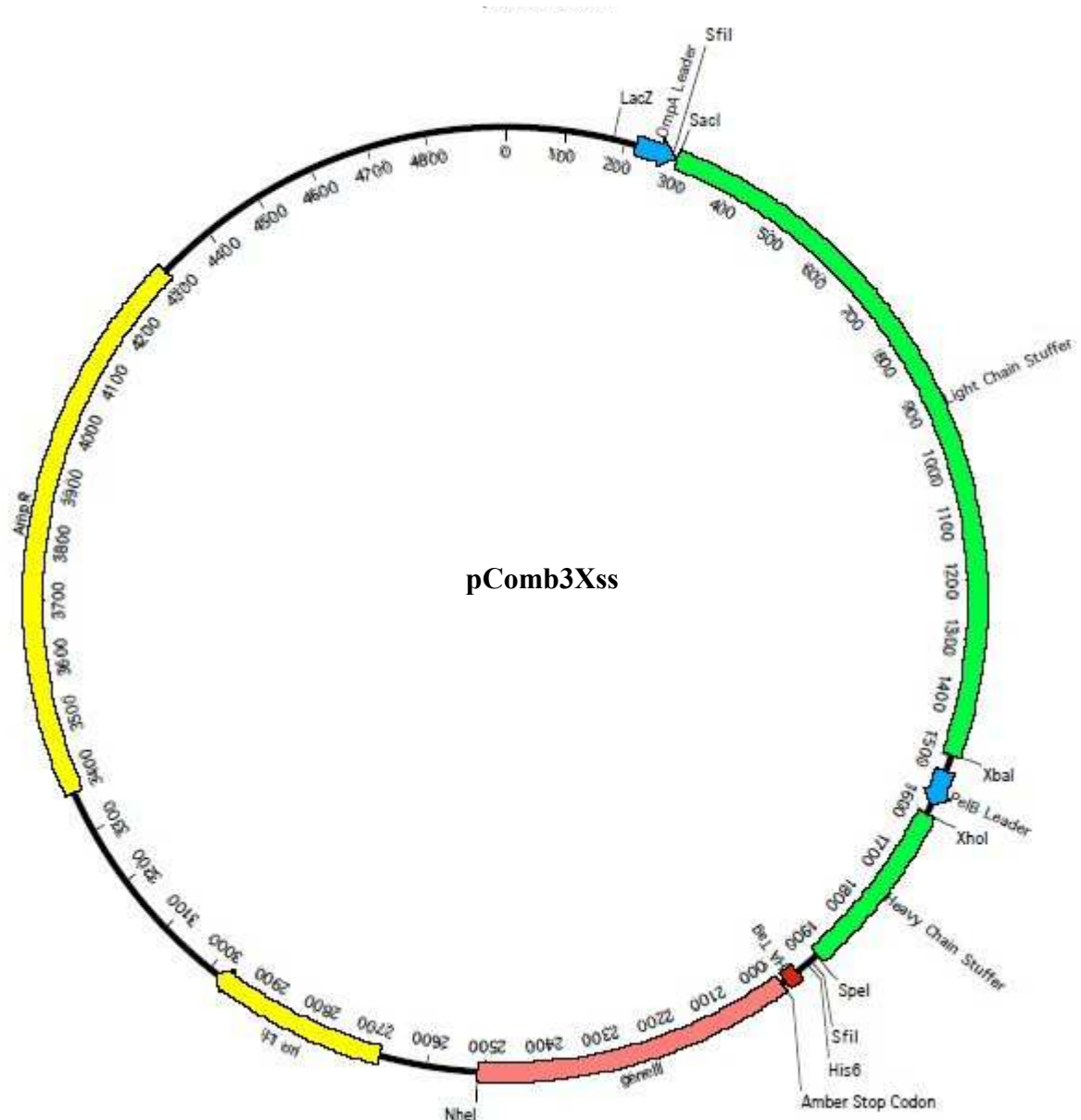
Fig. 2.1a PComb3Xss vector map (This vector map was sourced from GenBank with accession number AF268281). The vector map of pComb3XSS vector contains an amber codon, *SfiI* restriction sites, hemagglutinin (HA) and His tags.

Fig. 2.1b Plasmid map of pET-29a (This vector map was sourced from BVTech Plasmid, 2012). The pET-29a (+) vector contains an N-terminal thrombin restriction enzyme site, ampicillin resistance marker and His tag.

2.1.4 Composition of buffer and other solution

Table 2.4 List of buffers

Buffer	Composition
Phosphate buffered saline (PBS)	150 mM NaCl 2.5 mM KCl 10 mM Na_2HPO_4 18 mM KH_2PO_4, pH 7.4
PBS-Tween 20 (0.05%, v/v) (PBST)	0.15 M NaCl 2.5 mM KCl 10 mM Na_2HPO_4 18 mM KH_2PO_4 0.05% (v/v) Tween 20 Ph 7.4
PBST-milk (PBSTM)	0.15 M NaCl 2.5 mM KCl 10 mM Na_2HPO_4 18 mM KH_2PO_4 0.05% (v/v) Tween 20 Specified % (w/v) milk marvel powder Ph 7.4
Tris buffered saline (TBS)	20 mM Tris base 135 mM NaCl pH 7.5
TBS-Tween 20 (1% v/v) (TBST)	20 mM Tris base 135 mM NaCl 0.1 % (v/v) Tween 20 pH 7.5
TBST-milk (TBSTM)	20 mM Tris base 135 mM NaCl 0.1 % (v/v) Tween 20 Specified % (w/v) milk marvel powder, pH 7.5

10×electrophoresis buffer	500 mM MOPS 500 mM Tris base 1 % (w/v) SDS 10 mM EDTA
2.5×transfer buffer	125 mM Tris base 192 mM Glycine 20% (v/v) Methanol
Coomassie stain dye	0.2% (w/v) Coomassie blue R-250 45% (v/v) Methanol 10% (v/v)Acetic acid
Coomassie destain	25%(v/v) Acetic acid 25% (v/v) Methanol
FACS buffer	2% (w/v) FCS 0.05% (w/v) NaN_3 1 x PBS

2.1.5 Commercial kits used in this research

Table 2.5 List of commercial kits used in this research

Commercial kits	Catalog Number	Suppliers
Superscript III reverse transcriptase kit	18080-051	Invitrogen Corporation, 5791 Van Allen Way, Carlsbad, CA 92008, USA.
Plasmid Purification kit	NZ74058850	Fisher Thermo Scientific, 47341 Bayside Pkwy., Fremont, CA 94538, USA.
NucleoSpin® extract II	NZ740609.50	Fisher Thermo Scientific, 47341 Bayside Pkwy., Fremont, CA 94538, USA.
EZ-Link(R) Micro Sulfo-NHS-LC-Biotinylation kit	PN21935	Fisher Thermo Scientific, 47341 Bayside Pkwy., Fremont, CA 94538, USA.
Biotin Quantification kit	PN28005	Fisher Thermo Scientific, 47341 Bayside Pkwy., Fremont, CA 94538, USA.
BCA kit	PI-23252	Fisher Thermo Scientific, 47341 Bayside Pkwy., Fremont, CA 94538, USA.
Rat CGRP EIA kit	589001	Cayman Chemical Company, 1180 East Ellsworth Road, Ann Arbor, Michigan 48108, USA
Rat SP EIA kit	583751	Cayman Chemical Company, 1180 East Ellsworth Road, Ann Arbor, Michigan 48108, USA

2.1.6 Antigens and antibodies

2.1.6.1 Peptide-antigen selection and synthesis

Frequently there are problems associated with the generation of antibodies against integral membrane proteins. This arises from difficulties in their isolation and the generation of specific antibodies to domains external to the membrane that can effectively be used for localisation, and eventually, targeting. The use of peptide-antigens derived from proteins is becoming more and more popular as they can be easily obtained with high purity and specificity for a particular region (e.g. an extracellular domain). Moreover, antibodies raised against whole proteins are more likely to predomainantly recognize only selected regions of the whole immunizing protein and it may sometimes be hard to identify the exact region to which they bind (Angeletti, 1999). Therefore, peptide-antigens, may result in the generation of antibodies with higher purity and specificity, and are ideal substitutes for whole natural proteins.

There are four principles to follow for selection of peptides for immunisation:

1) An anti-P2X$_3$ scFv recombinant antibody will be used as the agent to deliver drugs to sensory neurons and, hence, the scFv should ideally bind to P2X$_3$ extracellular domains, e.g. Val$_{60}$-Phe$_{301}$ (Koshimizu *et al.*, 2002). Thus, the immunised peptide region should be chosen from an extracellular domain of P2X$_3$ (Fig. 2.2a).

2) The ideal peptide lengths are from 10 to 20 amino acid residues. Peptides longer than 20 amino acids will be hard to synthesize, while less than 10 residues may contain less epitope which may lead to less chance of the generation of a successful specific immune response (Brown *et al.*, 2011).

3) Ideally no cysteine should be present in peptides for immunisation, as it may lead to the formation of disulfide bonds and improper folding which may cause loss of epitope conformation (Kontermann and Dübel, 2010).

4) N-terminal and C-terminal sequences of a protein are good choices for synthesis, as these sequences are often exposed to the solvent and mobile in protein crystallographic structures. Antibodies developed against these

sequences are suggested to be more likely to work well in immunoblot analysis (Angeletti, 1999).

Human P2X$_3$ protein consists of 397 amino acids, and the extracellular domain is Val$_{60}$-Phe$_{301}$. No extracellular P2X$_3$ epitope has ever been published for antibody generation. Santa Cruz Biotechnology (U.S.A.) has two goat polyclonal antibodies against the P2X$_3$ extracellular domain which are commercially available. The exact immunogens used to generate Santa Cruz's peptide polyclonals are proprietary. They only provide peptides of approximately 50 amino acids range, i.e. 50-100 and 227-277 amino acids for these antibodies. After avoiding the Cys folding domain and taking into account N-terminal and C-terminal sequences, two extracellular domains, P2X$_3$-60 and P2X$_3$-257, were chosen for synthesis. P2X$_3$-60 contributes the protein sequence from amino acids 60 to 79 and P2X$_3$-257 is composed of the amino acid sequence from position 257 to 276.

The amino acid sequence of 60-79 amino acids range (P2X$_3$-60) is:

Val-Val-Thr-Lys-Val-Lys-Gly-Ser-Gly-Leu-Tyr-Ala-Asn-Arg-Val-Met-Asp-Val-Ser-Asp (VVTKVKGSGLYANRVMDVSD).

The amino acid sequence of 257-276 amino acids range (P2X$_3$-257) is:

Ile-Pro-Lys-Tyr-Ser-Phe-Thr-Arg-Leu-Asp-Ser-Val-Ser-Glu-Lys-Ser-Ser-Val-Ser-Pro (IPKYSFTRLDSVSEKSSVSP).
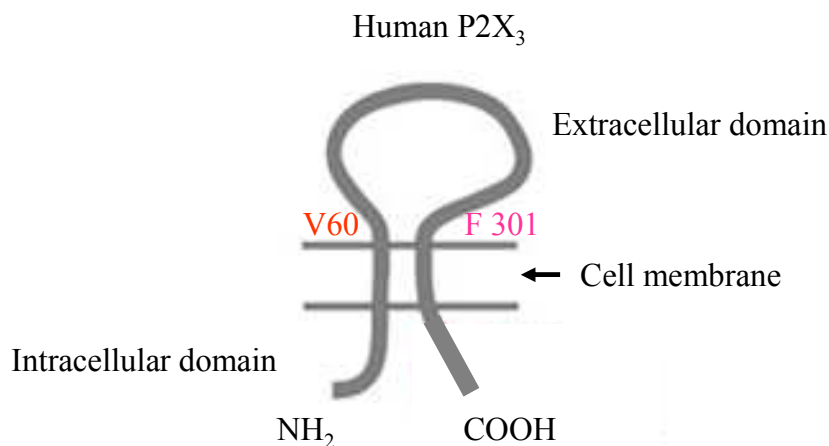
Human P2X$_3$

Fig. 2.2a Schematic structure of human P2X$_3$. The human P2X$_3$ extracellular domain, starts at amino acid V$_{60}$ and ends at F$_{301}$ (Modified from human P2X$_3$ purinoceptor model of Sundukova *et al.*, 2012).

Rat was chosen to be both the *in vitro* and *in vivo* model system for analysis of anti-human P2X$_3$ scFv antibody. The homology of human P2X$_3$ with rat P2X$_3$ was analysed using Basic Local Alignment Search Tool (BLAST). A high identity of 94% was observed and that confirmed the rationality of using the rat as the selected appropriate pain model. The two human regions (P2X$_3$-60 and P2X$_3$-257) chosen for immunisation also showed high identity with their respective regions of rat P2X$_3$. The identity of 60-79 amino acid sequence of the human showed a homoloty of 90% to rat, while for amino-acids 227-277 it was 95% (Fig. 2.2b).

Human P2X$_3$	MNCISDFFTYETTKSVVVKSWTIGIINRVVQLLIISYFVGWVFLHEKAYQVRDTAIESSV	**60**
Rat P2X$_3$	. . . . A	**60**
HumanP2X$_3$	VTKVKGSGLYANRVMDVSDYVTPPQGTSVFVIITKMIVTENQMQGFCPESEEKYRCVSDS	**120**
Rat P2X$_3$	. . . . . . F .R . . . . N	**120**
Human P2X$_3$	QCGPERLPGGGILTGRCVNYSSVLRTCEIQGWCPTEVDTVETPIMMEAENFTIFIKNSIR	**180**
Rat P2X$_3$	. . . . . F . . . . .M..	**180**
Human P2X$_3$	FPLFNFEKGNLLPNLTARDMKTCRFHPDKDPFCPILRVGDVVKFAGQDFAKLARTGGVLG	**240**
Rat P2X$_3$	. . . . .DK . I . R . . . . E .A	**240**
Human P2X$_3$	IKIGWVCDLDKAWDQCIPKYSFTRLDSVSEKSSVSPGYNFRFAKYYKMENGSEYRTLLKA	**300**
Rat P2X$_3$	. . . . .G	**300**
HumanP2X$_3$	FGIRFDVLVYGNAGKFNIIPTIISSVAAFTSVGVGTVLCDIILLNFLKGADQYKAKKFEE	**360**
Rat P2X$_3$	. . . . .H . . . R	**360**
HumanP2X$_3$	VNETTLKIAALTNPVYPSDQTTAEKQSTDSGAFSIGH **397**	
Rat P2X$_3$	. T . . . . .GT . S . . . . FA . . . A .V . . . . .Y **397**	

Fig. 2.2b BLAST analysis of homology of human P2X$_3$ and rat P2X$_3$ amino acid sequences. The 20 amino acids region P2X$_3$-60 is highlighted in red, and P2X$_3$-257 is highlighted in blue. Identity of human P2X$_3$ and rat P2X$_3$ is 94%.

The three-dimensional (3D) structure of human P2X$_3$ was predicted by free online software, RaptorX, based on the 3D structure of another P2X family member, P2X$_4$ (Kawate *et al.*, 2009; Kallberg *et al.*, 2012). This 3D structure showed that both P2X$_3$-60 and P2X$_3$-257 regions formed loops and were in the beta-sheet region which indicates that they are exposed on the surface for

antibody binding (Fig. 2.2c). Thus regions of P2X$_3$-60 and P2X$_3$-257 should be promising choices for antibody generation.
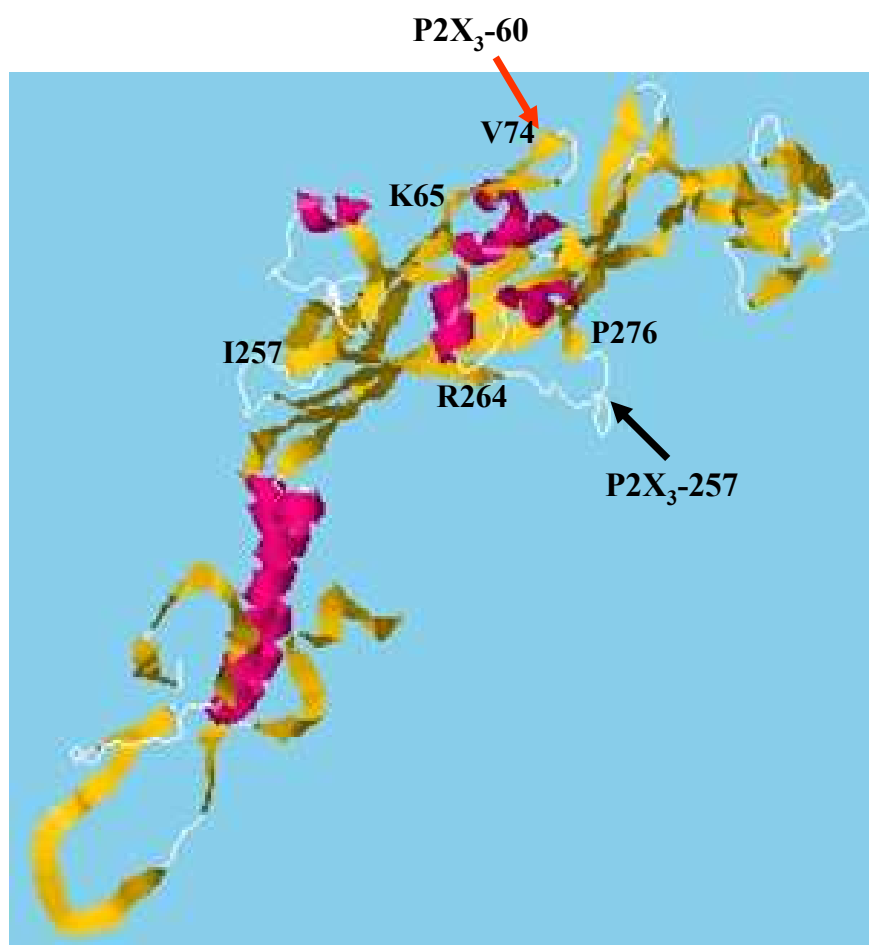
Fig. 2.2c Three-dimensional (3D) structure of human P2X$_3$ was predicted using RaptorX software (Xu Group, Chicago). The red arrow indicates the loop of P2X$_3$-60 and the black arrow the loop of P2X$_3$-257.

P2X$_3$-60, P2X$_3$-257 and all their BSA, KLH, bTg and biotin conjugates were then synthesized by Cambridge Bioscience Ltd. (Munro House, Trafalgar Way, Bar Hill, Cambridge, CB23 8SQ, United Kingdom).

2.1.6.2 Commercial antibodies used in this research

Table 2.6 List of commercial antibodies used in this research

Commercial antibodies	Catalog Number	Suppliers	Dilution Used
HRP-labelled mouse anti-M13 monoclonal antibody	27-9421-01	GE Healthcare Bio-Sciences AB, SE-751 84 Uppsala, Sweden.	1:1,000
HRP-labelled mouse anti-hemagglutinin (HA) IgG$_1$ monoclonal antibody	11988506001	Roche Diagnostics, Grenzacherstrasse 124, Basel 4070, Switzerland.	1:2,000
HRP-labelled goat anti-rabbit polyclonal antibody	A4914-1ML	Sigma Aldrich, 3050 Spruce Street, St. Louis, MO 63103, USA.	1:2,000
HRP-labelled goat anti-mouse polyclonal antibody	A8924	Sigma Aldrich, 3050 Spruce Street, St. Louis, MO 63103, USA.	1:2,000
HRP-labelled goat anti-chicken IgY polyclonal antibody	A9046	Sigma Aldrich, 3050 Spruce Street, St. Louis, MO 63103, USA.	1:2,000
Rabbit anti-rat P2X$_3$ polyclonal antibody	APR-016	Alomone labs Ltd., Har Hotzvim Hi-Tech Park, PO Box 4287, Jerusalem, 91042, Israel.	1:50 for IF; 1:300 for WB
Goat anti-human P2X$_3$ polyclonal antibody	sc-31494	Santa Cruz Biotechnology, Inc., 2145 Delaware Avenue, Santa Cruz, CA. 95060, U.S.A.	1:50 WB
Fluorescein-labelled rat anti-HA monoclonal antibody (3F10)	12013819001	Roche Diagnostics GmbH, Roche applied science, 68298 Mannheim, Germany.	2 µg/mL

HRP-labelled mouse anti-polyHistidine IgG$_{2a}$ monoclonal antibody	A7058-1VL	Sigma Aldrich, 3050 Spruce Street, St. Louis, MO 63103, USA.	1:2,000
Alexa Fluor-546-labelled goat anti-mouse IgG polyclonal antibody	A11003	Invitrogen, 5791 Van Allen Way, Carlsbad, CA 92008, USA.	1:200
Mouse anti-neurofilament (NF) monoclonal antibody	131300	Invitrogen, 5791 Van Allen Way, Carlsbad, CA 92008, USA.	1:500
Cy2-labelled goat anti-mouse IgM polyclonal antibody	115-225-062	Jackson ImmunoResearch, Europe Ltd., Unit 7, Acorn Business Centre, Oaks Drive, Suffolk, UK.	1:100
Rabbit anti-rat calcitonin gene-related peptide (CGRP) Ig G polyclonal antibody	ab47027	Abcam, 330 Cambridge Science Park Cambridge, CB4 0FL, UK.	1:500
Alexa Fluor-546-labelled goat anti-rabbit IgG polyclonal antibody	A-11035	Invitrogen, 5791 Van Allen Way, Carlsbad, CA 92008, USA.	1:200
Mouse anti-SNAP25 IgG$_1$ monoclonal antibody (SMI-81)	SMI-81R	Sternberger monoclonals, Inc. 5210 Eastern Avenue, Hopkins Bayview Research Campany, Baltimore, MD, USA.	1:2,000
Mouse anti-VAMP IgM monoclonal antibody (V2)	ab90433	Abcam, 330 Cambridge Science Park, Cambridge, CB4 0FL, UK.	1:2,000
Mouse anti-syntaxin-1 IgG$_1$ monoclonal antibody (HPC-1)	S0664-2ML	Sigma Aldrich, 3050 Spruce Street, St. Louis, MO 63103, USA.	1:2,000

2.1.7 Cell culture media

Table 2.7 List of media

Media	Composition
Super Broth (SB) Media	10 g/L MOPS
	20 g/L Yeast Extract
	30 g/L Tryptone
Super Optimal Catabolite (SOC) Media	20 g/L Tryptone
	5 g/L Yeast Extract
	0.5 g/L NaCl
	2.5 mM KCl
	20 mM MgCl$_2$
	20 mM Glucose
LB agar	10 g/L Tryptone
	5 g/L Yeast Extract
	10 g/L NaCl
	15 g/L agar
DMEM Culture medium	10% (v/v) FBS
	1% (v/v) P/S
	in DMEM
ZY Media	10 g/L N-Z-Amime
	5 g/L Yeast Extract

2.2 Methods

2.2.1 Isolation and culture of dorsal root ganglion cells (DRGs)

2.2.1.1 Animals, anesthesia and dissection

Postnatal day 5 Sprague-Dawley rats, bred in the approved Bioresources Unit at Dublin City University (DCU), were deeply anesthetized by intraperitoneal

(i.p.) injection of euthatal (Merial Animal Health Ltd., 20% (w/v) pentobarbitone sodium, 25 µL/rat). The dissection of DRG was performed in an open-front laminar flow hood (Microflow, #H50548/1, Class I). The inner surface of the hood was sprayed with 70% (v/v) IMS. Tissue culture plates (12-wells or 24-wells) were coated with poly-L-lysine for one hour at room temperature (100 µL per well). Plates were washed three times with sterile H_2O, and then dried in the hood for one hour (plates then can be stored at 4°C for a month). Laminin (20 µg/mL) was diluted with HBSS, and 100 µL was added per well, and incubated at room temperature for one hour, followed by washing three times with sterile 1 x PBS before culturing cells.

2.2.1.2 Dissection, dissociation and culture of DRG cells

Generally, 7-12 postnatal day 5 Sprague-Dawley rats were sacrificed for culturing 3-4 plates. Dorsal root ganglions (DRGs) were then collected in HBSS and placed on ice (Fig. 2.2.4.2). After dissection, DRGs were washed with ice-cold HBSS three times at 170 g for 1 min (HermLe Z233MK-2 refrigerated centrifuge). Then HBSS was carefully removed. Twenty three mg dispase II and 5 mg collagenase in 10 mL HBSS were then added to the DRGs and incubated for 30 min in a 37°C water bath for dorsal root ganglion membrane digestion. The tube was shaken from time-to-time. The DRG preparation was centrifuged (HermLe Z233MK-2 refrigerated centrifuge) at 170 g for 5 min, and then the pellet was washed with pre-warmed (37°C in a water bath) Dulbecco's Modified Eagle's Medium (DMEM) three times at 170 g for 5 min. The DRG cells preparation was resuspended in 35-50 mL DMEM culture medium with 10% (v/v) fetal bovine serum (FBS), 100 U/mL penicillin and 100 µg/mL streptomycin and passed through a 100 µm cell strainer. Nerve growth factor (NGF) was added to final concentration of 50 ng/ mL. DRG cells were plated into each well and incubated at 37°C in 5% (v/v) CO_2. Every two days the culture medium was replaced by fresh DMEM containing 10% (v/v) FBS, 100 U/mL penicillin, 100 µg/mL streptomycin, 50 ng/ mL NGF and 10 µM Ara-c. The cell images were recorded using an Olympus IX71 microscope with a charge-coupled device (CCD) camera by phase contrast.

Fig. 2.3 Location of DRGs. DRG cells locate in the intervertebral foramen along the spinal column as indicated by the arrows. This picture is taken from Malin *et al.* (2007).

2.2.1.3 Membrane protein enrichment

To harvest $P2X_3$, which is found on DRG membranes, a membrane protein enrichment was performed. After 4 days, medium was removed from each well of the DRG cell culture plate and 1 mL sterile of water containing 1:10 (v/v) protease inhibitor (Sigma, #P8849) was added per well. The cells were scraped from the wells of the cell culture plate. This action was followed by repeated pipetting and this served to break the cells' membranes. The final suspension was collected in a 1 mL tube and centrifuged (Eppendorf centrifuge 5810R) at 14,000 g for 1 min. The suspension was transferred to an ice-cold TL-100 ultracentrifuge tube (stored in the cold room) and centrifuged at 480,000 g (Beckman TL 100 ultracentrifuge) for 20 min at 4°C. The supernatant was removed carefully from the tube. A 200 µL volume of LDS buffer was then added to resuspend the membrane pellet wherein the $P2X_3$ protein should be found. The resuspended protein was heated to 80°C for 5min, and was subsequently loaded onto an SDS-PAGE gel. The protein was placed in long-term storage at -80°C, if not being used immediately.

2.2.1.4 Identification of DRGs by specific antibodies

DRG cells were cultured in a 24-well tissue culture plate for 5-7 days. The DRGs were washed three times with Dulbecco's phosphate buffer saline (D-PBS, lacking Mg^{2+} and Ca^{2+}) and fixed using 3.7% (v/v) paraformaldehyde for 20 min at room temperature. The plate was washed three times with D-PBS, and then blocked with 1% (w/v) BSA in D-PBS for one hour at room temperature. The blocking solution was removed. Mouse anti-neurofilament (NF) monoclonal antibody (1:500 dilution) or rabbit anti-calcitonin gene-related peptide (CGRP) polyclonal antibody (1:500 dilution) was added, and incubated at room temperature for one hour. The plate was washed three times with D-PBS, followed by the addition of secondary antibody Cy2-labelled goat anti-mouse IgG (1:100 dilution) or Alexa Fluor-546-labelled goat anti-rabbit antibody (1:200 dilution). After washing three times by addition of 1 mL of D-PBS into each well, the cells were ready for imaging using an Olympus IX71 microscope or a inverted confocal microscope (Leica Dmire 2) with a CCD camera. Images were then analysed using the Image-Pro Plus 5.1 or Leica confocal software. A negative control was included with rabbit anti-goat IgG (1:1,000 dilution) as primary antibody, followed by secondary antibody Alexa Fluor-546-labelled goat anti-rabbit IgG (1: 200 dilution).

2.2.1.5 Analysis of P2X3 expression on DRG cells with commercial anti-P2X$_3$ antibody

Both Western blotting and immunofluorescence staining were performed to check for P2X$_3$ expression on DRG cells using the protocol described in section 2.2.3.17. With the exception that a commercial anti-P2X$_3$ antibody (Alomone Labs Ltd.; 1:300 dilution for Western blotting and 1:50 dilution for immunofluorescence) was applied as the primary antibody.

2.2.1.6 Testing of DRGs sensitivity to botulinum neurotoxin (BoNT)

Different concentrations of BoNT (0-1,000 nM) were added into rat DRGs cultures (P5, 6 DIV) and incubated for 24 hours at 37°C in 5% (v/v) CO_2. After 24 hours, the medium was removed from each well and the DRGs were harvested using Lithium dodecyl sulfate (LDS) buffer (60 µL per well). DRG cells were harvested at 3-5 days *in vitro* (DIV 3-5) by lysing the cells with 100 µL 2 x LDS buffer.

A 160 µg quantity of DRGs lysis protein sample (in a total volume of 20 µL) was added into each well of 4-12% precast Bis-Tris gel (Invitrogen). The gels were placed in an electrophoresis apparatus and submerged in electrophoresis buffer. The electrophoresis buffer was prepared using 50 mM MOPS, 50 mM Tris, pH 8.3, 1 mM ethylenediaminetetraacetic acid (EDTA) and 0.1% (w/v) SDS. The apparatus is attached to a power supply and a voltage of 200 V applied to the gel. The gels were allowed to run until the tracker dye had reached the bottom of the gel.

Proteins were transferred from the gel to a PVDF membrane at 250 mA for 2.5 hours. The membrane was blocked with 5% (w/v) TBSTM for one hour at room temperature. Mouse anti-SNAP-25 antibody (SMI-81, 1:1,000 dilution) was added at 4°C overnight. The membrane was washed three times with 1 x TBST for 5 min. HRP-labelled anti-mouse IgG (1:2,000 dilution) was added as secondary antibody and incubated at room temperature for one hour. The membrane was washed three times with 1 x TBST for 5 min and TMB (0.4 g/L) was added for visualisation. When the bands appeared, the membrane was washed with ddH_2O to stop the reaction. A picture was taken using the G:BOX Gel & Blot Imaging Series.

2.2.2 Immunisation protocols

2.2.2.1 Immunisation of rabbits using P2X$_3$-60/257-BSA and P2X$_3$-60/257-KLH

Two New Zealand white rabbits (designated CKPH and DARP) were immunised by subcutaneous injections, using 200 µg P2X$_3$-60-KLH (in 700 µL PBS) and 200 µg P2X$_3$-257-BSA (in 700 µL PBS) in µL complete Freund's adjuvant (Sigma), and subsequently boosted four times with 100 µg P2X$_3$-60-KLH (in 400 µL PBS) and 100 µg P2X$_3$-257-BSA (in 400 µL PBS) in 400 µL incomplete Freund's adjuvant (Sigma), each given on day 21 after the former injection. Approximately 5 mL peripheral blood was removed from the ear vein on day seven following each boost; this was carried out to assess the serum antibody titre. Rabbits were sacrificed on day seven after the final boost. The RNA was extracted from the spleen and bone marrow, followed by cDNA synthesis and scFv library building.

2.2.2.2 Immunisation of mice with P2X$_3$-60-BSA and P2X$_3$-257-BSA

Six BALB/c mice were immunised by intraperitoneal injections. Three mice were immunised with 50 µg P2X$_3$-60-BSA (in 200 µL PBS) and the other three with 50 µg P2X$_3$-257-BSA (in 200 µL PBS) in 200 µL complete Freund's adjuvant (Sigma), and subsequently boosted four times with 25 µg P2X$_3$-60-BSA (in 100 µL PBS) and 25 µg P2X$_3$-257-BSA (in 100 µL PBS) in 100 µL incomplete Freund's adjuvant (Sigma) respectively, each given on days 14 after the previous injection except the fourth boost, which was given on day 67 after the previous injection. Approximately 200 µL blood was removed from the cheek 7 days after each boost, to check the serum antibody titre. Mice were sacrificed on day seven after the final boost. The RNA was extracted from the spleen, followed by cDNA synthesis and scFv library building.

2.2.2.3 Immunisation of chickens with P2X$_3$-60-KLH and P2X$_3$-257-BSA

Three chickens were immunised by subcutaneous injections. One was immunised with 200 µg P2X$_3$-60-KLH (in 600 µL PBS) and the remaining two were immunised with 200 µg P2X$_3$-257-BSA (in 600 µL PBS), in 600 µL complete Freund's adjuvant (Sigma), and subsequently boosted four times with 100 µg P2X$_3$-60-KLH (in 300 µL PBS) and 25 µg P2X$_3$-257-BSA (in 300 µL PBS), respectively, in 300 µL incomplete Freund's adjuvant (Sigma), each given on day 21 after the former injection. Approximately 5 mL blood was removed from the wing vein on day seven after each boost, to check for serum antibody titre. One chicken died before any injection and another three chickens gave little response after the third boost. No RNA was extracted from chickens after they were sacrificed.

2.2.2.4 Serum screening and antibody titre

Sera from the immunised animals were analysed for the presence of antibodies to P2X$_3$. After each boost, an enzyme-linked immunosorbent assay (ELISA) was carried out. Maxisorb 96-well plates were coated with 100 µL per well neutravidin (2.5 µg/µL) at 37°C for one hour. This was followed by addition of 100 µL per well of 5 µg/µL P2X$_3$-257/60-biotin conjugates coated at 4°C overnight. Plates were then blocked with 5% (w/v) PBSTM (200 µL per well) at 37°C for one hour. The serum was made up in a range of dilutions (1:100-1:400,000) in 3% (w/v) PBSTM and incubated at 37°C for one hour. Then, HRP-labelled antibody (1:1,000 dilution, 100 µL per well) directed against each of the species (i.e. HRP-labelled anti-rabbit IgG, HRP-labelled anti-mouse IgG and HRP-labelled anti-chicken IgG) was added and incubated at 37°C for one hour. TMB (0.4 g/L, 100 µL per well) was added and incubated at room temperature for 10 min. After stopping the reaction by addition of1 M HCl (50 µL per well), the absorbances were read at 450 nm using a Safire 2 plate reader.

2.2.2.5 Competitive enzyme-linked immunosorbent assay (ELISA)

Maxisorb 96-well plates were coated with 100 µL per well of 2.5 µg/µL neutravidin for one hour at 37°C. This was followed by addition of 100 µL per well of 5 µg/µL $P2X_3$-257/60-biotin conjugates overnight at 4°C. Plates were blocked with 200 µL per well 5% (w/v) PBSTM for one hour at 37°C. A range of concentrations of $P2X_3$-257/60 free peptide (0-2 µg/mL) were prepared and mixed with a fixed concentration of serum. This mixture (100 µL per well) was incubated for one hour at 37°C. Then 100 µL per well of anti-IgG antibody (whole molecule) labelled with HRP was applied as the secondary antibody for one hour at 37°C. TMB (0.4 g/L) was then added (100 µL per well) and incubated at room temperature for 10 min. The reaction was stopped by addition of 50 µL per well of 1 M HCl. The absorbances of the wells were read at 450 nm using a Safire 2 plate reader.

2.2.3 Production of anti-$P2X_3$ polyclonal antibody

2.2.3.1 Protein A purification of polyclonal IgG antibody from rabbit serum

Two mL of Protein A-Sepharose® 4B (Sigma, #P9424-5ML) was added to a 20 mL column (VWR). The column was washed five times with 2 mL of PBS. A cap was placed on the base of the column. Debris in the serum was removed by centrifugation at 3,220 g for 10 min at 4°C before addition of to the column. Five mL of serum was added to the resin and mixed gently on a roller overnight at 4°C before addition of to the column. The flow-through was reapplied to the column. This process was repeated four times. The column was washed five times with 10 mL 1 x PBS (pH 7.5). The antibody was eluted with 10 mL of 100 mM glycine-HCl buffer (pH 2.5). Individual 1 mL fractions were collected in tubes containing 100 µL of 1 M Tris-HCl, pH 8.0, for pH neutralization. The column was washed with 20 mL of PBS (pH 7.5) and was stored at 4°C with 20% (v/v) ethanol. The eluted fractions were analysed by determining the

absorbances at 280 nm. The fractions which contained the eluted antibodies were then combined, washed and concentrated through buffer exchange against filtered 20 mL of PBS (pH 7.5) using 10,000 MWCO Viva spin columns (Sartorius, #VS0601). Protein concentration was determined by the BCA assay. The purified polyclonal antibody (1 mL, 39.27 mg/mL) was divided into 100 µL aliquots and stored at -20°C.

2.2.3.2 Purification of anti-P2X$_3$ polyclonal antibody using streptavidin-agarose

P2X$_3$-257-biotin (138 µg) was mixed with 90 mg purified rabbit IgG antibody in a volume of 300 µL (from section 2.2.2.1) on a roller overnight at 4°C. Two mL of high capacity streptavidin-agarose resin (Fisher, #PN20359) was added to a 20 mL column (VWR). The resin was washed five times with 2 mL of PBS. A cap was placed on the base of the column. The serum and P2X$_3$-257-biotin mixture, was incubated overnight, and then applied to the column. This was mixed on a roller at room temperature for one hour. The flow-through was reapplied to the column four times. A total of 30 mL of wash buffer (sterile-filtered PBS) was passed through the column and, subsequently, the retained protein was eluted with 100 mM glycine-HCl buffer (pH 2.5). Fractions of eluate were collected in micro-centrifuge tubes containing 150 µL of neutralisation buffer (2 M Tris-HCl, pH 8.5). This served to rapidly neutralise the highly acidic environment of the elution buffer, thereby, preventing denaturation of the eluted IgG fraction. Each of the fractions was quantified using the NanoDrop™ ND-1000 using the pre-programmed 'IgG' option (mass extinction coefficient of 13.7 at 280 nm). The fractions containing high concentrations of IgG were pooled, desalted on a 10,000 MWCO Viva spin column (Sartorius, #VS0601) against PBS and stored at -20°C until required for further use.

2.2.3.3 Determination of anti-P2X$_3$ polyclonal antibody concentration using the bicinchoninic acid (BCA) protein assay

A range of BSA concentrations (0-2,000 µg/µL) were prepared, based on the BCA kit protocol, for the protein standard curve. Four dilutions (1/5, 1/10, 1/20, 1/40) were made for unknown samples. Twenty five µL of BSA standards and unknown sample dilutions (in duplicate) were added into ELISA plate wells. Two hundred µL of Reagent A and Reagent B mixture (50:1) from the BCA kit was added into the wells and mixed gently on a plate shaker for 30 seconds. The plate was covered with tinfoil and incubated at 37°C for 30 min. The plate was placed on a bench to cool it to room temperature. The absorbances of the wells were measured at 562 nm using a Safire 2 plate reader. Protein concentrations of unknown samples were then calculated from the linear range of the standard curve.

2.2.3.4 SDS-PAGE analysis of anti-P2X$_3$ antibody purity

Purified polyclonal antibody (15 µL in PBS; 0.1 mg) was mixed with 5 µL of 4 x lithium dodecyl sulfate (LDS) loading buffer and was added into each well of a 4-12% (w/v) NuPAGE Bis-Tris gel. The gel was resolved at 170 volts until the blue tracker dye reached the bottom of gel (took approximately 1.5 hours). The gel was removed and stained with Coomassie Blue for one hour. Finally, the stained gels were destained overnight using Coomassie destain solution.

2.2.3.5 Western blotting (WB) and Immunofluorescent (IF) stain analysis of polyclonal anti-P2X$_3$ antibody specificity for P2X$_3$ expressed on root ganglion cells (DRGs)

2.2.3.5.1 Western blotting

After grown 3-5 days in 24-well tissue plate, DRG cells were harvested after grown and membrane proteins were enriched as described in section 2.2.4.3. A 160 µg quantity of DRGs membrane protein sample (in a total volume of 20

µL) was added into each well of 4-12% precast Bis-Tris gel (Invitrogen). The gel was resolved at 170 volts for about one hour until the blue tracker dye reached the bottom of the gel. The proteins on the gel were transferred to a PVDF membrane at 250 mA for 2.5 hours. The membrane was blocked in 5% (w/v) TBSTM for one hour at room temperature. Purified polyclonal anti-P2X$_3$ antibody was used as the primary antibody and incubated overnight at 4°C. The membrane was washed three times with TBST for 5 min. HRP-labelled anti-rabbit IgG antibody (1:2,000 dilution) was added as secondary antibody and incubated at room temperature for 1 hour. The PVDF membrane was washed three times with TBST for 5 min and then developed by addition of 1 mL of TMB (0.4 g/L) to the membrane until the bands appeared. The membrane was washed with ddH$_2$O to stop the reaction. An image was taken using the G:BOX Gel & Blot Imaging Series.

2.2.3.5.2 Immunofluorescent staining

DRG cells were cultured in a 24-well tissue plate for 5-7 days. They were then washed three times with Dulbecco's phosphate buffer saline (D-PBS, lacking Mg^{2+} and Ca^{2+}) and fixed using 3.7% (v/v) paraformaldehyde for 20 min at room temperature. The plate was washed three times with D-PBS, and then blocked with 1% (w/v) BSA in D-PBS for one hour at room temperature. The blocking solution was removed. Polyclonal anti-P2X$_3$ antibody was added as primary antibody and incubated at room temperature for one hour. The plate was washed three times with D-PBS, followed by addition of the secondary antibody which was Alexa Fluor-488-labelled goat anti-rabbit IgG (1: 200 dilution). After washing three times with D-PBS, the cells were imaged using an Olympus IX71 microscope or a inverted confocal microscope (Leica Dmire 2) with a CCD camera. The images were then analysed using the Image-Pro Plus 5.1 or Leica confocal software. A negative control was included which contained rabbit anti-goat IgG (1:1,000 dilution) as primary antibody, followed by secondary antibody Alexa Fluor-488-labelled goat anti-rabbit IgG (1: 200 dilution).

2.2.4 Generation of anti-P2X$_3$ scFv library

2.2.4.1 Extraction and isolation of total RNA from immunised animals

The inner surface of a Gelaire BSB 4 laminar flow hood was sprayed with both 70% (v/v) IMS and RNaseZAP (Sigma, #R2020) to prevent RNA degradation by RNase. The spleens and bone marrow from rabbits, and the spleens from mice were removed and transferred into a 50 mL 'RNase-free' tube containing 10 mL TRIzol ™ reagent. A homogenizer, previously autoclaved and baked overnight at 60°C, was used to homogenize the spleen/bone marrow. The homogenized tissue was transferred to a 85 mL polypropylene Oakridge 'RNase-free' tube and incubated for 5 min at room temperature, to allow complete dissociation of nucleoprotein complexes. Chloroform (2 mL) was then added to the tube. The tube was shaken vigorously for 15 seconds and then incubated for 15 min at room temperature. After centrifugation (Eppendorf centrifuge 5810R) at 19,000 g for 20 min at 4°C, the suspension was separated into 3 distinct layers. The top aqueous and transparent layer which contains RNA, was carefully transferred into a new 85 mL polycarbonate Oakridge 'RNase-free' tube and precipitated by addition of 5 mL of isopropanol. This tube was incubated for 10 min at room temperature, and then centrifuged (Eppendorf centrifuge 5810R) at 19,000 g for 25 min at 4°C. The supernatant was carefully removed and the white RNA pellet was washed with 30 mL 75% (v/v) ethanol by centrifugation at 19,000 g for 10 min at 4°C. The RNA pellet was air-dried in the laminar hood and then resuspended in 800 µL of molecular grade water. RNA concentrations were measured with the NanoDrop™ spectrophotometer ND-1000 (Thermo Fisher Scientific, USA).

2.2.4.2 Reverse transcription of total RNA to cDNA

Total RNA was reverse transcribed into cDNA using Superscript III Reverse Transcriptase kit (Invitrogen, USA). A '20 X mixture 1' was set up on ice and then 20 X 10 µL aliquots were made in sterile PCR tubes. Mixture 1 was

incubated at 65°C on Biometra T$_{GRADIENT}$ PCR machine (Labrepco, USA) for 5 min. At the same time, a '20 x mixture 2' was set up. Mixture 1 was placed on ice. Ten µL of mixture 2 was added to 10 µL aliquots of mixture 1 and incubated at 50°C for 50 min, and then 85°C for 5 min. Five µL of RNase ™ H was added into each of the 20 µL reactions and incubated at 37°C for 20 min. The cDNA samples were stored at -20°C for subsequent light chain and heavy chain amplification.

The following components were used for mixture 1:

Mixture 1 Component	10 µL Volume	Conc. In 10 µL reaction
Total RNA	x µL	5 µg/reaction
Oligo (dT) primer	1 µL	0.5 µg/reaction
dNTP mix	1 µL	1 mM
Molecular grade H$_2$O	(8-x) µL	N/A

The following components were used for mixture 2:

Mixture 2 Component	10 µL Volume	Conc. In 10 µL reaction
10xRT Buffer	2 µL	2x
MgCl$_2$	4 µL	2.5 mM
DTT	2 µL	20 mM
RNase Out	1 µL	1 U/µL
Superscript III enzyme	1 µL	200 U/µL

2.2.4.3 PCR primers for the amplification of anti-P2X$_3$ scFv (pComb series)

2.2.4.3.1 PCR primers for amplification of rabbit anti-P2X$_3$ scFv

All primers listed below were synthesized by Eurofins-MWG-Operon (318 Worple Road, Raynes Park, London, SW20 8QU).

Vκ 5′ Sense Primers

RSCVK1	5′ GGG CCC AGG CGG CCG AGC TCG TGM TGA CCC AGA CTC CA 3′
RSCVK2	5′ GGG CCC AGG CGG CCG AGC TCG ATM TGA CCC AGA CTC CA 3′
RSCVK3	5′ GGG CCC AGG CGG CCG AGC TCG TGA TGA CCC AGA CTG AA 3′

Vκ 3′ Reverse Primers, long linker

(linker amino acid sequence: SSGGGGSGGGGGGSSRSS)

RKB9J1o-BL	5′ GGA AGA TCT AGA GGA ACC ACC CCC ACC ACC GCC CGA GCC ACC GCC ACC AGA GGA TAG GAT CTC CAG CTC GGT CCC 3′
RKB9Jo-BL	5′ GGA AGA TCT AGA GGA ACC ACC CCC ACC ACC GCC CGA GCC ACC GCC ACC AGA GGA TAG GAT CTC CAG CTC GGT CCC 3′
RKB42Jo-BL	5′ GGA AGA TCT AGA GGA ACC ACC CCC ACC ACC GCC CGA GCC ACC GCC ACC AGA GGA TTT GAC SAC CAC CTC GGT CCC 3′

V$_H$ 5′ Sense Primers

RSCVH1	5′ GGT GGT TCC TCT AGA TCT TCC CAG TCG GTG GAG GAG TCC RGG 3′
RSCVH2	5′ GGT GGT TCC TCT AGA TCT TCC CAG TCG GTG AAG GAG TCC GAG 3′
RSCVH3	5′ GGT GGT TCC TCT AGA TCT TCC CAG TCG YTG GAG GAG TCC GGG 3′
RSCVH4	5′ GGT GGT TCC TCT AGA TCT TCC CAG SAG CAG CTG RTG GAG TCC GG 3′

<u>V$_H$ 3′ reverse primers</u>

RSCG-B	5′ CCT GGC CGG CCT GGC CAC TAG TGA CTG AYG GAG CCT TAG GTT GCC C 3′

<u>Overlap extension primers</u>

RSC-F (sense)	5′ GAG GAG GAG GAG GAG GAG GCG GGG CCC AGG CGG CCG AGC TC 3′
RSC-B (reverse)	5′ GAG GAG GAG GAG GAG GAG CCT GGC CGG CCT GGC CAC TAG TG 3′

<u>pComb rabbit anti-P2X$_3$ scFv primer combinations</u>

<u>Variable Heavy chain combinations</u>

Heavy chain	Forward	Reverse
V$_H$1	RSCVH1	RSCG-B
V$_H$2	RSCVH2	RSCG-B
V$_H$3	RSCVH3	RSCG-B
V$_H$4	RSCVH4	RSCG-B

<u>Variable kappa light chain combinations</u>

Light chain	Forward	Reverse
VK1	RSCVK1	RKB9J10-BL
VK2	RSCVK1	RKB9J0-BL
VK3	RSCVK1	RKB42J0-BL
VK4	RSCVK2	RKB9J10-BL
VK5	RSCVK2	RKB9J0-BL
VK6	RSCVK2	RKB42J0-BL
VK7	RSCVK3	RKB9J10-BL
VK8	RSCVK3	RKB9J0-BL
VK9	RSCVK3	RKB42J0-BL

2.2.4.3.2 PCR primers for amplification of mouse anti-P2X₃ scFv

All primers listed below were synthesized by Eurofins-MWG-Operon (318 Worple Road, Raynes Park, London, SW20 8QU).

<u>V$_H$ 5′ Sense Primers</u>

MSCVH1	5′ GGT GGT TCC TCT AGA TCT TCC CTC GAG GTR MAG CTT CAG GAG TC 3′
MSCVH2	5′ GGT GGT TCC TCT AGA TCT TCC CTC GAG GTB CAG CTB CAG CAG TC 3′
MSCVH3	5′ GGT GGT TCC TCT AGA TCT TCC CTC GAG GTG CAG CTG AAG SAS TC 3′
MSCVH4	5′ GGT GGT TCC TCT AGA TCT TCC CTC GAG GTC CAR CTG CAA CAR TC 3′
MSCVH5	5′ GGT GGT TCC TCT AGA TCT TCC CTC GAG GTY CAG CTB CAG CAR TC 3′
MSCVH6	5′ GGT GGT TCC TCT AGA TCT TCC CTC GAG GTY CAR CTG CAG CAG TC 3′
MSCVH7	5′ GGT GGT TCC TCT AGA TCT TCC CTC GAG GTC CAC GTG AAG CAG TC 3′
MSCVH8	5′ GGT GGT TCC TCT AGA TCT TCC CTC GAG GTG AAS STG GTG GAA TC 3′
MSCVH9	5′ GGT GGT TCC TCT AGA TCT TCC CTC GAG GTG AWG YTG GTG GAG TC 3′
MSCVH10	5′ GGT GGT TCC TCT AGA TCT TCC CTC GAG GTG CAG SKG GTG GAG TC 3′
MSCVH11	5′ GGT GGT TCC TCT AGA TCT TCC CTC GAG GTG CAM CTG GTG GAG TC 3′
MSCVH12	5′ GGT GGT TCC TCT AGA TCT TCC CTC GAG GTG AAG CTG ATG GAR TC 3′
MSCVH13	5′ GGT GGT TCC TCT AGA TCT TCC CTC GAG GTG CAR

	CTT GTT GAG TC 3′
MSCVH14	5′ GGT GGT TCC TCT AGA TCT TCC CTC GAG GTR AAG CTT CTC GAG TC 3′
MSCVH15	5′ GGT GGT TCC TCT AGA TCT TCC CTC GAG GTG AAR STT GAG GAG TC 3′
MSCVH16	5′ GGT GGT TCC TCT AGA TCT TCC CTC GAG GTT ACT CTR AAA GWG TST G 3′
MSCVH17	5′ GGT GGT TCC TCT AGA TCT TCC CTC GAG GTC CAA CTV CAG CAR CC 3′
MSCVH18	5′ GGT GGT TCC TCT AGA TCT TCC CTC GAG GTG AAC TTG GAA GTG TC 3′
MSCVH19	5′ GGT GGT TCC TCT AGA TCT TCC CTC GAG GTG AAG GTC ATC GAG TC 3′
MSCJL-B	5′ GGA AGA TCT AGA GGA ACC ACC GCC TAG GAC AGT CAG TTT GG 3′

V_H 3′ Reverse Primers

MSCM-B	5′ CCT GGC CGG CCT GGC CAC TAG TGA CAT TTG GGA AGG ACT GAC TCT C 3′
MSCG3-B	5′ CCT GGC CGG CCT GGC CAC TAG TGA CAG ATG GGG CTG TTG TTG T 3′
MSCG1ab-B	5′ CTG GCC GGC CTG GCC ACT AGT GAC AGA TGG GGS TGT YGT TTT GGC 3′

MSCVK-1	5′ GGG CCC AGG CGG CCG AGC TCG AYA TCC AGC TGA CTC AGC C 3′
MSCVK-2	5′ GGG CCC AGG CGG CCG AGC TCG AYA TTG TTC TCW CCC AGT C 3′
MSCVK-3	5′ GGG CCC AGG CGG CCG AGC TCG AYA TTG TGM TMA CTC AGT C 3′
MSCVK-4	5′ GGG CCC AGG CGG CCG AGC TCG AYA TTG TGY TRA CAC AGT C 3′
MSCVK-5	5′ GGG CCC AGG CGG CCG AGC TCG AYA TTG TRA TGA CMC AGT C 3′
MSCVK-6	5′ GGG CCC AGG CGG CCG AGC TCG AYA TTM AGA TRA MCC AGT C 3′
MSCVK-7	5′ GGG CCC AGG CGG CCG AGC TCG AYA TTC AGA TGA YDC AGT C 3′
MSCVK-8	5′ GGG CCC AGG CGG CCG AGC TCG AYA TYC AGA TGA CAC AGA C 3′
MSCVK-9	5′ GGG CCC AGG CGG CCG AGC TCG AYA TTG TTC TCA WCC AGT C 3′
MSCVK-10	5′ GGG CCC AGG CGG CCG AGC TCG AYA TTG WGC TSA CCC AAT C 3′
MSCVK-11	5′ GGG CCC AGG CGG CCG AGC TCG AYA TTS TRA TGA CCC ART C 3′
MSCVK-12	5′ GGG CCC AGG CGG CCG AGC TCG AYR TTK TGA TGA CCC ARA C 3′
MSCVK-13	5′ GGG CCC AGG CGG CCG AGC TCG AYA TTG TGA TGA CBC AGK C 3′
MSCVK-14	5′ GGG CCC AGG CGG CCG AGC TCG AYA TTG TGA TAA CYC AGG A 3′
MSCVK-15	5′ GGG CCC AGG CGG CCG AGC TCG AYA TTG TGA TGA CCC AGW T 3′
MSCVK-16	5′ GGG CCC AGG CGG CCG AGC TCG AYA TTG TGA TGA

	CAC AAC C 3′
MSCVK-17	5′ GGG CCC AGG CGG CCG AGC TCG AYA TTT TGC TGA CTC AGT C 3′

Vκ light chain 3′ reverse primers, long linker

MSCJK12-BL	5′ GGA AGA TCT AGA GGA ACC ACC CCC ACC ACC GCC CGA GCC ACC GCC ACC AGA GGA TTT KAT TTC CAG YTT GGT CCC 3′
MSCJK4-BL	5′ GGA AGA TCT AGA GGA ACC ACC CCC ACC ACC GCC CGA GCC ACC GCC ACC AGA GGA TTT TAT TTC CAA CTT TGT CCC 3′
MSCJK5-BL	5′ GGA AGA TCT AGA GGA ACC ACC CCC ACC ACC GCC CGA GCC ACC GCC ACC AGA GGA TTT CAG CTC AGC TT GGT CCC 3′

Vκ light chain 3′ reverse primers

MSCJK5-B	5′ GGA AGA TCT AGA GGA ACC ACC TTT CAG CTC CAG CTT GGT CCC 3′
MSCJK4-B	5′ GGA AGA TCT AGA GGA ACC ACC TTT TAT TTC CAA CTT TGT CCC 3′
MSCJK12-B	5′ GGA AGA TCT AGA GGA ACC ACC TTT KAT TTC CAG YTT GGT CCC 3′

λ light chain 5′ sense primers

MSCVL-1	5′ GGG CCC AGG CGG CCG AGC TCG ATG CTG TTG TGA CTC AGG AAT C 3′

<u>λ light chain 3′ back reverse primers</u>

MSCJL-BL	5′ GGA AGA TCT AGA GGA ACC ACC CCC ACC ACC GCC CGA GCC ACC GCC ACC AGA GGA GCC TAG GAC AGT CAG TTT GG 3′

<u>Overlap Extension Primers</u>

RSC-F (sense)	5′ GAG GAG GAG GAG GAG GAG GCG GGG CCC AGG CGG CCG AGC TC 3′
RSC-B (reverse)	5′ GAG GAG GAG GAG GAG GAG CCT GGC CGG CCT GGC CAC TAG TG 3′

2.2.4.4 Amplification of antibody variable domain genes using pComb3X series primers

The components for a 1x reaction with 50 µL total volume were as follows:

Component	50 µL Volume	Conc. in 50 µL
GoTaq Buffer (5 x)	10.0 µL	1 x
V_L/V_H sense Primer	0.5 µL	60 pM
V_H/V_L reverse Primer	0.5 µL	60 pM
$MgCl_2$	3.0 µL	1.5 mM
cDNA	1.0 µL	0.5 µg
dNTP	1.0 µL	0.2 mM
H_2O	33.75 µL	N/A
GoTaq ™ Polymerase	0.25 µL	5 U/µL

The PCR for the amplification was performed using a Biometra $T_{GRADIENT}$ PCR machine with the following conditions:

Stage	Temperature (°C)	Time (seconds)
1 (1 cycle)	94	120
2 (25 cycles)	94	15
	56	30
	72	90
3 (1 cycle)	72	600
	4	Pause

2.2.4.5 Purification of V_H and V_L variable gene fragments using a NucleoSpin® Extract II kit

After each V_H and V_L variable gene fragment was obtained via PCR, V_H and V_L amplifications were ethanol-precipitated with 10% (w/v) 3 M sodium acetate (pH 5.5) and twice the total sample volume of 100% ethanol. The solution was then incubated overnight at -20°C and subsequently centrifuged (Eppendorf centrifuge 5810R) at 13,220 g for 15 min at 4°C. The ethanol supernatant was discarded and the pellet was washed by addition of 750 µL of 70% (v/v) ice cold ethanol. It was then centrifuged (Eppendorf centrifuge 5810R) at 13,220 g for 4 min at 4°C. The pellet was then allowed to air-dry (but not over dry) before dissolving in 20 µL of molecular grade H_2O.

V_H and V_L amplifications were loaded on a 1% (w/v) agarose gel and run at 60 volts using 1 × TAE buffer until single bands at 386-440 bp (V_H chain) and 375-402 bp (V_L chain) were observed and had separated clearly from non-specific bands. Both V_H and V_L bands were then separated using sterile scalpels and transferred into a new sterile 1.5 mL micro-centrifuge tubes. For each 100 mg agarose gel, 200 µL buffer NT was added. The mixture was incubated at 50°C for approximately 10 min until the gel had completely dissolved. The mixture was then transferred to a NucleoSpin® extract column which was placed into a clean collection tube and was then centrifuged

(Eppendorf centrifuge 5810R) at 13,220 g for 1 min to remove residual buffer. The 'flow-through' was discarded and the column was washed with 700 µL of 'buffer NT3' by centrifugation at 13,220 g for 1 min. After discarding the 'flow-through' the column was centrifuged (Eppendorf centrifuge 5810R) at 13,220 g for 2 min to remove residual buffer NT3. Finally, DNA was eluted from the column using 30 µL molecular grade H_2O. The concentration of purified DNA was measured using the Nanodrop™ ND-1000.

2.2.4.6 Splice by Overlap extension (SOE) polymerase chain reaction (PCR)

The V_H and V_L purified fragments were joined by SOE-PCR via a long glycine-serine linker $(Gly_4Ser)_3$ to produce a fragment of approximately 800 bp.

The following components were used for SOE-PCR:

RSC-F (sense)	GAG GAG GAG GAG GAG GAG GCG GGG CCC AGG CGG CCG AGC TC
RSC-B (reverse)	GAG GAG GAG GAG GAG GAG CCT GGC CGG CCT GGC CAC TAG TG

Component	50 µL Volume	Conc. in 50 µL reaction
GoTaq Buffer (5 x)	10 µL	1 x
RSC-F	0.5 µL	60 Pm
RSC-B	0.5 µL	60 pM
V_H chain	2.5 µL	100 ng/reaction
V_L chain	2.5 µL	100 ng/reaction
dNTP	1 µL	0.2 mM
$MgSO_4$	2 µL	2 mM
H_2O	30.75 µL	N/A
Go ™ Taq	0.25 µL	5 U/ µL

The SOE-PCR was performed using Biometra $T_{GRADIENT}$ PCR machine under the following conditions:

Stage	Temperature (°C)	Time (seconds)
1 (1 cycle)	94	300
2 (25 cycles)	94	15
	56	15
	72	120
2 (1 cycle)	72	600
	4	Pause

2.2.4.7 *Sfi*I restriction digestion of purified SOE-PCR fragment and ligation into pComb3XSS vector

The SOE product and pComb3XSS vector were digested using the *Sfi*I restriction enzyme which enables the unidirectional cloning of the scFv fragment into the pComb3XSS phage display vector. *Sfi*I recognises 8 bases which are interrupted by 5 non-recognised nucleotides (5′ggccnnnnnggcc3′). The *Sfi*I sites on both forward and reverse SOE primers are different and similar to that of the *Sfi*I sites on the pComb3XSS phage display vector, thus allowing unidirectional cloning of the scFv gene into phagemid vector. Digestion was carried out for 5 hours at 50°C on a heating block.

Components of SOE product *Sfi*I digestion:

Component	Volume
SOE product (10 μg)	60 μL
10 x buffer 2	15 μL
100 x BSA	1.5 μL
H$_2$O	58.5 μL
*Sfi*I	15 μL
Total volume	150 μL

Components of pComb3XSS vector *Sfi*I digestion:

Component	Volume
pComb3XSS vector (40 μg)	44 μL
10 x Buffer 2	20 μL
100 x BSA	2 μL
H₂0	114 μL
*Sfi*I	20 μL
Total volume	200μL

After 5 hours incubation at 50°C, the *Sfi*I digested pComb3XSS (~ 3,400 bp) and SOE products (800 bp) were ethanol-precipitated and gel-purified following the protocol in section 2.2.3.5. The restriction digested scFv gene was then ligated into the pComb3XSS vector with the following conditions and incubated on a bench at room temperature overnight.

Components of *Sfi*I digested SOE and pComb3XSS vector ligation:

Component	Volume
5 x Ligase buffer	20 μL
Digested pComb3X vector (1.4 μg)	12 μL
Digested scFv gene (700 ng)	4 μL
H₂O	54 μL
T₄ DNA ligase	10 μL
Total Volume	100 μL

The ligated samples were ethanol-precipitated and gel-purified following the protocol in section 2.2.3.5. For scFv library construction, 30 μL of the ligation mixture was used.

2.2.4.8 Electro-transformation of scFv-containing plasmid into XL-1 Blue *E. coli* cells

The ligated products were transformed into electrocompetent XL-1 Blue cells by Gene Pulser Xcell ™ electroporation at 25 μF, 1.25 kV and 200 Ω for the

gene pulse controller. The 30 μL ligation for each library was split into three aliquots of 10 μL. After thawing on ice, 100 μL of the competent cells was quickly added to each of the ice cold ligated product aliquots, mixed by pipetting up and down once gently and incubated on ice for 30 seconds. The mixture was then transferred to a chilled 0.2 cm electroporation cuvette and placed in the 'ShockPod'. After pulsing the cuvette, the transformant was immediately flushed with 1 mL of 37°C pre-warmed SOC medium, using a sterile tip. A further 2 mL of SOC media were added to flush the cuvette. The processes between applying the pulse and transferring the cells to growth media must be as rapid as possible to allow for better recovery of XL-1 Blue cells. The rescued ligations for both libraries (spleen and bone marrow) were then incubated for 1 hour at 250 rpm at 37°C. Following incubation, the rescued transformants were centrifuged (HermLe Z233MK-2 refrigerated centrifuge) down for 10 min at 3,220 g at 4°C. The pellets from each library were resuspended in 1 mL of SB medium which were then plated out on LB agar plates containing 100 μg/mL carbenicillin. A negative control was also provided by plating the XL-1 Blue cells containing no plasmid onto a LB agar plate with 100 μg/mL carbenicillin. All agar plates were incubated overnight at 37°C and then scraped into SB medium containing 20% (v/v) glycerol at -80°C for long-term storage.

2.2.4.9 Rescue of anti-P2X$_3$ scFv-displaying phage

The scraped library (200 μL) (section 2.2.3.8) was inoculated into 200 mL of SB medium (50 μg/mL carbenicillin and 10 μg/mL tetracycline) for both of the rabbit scFv libraries (spleen and born marrow). The culture was left to grow by shaking at 37°C for one hour at 220 rpm. More carbenicillin was then added to a final concentration of 100 μg/mL. When the OD reached 0.6, 200 μL of commercial M13K07 helper phage (ISIS, # N0315S) was added to each of the libraries, and left static at 37°C for 20 min. The culture was then grown in a rotating incubator at 37°C for two hours at 220 rpm. Kanamycin was then added to a final concentration of 70 μg/mL. The culture was then left to grow overnight at 37°C at 250 rpm.

2.2.4.10 Enrichment of the phage library via biopanning against immobilised antigens

2.2.4.10.1 Immunotube-based biopanning

2.2.4.10.1.1 Phage preparation

A Nunc-immunotube was coated overnight at 4°C with 500 µL of dilution of P2X$_3$-biotin in PBS solution (Table 2.2.3.10.1), and blocked with 3% (w/v) BSA-PBS. This was left for 2 hours at 37°C. Meanwhile, the overnight-rescued phage-induced libraries were pelleted by centrifuging (HermLe Z233MK-2 refrigerated centrifuge) at 15,000 g for 20 min with the 'brake-on' option. The phage supernatants were decanted into 85 mL sterile polycarbonate Oakridge tubes, to which 4 g of PEG and 3 g of NaCl were added for every 100 mL of phage supernatants. The tubes were placed in a 37°C shaking incubator for 5-10 min at 220 rpm to ensure all the PEG and NaCl was dissolved. The tubes were placed on ice and left in a cold room for 45 min. Subsequently, the PEG-precipitated phage were harvested by centrifugation (HermLe Z233MK-2 refrigerated centrifuge) at 19,000 g for 20 min with the 'brake-off' option and the supernatant was decanted carefully. The phage pellets were thoroughly resuspended in 1 mL of 1% (w/v) BSA-PBS and 0.1% (w/v) KLH-PBS, and transferred into 2 mL centrifuge tubes. They were centrifuged (Eppendorf centrifuge 5810R) at 13,220 g for 5 min at 4°C to pellet excess bacterial cells and the phage supernatants were transferred into clean 1.5 mL micro-centrifuge tubes kept on ice.

2.2.4.10.1.2 Biopanning using immunotubes

The process was continued using blocked immunotubes (Table 2.8). The blocking solution was decanted out of the immunotube and 150 µL input phage incubated at 37°C for two hours. The phage solution was decanted out, the immunotube washed five times with PBST (4 mL) and then five times with

PBS (4 mL). To elute the bound phage, freshly prepared 10 mg/ml trypsin was added into the washed immunotube at 500 µL volume and incubated at 37°C for 30min. The trypsin was vigorously pipetted up and down for 10 times. The trypsin eluted phage were then infected to 5mL XLI-Blue (OD 600nm of 0.4-0.6) and incubated for 15 min at room temperature. Subsequently, 5 mL SB media was added containing 2 µL of 100 mg/mL carbenicillin and 12 µL of 5 mg/mL tertracycline. Ten mL of phage infected XLI-Blue culture were incubated in the rotating incubator at 220 rpm for 1.5 hours at 37°C followed by centrifugation (HermLe Z233MK-2 refrigerated centrifuge) at 3,220 g for 10min at 4°C. The supernatant was discarded and 500 µL SB was added to resuspend the pellet. Finally, five LB agar plates (containing 100 µg/mL carbenicillin) with 100 µL of the phage-infected XLI-Blue suspension were plated out and incubated at 37°C overnight.

Table 2.8 Culture volumes, concentration of coating antigen and competitive peptide, and wash times for each round of immunotube-based panning of the rabbit anti-P2X$_3$ scFv library.

Round number	Culture volume (mL)	[P2X$_3$-257-biotin] nM	Helper phage (µL)	Washing
1	200	400	400	PBSTx5, PBSx5
2	100	200	200	PBSTx5, PBSx5
3	100	40	200	PBSTx10, PBSx10
4	100	20	200	PBSTx10, PBSx10

* Phage was dissolved in sterile 1% (w/v) BSA and 0.1% (w/v) KLH to 'deplete' potential cross reacting scFvs.

2.2.4.10.1.3 Output and input titres

To determine the output titre, 2 µL of phage-infected bacteria were diluted [sample after infecting into XLI-Blue (OD600 nm of ~0.5) and addition of 5mL SB media] in 400 µL SB media to make the 1/100 dilution. Two LB agar plates (containing 100 µg/mL carbenicillin) were plated with 100 uL of the 1 in 100 dilution of the culture. Two further LB agar plates (containing 100 µg/mL carbenicillin) were plated with 10 µL of the 1:100 dilution of the culture. Plates were labelled "output titre" and incubated stationary at 37°C overnight.

To determine the input titre, phage were diluted to 1:1,000,000, 1:10,000,000 and 1:100,000,000, and 1 µL of each dilution was infected into 50 µL XLI-Blue cells (OD 600 nm of 0.4-0.6) and incubated at room temperature for 15 min. Each dilution (in duplicate) was plated onto LB agar plates (containing 100 µg/mL carbenicillin) and incubated at 37°C overnight.

2.2.4.10.2 Biopanning using streptavidin-labelled magnetic beads

2.2.4.10.2.1 Phage preparation

Streptavidin-labelled magnetic beads (BioLabs; 2 x 20 µL) were blocked in 1.5 mL tubes by filling with 5 % (w/v) PBSM and incubated overnight at 4°C. The following day, the overnight-rescued phage-induced libraries were pelleted by centrifuging (HermLe Z233MK-2 refrigerated centrifuge) at 15,000 g for 20 min (brake-on). The phage supernatants were decanted into 85 mL sterile polycarbonate Oakridge tubes, to which, 4 g of PEG and 3 g of NaCl were added for every 100 mL of phage supernatant. The polycarbonate Oakridge tubes were placed in a 37°C shaking incubator for 5-10 min at 220 rpm to ensure all the PEG and NaCl has dissolved. The tubes were placed in ice and left in the cold room for 45 min. Then the PEG-precipitated phage were harvested by centrifugation (HermLe Z233MK-2 refrigerated centrifuge) at 19,000 g in for 20 min using the 'brake-off' option and the supernatant was decanted carefully. The phage pellets were thoroughly resuspended in 1 mL of

1% (w/v) BSA-PBS and 0.1% (w/v) KLH-PBS to 'deplete' potential cross reacting phage, and transferred into 2 mL centrifuge tubes. They were then centrifuged (Eppendorf centrifuge 5810R) at 13,220 g for 5 min at 4°C to pellet excess bacterial cells. The supernatant was transferred into a sterile 1.5 mL tube on ice.

2.2.4.10.2.2 Streptavidin-labelled magnetic bead-based biopanning

The blocked beads were washed three times with 1 x PBST, followed by three times with 1 x PBS. Input phage (180 µL) were incubated in one tube with washed beads at 37°C for 15 min to deplete the non-specific binding phage. The beads were then pelleted using a Magnetic Separation Rack (New England Biolabs Ltd.), and 150 µL depleted phage solution was taken out and incubated with 50 µL of a serial dilution of P2X$_3$-biotin (Table 2.9) at 37°C for 45 min. The phage and P2X$_3$-biotin mixture were than added into 1.5 mL tube with blocked beads and incubated at 37°C for 15 min. The beads were washed five or ten times (Table 2.9) with PBST, followed by PBS. To elute the bound phage, the beads were resuspended in 500 µL freshly prepared trypsin (10 mg/ml) and incubated for 30 min at 37°C. The beads were pelleted and the phage solution was taken out, infected into 5 mL XLI-Blue (OD 600 nm of 0.4-0.6) and incubated at room temperature for 15 min. Following this, 5 mL SB media containing 2 µL 100 mg/mL carbenicillin and 12 µL 5 mg/mL tertracycline was added. A 10 mL culture was shaken at 220 rpm for 1.5 hours at 37°C followed by centrifugation at 3,220 g for 10 min at 4°C. The supernatant was discarded and 500 µL of SB was added to resuspend the pellet. Finally, five LB agar plates with 100 µL suspension of phage-infected XLI-Blue, were incubated at 37°C overnight.

Table 2.9 Culture volumes, concentration of coating antigen and wash times for each round of magnetic bead-based panning of the rabbit anti-P2X$_3$ scFv library.

Round number	Culture volume (mL)	[P2X$_3$-257-biotin] nM	Helper phage (µL)	Washing
1	200	400	400	PBSTx5, PBSx5
2	100	200	200	PBSTx5, PBSx5
3	100	40	200	PBSTx10, PBSx10
4	100	20	200	PBSTx10, PBSx10

* Phage was dissolved in sterile 1% (w/v) BSA and 0.1% (w/v) KLH to 'deplete' potential cross reacting scFvs.

2.2.4.10.1.3 Output and input titres

To determine the output titre, 2 µL of phage infected bacteria was diluted [sample after infecting into XLI-Blue (OD600 nm of ~0.5) and addition of 5mL SB media] in 400 µL SB media to make the 1/100 dilution. Two LB agar plates (containing 100 µg/mL carbenicillin) were plated with 100ul of the 1 in 100 dilution of the culture. Two further LB agar plates (containing 100 µg/mL carbenicillin) were plated with 10 µL of the 1/100 dilution of the culture. Plates were labelled pan output titre plates and incubated stationary at 37°C O/N.

To determine the input titre, phage were diluted to 1:1,000,000, 1:10,000,000 and 1:100,000,000, and 1 µL of each dilution was infected into 50 µL XLI-Blue (OD 600 nm of 0.4-0.6) and incubated at room temperature for 15 min. Each dilution (in duplicate) was plated onto LB agar plates (containing 100 µg/mL carbenicillin) and incubated at 37°C overnight.

2.2.4.11 Polyclonal phage ELISA

A 96-well plate (Maxisorp™, Nunc) was coated with 2 µg/mL P2X$_3$-biotin, P2X$_3$-BSA, P2X$_3$-BTG, neutravidin, BSA, BTG and KLH, incubated overnight at 4°C. The coating solution was decanted and the plate was blocked with 5% (w/v) PBSM for one hour at 37°C. The phage inputs for each round of panning were diluted 1:1 with 3% (w/v) PBSTM. Then 100 µL of each diluted phage was added to a designated well of the ELISA plate and incubated for one hour at 37°C. M13K07 helper phage and 3% (w/v) PBSTM were also diluted and added to certain wells as negative controls to identify any background binding. After washing the plate three times with PBST and three times with PBS, 100 µL of 1:2,000 dilution of a HRP-conjugated anti-M13 antibody (GE Healthcare Life Sciences) in PBST was added to each well as secondary antibody and incubated for one hour at 37°C. After washing the plate three times with PBST and three times with PBS, 100 µL of TMB substrate (0.4 g/L) was added and the colour was allowed to develop for 15 min at room temperature. Finally, the reaction was stopped by applying 50 µL of 1 M HCl. The absorbances of the wells were read at 450 nm using a Safire 2 plate reader.

2.2.4.12 Infection of the eluted phage output into *E. coli* Top 10 F′ (non-suppressor strain) for soluble expression

A 5 µL aliquot of output phage, from the last round of panning, was infected into 5 mL of Top 10 F′ cells (OD 600 nm of ~0.5) containing 12 µg/mL tetracycline and incubated for 15 min at room temperature. Subsequently, 1:1,000,000, 1:10,000,000 and 1:100,000,000 dilutions were prepared for obtaining single colonies for further analysis. Each dilution (in duplicate) was plated on LB agar plates (containing 100 µg/mL carbenicillin) and incubated at 37°C overnight.

2.2.4.13 Direct and inhibition ELISA of solubly expressed scFv fragments

Single colonies of scFv fragments were picked from overnight plates, as described in section 2.2.3.12, and inoculated into 96-well plates containing 100 µL SB media per well (containing 50 µg/mL of carbenicillin) and were grown overnight at 220 rpm at 37°C (stock plates). The 96-well stock plates were then subcultured into fresh SB media (150 µL) containing 1 x 505 [0.5% (v/v) glycerol, 0.05% (w/v) glucose, sterile-filtered], 1mM $MgSO_4$ and 100 µg/mL carbenicillin (subcultured plates). For the stock plates, glycerol was added to a final concentration of 20% (v/v) and kept at -80°C for long-term storage. The subcultured plates were incubated at 37°C and rotated at 200 rpm until the cells appeared to be cloudy (OD 600 nm of 0.4-0.6). Expression was then induced by addition of 1 mM IPTG overnight at 30°C (220 rpm). For each plate of colonies, a 96-well plate (Maxisorp™, Nunc) was coated with 1 µg/mL neutravidin (100 µL per well) incubated for one hour at 37°C, and washed with 1 × PBS twice. Two µg/mL $P2X_3$-biotin (100 µL per well) was then added and incubated overnight at 4°C, followed by blocking with a 5% (w/v) PBSM (200 µL per well) for 1 hour at 37°C. The overnight expression plates were frozen (-80°C) and thawed (37°C) three times to break open the cells to produce a scFv-containing lysate. The plates were centrifuged (HermLe Z233MK-2 refrigerated centrifuge) at 3,220 g for 10 min at 4°C, and the lysate supernatant was added (100 µL per well) to its corresponding coated/blocked well and incubated at 37°C for one hour. For the inhibition ELISA, at this step, the lysate was pre-incubated with several concentrations of the free $P2X_3$-257/60 and then added to the corresponding coated/blocked well and incubated at 37°C for 1 hour. After washing the plates three times with 1 x PBST and three times with 1 x PBS to remove any unbound scFv, the scFv-bound $P2X_3$ complex was detected using HRP-labelled anti-HA secondary monoclonal antibody (1:2,000 dilution, 100 µL per well). After incubating for one hour at 37°C, TMB (0.4 g/L) was added (100 µL per well) and incubated for 15 min at 37°C. The reaction was stopped by the addition of 10% (v/v) HCl (100 µL per well), and absorbances of the wells was read at 450 nm using a Safire 2 plate reader.

2.2.4.14 'Colony-pick' PCR and restriction enzyme digestion of scFv

Individual colonies were picked with a sterile 200 µL pipette tip and added to an SOE-PCR reaction mixture containing the following components:

Component	50 µL Volume	Conc. in 50 µL reaction
GoTaq buffer (5x)	10 µL	1x
MgCl$_2$	3.0 µL	1.5 mM
RSC-F	0.5 µL	60 pM
RSC-B	0.5 µL	60 pM
dNTP	1.0 µL	0.2 mM
H$_2$O	34.75 µL	N/A
GoTaq ™ Polymerase	0.25 µL	5 U/µL

The mixture above was placed into PX2 thermal cycler (Thermo Electron Corporation) and proceed reactions under the following conditions:

Stage	Temperature (°C)	Time (seconds)
1 (1 cycle)	94	300
2 (26 cycles)	94	45
	56	60
	72	150
3 (1 cycle)	72	600
	4	Pause

81

Following by analysis of PCR reactions using 1% (w/v) agarose gel electrophoresis. The successfully amplified products were restriction digested by *Alu*I (New England Biolabs) under the following conditions:

scFv gene *Alu*I digest	
Component	**24 µL Volume**
SOE product	8 µL
10 x buffer 2	2.4 µL
100 x BSA	0.24 µL
H_2O	12.86 µL
*Alu*I	0.5 µL

The *Alu*I digestion was carried out for two hours at 37°C. Then the digested samples were run on a 3% (w/v) agarose gel for analysis.

2.2.4.15 ScFv purification by immobilised metal affinity chromatography (IMAC)

A 3 mL aliquot of Ni^+-NTA agarose resin (QIAgen) was added to a 20 mL column and equilibrated with 20 mL of running buffer (1 x PBS, 0.5 M NaCl, 20 mM imidazole and 1% (v/v) Tween-20). The filtered lysate was then applied to the equilibrated column and the 'flow-through' collected in a 50 mL tube. The column was washed with 30 mL of running buffer to remove any loosely bound non-specific proteins, again collecting the 'flow-through' in a 50 mL tube. The scFv fraction was eluted using 100 mM NaAc (pH 4.4) and collected in 24 x 400 µL aliquots in 1.5 mL micro-centrifuge tubes containing 100 µL of filtered neutralisation buffer (50 µL 100 mM NaOH and 50 µL of 10 x PBS). The neutralised scFv (12 mL) was then thoroughly buffer exchanged against filtered 1 x PBS using a 5 kDa 'cut-off' Vivaspin™ 6 column (AGB, VS0611). The buffer-exchanged scFv was then quantified using the Nanodrop™ ND-1000 and aliquoted into clean PCR tubes and stored at -20°C.

2.2.4.16 ScFv titre and competitive ELISA

Maxisorb 96-well plates were coated with 100 µL per well 2.5 µg per µL neutravidin at 37°C for one hour. Then the plates were washed once with 1 × PBS, followed by the addition of 100 µL per well 5 µg/µL P2X$_3$-257/60-biotin conjugates overnight at 37°C. Plates were blocked with 200 µL per well 5 % (w/v) PBSTM at 37°C for one hour. A range of dilutions of purified scFv in 3% (w/v) PBSTM (1:2-1:1,000 dilution; 100 µL per well) was applied as primary antibody at 37 ℃ for one hour. To carry out the competitive ELISA, a range of concentrations of P2X$_3$-257/60 peptide (0-2 µg/mL) were prepared and mixed with a fixed concentration of purified scFv. One hundred µL per well of this mixture was incubated at 37°C for one hour. Then HRP-labeled HA antibody (100 µL per well) was added as secondary antibody and incubated at 37°C for one hour. TMB (0.4 g/L, 100 µL per well) was added and incubated at room temperature for 10 min. The reaction was stopped by addition of 50 µL of 1 M HCl per well. The absorbances of the wells were read at 450 nm using Safire 2 plate reader.

2.2.4.17 SDS-PAGE, Western blotting (WB) and Immunofluorescent (IF) staining analysis of rabbit anti-P2X$_3$ scFv specificity to rat root ganglion cells (DRGs) expressing P2X$_3$.

2.2.4.17.1 SDS-PAGE and Western blotting

DRG cells were harvested at 3-5 days *in vitro* (DIV 3-5) by lysing the cells with 100 µL 2 x LDS buffer. A 160 µg quantity of DRGs lysis protein sample (in a total volume of 20 µL) was added into each well of 4-12% precast Bis-Tris gel (Invitrogen). The gels were placed in an electrophoresis apparatus and submerged in electrophoresis buffer. The electrophoresis buffer was prepared using 50 mM MOPS, 50 mM Tris, pH 8.3, 1 mM ethylenediaminetetraacetic acid (EDTA) and 0.1% (w/v) SDS. The apparatus is attached to a power supply and a voltage of 200 V is applied to the gel. The

gels were allowed to run until the tracker dye had reached the bottom of the gel. The gels were taken out and stained using Coomassie stain [0.2% (w/v) Coomassie blue R-25, 45% (v/v) methanol, 45% water, 10% (v/v) acetic acid] for 1-2 hours. Finally, the stained gels were destained overnight using Coomassie blue destain [10% (v/v) acetic acid, 25% (v/v) methanol, 65% (v/v) water], changing the destain several times.

For Western blotting, proteins were transferred from the gel to a PVDF membrane at 250 mA for 2.5 hours. The membrane was blocked with 5% (w/v) TBSTM for one hour at room temperature. Purified scFv antibody (prepared in section 2.2.3.15) was added overnight at 4°C. The membrane was washed three times with 1 x TBST for 5 min. HRP-labelled anti-HA (1:2,000 dilution) secondary antibody was added and incubated at room temperature for one hour. The membrane was washed three times with 1 x TBST for 5 min, and TMB (0.4 g/L) was added for visualisation. When the bands appeared, the membrane was washed with ddH$_2$O to stop the reaction. A picture was then taken using the G:BOX Gel & Blot Imaging Series.

2.2.4.17.2 Immunofluorescent staining

A 24-well tissue culture plate with DRG cells cultured for 5-7 day were washed three times with Dulbecco's phosphate buffer saline (D-PBS, lacking Mg^{2+} and Ca^{2+}) and fixed using 3.7% (v/v) paraformaldehyde for 20 min at room temperature. The plate was washed three times with D-PBS, and then blocked with 1% (w/v) BSA in D-PBS for one hour at room temperature. The blocking solution was removed, purified anti-P2X$_3$-scFv was added as primary antibody and the cells were incubated at room temperature for one hour. The plate was washed three times with D-PBS, followed by addition of fluorescein-labelled rat anti-HA monoclonal antibody (2 µg/mL, 200 µL). After washing three times with D-PBS, the cells were ready to image using an Olympus IX71 microscope or inverted confocal microscope (Leica Dmire 2) with a CCD camera. Images were then analysed using the Image-Pro Plus 5.1 or Leica confocal software. A negative control was included with rabbit anti-goat-IgG (1:1,000 dilution) as primary antibody instead of purified

anti-P2X$_3$-scFv, followed by secondary antibody Alexa Fluor-488-labelled goat anti-rabbit IgG (1: 200 dilution).

2.2.4.18 Determination of rabbit anti-P2X$_3$ scFv stability in solution

Purified rabbit scFv was stored in autoclaved glycerol or sterile filtered BSA or in a protease inhibitor cocktail (PIC) according to conditions shown in table 2.10. The scFv titre was measured on days 1, 6, 12, 19, 30, 60 and 90. The scFv titre determination was described in section 2.2.3.16.

Table 2.10 Different storage conditions with different additions for rabbit anti-P2X$_3$ scFv.

Component added	Storage temperature
1:1 (v/v) glycerol	4°C
10 mg/mL BSA	4°C
1:10 (v/v) PIC	4°C
10 mg/mL BSA + 1:10 (v/v) PIC	4°C
10 mg/mL BSA	-80°C

2.2.4.19 ScFv mutation of Cys$_{80}$ to Ala

Cys$_{80}$ mutation Primers

Mutation sense primer	5′ CGG ACG ATG CTG CCA CTT ACT ACT G 3′
Mutation reverse primer	5′ CCT GCA CGT CGC TGA TGG TGA GAG 3′

The components for a 1 x reverse PCR reaction with 50 µL total volume were as follows:

Component	50 µL Volume	Conc. in 50 µL
Accu Pfx Buffer (10x)	5.0 µL	1x
Mutation sense primer	1 µL	60 pM
Mutation reverse primer	1 µL	60 pM
ScFv plasmid (H7C; 500 ng)	5.0 µL	0.5 µg
H_2O	37.2 µL	N/A
Accu Pfx	0.8 µL	5 U/µL

The PCR for the amplification was performed using a Biometra $T_{GRADIENT}$ PCR machine with the following conditions:

Stage	Temperature (°C)	Time (seconds)
1 (1 cycle)	94	120
2 (15 cycles)	94	30
	55	53
	68	285
3 (1 cycle)	68	600
	4	Pause

The reverse PCR mutated samples were ethanol-precipitated and gel-purified following the protocol in section 2.2.3.5, followed by transformation into Top 10 electrocompetent *E.coli*, as described in section 2.2.3.8. Six single colonies were picked and plasmids were extracted as described in section 2.2.3.8, and then *sfi*I restriction digestion was performed for selection of positive colony (section 2.2.3.7).

2.2.4.20 Fluorescence-activated cell sorting (FACS) analysis of rat DRG expressed-P2X$_3$ staining

Fluorescence-activated cell sorter (FACS), an instrument based on flow cytometry, is effectively used for detecting antibody specific binding on antigen expressed by cells (Geuijen *et al.*, 2005). The principle of FACS analysis is a fluorescence-labelled suspension containing individual cells passes a focused laser-beam, and then the fluorescence-labels are stimulated by the laser light. The emitted flurescent light from the flurophores (correspond to the number of antibody) and the scattered-light (correspond to size of cell) are detected separately (Nunez, 2001). Thus, FACS enables quantification of specific-binded antibodies which can not be achieved by merely immunofluorescent staining and observed using microscope.

Rat DRG cells cultured for 4 days were fixed and stained as described in section 2.2.4.17.2. After proper wash with D-PBS, 0.5 mL per well D-PBS was added and DRG cells were scraped from the wells of the cell culture plate. DRG cells were then transferred to labelled FACs tubes (Becton Dickson, U.S.A.). Samples were acquired immediately or left overnight at 4°C in the dark. 10,000 events were acquired per sample using a 4-colour FACS Calibur (fluorescence activated cell sorter) Becton Dickson. Data was analysed using FlowJo software. For negative control, the primary antibody was omitted and only applied with secondary antibody. For positive control, commercial rabbit anti-P2X$_3$ polyclonal antibody was added instead of scFv antibody.

2.2.4.21 Immunohistochemical analysis of specificity of anti-P2X$_3$ antibody

Sections of 4 μm thickness were cut from the whole section blocks for the purpose of immunohistochemistry. Sections were immunostained with rabbit anti-P2X$_3$-257 scFv antibody (50 μM) or rabbit anti-P2X$_3$-257 polyclonal antibody (50 μM) after antigen heat retrieval on an automated platform (Bond system-Leica Microsystems, Bannockburn, IL, U.S.A.) in Beaumont Hospital. Briefly, cut sections were subjected to on-board dewaxing and the following

conditions were applied: P2X$_3$ antigen retrieval in tri-sodium citrate buffer (Bond Epitope Retrieval 1 solution) for 20 mins. Detection of the antibody–antigen complex was achieved using a polymer-based kit (Bond Refine) with DAB as the chromogen. All sections were counterstained with haematoxylin. Negative controls were included for all sections by omitting the primary antibody; competition controls were performed by preincubating antibodies with P2X$_3$ peptides (1 µg peptide per 1 µg antibody); positive controls included rat DRG sections stained by commercial rabbit anti-P2X$_3$ polyclonal antibody (50 µM).

2.2.5 Expression and purification of LC-H$_N$/A-core streptavidin (CS5)

2.2.5.1 Expression and purification of LC-H$_N$/A-core streptavidin (CS5)

The principle of P2X$_3$ delivering BoNT for treating inflammatory pain was proved by LC-H$_N$/A-anti-P2X$_3$ pAb conjugates (BoNT/E light chain and heavy chain translocation domain and anti-P2X$_3$ polyclonal antibody conjugates), which were obtained by conjugating biotinylated rabbit polyclonal anti-P2X$_3$ antibody and LC-H$_N$/A-core streptavidin (CS5) via the high affinity biotin-streptavidin bond. A description of how LC-H$_N$/A-core streptavidin (CS5) was expressed and purified follows.

One clone of LC-H$_N$/A-core streptavidin was picked and added into 5 mL LB medium and incubated overnight at 220 rpm and 37°C. LC-H$_N$/A-core streptavidin overnight culture (0.5 mL) was inoculated into 500 mL of ZY medium in 2 L flask and the culture was shaken at 220 rpm and 37°C. After five hours, the temperature was changed from 37°C to 22°C for self-induction of LC-H$_N$/A-core streptavidin expression and it was incubated overnight with shaking at 220 rpm. The culture was centrifuged (Beckman J2-HS centrifuge) at 8,500 g for 20 min at 4°C. The pellet was resuspend in 25 mL of lysis buffer (25 mM HEPES, 500 mM NaCl and 10% (v/v) glycerol, pH 7.8) containing 150 µL protease inhibitor (CalBiochem, #539134), 20 µL benzonase (Novagen, #70746-3) and 45 mg lysozyme (Sigma, #L6876-10G). The sample was mixed

gently on a roller for 40 min at room temperature, then frozen (-80°C) and thawed (37°C) three times to break open the bacterial cells to release expressed LC-H_N/A-core streptavidin. The sample was either kept at -80°C for long-term storage or purification steps undertaken.

For purification, 1 mL of metal affinity resin (Talon superflow, # 635507) was equilibrated twice with 10 mL lysis buffer, and then the freeze-thawed sample was centrifuged (Beckman J2-HS centrifuge) at 18,000 g for 20 min. A 2 mL volume of supernatant was added to the column and mixed resin with supernatant for one hour at 4°C. The mixture was transferred to the column and incubated for 10 min to allow the solution pass through the column. The column was washed twice with 6 mL wash buffer (25 mM HEPES, 500 mM NaCl, 10% (v/v) glycerol and 5 mM imidazole, pH 7.8). The LC-H_N/A-core streptavidin was then eluted with 6 mL elution buffer (25 Mm HEPES, 500 mM NaCl, 10% (v/v) glycerol and 500 mM imidazole, pH 7.8). The eluate was collected in 6 x 1.5 mL tubes and the protein concentration was then measured with a BCA kit (section 2.2.2.3).

Subsequently, the eluted fractions were desalted using a Zeba Desalt Spin Column (Pierce, # 89893). The desalting column was equilibrated with running buffer (20 mM HEPES, 145 mM NaCl, pH 7.4). Eluted fractions from the last step were added to the column, the 'flow-through' discarded, and the LC-H_N/A-core streptavidin was eluted with 3.5 mL nicking buffer (25 mM HEPES, 145 mM NaCl, 2 mM CaCl$_2$, pH 7.8). Eluted desalted LC-H_N/A-core streptavidin was added to a 50,000 MWCO Vivaspin, and centrifuged (HermLe Z233MK-2 refrigerated centrifuge) at 2,465 g for 5-10 min at 4°C until 1 mL of solution was left. The concentrated sample was transferred to a 1.5 mL tube, and centrifuged (Eppendorf centrifuge 5810R) at 18,000 g for 10 min at 4°C to remove debris.

At this stage, the purified LC-H_N/A-core streptavidin protein was in single chain (SC) form, which is inactive, and needed to be nicked to the di-chain (DC) active form by thrombin (1:250 dilution) treatment at 27°C for 40 mins. Then a thrombin inhibitor, APMSF (250 μM), was added to the solution to inactive the thrombin. The concentration of LC-H_N/A-core streptavidin was measured with a BCA protein determinationkit (section 2.2.2.3).

2.2.5.2 Analysis of expression and purity of LC-H$_N$/A-core streptavidin (CS5) via SDS-PAGE

For SDS-PAGE analysis, 0.1 mg of purified LC-H$_N$/A-core streptavidin (CS5, in a total volume of 20 µL) was loaded into each well of 4-12% (w/v) NuPAGE Bis-Tris Gel. The gels were placed in an electrophoresis apparatus and submerged in electrophoresis buffer. The electrophoresis buffer was prepared using 50 mM MOPS, 50 mM Tris, pH 8.3, 1 mM EDTA and 0.1% (w/v) SDS. The apparatus was attached to a power supply and a voltage of 170 V applied to the gel. The gels were allowed to run until the tracker dye had reached the bottom of the gel, taking approximately 45-60 minutes. The gel was taken out and stained using Coomassie stain [0.2% (w/v) Coomassie blue R-25, 45% (v/v) methanol, 45% water, 10% (v/v) acetic acid] for 1 hour. Finally, the stained gels were destained for 2 hours using Coomassie destain [10% (v/v) acetic acid, 25% (v/v) methanol, 65% (v/v) water], changing the destain twice.

2.2.5.3 Biotin-binding capacity of LC-H$_N$/A-core streptavidin (CS5)

A Maxisorb 96-well plate was coated with a range of concentrations (0.004, 0.01, 0.02, 0.04, 0.1, 0.2, 0.4, 1, 2 and 4 nM) of LC-H$_N$/A-core streptavidin (100 µL per well) overnight at 4°C. The plate was blocked with 200 µL/well 5 % (w/v) PBSTM at 37°C for one hour. One hundred µL per well of HRP-labelled biotin was added as secondary antibody and the plate was incubated at 37°C for one hour. Subsquently, 100 µL per well TMB (0.4 g/L) was added and incubated at room temperature for 15 min. The reaction was stopped by addition of 50 µL per well of 1 M HCl, and the absorbances of the wells read at 450 nm using a Safire 2 plate reader.

2.2.5.4 Activity determination of purified LC-H$_N$/A-core streptavidin (CS5)

Different amounts of LC-H$_N$/A-core streptavidin (0, 0.013, 0.13, 1.3, 13 µg) were added into rat DRGs cultures (P5, 6 DIV) and incubated for 16 hours at 37°C in 5% (v/v) CO$_2$. Culture medium was carefully removed and DRG cells were lysed using LDS buffer (60 µL per well). Western blotting was performed for checking P2X$_3$ expression on DRG cells using the protocol described in section 2.2.3.17, with mouse anti-SNAP-25 antibody (SMI-81, 1:1,000 dilution) applied as the primary antibody, and followed by HRP-labelled anti-mouse IgG secondary antibody.

2.2.6 Anti-P2X$_3$ polyclonal antibody-LC-H$_N$/A-core streptavidin conjugates

2.2.6.1 Biotinylation of rabbit anti-P2X$_3$ polyclonal antibody and quantitation

An EZ-Link(R) Micro Sulfo-NHS-LC-biotinylation kit (Fisher Thermo Scientific, #PN21935) was used for labeling antibody with biotin. Polyclonal antibody was prepared in 1 x PBS to a final concentration of 1-10 mg. One vial of Sulfo-NHS-LC-biotin, stored at -20°C, was placed at room temperature for equilibration. Ultrapure water (180 µL) was added to the 1 mg microtube to give a 10 mM biotin reagent solution. An appropriate volume of 10 mM biotin reagent solution was added to the polyclonal antibody solution based on the following formulae (from the EZ-Link(R) Micro sulfo-NHS-LC-biotinylation kit protocol):

1) Caculation of millimoles of sulfo-NHS-LC-biotin to add to the reaction to give a 20-fold molar excess:

$$\text{mL (protein)} \times \frac{\text{mg (protein)}}{\text{mL (protein)}} \times \frac{\text{mol (protein)}}{\text{mg (protein)}} \times \frac{20\,\text{mmol (biotin)}}{\text{mmol (protein)}} = \text{mmol}$$

biotin

20 = Recommemded molar fold excess of biotin per 1-10 mg/mL protein sample

2) Calculation of microliters of 10 mM Sulfo-NHS-LC-biotin to add to the reaction:

$$\text{mmol biotin} \times \frac{557\,\text{mg}}{\text{mmol (biotin)}} \times \frac{400\,\mu L}{\text{mmol (biotin)}} = \mu L \text{ biotin colution}$$

577 = Molecular weight of Sulfo-NHS-LC-biotin
400 = Microliters of water in which 2.2 mg of Sulfo-NHS-LC-biotin is dissolved to make a 10 mM solution

The biotin reagent and antibody mixture were placed on ice and incubated for two hours. The biotinylated polyclonal antibody was desalted and concentrated using 10,000 MWCO viva spin (Sartorius, #VS0601) by applying 3 times 1 X PBS (pH 7.5). The concentration was determined by the BCA assay. The biotinylated polyclonal antibody sample was dispensed into 50 µL volumes and stored at -20°C for future use.

A kit (Fisher Thermo Scientific, # PN28005) was used for biotin quantitation. One microtube of HABA/Avidin Premix was removed from the kit at -20°C and left at room temperature for equilibration. Ultrapure water (100 µL) was added and mixed by pipetting up and down. PBS (160 µL) was added into each Maxisorb plate well, followed by 20 µL of the HABA/Avidin Premix solution. Mixing was achieved by manually shaking the plate on the bench 10 times. The absorbances of the wells were read at 500 nm using a Safire 2 plate reader and the values recorded as A_{500} H\A. Twenty µL biotinylated sample or biotinylated-HRP (positive control) was added as secondary antibody and mixed by manually shaking the plate on the bench 10 times. The plate was read at 500 nm and the value was recorded as A_{500} H\A\B sample. Finally, the moles

of biotin conjugated per mole of protein was calculated based on the following formulae (from the Biotin Quantification Kit protocol):

1) Calculation No. 1 is for the concentration of biotinylated protein in mmol/mL (before any dilution for the assay procedure)

$$\text{mmol protein per Ml} = \frac{\text{Protein concentration (mg/mL)}}{\text{MW protein (mg/mmol)}} = \text{Calc No.1}$$

MW = Molecular weight

Calc No. 1 = Calculation number 1

2) Calculation No. 2 is for the change in absorbance at 500nm:

Cuvette:

$$\triangle A_{500} = (0.9 \times A_{500} \text{ H\textbackslash A}) - (A_{500} \text{ H\textbackslash A\textbackslash B}) = \text{Calc No. 2}$$

Microplate:

$$\triangle A_{500} = (A_{500} \text{ H\textbackslash A}) - (A_{500} \text{ H\textbackslash A\textbackslash B}) = \text{Calc No. 2}$$

A_{500} H\A = Absorbance at 500nm for PBS

A_{500} H\A\B = Absorbance at 500nm for biotinylated sample

Calc No. 2 = Calculation number 2

> Note: The cuvette format requires the 0.9 correction factor to adjust for dilution of the H/A mixture by the biotinylated protein sample. The microplate format does not require this correction factor because the dilution effect is exactly offset by the increased height and light path length of solution in the well.

3) Calculation No. 3 is for the concentration of biotin in mmol per mL of reaction mixture:

$$\frac{\text{mmol biotin}}{\text{mL reaction mixture}} = \frac{\Delta A500}{(34,000 \times b)} = \frac{\text{Calc. No.2}}{(34,000 \times b)} = \text{Calc. No.3}$$

Calc No. 3 = Calculation number 3

Note: b is the light path length (cm) of the sample. Use $b = 1$ with cuvette format. Use $b = 0.5$ with the microplate format when using a standard 96-well plate and the volumes specified in the procedure. The exact path length is the height of the solution through which the plate reader measures the absorbance.

4) Calculation No. 4 is for the mmol of biotin per mmol of protein:

$$= \frac{\text{mmol biotin in original sample}}{\text{mmol protein in original sample}}$$

$$= \frac{(\text{mmol per mL biotin in reaction mixture}) (10) (\text{dilution factor})}{\text{mmol per mL protein in original sample}}$$

$$= \frac{(\text{Calc No.3}) \times 10 \times \text{dilution factor}}{\text{Calc No.1}} = \text{Calc No.4}$$

Calc No. 4 = Calculation number 4

Note: The original biotinylated protein sample was diluted 10-fold in the reaction mixture. Therefore, a multiplier of 10 is used in this step to convert the biotin concentration in the original sample. If the original sample was diluted before performing the assay, then the dilution factor must be used as well. Calculation No. 4 yields the biotin: protein molar ratio (average number of biotin molecules per protein molecule).

2.2.6.2 Avidin-binding capacity of biotinylated rabbit anti-P2X$_3$ polyclonal antibody

A Maxisorb 96-well plate was coated overnight at 4°C with 100 µL per well of 2.5 µg/µL neutravidin. The plate was blocked with 200 µL per well 5 % (w/v) PBSTM at 37°C for one hour. A range of concentrations (2, 4, 10, 20, 40, 100,

200, 400, 1,000 and 2,000 ng) of biotinylated rabbit anti-P2X$_3$ polyclonal antibody was prepared and added into separate wells (100 µL per well), and incubated at 37°C for one hour, followed by the secondary antibody HRP-labelled anti-rabbit antibody (100 µL per well) and incubated for one hour at 37°C. Then, 100 µL per well TMB (0.4 g/L) was added and incubated at room temperature for 15 min. The reaction was stopped by addition of 50 µL per well 1 M HCl, and the absorbances of the wells were read at 450 nm using a Safire 2 plate reader.

2.2.6.3 Western blotting and immunofluorescent staining analysis of biotinylated rabbit anti-P2X$_3$ polyclonal antibody and its specificity to P2X$_3$ expressed on rat DRG cells

The same protocol was followed, as described in section 2.2.2.5, with 20 µg (in 250 µL) biotinylated rabbit anti-P2X$_3$ polyclonal antibody as the primary antibody.

2.2.6.4 The conjugation of biotinylated rabbit anti-P2X$_3$ polyclonal antibody to purified LC-H$_N$/A-core streptavidin (CS5)

Biotin-streptavidin bond is known to be the strongest noncovalent biological interaction (Holmberg *et al.*, 2005), and one molecule of core streptavidin binds to one molecules of biotin. Therefore, LC-H$_N$/A-core streptavidin and biotinylated polyclonal antibody were mixed at a molecular ratio of 2:1 to ensure sufficient binding occurred. The mixture was incubated at 4°C on a roller for two hours to maximum binding.

2.2.6.5 SDS-PAGE and Western blotting (WB) analysis of successful conjugation of rabbit anti-P2X$_3$ pAb and LC-H$_N$/A-core streptavidin (CS5)

A 160 µg quantity of rabbit anti-P2X$_3$ pAb-LC-H$_N$/A-core streptavidin (CS5) conjugates (in a total volume of 20 µL) in 1 x LDS loading buffer was added into each well of 4-12% (v/v) precast Bis-Tris gel (Invitrogen). The gels were

placed in an electrophoresis apparatus and submerged in electrophoresis buffer. The electrophoresis buffer was prepared using 50 mM MOPS, 50 mM Tris, pH 8.3, 1 mM ethylenediaminetetraacetic acid (EDTA) and 0.1% (w/v) SDS. The apparatus is attached to a power supply and a voltage of 200 V applied to the gel. The gels were allowed to run until the tracker dye had reached the bottom of the gel. The gels were taken out and stained using Coomassie stain [0.2% (w/v) Coomassie blue R-25, 45% (v/v) methanol, 45% (v/v) water, 10% (v/v) acetic acid] for 1-2 hours. Finally, the stained gels were destained overnight using Coomassie blue destain [10% (v/v) acetic acid, 25% (v/v) methanol, 65% (v/v) water], changing the destain several times.

For Western blotting, proteins were transferred from the gel to a PVDF membrane at 250 mA for 2.5 hours. The membrane was blocked with 5% (w/v) TBSTM for one hour at room temperature. HRP-labelled anti-rabbit IgG (1:2,000 dilution) was added as secondary antibody and incubated at room temperature for one hour. The membrane was washed three times with 1 x TBST for 5 min, and TMB (0.4 g/L) was added for visualisation. When the bands appeared, the membrane was washed with ddH$_2$O to stop the reaction. A picture was taken using the G:BOX Gel & Blot Imaging Series.

2.2.6.6 Immunofluorescent (IF) staining analysis of rabbit anti-P2X$_3$ pAb-CS5 specificity to rat root ganglion cells (DRGs) expressing P2X$_3$

A 24-well tissue culture plate with DRG cells cultured 5-7 days *in vitro* were washed three times with Dulbecco's phosphate buffer saline (D-PBS, lacking Mg^{2+} and Ca^{2+}) and fixed using 3.7% (v/v) paraformaldehyde for 20 min at room temperature. The plate was washed three times with D-PBS, and then blocked with 1% (w/v) BSA in D-PBS for one hour at room temperature. The blocking solution was removed, rabbit anti-P2X$_3$ pAb-CS5 was added as primary antibody and the cells were incubated at room temperature for one hour. The plate was washed three times with D-PBS, followed by addition of secondary antibody Alexa Fluor-546-labelled goat anti-rabbit polyclonal antibody. After washing three times with D-PBS, the cells were ready to image using an Olympus IX71 microscope or inverted confocal microscope (Leica

Dmire 2) with a CCD camera. Images were then analysed using the Image-Pro Plus 5.1 or Leica confocal software. A negative control was included with contained anti-goat IgG (1:1,000 dilution) as primary antibody, followed by secondary antibody Alexa Fluor-488-labelled goat anti-rabbit IgG (1: 200 dilution).

2.2.6.7 Endopeptidase activity of Rabbit anti-P2X$_3$ polyclonal antibody-CS conjugates

Different concentrations of anti-P2X$_3$ pAb-CS5 (0, 0.013, 0.13, 1.3, 13 µg in a total volume of 200 µL) in DMEM culture medium were added into rat DRGs cultures (P5, 6 DIV) and incubated for 16 hours at 37°C in 5% (v/v) CO$_2$. The medium was removed, and DRGs were harvested by lysing with 2 x LDS buffer (60 µL per well). Western blotting was performed to check P2X$_3$ expression on DRG cells using the protocol described in section 2.2.3.17, with anti-SNAP-25 antibody (SMI-81, 1:1,000 dilution) applied as the primary antibody.

2.2.7 P2X$_3$ scFv-BoNT genetic fusion

2.2.7.1 Generation, expression and purification of BoNT-rabbit anti-P2X$_3$ scFv fusion

These processes were carried out by Dr. Jiafu Wang in the International Centre for Neurotherapeutics (ICNT), Dublin City University (DCU). BoNT-scFv fusions [joined with an (GGGGS)$_3$ linker] with C-terminal His-tag (for BoNT-scFv fusion detection and purification), with or without a linker, and with or without the C-terminal banding domain, were designed and generated, followed by primer design, and amplification of fusions via PCR. BoNT-scFv fusions were then ligated onto the pET-29a plasmid vector and transferred to BC21(DE3) or Origami 2(DE3) competitive *E.coli* cells for expression. Finally, the BoNT-scFv fusions were purified by both IMAC and ion exchange chromatography (Fig. 2.4).
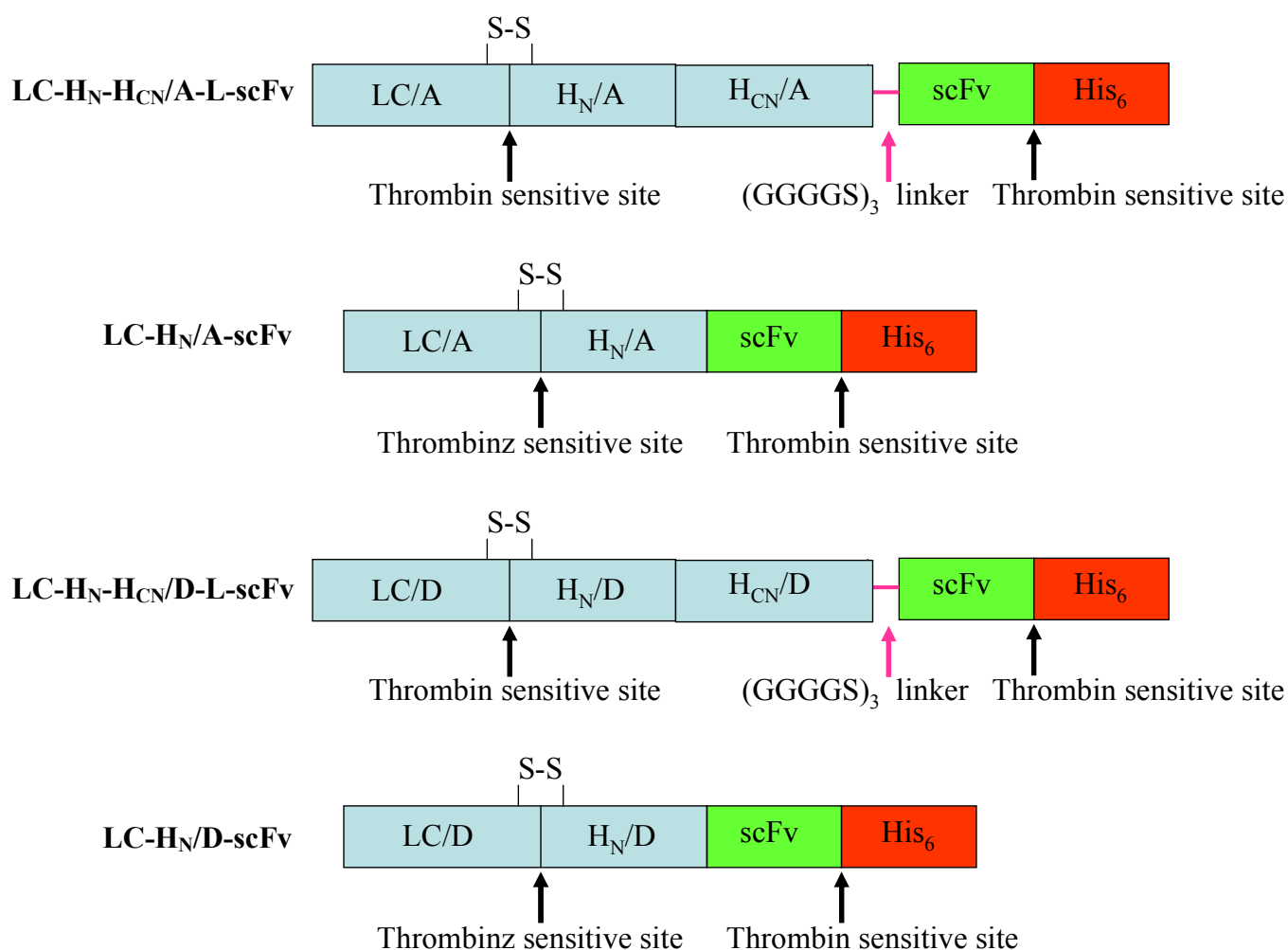
Fig. 2.4 Structure of BoNT-scFv fusion. LC = light chain; H_N = heavy chain translocation domain; H_{CN} = heavy chain C-terminal binding domain; LC/A = light chain of BoNT/A; H_N/A= heavy chain translocation domain of BoNT/A; H_{CN}/A= heavy chain C-terminal binding domain of BoNT/A; LC/D = light chain of BoNT/D; H_N/D= heavy chain translocation domain of BoNT/D; H_{CN}/D= heavy chain C-terminal binding domain of BoNT/D; L = linker, S-S = disulfide bond; scFv = single-chain variable fragment; His_6 = histidine tag.

98

2.2.7.2 Analysis of expression and purity of BoNT/A(or/D)-rabbit anti-P2X$_3$ scFv fusion via SDS-PAGE and Western blotting

A 160 µg quantity of BoNT/A(or/D)-rabbit anti-P2X$_3$ scFv fusion (in a total volume of 20 µL) in 1 x LDS loading buffer was added into each well of 4-12% (v/v) precast Bis-Tris gel (Invitrogen). The gels were placed in an electrophoresis apparatus and submerged in electrophoresis buffer. The electrophoresis buffer was prepared using 50 mM MOPS, 50 mM Tris, pH 8.3, 1 mM ethylenediaminetetraacetic acid (EDTA) and 0.1% (w/v) SDS. The apparatus is attached to a power supply and a voltage of 200 V applied to the gel. The gels were allowed to run until the tracker dye had reached the bottom of the gel. The gels were taken out and stained using Coomassie stain [0.2% (w/v) Coomassie blue R-25, 45% (v/v) methanol, 45% (v/v) water, 10% (v/v) acetic acid] for 1-2 hours. Finally, the stained gels were destained overnight using Coomassie blue destain [10% (v/v) acetic acid, 25% (v/v) methanol, 65% (v/v) water], changing the destain several times.

For Western blotting, proteins were transferred from the gel to a PVDF membrane at 250 mA for 2.5 hours. The membrane was blocked with 5% (w/v) TBSTM for one hour at room temperature. As His-tag was located in the C-terminal of BoNT/A(or/D)-rabbit anti-P2X$_3$ scFv fusion (Fig. 2.4), complete His-tag expression may indicate successful and complete expression of the fusion. Therefore, HRP-labelled anti-His antibody (1:500 dilution) was added as secondary antibody (detect BoNT/A(or/D)-rabbit anti-P2X$_3$ scFv fusion) and incubated at room temperature for one hour. The membrane was washed three times with 1 x TBST for 5 min, and TMB (0.4 g/L) was added for visualisation. When the bands appeared, the membrane was washed with ddH$_2$O to stop the reaction. A picture was taken using the G:BOX Gel & Blot Imaging Series.

2.2.7.3 Western blot analysis of BoNT/A(or/D)-rabbit anti-P2X$_3$ scFv specificity to rat DRG-expressed P2X$_3$

After DRG cells were grown in 24 wells plate for 4 days, the membrane proteins were enriched, as described in section 2.2.4.3. A 160 µg quantity of

DRG membrane protein (in a total volume of 20 µL) was added into each well of a 4-12% precast Bis-Tris gel (Invitrogen). The gel was resolved at 170 volts for about one hour until the blue tracker dye reached the bottom of the gel. The proteins on the gel were transferred to a PVDF membrane at 250 mA for 2.5 hours. The membrane was blocked in 5% (w/v) TBSTM for one hour at room temperature. Purified BoNT/A(or/D)-rabbit anti-P2X$_3$ scFv was used as the primary antibody and incubated overnight at 4°C. The membrane was washed three times with TBST for 5 min. The His-tag was located in the C-terminal of BoNT/A(or/D)-rabbit anti-P2X$_3$ scFv fusion (Fig. 2.4), hence, complete His-tag expression may indicate successful and complete expression of the fusion. Therefore, HRP-labelled anti-His antibody (1:500 dilution) was added as secondary antibody (detect BoNT/A(or/D)-rabbit anti-P2X$_3$ scFv fusion) and incubated at room temperature for 1 hour. The PVDF membrane was washed three times with TBST for 5 min and then developed by addition of 1 mL of TMB (0.4 g/L) to the membrane until the bands appeared. The membrane was washed with ddH$_2$O to stop the reaction. An image was taken using the G:BOX Gel & Blot Imaging Series.

2.2.7.4 Activity of BoNT/A(or/D)-rabbit anti-P2X$_3$ scFv fusion

2.2.7.4.1 Analysis of BoNT/A(or/D)-rabbit anti-P2X$_3$ scFv fusion inhibition K$^+$-evoked release of CGRP and SP from rat cultured DRG neurons

After DRGs were cultured 7 days *in vitro*, medium was gently aspirated from DRG cell cultures. Different concentrations of anti-P2X$_3$ scFv antibody-BoNT fusion (1.6, 8, 40 200 and 1000 nM) were added to the rat DRG cultures and incubated for 24 hours at 37°C in 5% (v/v) CO$_2$. The cells were washed three times with 0.5 mL/well basal release (low K$^+$) buffer [22.5 mM HEPES, 135 mM NaCl, 3.5 mM KCl, 1 mM MgCl$_2$, 2.5 mM CaCl$_2$, 3.3 mM glucose, BSA (0.1%, w/v), pH 7.4] and incubated in 0.5 mL of basal release buffer at 37°C in 5% (v/v) CO$_2$ for 5 min to get the basal release samples. The basal release samples were then collected into sterile 1.5 mL EP tubes, followed by added 0.5 mL of high K$^+$ buffer [22.5 mM HEPES, 76 mM NaCl, 60 mM KCl, 1 mM

MgCl$_2$, 2.5 mM CaCl$_2$, 3.3 mM glucose, BSA (0.1%, w/v), pH 7.4] into each well and incubated at 37°C in 5% (v/v) CO$_2$ for 5 min to stimulate K$^+$-evoked (Ca^{2+}-dependent) release. The stimulated release samples were collected into sterile 1.5 mL EP tubes.

2.2.7.4.2 Enzyme immuno-assay (EIA) of calcitonin gene-related peptide (CGRP)

This enzyme immuno-assay (EIA) was based on a double-antibody sandwich technique that permits measurement of calcitonin gene-related peptide (CGRP) within the range of 1-500 pg/mL. The wells of the plates supplied with the kits were coated with a monoclonal antibody specific for CGRP. This monoclonal antibody binds CGRP (100 µL per well) added in the wells (samples and standards supplied with the kits). This was followed by addition of an acetylcholinesterase (AChE)-Fab conjugate (anti-CGRP AChE tracer) (100 µL per well) which binds to an epitope on the CGRP molecule This allowed the two antibodies to form a sandwich by binding of different epitopes of the CGRP molecule, which remained immobilised on the plate. The excess reagents were then removed by washing five times with wash buffer (300 µL per well) supplied in the kit. The concentration of CGRP was then determined by measuring the enzymatic acitivity of the AChE using Ellman's reagent, which contains acetylthiocholine as substrate. The final product of the enzymatic reaction, 5-thio-2-nitrobenzoic acid, is bright yellow and its absorbance can be determined at 405-420 nm. The intensity of the yellow colour, determined spectrophotometrically, is proportional to the amount of the CGRP present in the well.

For determining the amount of released CGRP, 0.1 mL of sample or standard was added to the plate (supplied with kit) followed by 0.1 mL of CGRP-tracer solution and incubated at 4°C overnight. After the plate was washed five times with wash buffer (300 µL per well) supplied in the kit, Ellman's reagent (200 µL per well) was added and incubated in dark at room temperature for 30 min. The absorbances of the wells were read at 405 nm using a Safire 2 plate reader. For data analysis, a standard curve was generated for each assay and the

best-fit line through the points drawn using Excel software. Concentrations of released CGRP were then calculated from the linear range of the standard curve.

2.2.7.4.3 Analysis of SNAP-25 and VAMP2 cleavage in cultured DRGs for BoNT/A-anti-P2X$_3$-scFv and BoNT/D-anti-P2X$_3$-scFv

After being exposed to different concentrations of anti-P2X$_3$ scFv antibody-BoNT fusion (1.6, 8, 40 200 and 1000 nM) and being treated with basal and stimulated release buffers in section 2.2.7.4.1, DRGs (same DRGs is in section 2.2.7.4.1) were harvested by scraping from the wells of cell culture plate using LDS buffer (60 µL per well).

Western blot analysis was performed to check SNAP-25 and VAMP2 using the protocol described in section 2.2.3.17, with mouse anti-SNAP-25 antibody (SMI-81; 1:1,000 dilution) or mouse anti-VAMP IgM monoclonal antibody (V2; 1:1,000 dilution) as the primary antibody followed by HRP-labelled goat anti-mouse secondary antibody (1:1,000 dilution).

Chapter 3

Isolation and Culturing of Rat Dorsal Root Ganglion Cells (DRGs)

3.1 Introduction

In this chapter, a description is given of culturing dorsal root ganglion cells (DRGs), including their expression of sensory neuron markers and P2X purinoceptor 3 (P2X$_3$), and their susceptibility to botulinum neurotoxin type A and type D BoNT/A and BoNT/D. Successful establishment of rat DRG cell cultures was demonstrated by their expression of peptidergic sensory neuron markers and targeting was achieved by use of an anti-P2X$_3$ receptor antibody.

DRGs are among the most common and major sensory neurons in vertebrata (Bessac *et al.*, 2008). It was reported that inflammation can activate multiple intracellular signalling pathways in DRGs. During persistent inflammatory pain, DRGs were found to be sensitized by a majority of identified signalling cascades (Kallenborn and Schmidtko, 2011).

BoNT/A and BoNT/D are two different types of BoNT. BoNT/A was shown to be a promising means of treating inflammatory pain (Mahowald *et al.*, 2009). BoNT/D inhibits inflammatory pain peptide calcitonin gene-related peptide (CGRP) release in cultured sensory neurons (Meng *et al.*, 2007).

P2X$_3$, one of purinergic receptors, plays a crucial role in signalling that leads to chronic inflammatory pain. Anti-P2X$_3$ antibody can be used as a targeting agent to deliver BoNT to pain-signalling neurons.

Rat neurons are sensitive to BoNT (Foran *et al.*, 2003; Meng *et al.*, 2007). Rat animal pain models are stable (Kim *et al.*, 1997), easily dissected and readily cultured with sufficient dorsal root ganglions (60 pairs) with large size (20-51µm). A high percentage of rat DRGs express P2X$_3$ receptor on postnatal day seven (P7) and 72.6 ± 3.4% of DRGs were identified as P2X$_3$ receptor-positive cells (Ruan *et al.*, 2004). Thus, rat DRGs were chosen for analysis of the antibody specificity and targeting ability to P2X$_3$, and for the capacity of delivering BoNT endopeptidase and the resultant inhibition of transmitter release *in vitro*.

3.2 Results

3.2.1 Images for morphology of cultured rat DRGs using immunofluorescent staining and microscopic examination

3.2.1.1 Phase contrast microscopy of rat DRGs

Using the phase contrast mode of the Olympus IX71 microscope, DRGs isolated from postnatal day 5 (P5) rats and cultured in DMEM medium, as described in section 2.2.4.1 and 2.2.4.2, were easily recognised by the presence of large, opaque and round cell bodies with fine neuritis (Fig. 3.1, 1DIV). After seven days *in vitro* (7 DIV), cells were pure and mature compared with DRGs of earlier stages, with less satellite cells and astrocytes, but with extensive neuritis, which can be observed using the Olympus IX71 inverted microscope (Fig. 3.1, 7 DIV).
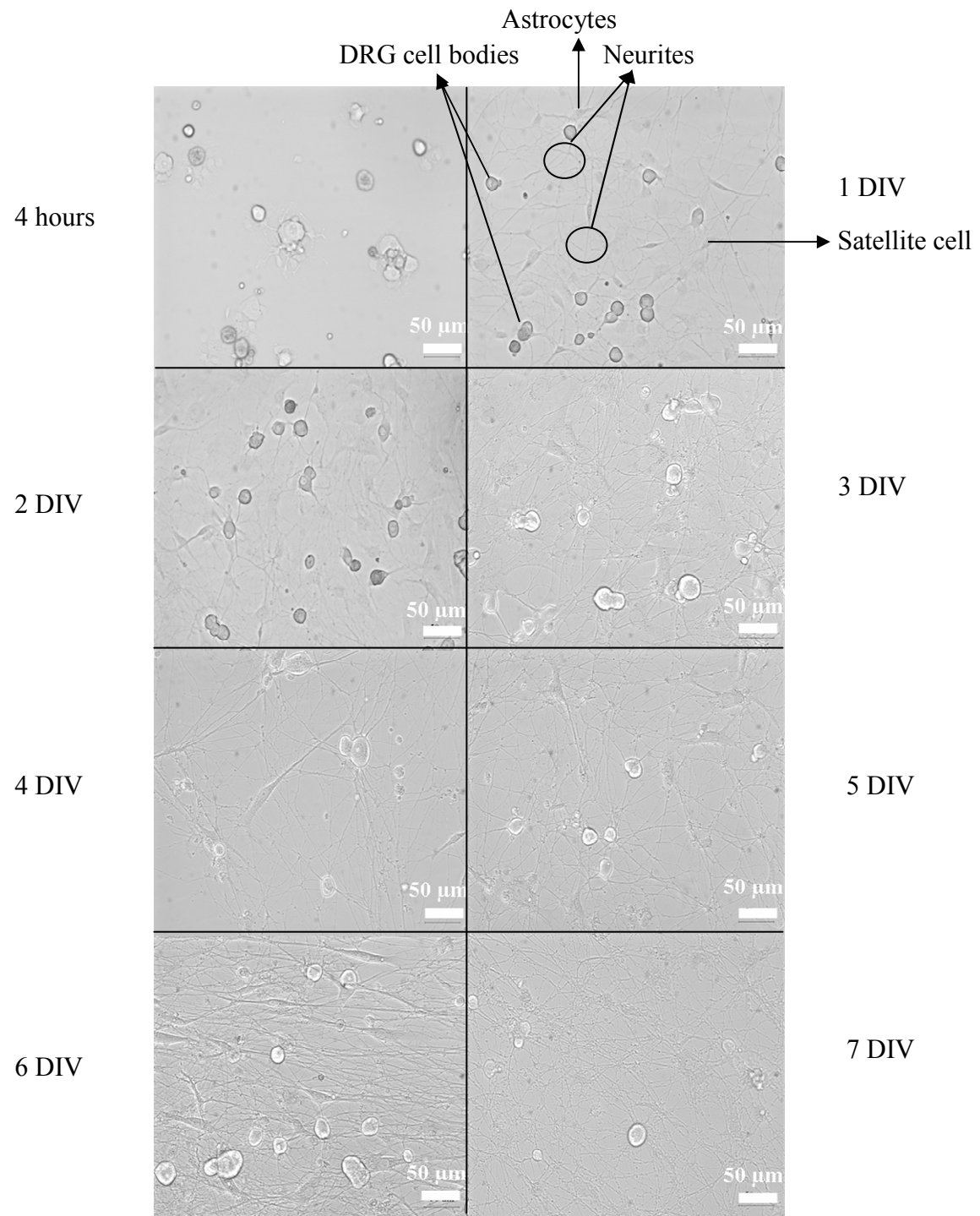
Fig. 3.1 Visualization of the DRG cell culture process after plating for periods of 4 hours to 7 days in 24-well cell culture plates. DRGs were isolated from P5 rats and cultured from four hours to 7 DIV. Original magnification x 20; scale bars are 50 μm.

3.2.1.2 Identification of DRGs by specific antibodies for neuron and nociceptive markers

3.2.1.2.1 DRGs display neuron-specific proteins

In order to prove that the cultured cells were enriched with nerve cells, the cells were stained using anti-neurofilament (NF) heavy chain antibody, which is specific to neurons, as described in section 2.2.4.4. The high majority of all cultured cells were successfully stained by anti-NF antibody (Fig. 3.2) indicating that the cultured cells were neuronal in origin.
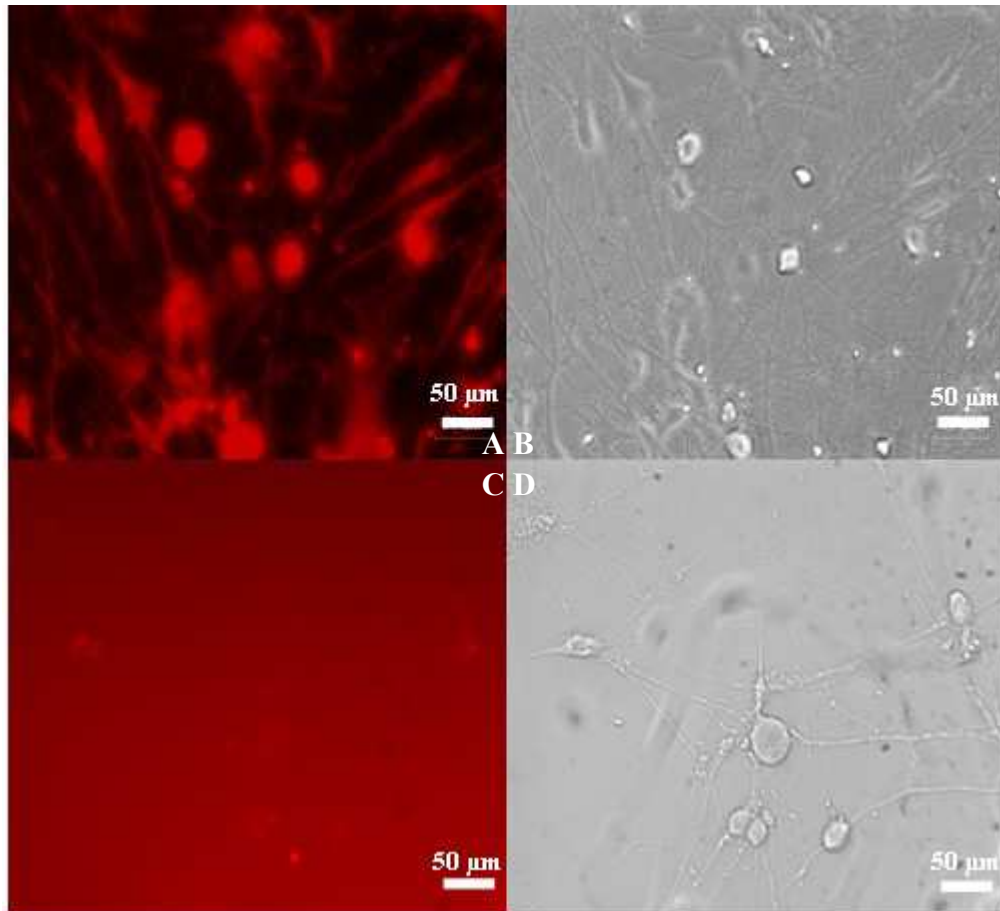
Fig. 3.2 Demonstration of the presence of neurofilament (NF) in rat DRG culture by immunofluorescent staining. Images were viewed in an Olympus IX71 inverted microscope by both phase contrast (B, D) and in epifluorescence mode (A, C). Rat DRGs grown in 24 wells plate for 6 days *in vivo* (6 DIV) were fixed, permeabilised and then stained by mouse anti-NF antibody (1:500 dilution), followed by Cy2-labelled goat anti-mouse IgG (1:100 dilution) (A). For control, rabbit anti-goat IgG (1:1,000 dilution) was added instead of NF antibody, followed by secondary antibody Alexa Fluor-546-labelled goat anti-rabbit polyclonal antibody (1: 200 dilution) (C). Original magnification x 20; scale bars are 50µm.

3.2.1.2.2 DRGs display sensory neuron specific proteins

To demonstrate that the cultured cells were sensory nerve cells, the cells were stained with anti-calcitonin gene-related peptide (CGRP) antibody, which is

specific to sensory nerve cell, as described in section 2.2.4.4. Fig. 3.3 showed that the cells were successfully stained by anti-CGRP antibody, and thus indicated that the cultured cells were sensory nerve cells in origin.
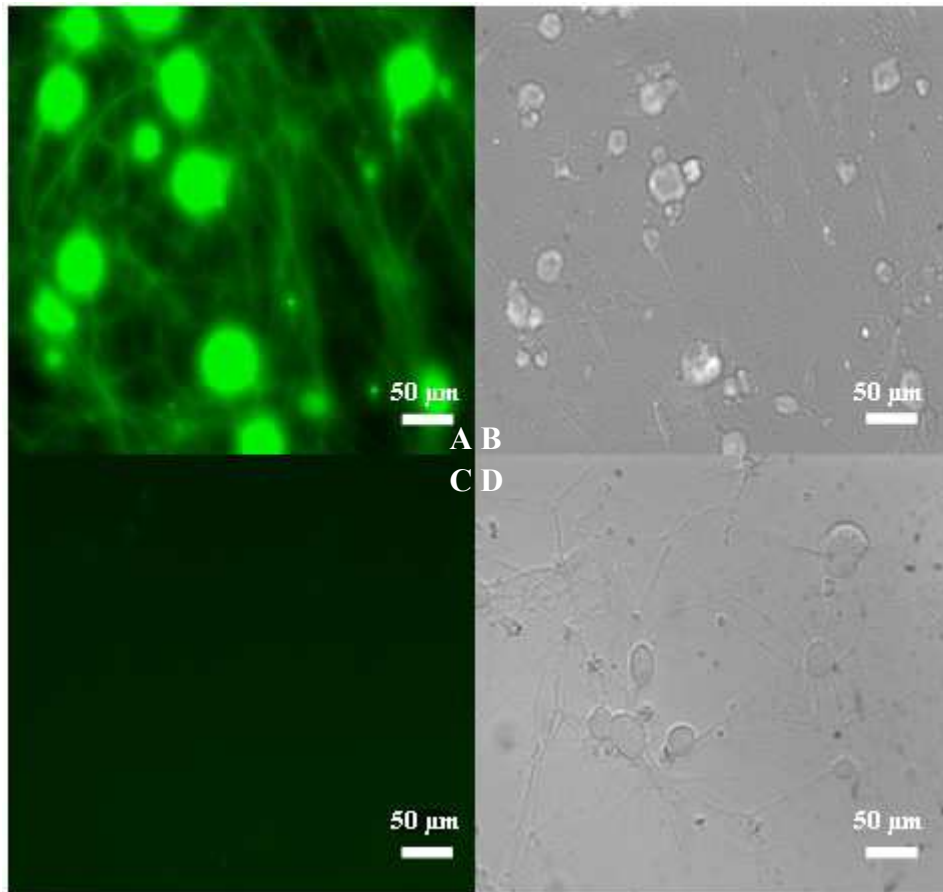
Fig. 3.3 Demonstration of the presence of anti-calcitonin gene-related peptide (CGRP) in rat DRG culture (P5, 5 DIV) by immunofluorescent staining. Images were viewed in an Olympus IX71 inverted microscope by both phase contrast (B, D) and in epifluorescence mode (A, C). Rat DRGs grown in 24 wells plate for 6 days *in vivo* (6 DIV) were fixed, permeabilised and then stained by rabbit anti-CGRP antibody (1:500 dilution), followed by Alexa Fluor-488-labelled goat anti-rabbit IgG (1:200 dilution) (A). For control, rabbit anti-goat IgG (1:1,000 dilution) was added instead of CGRP antibody, followed by secondary antibody Alexa Fluor-488-labelled goat anti-rabbit IgG (1:200 dilution) (C). Original magnification x 20; scale bars are 50 μm.

3.2.2 Demonstration of P2X$_3$ expression in cultured rat DRGs using commercial anti-P2X$_3$ antibody

3.2.2.1 P2X$_3$ expression on cultured rat DRGs

Cultured DRGs (P7, 7 DIV) were fixed, permeabilized and blocked, as described in section 2.2.4.5. Then rabbit anti-rat P2X$_3$ polyclonal antibody (1:50 dilution) was applied, followed by secondary antibody Alexa Fluor-546-labelled goat anti-rabbit polyclonal antibody (1:200 dilution). Strong and punctate red fluorescence signal was shown on cell bodies and their extensive neurites (Fig. 3.4), as reported by Kaan *et al.* (2010), demonstrating that P2X$_3$ is expressed in these DRGs.
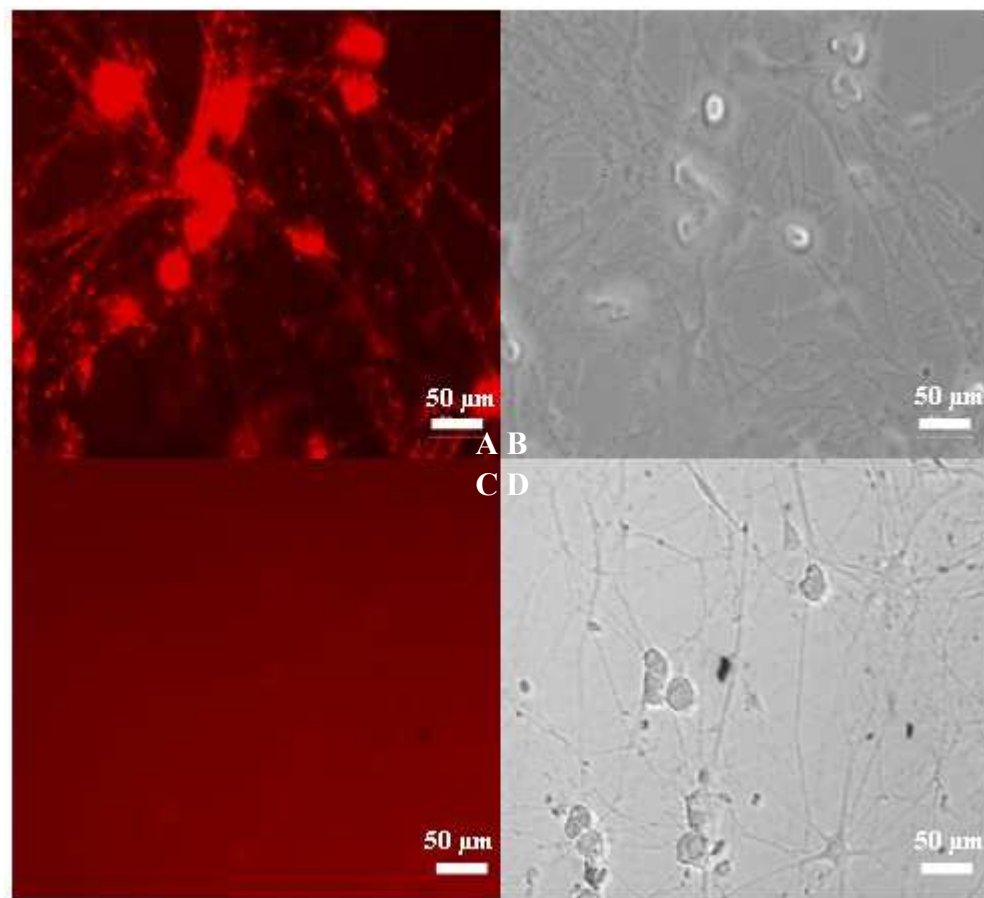
Fig. 3.4 Immunofluorescent staining of cultured DRG by P2X$_3$ antibody. Samples were viewed in an Olympus IX71 inverted microscope by both phase contrast (B, D) and in fluorescence mode (A, C). Rat DRGs, grown in 24 wells plate for 7 days *in vivo* (7 DIV), were fixed and stained by rabbit anti-rat P2X$_3$ polyclonal antibody (1:50 dilution), followed by secondary antibody Alexa Fluor-546-labelled goat anti-rabbit polyclonal antibody (1: 200 dilution). For control, rabbit anti-goat IgG (1:1,000 dilution) was added instead of anti-P2X$_3$ antibody, followed by secondary antibody Alexa Fluor-546-labelled goat anti-rabbit polyclonal antibody (1: 200 dilution) (C, D). Original magnification x 20; scale bars are 50 μm.

3.2.2.2 P2X₃ expression on DRGs culture detected using immunoblot analysis

Cultured DRGs (P7, 7 DIV) were harvested and lysed, as described in section 2.2.4.3. Lysed samples were loaded and run on a SDS-PAGE gel, and the proteins transferred to a PVDF membrane, as described in section 2.2.3.17.1, for Western blotting. Rabbit anti rat-P2X$_3$ polyclonal antibody (1:300 dilution) was applied to the membrane, followed by HRP-labelled anti-rabbit secondary antibody (1:2,000 dilution). A strong band at the expected size of P2X$_3$ (50-55 kDa) is shown indicating that P2X$_3$ was expressed by cultured DRGs (Fig. 3.5; A and B).
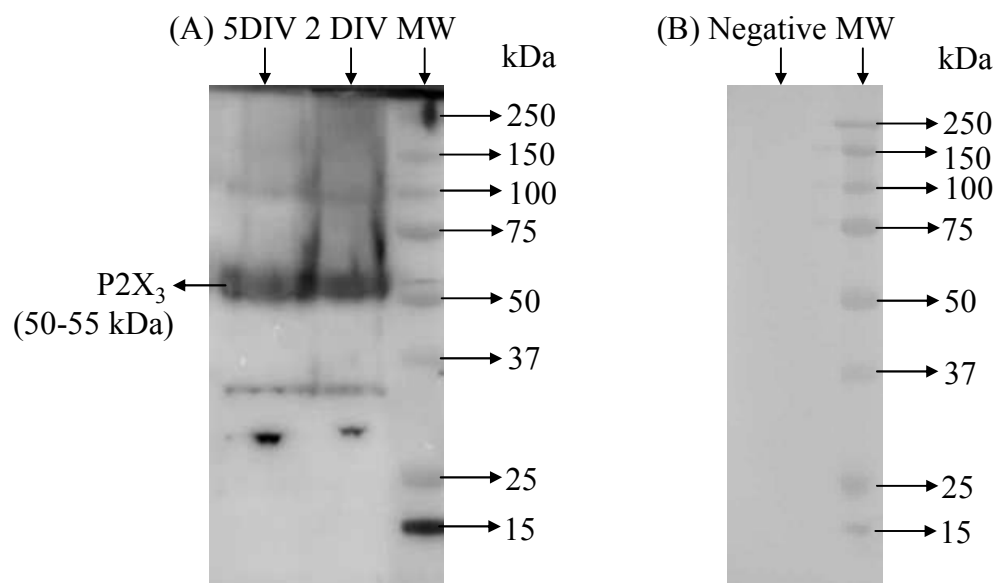
Fig. 3.5 Western blot analysis of DRGs for $P2X_3$ (50-55 kDa) expression. DRGs were isolated from postnatal day 5 rats and cultured for 2 or 5 days *in vitro* before harvesting in SDS sample buffer and analysis by SDS-PAGE and Western blotting (400 µg protein lysate per lane). After Western blotting, the membranes were stained by rabbit anti rat-$P2X_3$ polyclonal antibody (1:300 dilution), followed by HRP-labelled anti-rabbit secondary antibody (1:2,000 dilution) (Fig. 3.5 A). For the negative control, rabbit anti-goat IgG (1:1,000 dilution) was added instead of anti-$P2X_3$ antibody, followed by followed by HRP-labelled anti-rabbit secondary antibody (1:2,000 dilution) (Fig. 3.5 B). DIV = days *in vitro* and MW = molecular weight markers.

3.2.3 Sensitivity of DRGs to BoNT

3.2.3.1 Demonstration that cultured DRGs are sensitive to BoNT/A

Different concentrations of BoNT/A (0, 10, 100 and 1,000 nM) were added into rat DRGs cultures (P5, 6 DIV) and incubated for 24 hours at 37°C in 5% (v/v) CO_2, as described in section 2.2.4.6. Initially, the sensitivity of DRGs to BoNT/A was observed by cleavage of its intracellular substrate, SNAP-25,

using anti-SNAP-25 antibody (SMI-81) which detects both cleaved SNAP-25 (~ 25 kDa) and full length SNAP-25 (~ 27 kDa) (Morris *et al.*, 2002). Another SNARE protein, syntaxin 1 (~ 35 kDa) was simultaneously detected by mouse anti-syntaxin-1 antibody (HPC-1) and was used as an internal control due to the lack of cleavage. The generation of the cleaved form of SNAP-25 demonstrated that cultured DRGs were sensitive to BoNT/A (Fig. 3.6).
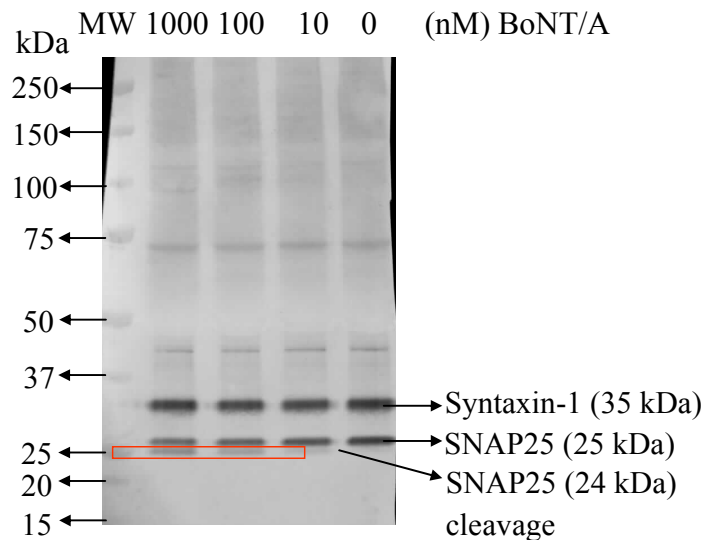
Fig. 3.6 Western blot analysis of cleavage of SNAP-25 by BoNT/A in cultured rat DRGs. After Western blotting, the membrane was stained by mouse anti-SNAP-25 antibody (SMI-81; 1:1,000 dilution) and mouse anti-syntaxin-1 antibody (HPC-1; 1:1,000 dilution), then followed by addition of alkaline phosphatase-conjugated anti-mouse IgG (1:5,000 dilution) secondary antibody. Syntaxin 1 was used as an internal control. The SNAP-25 cleaved form (~ 24 kDa; lower band) was enhanced with increasing concentration of BoNT/A-2T from 0 to 1,000 nm. MW = molecular weight markers.

3.2.3.2 Sensitivity of cultured DRGs to BoNT/D

Rat DRGs, cultured for 5 days *in vivo*, were incubated with BoNT/D for 24 hours to cleave vesicle-associated membrane protein (VAMP2), a pain-related protein. Cells were then solubilized in 2 x LDS sample buffer and subjected to SDS-PAGE and Western blotting, as described in section 2.2.4.6. The sensitivity of the DRG to BoNT/D was also successfully observed by the presence of VAMP2 (~ 18 kDa) cleavage detected using mouse anti-VAMP2 antibody (V2). Another SNARE protein, syntaxin 1 (~ 35 kDa) was simultaneously detected by mouse anti-syntaxin-1 (HPC-1) used as an internal control due to the lack of cleavage. Fig 3.7 shows the absence of VAMP2 following exposure to 1000 nM BoNT/D and a significant reduction when treated with 100 nM BoNT/D compared to 10 nM and 0 of BoNT/D, indicating that VAMP2 is cleaved by BoNT/D.
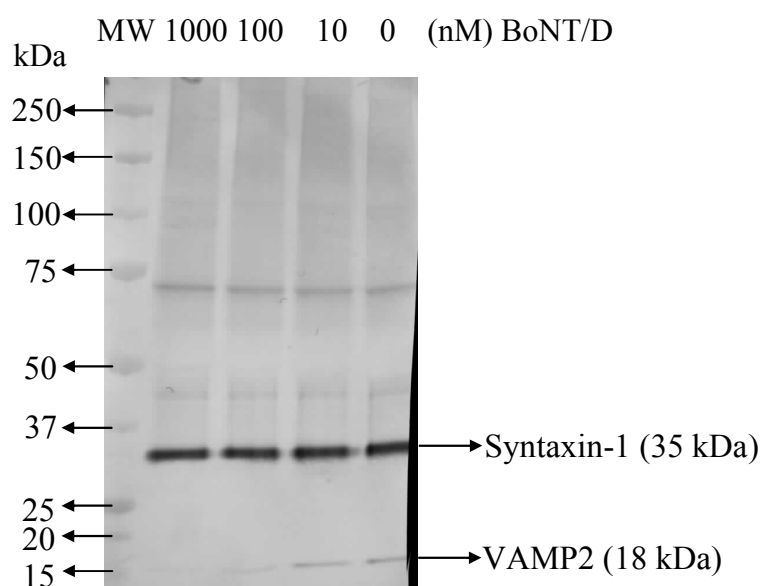
Fig. 3.7 Western blot analysis of cleavage of VAMP2 by BoNT/D-2T in cultured rat DRGs. After Western blotting, the membrane was stained by mouse anti-VAMP2 (V2; 1:10,000 dilution) and mouse anti-syntaxin-1 antibody (HPC-1; 1:1,000 dilution), followed by addition of alkaline phosphatase-conjugated anti-mouse IgG (1:5,000 dilution) secondary antibody. VAMP2 levels were reduced with increased concentrations of BoNT/D-2T (0 to 1,000 nM). MW = molecular weight markers.

3.3 Discussion

The dissection, isolation and culturing of rat DRGs was difficult with several attempts required before success was achieved. It was also important to choose rat pups of the correct age. Postnatal days five to seven was found to be the optimal age range since pups which were less than postnatal day five had DRGs of tiny size and nearly transparent colour, making them difficult to see and, therefore, to dissect. However, pups more than postnatal day seven expressed less $P2X_3$ in their DRGs with the percentage of $P2X_3$-immunopositive DRG cell bodies decreasing from 72.6 ± 3.4 to 44.3 ± 3.5 (Ruan, 2004).

The cultured cells from rat dorsal root ganglions were shown to successfully

express sensory neuron markers and the P2X purinoceptor 3 (P2X$_3$), which indicated that the cultured cells are DRGs. Over 70% of the cells stained positively for P2X$_3$, which is consistent with the reported value of 72.6 ± 3.4% (Ruan, 2004).

Cultured DRGs have been proven to be an ideal *in vitro* pain model through evaluation of cleavage of SNAP-25 or VAMP2 (Morenilla-Palao *et al.*, 2004; Meng *et al.*, 2007). The cultured DRGs showed sensitivity to BoNT/A and BoNT/D, by cleavage of pain-related proteins SNAP-25 and VAMP2, which implies that the cultured rat DRGs may be suitable as an *in vitro* model for investigating the specificity and effect of this new targeted therapeutic (i.e. use of anti-P2X$_3$ antibody as a targeting agent to deliver BoNT/A/D to pain-signalling neurons for inhibiting inflammatory pain peptides).

For further applications, for instance, analysis of anti-P2X$_3$ antibody specificity, the polyclonal anti-P2X$_3$ antibody and recombinant anti-P2X$_3$ scFv antibodies can be applied to cultured rat DRGs to prove their specificity to P2X$_3$ (expressed in rat DRGs) via Western blotting and immunofluorescence (Sokolova *et al.*, 2004; Liu *et al.*, 2011); for evaluation of BoNT-antibody efficacy, BoNT-polyclonal anti-P2X$_3$ antibody conjugates and the BoNT-anti-P2X$_3$ scFv fusion will be applied to cultured rat DRGs for analysis of cleavage of pain-related proteins SNAP-25 and VAMP2 via Western blotting, as described by Meng (2009). The availability and use of cultured DRGs makes the further analysis of novel treatment of pain possible.

Chapter 4

Generation of Anti-P2X$_3$ Antibodies

4.1 Introduction

$P2X_3$, a member of the family of purinoceptors for ATP, is involved in inflammatory pain signalling. Cockayne and colleagues found that after an intraplantar injection of formalin into $P2X_3$-knock-out mice reduced pain behaviour, such as hind paw licking and lifting, was displayed (Cockayne *et al.*, 2000). It was subsequently suggested that $P2X_3$ may provide a promising delivery target for inflammatory pain treatment (North, 2003). $P2X_3$ is a transmembrane protein and hence, anti-$P2X_3$ antibodies required for inflammatory pain therapy should be against the $P2X_3$ extracellular domain (Val_{60}-Phe_{301}) in order to target $P2X_3$ on neuron cell bodies. Therefore, anti-$P2X_3$ antibody and the associated drug complex could enter into the pain signalling pathway as a treatment strategy (Koshimizu *et al.*, 2002).

This chapter describes the generation of polyclonal and recombinant antibodies to the extracellular domain of $P2X_3$ in rabbits, mice and chickens following immunization with $P2X_3$.

Two human extracellular $P2X_3$ peptides ($P2X_3$-60: Val_{60}-Asp_{79} and $P2X_3$-257: Ile_{257}-Pro_{276}) were identified (section 2.1.6.1) and then subsequently conjugated to bovine serum albumin (BSA), keyhole limpet hemocyanin (KLH), biotin and bovine thyroglobulin (bTg). Both $P2X_3$-257-BSA and $P2X_3$-60-BSA conjugates were used to immunise two rabbits (CKPH and DARP) and high serum titres were achieved (Table 3.1). In addition, $P2X_3$-257-BSA and $P2X_3$-60-BSA conjugates were used to immunise a group of three mice per conjugate. After the final boost, each mouse had shown a sufficient immune response with high serum titres (Table 3.1). These mice were then sacrificed and RNA was extracted from the spleens. This genetic material was used to generate a mouse scFv library.

Four chickens were also immunised with $P2X_3$-257-BSA or $P2X_3$-60-KLH conjugates, but failed to provide an adequate immune response.

Table 4.1 Antibody titre of rabbits, mice and chickens immunised with P2X$_3$-257/60.

Immunised animal	Serum titre to P2X$_3$-257-biotin	Serum titre to P2X$_3$-60-biotin
Rabbit-CKPH (immunised with both P2X$_3$-257/60)	1:20,000	1:10,000
Rabbit-DARP (immunised with both P2X$_3$-257/60)	1:20,000	1:4,000
Mouse number 1 (immunised with P2X$_3$-60)	---	1:20,000
Mouse number 2 (immunised with P2X$_3$-60)	---	1:40,000
Mouse number 3 (immunised with P2X$_3$-60)	---	1:40,000
Mouse number 4 (immunised with P2X$_3$-257)	1:200,000	---
Mouse number 5 (immunised with P2X$_3$-257)	1:200,000	---
Mouse number 6 (immunised with P2X$_3$-257)	---	---
Chicken number 1 (died before any injection)	---	---
Chicken number 2 (immunised with P2X$_3$-60)	---	---
Chicken number 3 (immunised with P2X$_3$-257)	---	---
Chicken number 4 (immunised with P2X$_3$-257)	---	---

RNA was extracted from both the spleen and bone marrow of rabbits, cDNA synthesis performed, and it was used to generate scFv libraries. These were then screened for scFvs specific to $P2X_3$ using phage display. Five rounds of iterative bio-panning were performed and up to 52% of positive colonies were screened with $P2X_3$-257-biotin. Some $P2X_3$-positive colonies without cross reactivity to neither carrier protein (BSA and KLH) or ELISA-test protein (neutravidin) were picked for DNA sequencing. ELISA, Western blotting and immunofluorescence-based staining were performed to choose positive colonies with high antibody titres, IC_{50} and high specificity to $P2X_3$.

4.2 Results

4.2.1 Production of rabbit polyclonal antibodies

4.2.1.1 Titres and competitive ELISA of sera from New Zealand white rabbits (designated DARP and CKPH)

The rabbit immunisation procedure was followed, as described in section 2.2.1.1. Rabbit bleeds were taken seven days after the final boost and the serum anti-$P2X_3$ titre was performed using a direct ELISA format to detect IgG antibodies against the two $P2X_3$ extracellular domains, $P2X_3$-257 and $P2X_3$-60 (section 2.1.6.1). Serum antibody titres were determined (the serum dilutions required to produce an absorbance three times greater than the background signals of pre-bleed serum, neutravidin, KLH and BSA). For rabbit-CKPH, the serum titre against $P2X_3$-60 was 1:10,000 (Fig. 4.1a) and 1:20,000 against $P2X_3$-257. For rabbit-DARP, the titre against $P2X_3$-60 was 1:4,000 and against $P2X_3$-257 was 1:20,000 (Fig. 4.1b).
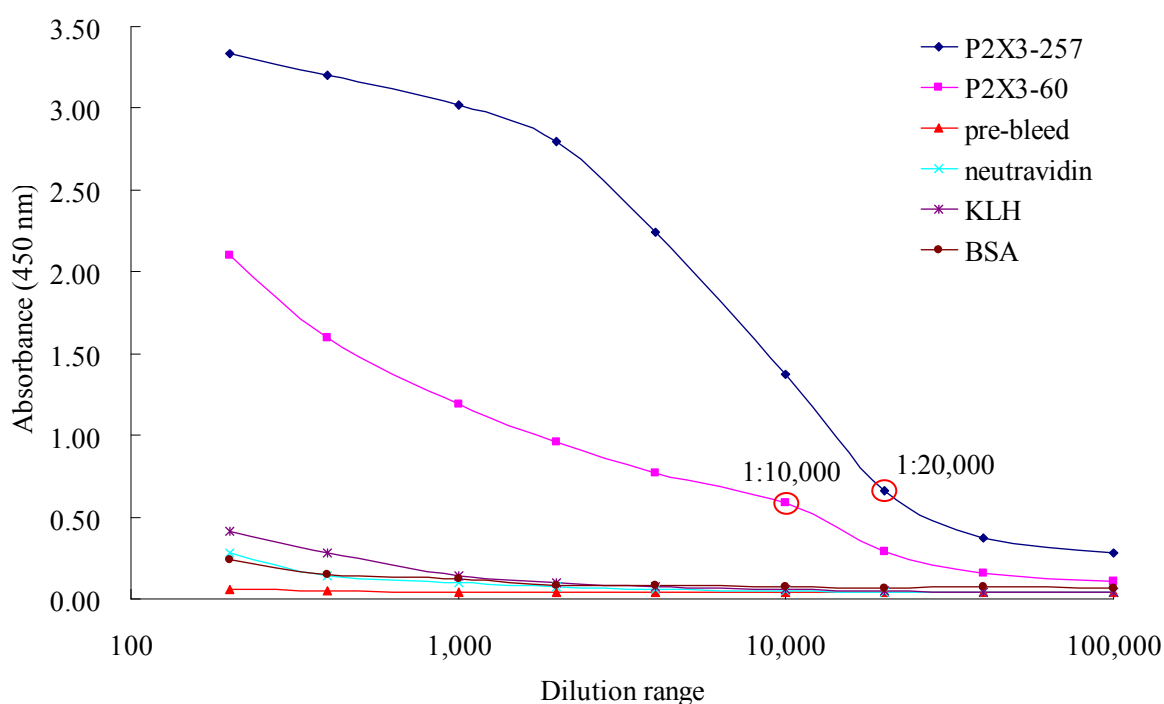
Fig. 4.1a Rabbit anti-P2X$_3$-60/257 antibody for titre after the fourth boost (P2X$_3$-60/257-biotin was applied for screening). An ELISA plate was coated with 5 µg/mL P2X$_3$-257-biotin conjugate. For competition, various dilutions of rabbit sera were added, followed by HRP-labelled anti-rabbit secondary antibody. Sera were diluted in 1% (w/v) BSA and 0.1% (w/v) KLH to 'deplete' potential cross reacting antibodies. The titre was 1:10,000 against P2X$_3$-60 and 1:20,000 against P2X$_3$-257.
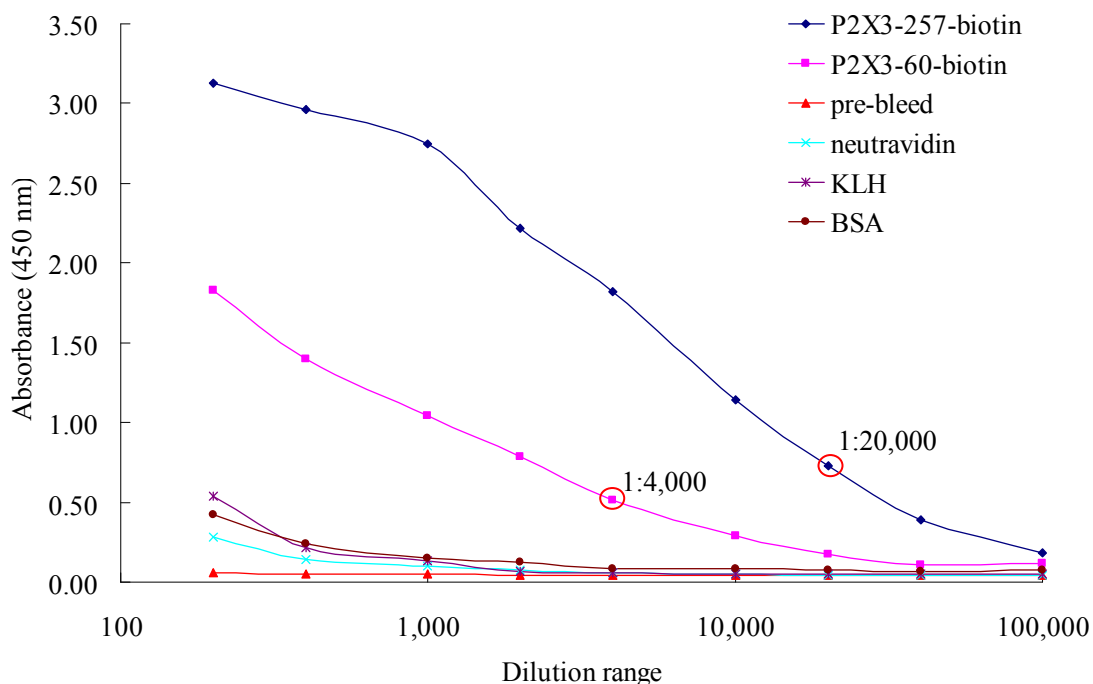
Fig. 4.1b Anibody titre to $P2X_3$-257 for rabbit-DARP after the fifth boost ($P2X_3$-60/257-biotin was applied for screening). An ELISA plate was coated with 5 µg/mL $P2X_3$-257-biotin conjugate. For competition, various dilutions of rabbit sera were added, followed by HRP-labelled anti-rabbit secondary antibody. Sera were diluted in 1% (w/v) BSA and 0.1% (w/v) KLH to 'deplete' potential cross reacting antibodies. The titre was 1:4,000 against $P2X_3$-60, and 1:20,000 against $P2X_3$-257.

To verify that the rabbit polyclonal antibody response for the injected $P2X_3$ ($P2X_3$-257) was also competitive, competitive ELISA with free $P2X_3$-257 and $P2X_3$-60 peptides was performed using the polyclonal sera (section 2.2.1.5). ELISA analysis revealed that the rabbit antibodies were competitive, which was shown by major reduction in signal in the presence of free competing peptide (Fig. 4.1c).

All of the titres and competitive ELISA results indicated a high level of specific mRNA for the creation of a recombinant anti-$P2X_3$-257 antibody library. However, there was a very low level titre against $P2X_3$-60. Thus, $P2X_3$-257 was chosen as the target for further experiments.
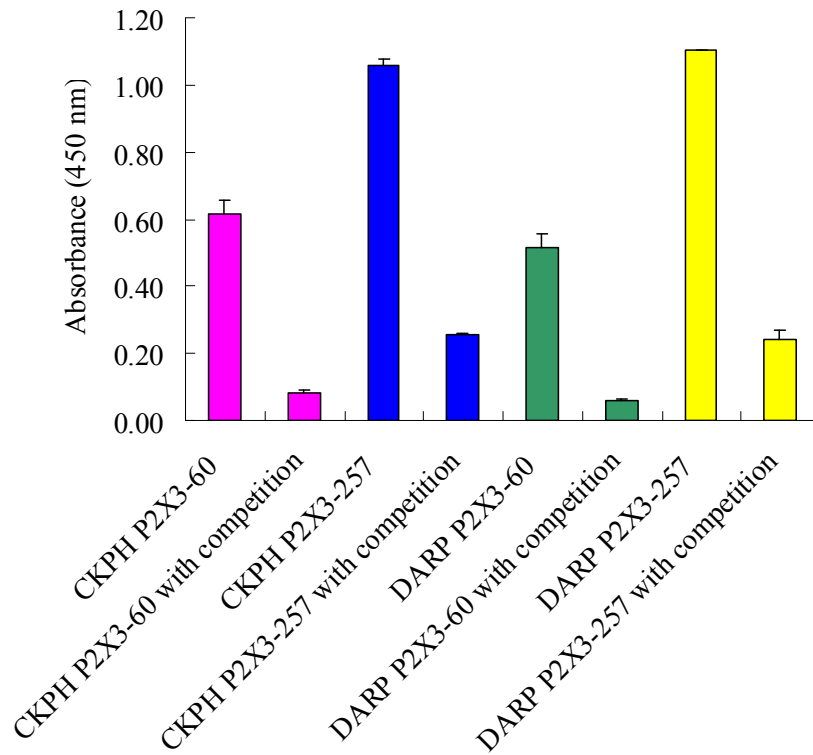
Fig. 4.1c Competitive ELISA analysis of rabbit sera specificity to $P2X_3$-60/257 after the fourth boost for CKPH and after the fifth boost for DARP. An ELISA plate was coated with 5 μg/mL $P2X_3$-257-biotin conjugate. For competition, the $P2X_3$-257/60 free peptide (25 μg/mL) was added to a fixed dilution (the dilution of $P2X_3$-257 was 1:20,000; the dilution of $P2X_3$-60 was 1:5,000) of sera. Sera were dissolved in 1% (w/v) BSA and 0.1% (w/v) KLH. HRP-labeled anti-rabbit IgG was applied as secondary antibody. Rabbit sera were shown to have antibody specific to $P2X_3$-60/257, which was demonstrated by a large decrease in signal response in the presence of free competing peptide. The results are the mean ± standard deviation (S.D.), where n = 3.

4.2.1.2 Purification and analysis of rabbit anti-P2X$_3$ polyclonal antibodies

Rabbit serum was purified using both Protein A and streptavidin-agarose (used to bind P2X$_3$-257/60-biotin to make a P2X$_3$-257/60 specific column), polyclonal IgG antibodies (pAbs) (section 2.2.2.1-2) and fractions containing protein were analysed using SDS-PAGE and Western blotting. SDS-PAGE indicated a high level of IgG purity after purification by the presence of two single bands, i.e. the light chain (~25 kDa) and heavy chain (~50 kDa) (Fig. 4.2a). Western blotting showed the purified IgG was specific to P2X$_3$ indicated by a P2X$_3$ specific band (Fig. 4.2b). In total, 8.67 mg of purified rabbit anti-P2X$_3$ IgG (1.7 mg/mL) were obtained.
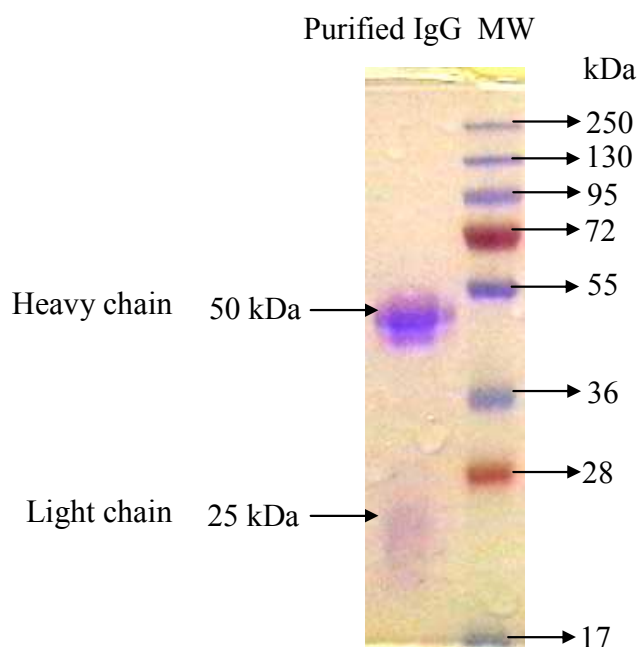
Fig. 4.2a SDS-PAGE analysis of rabbit (DARP) serum purified by protein A-sepharose followed by streptavidin-agarose resins. After purification, a high level of IgG purity was indicated by the presence of two single bands; the light chain (~25 kDa) and the heavy chain (~50 kDa). MW = molecular weight markers.
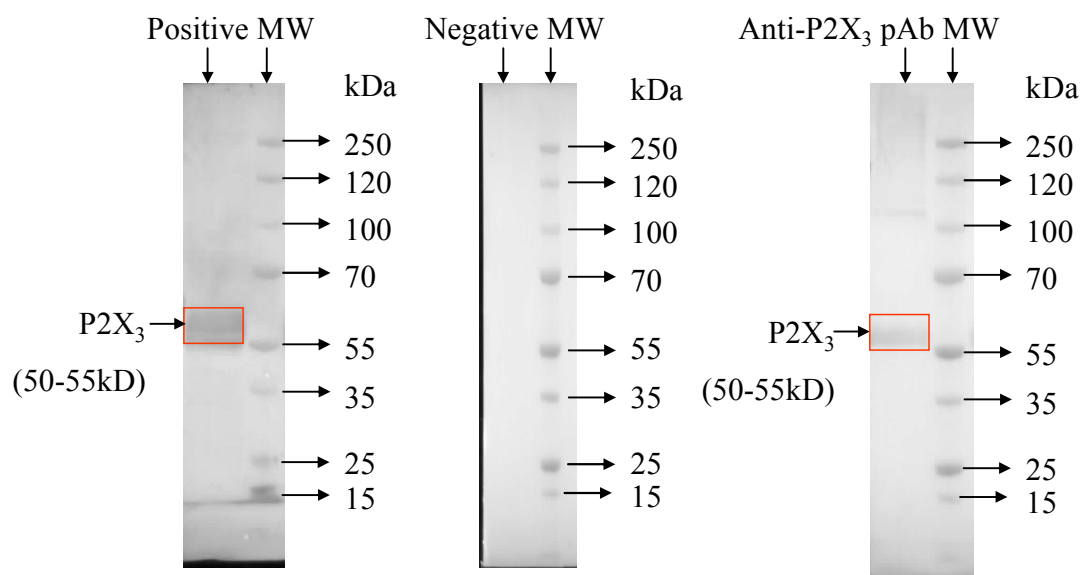
Fig. 4.2b Western blot analysis of polyclonal anti-P2X$_3$ antibodies specificity by applying rat DRG-expressed P2X$_3$. DRG samples were harvested from 2 days *in vitro* (2 DIV) culture. After Western blotting, the membranes were stained by purified anti-P2X$_3$ Ab (1:200 dilution), followed by HRP-labelled anti-rabbit secondary antibody (1:2,000 dilution). For the positive control, commercial anti-P2X$_3$ antibody was applied. For the negative control, rabbit anti-goat IgG (1:1,000 dilution) was added as the primary antibody instead of the anti-P2X$_3$ antibody. MW = molecular weight markers.

4.2.1.3 Examination of purified rabbit anti-P2X$_3$ polyclonal antibody specificity to rat DRG-expressed P2X$_3$

In order to analyze the specificity of rabbit anti-P2X$_3$ polyclonal antibodies to P2X$_3$ on rat DRG cells, DRG cultures grown in 24 wells plate for 5 days were fixed and incubated with rabbit anti-P2X$_3$ polyclonal antibodies, followed by addition of Alexa Fluor-488-labelled goat anti-rabbit secondary antibody (section 2.2.2.5.2). Samples were then viewed in an inverted microscope under both phase contrast and fluorescence modes using an Olympus IX71 microscope. Immunofluorescence staining further indicated purified IgG was specific to P2X$_3$ on DRG cultures by green fluorescence evident on DRG cell bodies. A similar result was shown with commercial rabbit anti-P2X$_3$ polyclonal antibody-stained DRG cells (Fig. 4.3). For the negative control,

anti-goat IgG was added as primary antibody instead of anti-P2X$_3$ antibody, and no DRG cells were stained as no green florescence was observed.
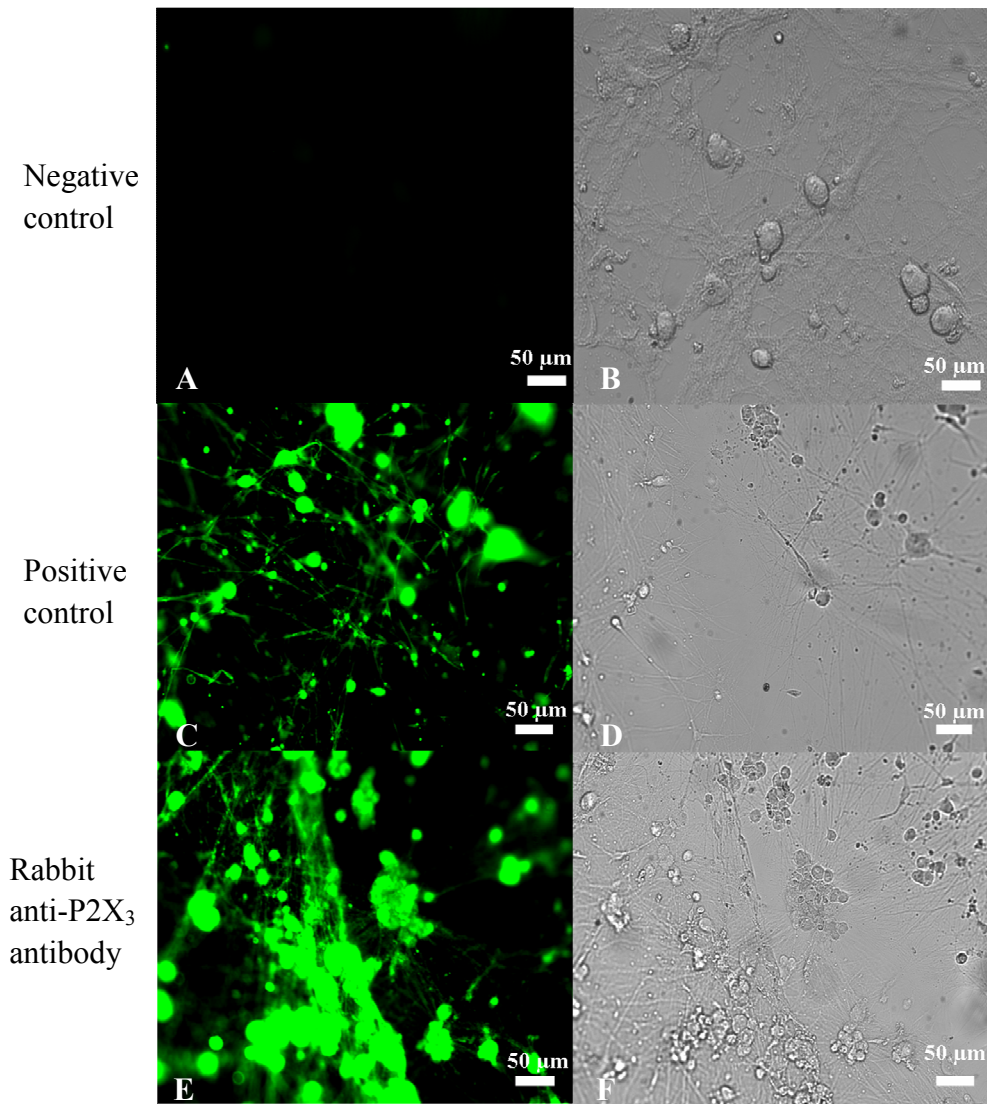
Fig. 4.3 Immunofluorescence-based microscopic analysis of anti-P2X$_3$ antibody binding in rat DRG culture cells (P4, 5 DIV). Samples were viewed in an inverted microscope by phase contrast (B, D and F) and in fluorescence modes (A, C and E). Rat DRG cells grown in 24 wells plate for 5 days were fixed, permeabilised and then stained by purified anti-P2X$_3$ pAbs (3.2 μg/well), followed by Alexa Fluor-488-labelled goat anti-rabbit secondary antibody (1:200 dilution) (E and F). For the negative control (A and B), anti-goat IgG (1:1,000 dilution) was added as primary antibody instead of anti-P2X$_3$ antibody (A and B). For positive control, commercial rabbit anti-P2X$_3$ Ab (1:50 dilution) was added instead of polyclonal anti-P2X$_3$ antibody (C and D). Original magnification x 20; scale bars are 50 μm.

4.2.1.4 Competitive ELISA analysis to determine the half-maximal inhibitory concentration (IC_{50}) of anti-P2X$_3$ polyclonal antibodies

In order to compare the binding of anti-P2X$_3$-257 IgG (after purification) with recombinant anti-P2X$_3$-257-scFv (which will be generated later), the half-maximal inhibitory concentration (IC_{50}) was measured by competing immobilised P2X$_3$-257-biotin with solution-phase P2X$_3$-257.

Anti-P2X$_3$-257 IgG was purified and the concentration of anti-P2X$_3$-257 IgG with an absorbance of approximately 1.00 was chosen as the primaryantibody (anti-P2X$_3$-257 IgG) concentration for competitive ELISA. The binding activity was evaluated by the IC_{50}: the concentration at which half-maximal inhibition of antibody-antigen interactions by competing antigen is achieved. With indirect competition ELISA, the value of IC_{50} for anti-P2X$_3$-257 Ig was approximately 20,000 ng/mL (Fig. 4.4).
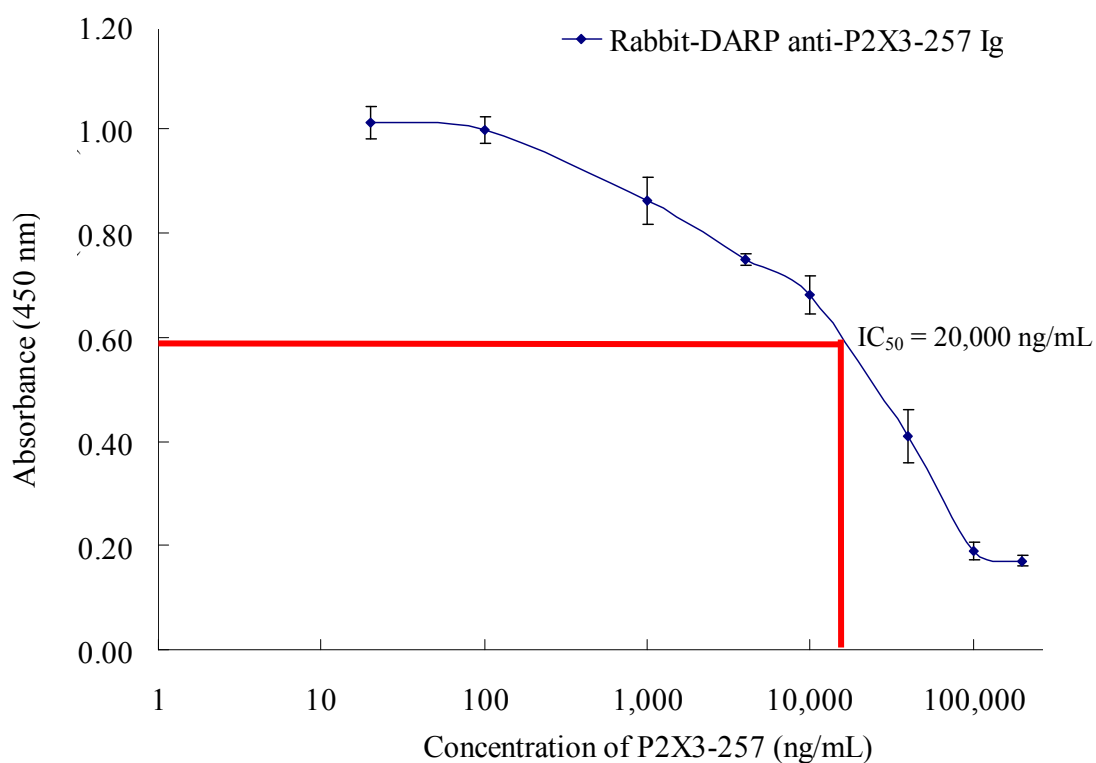
Fig. 4.4 Competitive ELISA analysis of IC_{50} of purified anti-P2X$_3$ polyclonal antibody. An ELISA plate was coated with 5 µg/mL P2X$_3$-257-biotin conjugate. The plate was blocked with 5% (w/v) milk in PBST. The P2X$_3$-257 free peptide was added at varying concentrations to a fixed concentration (400 µg/mL) of purified anti-P2X$_3$-257 Ig. This mixture (100 µL per well) was incubated for one hour at 37°C, followed by addition of HRP-labelled anti-rabbit secondary antibody (1:1,000 dilution). The IC_{50} for anti-P2X$_3$-257 Ig was approximately 20,000 ng/mL (8.70 nM). The results are the mean ± standard deviation (S.D.), for n=3.

4.2.1.5 Biotinylated anti-P2X$_3$ polyclonal antibodies specific to rat DRGs expressed P2X$_3$

Conjugation of rabbit anti-P2X$_3$ polyclonal antibodies to BoNT (which is conjugated with streptavidin) was necessary for proof of principle studies before fusion of anti-P2X$_3$-scFv with BoNT. The rabbit anti-P2X$_3$ polyclonal antibodies had first to be biotinylated. After biotinylation of anti-P2X$_3$

polyclonal antibodies with EZ-Link(R) micro Sulfo-NHS-LC-biotinylation kit (section 2.2.6.1), the specificity of biotinylated IgG to rat DRG-expressed P2X$_3$ was demonstrated by both Western blotting (Fig. 4.5a). Confocal microscopic studies were also applied to demonstrate biotinylated anti-P2X$_3$ antibody-specific binding to P2X$_3$, which is a transmembrane membrane protein as shown, by the striking red staining which outlined the surface of the DRG cells (Fig. 4.5b).
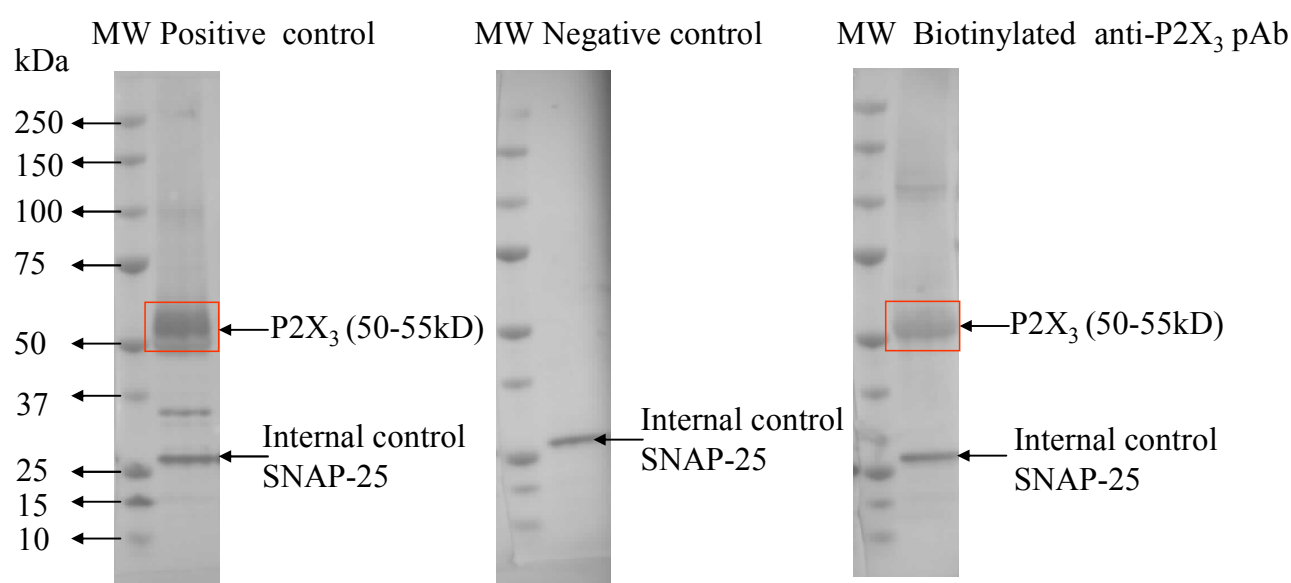
Fig. 4.5a Western blot analysis of biotinylated polyclonal anti-P2X$_3$ Ab specificity on rat DRG-expressed P2X$_3$. P2X$_3$ was harvested from 2 days *in vitro* (2 DIV) cultures and 160 µg of protein applied per lane. After Western blotting, the membranes were stained by biotinylated rabbit anti-P2X$_3$ antibody (20 µg) and mouse anti-SNAP-25 monoclonal antibody (1:1000 dilution), followed by HRP-labelled anti-rabbit secondary antibody (1:1,000 dilution) and HRP-labelled anti-mouse secondary antibody (1:1,000 dilution). For the positive control, commercial anti-P2X$_3$ antibody (1:300 dilution) was applied. For the negative control, anti-goat IgG (1:1,000 dilution) was added as primary antibody instead of anti-P2X$_3$ antibody. MW = molecular weight markers.
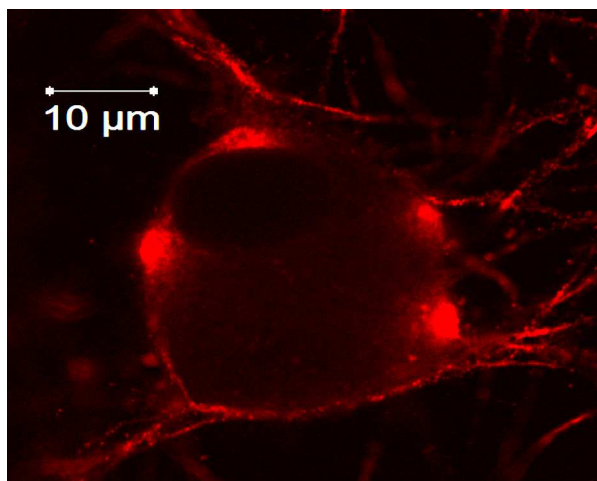
Fig. 4.5b Confocal micrograph analysis of biotinylated anti-P2X$_3$ antibody specific binding to P2X$_3$. Rat DRG cultures grown in 24 wells plate for 5 days were fixed and stained by biotinylated anti-P2X$_3$ antibody (3.2 µg/well), followed by Alexa Fluor-546-labelled goat anti-rabbit secondary antibody (1:200 dilution). Binding of the biotinylated anti-P2X$_3$ antibody specific to rat DRG-expressed P2X$_3$ (a membrane protein) was demonstrated by the striking red staining which clearly outlined the surface of the DRG cell body. Original magnification x 60.

4.2.1.6 Avidin-binding activity of biotinylated rabbit anti-P2X$_3$ polyclonal antibody

In order to demonstrate that biotinylated rabbit anti-P2X$_3$ polyclonal antibodies can bind BoNT-core streptavidin correctly, the avidin-binding activity was analyzed using direct ELISA. As described in section 2.2.6.2, ELISA plate was coated with neutravidin. A range of concentrations of biotinylated rabbit anti-P2X$_3$ polyclonal antibody or commercial biotinylated chicken anti-human IgG was prepared and added into separate wells, followed by the HRP-labelled anti-rabbit secondary antibody or HRP-labelled anti-chicken antibody. For the negative control, rabbit anti-P2X$_3$ polyclonal antibodies were added instead of biotinylated antibodies.

132

The biotinylated anti-P2X$_3$ polyclonal antibody limit of detection (LOD, three times greater than negative control) for neutravidin was 0.04 nM, which was very similar to the LOD of the commercial biotinylated anti-human antibody (Fig. 4.6). The avidin-binding activity of biotinylated rabbit anti-P2X$_3$ polyclonal antibody was then proved to be as good as the commercial source.
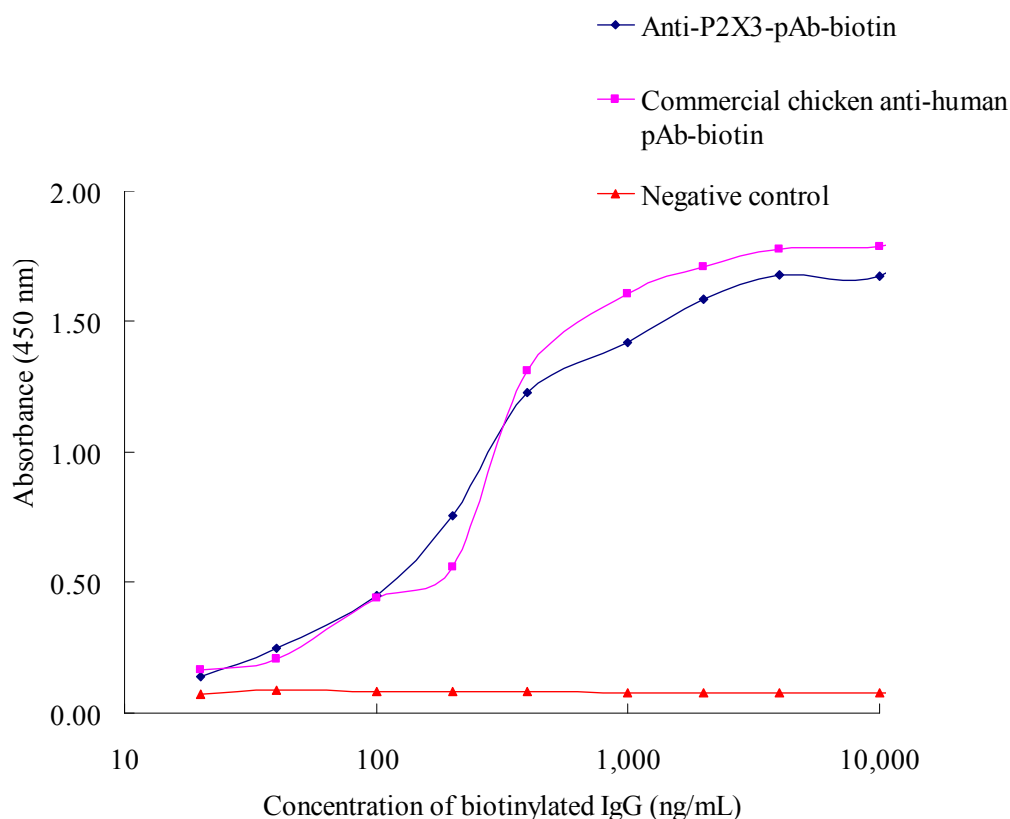
Fig. 4.6 Avidin-binding activity of biotinylated rabbit anti-P2X$_3$ polyclonal antibody. A 96-well ELISA plate was coated with neutravidin (2.5 µg/mL) and blocked with 5 % (w/v) PBSTM. A range of concentrations (20-10,000 ng/mL) of biotinylated rabbit anti-P2X$_3$ polyclonal antibody or commercial biotinylated chicken anti-human IgG was prepared and added into separate wells, followed by the HRP-labelled anti-rabbit secondary antibody (1:1,000 dilution) or HRP-labelled anti-chicken antibody (for positive control, 1:1,000 dilution). Both biotinylated rabbit anti-P2X$_3$ IgG and commercial biotinylated anti-human IgG gave similar binding profiles demonstrating that biotinylation of the rabbit anti-P2X$_3$ antibody was successfully achieved.

133

4.2.2 Generation of rabbit recombinant scFv antibodies

Due to the impressive performance of the purified rabbit anti-P2X$_3$ polyclonal antibody, it was decided to construct scFv recombinant libraries from the previously harvested bone marrow and spleen cDNA from both P2X$_3$-BSA/KLH immunised rabbits (CKPH and DARP).

In rabbit, very few antibody gene segments are rearranged and accessed during immune responses, which greatly reduces the number of PCR primers required for cloning of the entire immune repertoire (section 2.2.3.3.1). Consequently, each primer combination for the heavy and light chains was individually optimised and then combined in equimolar ratios for the SOE-PCR, which may lead to the overall library diversity being considerably enhanced.

4.2.2.1 Rabbit variable heavy and light chain amplification optimization

For rabbit CKPH, 4.8 mg spleen RNA and 1.6 mg bone marrow RNA were produced, and stored at -80°C. Spleen cDNA (600 μg) and bone marrow cDNA (445 μg) were generated and stored at -20°C. For DARP, 4.0 mg spleen RNA and 1.8 mg bone marrow RNA were produced and stored at -80°C. Six hundred μg spleen cDNA and 600 μg bone marrow cDNA was synthesized, and stored at -20°C. Before sacrifice, 50 mL serum was collected. Subsequently, the amplification of the variable heavy (V_H) and variable light (V_L) genes used rabbit spleen and bone marrow cDNA as template (Fig. 4.7).

The V_H and V_L amplifications were resolved on a 1% (w/v) agarose gel and single bands at 386-440 bp (V_H chain) and 375-402 bp (V_L chain) were observed (Fig.4.7a and Fig.4.7b). A large-scale PCR amplification was then performed, using the conditions described in section 2.2.3.4, for each of the variable chains in their respective buffers. Following purification of the VH and VL chains (see section 2.2.3.5), a SOE-PCR (section 2.2.3.6) was employed to fuse the two chains via a serine-glycine linker (Gly$_4$Ser)$_4$ resulting in the formation of the scFv fragment.
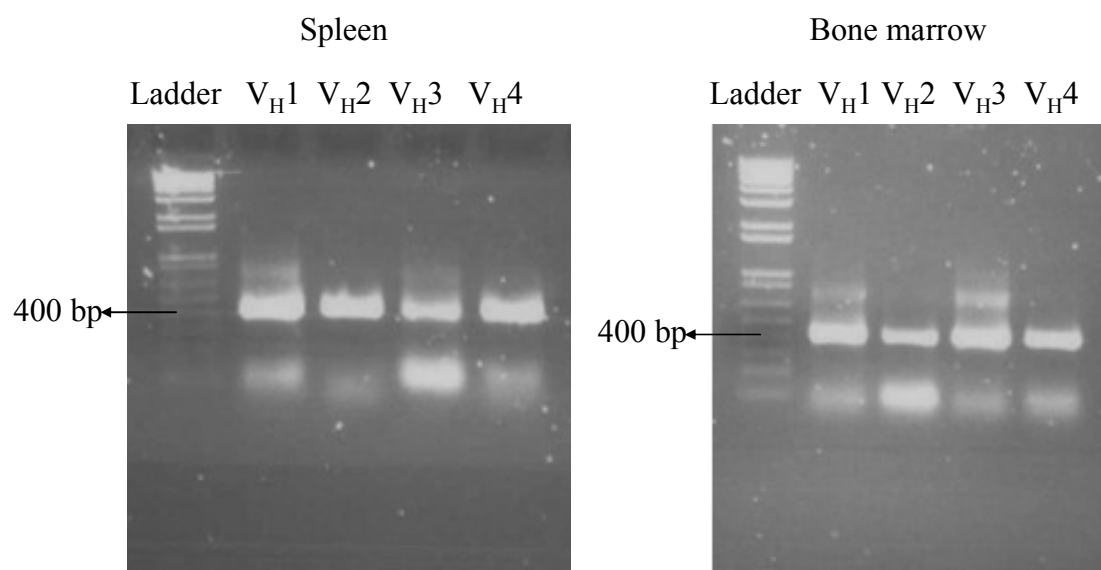
Fig. 4.7a PCR amplifications for the four variable heavy chains for both rabbit spleen and bone marrow libraries. Lanes V_H1-4 = heavy chains 1-4.

Spleen ($V_{\kappa 3}$ + 42JoB) Bone marrow ($V_{\kappa 3}$ + 42JoB)

Ladder 1.5 3   4 (mM MgCl$_2$)   Ladder 0   6% 8% 12% (DMSO)

400 bp◄

400 bp◄
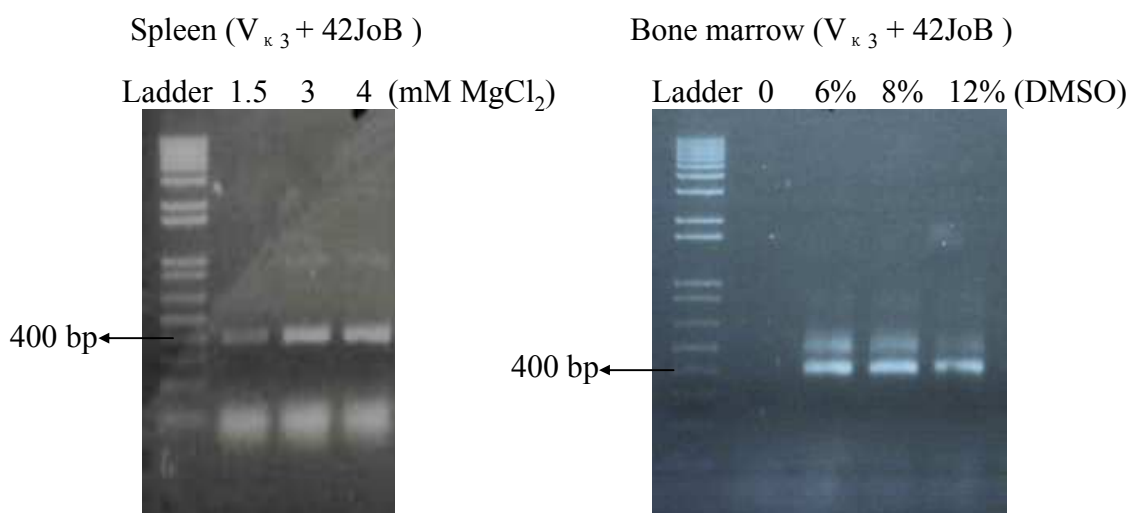
Fig. 4.7b Optimization of variable light (kappa) chains for both rabbit spleen and bone marrow. There are nine different primer combinations for rabbit spleen and bone marrow, respectively. Here one primer combination ($V_{\kappa 3}$+42JoB) for each of rabbit spleen and bone marrow variable light (kappa) chain is shown. For spleen $V_{\kappa 3}$+42JoB primer combination, 1.5 mM, 3 mM and 4 mM MgCl$_2$ was tested. A concentration of 3 mM MgCl$_2$ was selected for large-scale amplification as high amount of ligh chain product was already amplified with 3 mM MgCl$_2$, no higher concentration of MgCl$_2$ was needed. For the bone marrow $V_{\kappa 3}$+42JoB primer combination, 0, 6% (v/v), 8% (v/v) and 12% (v/v) DMSO concentrations were tested. A concentration of 6% (v/v) DMSO was selected for large-scale amplification.

4.2.2.2 SOE-PCR of variable heavy and light chains for rabbit library

Purified V_H and V_L fragments were linked with a glycine-serine linker (Gly$_4$Ser)$_4$ by SOE primers RSC-F and RSC-B (section 2.2.3.6) via PCR to generate the scFv fragment (~ 800 bp). The optimization shown below involved using various DMSO concentrations. A 1 kb Plus DNA molecular weight marker was added and several DMSO concentrations [2-12% (v/v)] were investigated (Fig. 4.8a). The PCR mixture with a final DMSO concentration of 10% (v/v) proved to be the most optimal (with the clearest

band at the correct position, 800 bp, with less non-specific bands). This was therefore used for the large-scale SOE-PCR of the scFv gene.

PComb3XSS vector was restriction digested with *Sfi*I using the protocol described in section 2.2.3.7. The digested pComb vector (~ 3,400 bp) and Stuffer fragments (~ 1,400 bp) as well as the PCR SOE (~ 800 bp) product were resolved on 1% (w/v) agarose gel (Fig. 4.8b).

Spleen (SOE)   Bone marrow (SOE)

Ladder 2% 4% 6% 8% 10% 12% (DMSO) Ladder 2% 4% 6%   8% 10% 12% (DMSO)
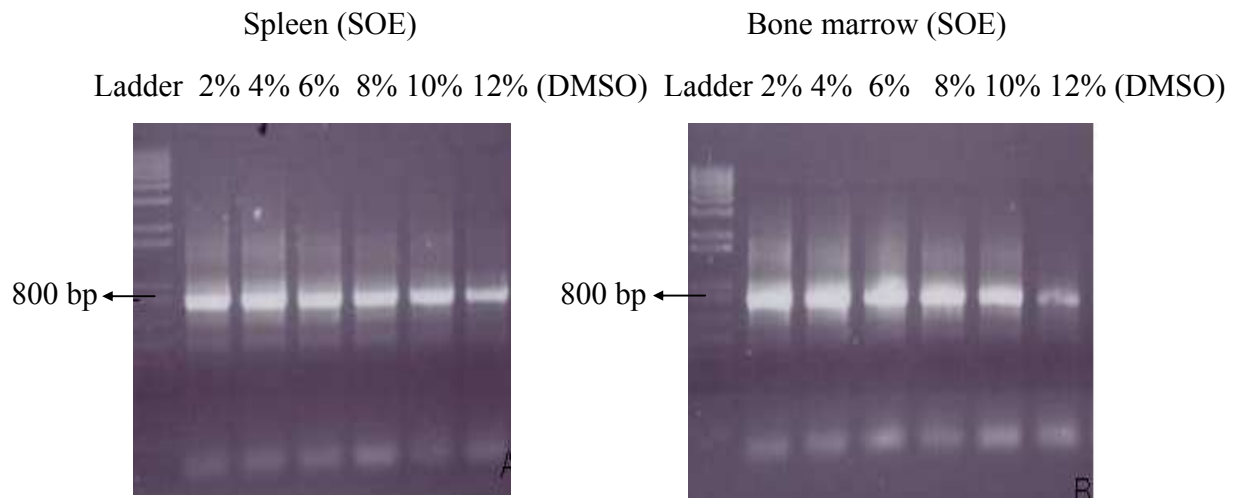
Figure 4.8a Optimization of SOE-PCR for both spleen (SP) and bone marrow (BM) scFv fragments. The PCR optimization was performed using a series of DMSO concentrations (2%, 4%, 6%, 8%, 10% and 12%). The annealing temperature was set at 56°C. The optimal condition selected was 10% DMSO.
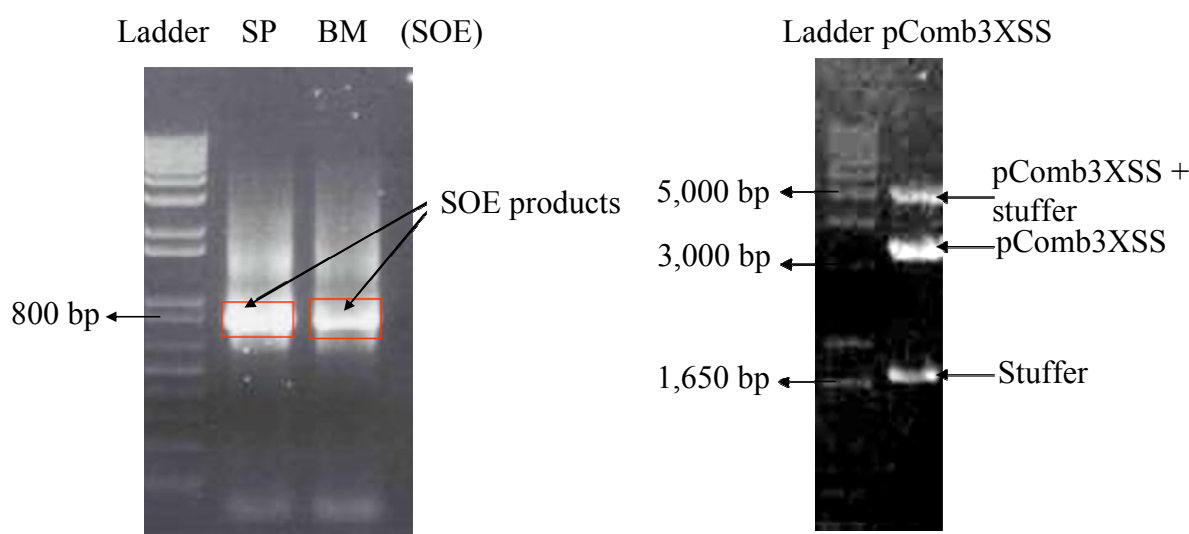
Fig. 4.8b A large-scale SOE-PCR was performed and the PCR product was extracted as described in section 2.2.3.5. A clear band (~ 800 bp) in lane SP and BM indicated the SOE-PCR product. In lane pComb3XSS, the upper band between 3,000 bp and 4,000 bp indicated the pComb3XSS vector and lower band near 1,650 bp marker band indicated the stuffer fragment. SP = spleen, BM = bone marrow.

4.2.2.3 Rabbit scFv library construction and subsequent enrichment via bio-panning

SOE PCR products were gel purified, digested, and ligated into pComb3XSS (section 2.2.3.5-2.2.3.7), which facilitates the expression, detection and purification of soluble scFv during phage display. The ligated sample was ethanol precipitated and then transformed into electrocompetent *E. coli* XL1-Blue cells by electroporation, as described in section 2.2.3.8.

Four transformed rabbit scFv libraries were generated and stored at -80°C. The rabbit-CKPH spleen scFv library size was 2.5×10^8 colony forming units (cfu)/mL; rabbit-CKPH spleen and bone marrow pre-mixed scFv library size: 3.5×10^9 cfu/mL and the DARP spleen scFv library size was 5×10^7 cfu/mL. The DARP bone marrow library size was 6.4×10^7 cfu/mL.

Recombinant rabbit anti-P2X$_3$-257 scFv colonies were successfully selected from the rabbit-DARP scFv library by performing five rounds of phage display biopanning (immunotube-based and streptavidin-labelled magnetic bead-based biopanning) against immobilised P2X$_3$–biotin conjugate as described in section 2.2.3.10 (Table 4.2a-b). However, rabbit-CKPH scFv were not successfully obtained after five rounds of phage display biopanning with conditions shown in table 4.3c.

Table 4.2a Immunotube-based biopanning with rabbit-DARP scFv library. Coated P2X$_3$-257-biotin concentrations, phage input and output titres of each round of biopanning are shown.

	[Neutravidin] nM	[P2X$_3$-257-biotin] Nm	Input	Output
Round 1	200	400	1.03×10^{13}	7.00×10^{5}
Round 2	100	200	7.90×10^{12}	1.30×10^{6}
Round 3	20	40	4.90×10^{12}	9.00×10^{4}
Round 4	10	20	7.30×10^{12}	6.00×10^{5}

Table 4.2b Streptavidin-labelled magnetic bead-based biopanning with rabbit-DARP scFv library. Coated P2X$_3$-257-biotin concentration, phage input and output titres of each round of biopanning are shown.

	[P2X$_3$-257-biotin] nM	[P2X$_3$-257-biotin] ug/mL	Input	Output
Round 1	400	1.00	1.03×10^{13}	1.80×10^{6}
Round 2	200	0.50	8.10×10^{12}	1.06×10^{6}
Round 3	40	0.10	1.03×10^{13}	4.00×10^{5}
Round 4	20	0.05	1.06×10^{13}	1.20×10^{6}

Table 4.2c Immunotube-based biopanning with rabbit-CKPH scFv library. Coated P2X$_3$-257-biotin concentration, phage input and output titres of each round of biopanning are shown.

	[Neutravidin] nM	[P2X$_3$-257-biotin] nM	Input	Output
Round 1	10,000	20,000	5.00×10^{12}	9.70×10^{5}
Round 2	1,000	2,000	7.50×10^{12}	1.50×10^{5}
Round 3	400	800	8.60×10^{12}	1.80×10^{5}
Round 4	40	80	1.85×10^{13}	2.00×10^{5}
Round 5	20	40	4.00×10^{13}	8.00×10^{4}

Phage output titres may indicate successful enrichment of specific scFv, since increasing numbers of phage should remain bound to the antigen which will lead to higher output titres. After comparison of Table 4.3a, Table 4.3b and Table 4.3c, the output titres for both immunotube-based and streptavidin-labelled magnetic beads-based biopanning of rabbit-DARP scFv library (10^{6}) were almost 100 times higher than that of immunotube-based biopanning of rabbit-CKPH scFv library (10^{4}). This may suggest successful enrichment of specific scFv with rabbit-DARP scFv library, while unsuccessful enrichment of specific scFv with rabbit-CKPH scFv library, which needs to be further examined by both polyclonal and monoclonal phage ELISA.

4.2.2.4 Rabbit polyclonal phage ELISA

The precipitated input phage particles from each round of panning were then tested for P2X$_3$-257 binding via a polyclonal phage ELISA (section 2.2.3.10). Phage pools were dissolved in sterile 1% (w/v) BSA and 0.1% (w/v) KLH to 'deplete' potential cross-reacting scFvs. All the phage pools were analyzed against P2X$_3$-257-biotin, P2X$_3$-257-BSA, neutravidin, bovine serum albumin (BSA), keyhole limpet hemocyanin (KLH) (BSA and KLH were conjugated to immunise P2X$_3$-257). Neutravidin, BSA and KLH-coated wells were used to identify cross-reactivity.

The scFv-displaying phage were detected using a HRP-conjugated mouse anti-M13 secondary antibody (1:1,000 dilution) and the absorbance read at 450 nm following a 20 min incubation with TMB. The increase of absorbance from the second round (Fig. 4.9a) suggested the enrichment of $P2X_3$-257-specific scFvs. Little binding was observed against neutravidin, BSA or KLH.

The largest enrichment of anti-$P2X_3$-257 polyclonal phage pool were detected in the fourth round of phage panning for both immunotube-based and streptavidin-labelled magnetic bead-based biopanning of the rabbit-DARP scFv library (Fig. 4.9a). No enrichment of anti-$P2X_3$-257 polyclonal phage pool was observed for the rabbit-CKPH scFv library (Fig. 4.9b).
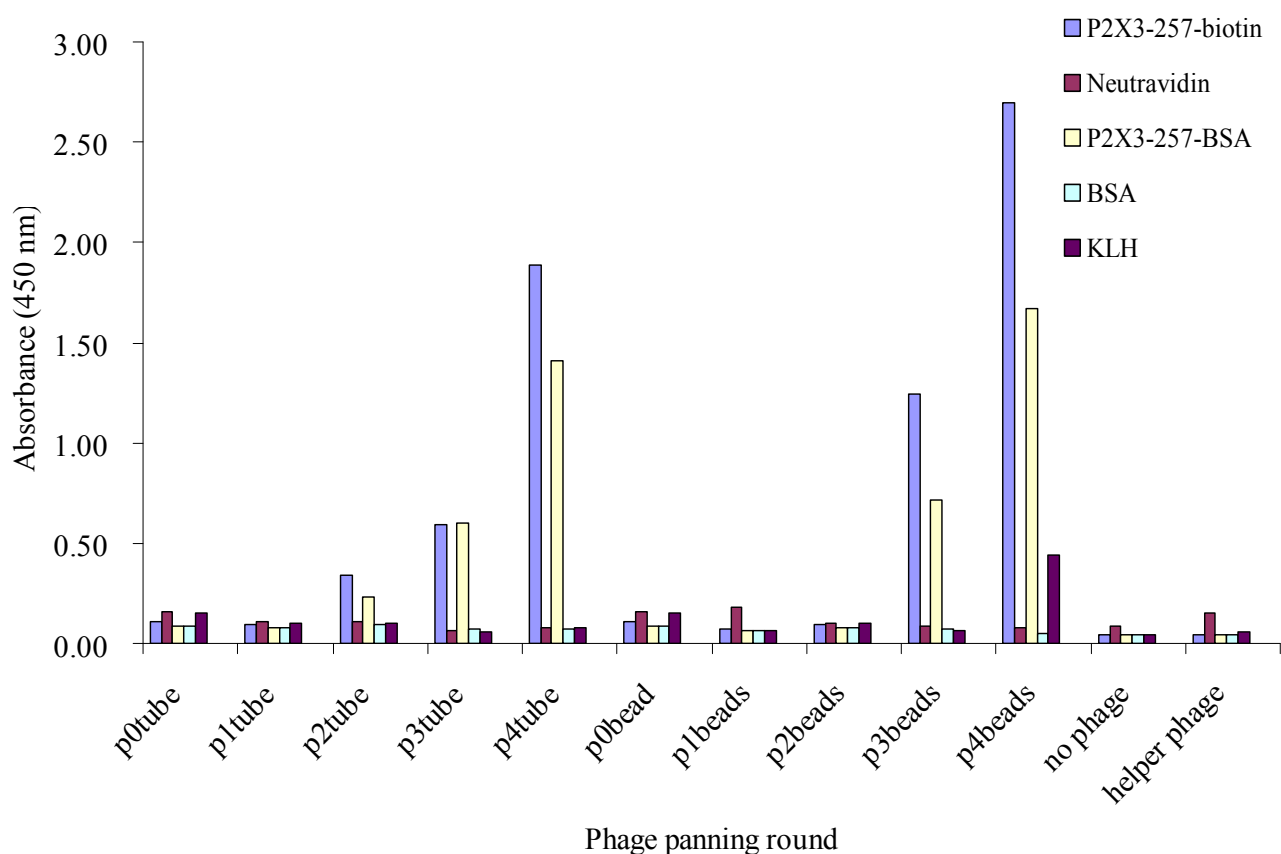
Fig. 4.9a Polyclonal phage ELISA involving all precipitated phage input samples from each round of panning of the rabbit DARP anti-P2X$_3$-257 scFv library. The phage pools from each round of panning were tested in a direct ELISA format against the biotin and BSA conjugates of the target antigen (P2X$_3$-257). Neutravidin, BSA and KLH were also tested as negative controls. Bound phage was detected with the HRP-conjugated anti-M13 secondary antibody and the absorbances measured at 450 nm. A significant absorbance signal increased in round 3 and 4 suggesting the presence of anti-P2X$_3$-257 scFv-phage fragments. P0 = before panning, P1-4 = phage panning round 1-4.
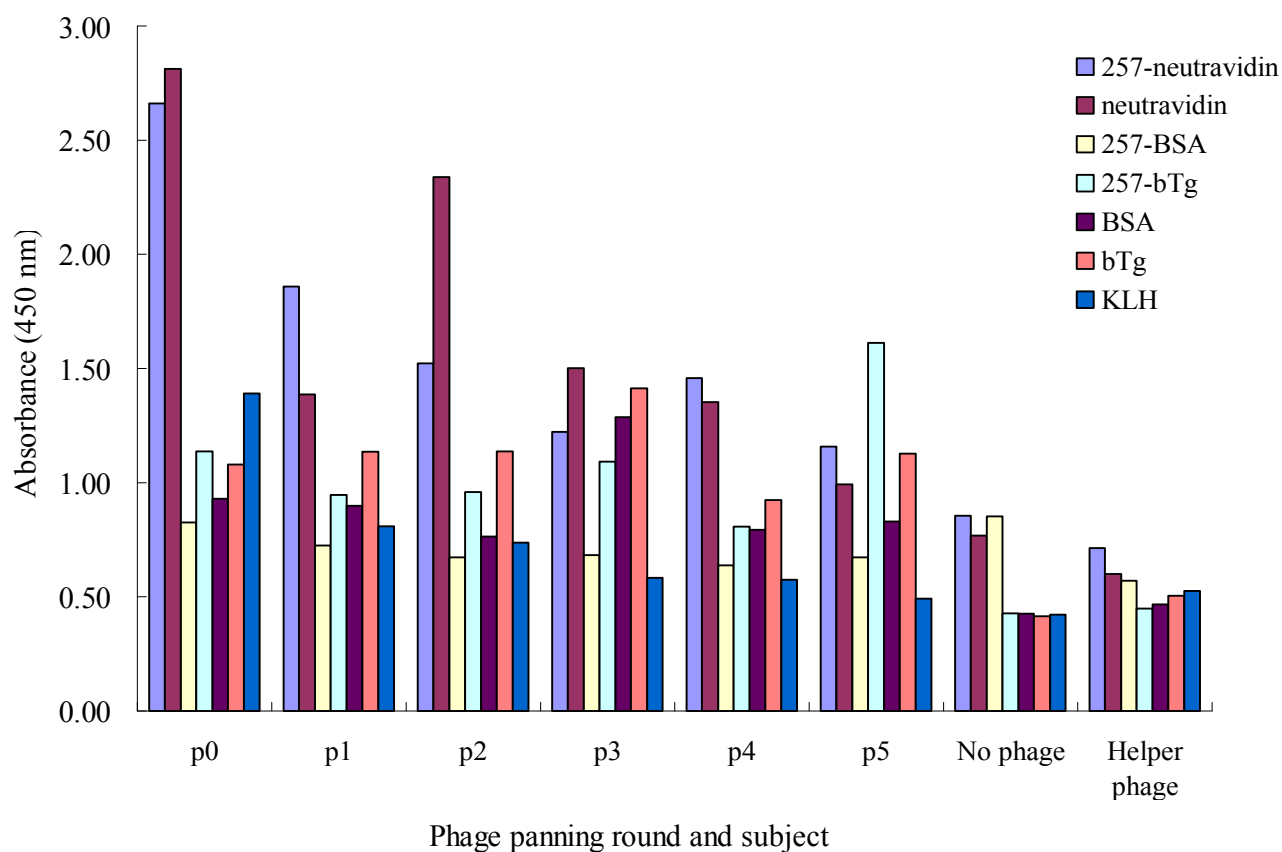
Fig. 4.9b Polyclonal phage ELISA involving all precipitated phage input samples from each round of panning of rabbit CKPH anti-P2X$_3$-257 scFv library. The phage pools from each round of panning were tested in a direct ELISA format against the biotin and BSA and bTg conjugates of target antigen (P2X$_3$-257). Neutravidin, BSA, KLH and bTg were used as negative controls. Bound phage was detected with an HRP-conjugated anti-M13 secondary antibody and the absorbance read at 450 nm. No significant absorbance signal increased in pan five suggested no presence of anti-P2X$_3$-257 scFv-phage fragment. P = Phage, P0-5 = Phage from round 0-5.

4.2.2.5 Soluble expression, direct ELISA and inhibition ELISA of rabbit anti-P2X$_3$ scFv colonies

At this stage, scFvs expressed in XL1-Blue contained the gene*III* product (pIII) which was used in phage display selection but may cause problem with scFv unsoluble expression. The pIII needed to be deleted for scFv soluble expression, which can be achieved in Top10F´ cells. Therefore, the pan 4 output phage was infected into Top10F´ cells (section 2.2.3.12) for analysis of solubly expressed scFv colonies via monoclonal ELISA (section 2.2.3.13).

189 single colonies were then grown, solubly expressed and incorporated into a direct ELISA to identify scFv candidates for specificity analysis. The scFv-enriched lysate was tested against P2X$_3$-257-biotin, the target protein. HRP-labelled anti-HA antibody (1:2,000 dilution) was added as secondary antibody. Figure 4.10 showed up to 51% of colonies had absorbance values more than three-fold higher than that of the negative controls, namely, neutravidin, BSA, KLH. Hence, 51% of scFv colonies have the capacity to bind P2X$_3$-257.
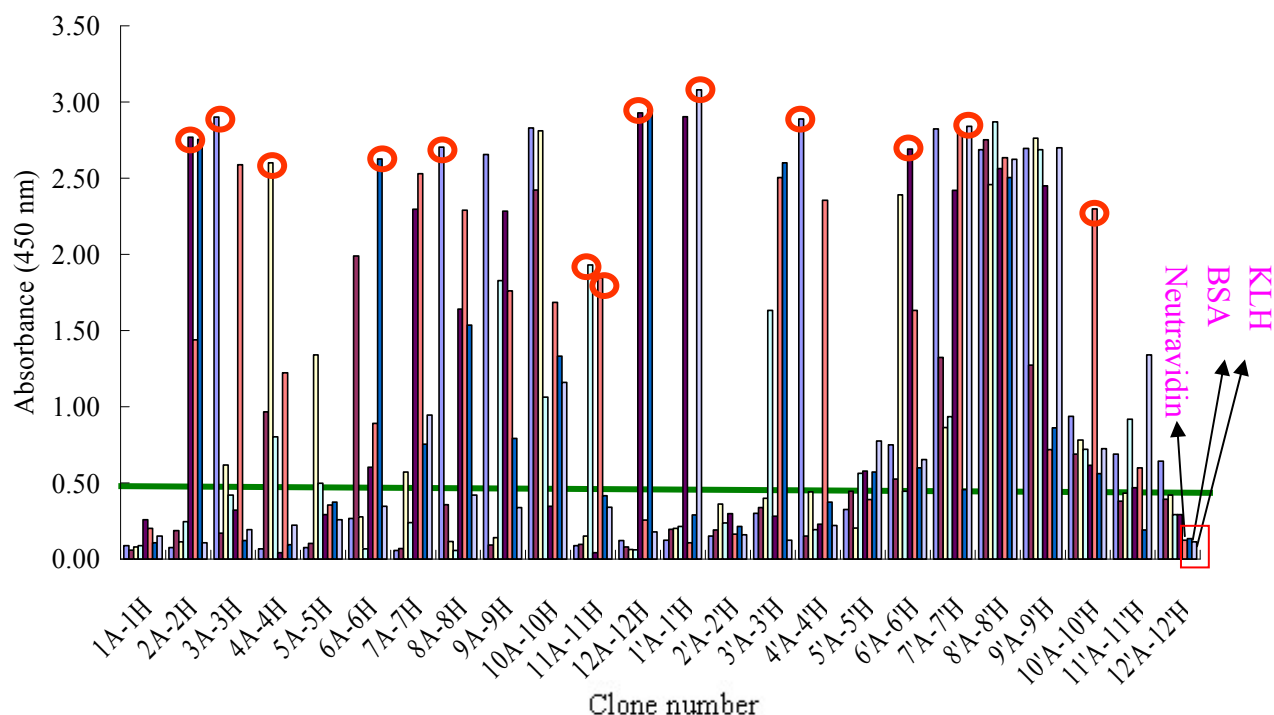
Fig. 4.10 Direct soluble ELISA involving scFv-enriched lysates expressed by 189 rabbit scFv clones against P2X3-257-biotin after 5 rounds of biopanning. A green horizontal line marked at the absorbance value of 0.5 indicated the background level (three fold of negative controls: neutravidin, BSA, KLH). 97 positive clones were detected indicating that 51% of the total colonies showed positive binding against P2X$_3$-257. Each vertical bar represents a single anti-P2X$_3$-257 scFv antibody. The red circles represent the clones chosen for further experiment.

4.2.2.6 Cross-reactivity analysis of the soluble anti-P2X$_3$-257 scFv antibodies

For cross-reactivity analysis, 13 positive colonies selected from the previous step were tested against P2X$_3$-257-biotin, P2X$_3$-257-BSA, neutravidin and BSA (section 2.2.3.13). All the 13 clones showed no cross-reactivity to the carrier protein (BSA) or detection protein (neutravidin), but shown specific binding to P2X$_3$-257 (Fig. 4.11).

145
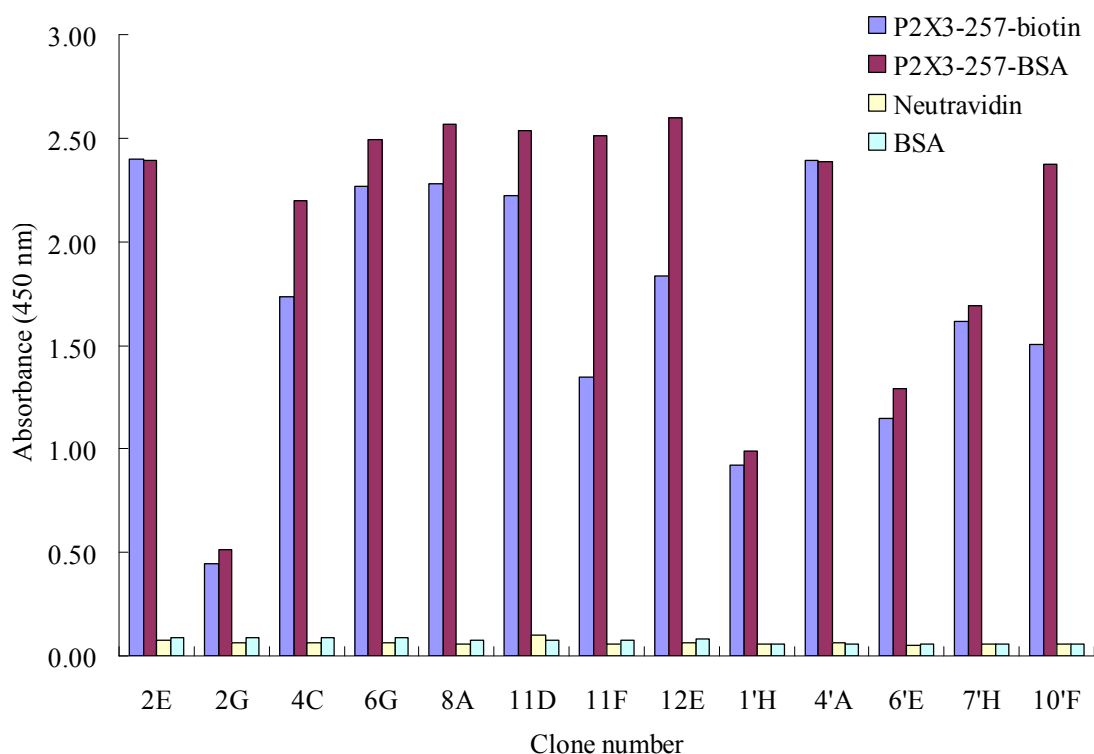
Fig. 4.11 ELISA analysis of cross-reactivities of anti-P2X$_3$-257 scFv antibodies. Crude bacterial lysate was used as the primary antibody and HRP-labelled anti-HA antibody (1:2,000 dilution) was added as secondary antibody. The 96-well plate was coated with either 2 µg/mL P2X$_3$-257-biotin, P2X$_3$-257-BSA, neutravidin or BSA. All 13 antibodies bound specifically to P2X$_3$-257 without cross-reaction to BSA or neutravidin.

4.2.2.7 Diversity analysis of panned rabbit scFv library via restriction mapping

'Restriction mapping' of the scFv genes provided a simple method for analyzing the diversity of the enriched library. It involved amplification of the scFv gene using a 'colony-pick' PCR (Fig. 4.12a) to prove the 10 randomly picked colonies contained scFv insert fragments (~ 800 bp). The negative control produced no scFv insert fragments, indicating the absence of any potential contamination.

146

The high-frequency cutting enzymes *Alu*I was applied for digesting each of the successfully amplified scFv gene products, and produced a restriction pattern specific to each different scFv gene sequence (Fig. 4.12b). High clonal heterogeneity, which was observed within the enriched library, indicated a high level of scFv antibody diversity (section2.2.3.14).

Ladder N   C1   C2 C3   C4   C5   C6   C7   C8   C9 C10
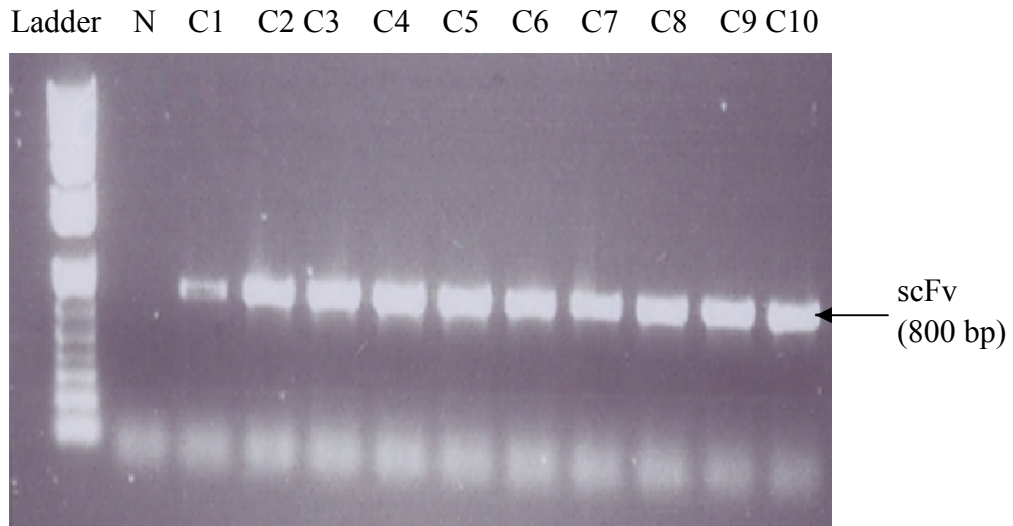
scFv
(800 bp)

Fig. 4.12a 'Colony-pick' PCR showed amplification of 10 scFv gene inserts from rabbit anti-P2X$_3$ scFv colonies. Lane 1 contained 1 Kb Plus DNA molecular weight ladder (Invitrogen), lane 2 contained the negative control (without scFv colony) and lanes 3-11 contained scFv insert amplifications from randomly selected colonies. N = negative control and lanes C1-10 = clones 1-10.
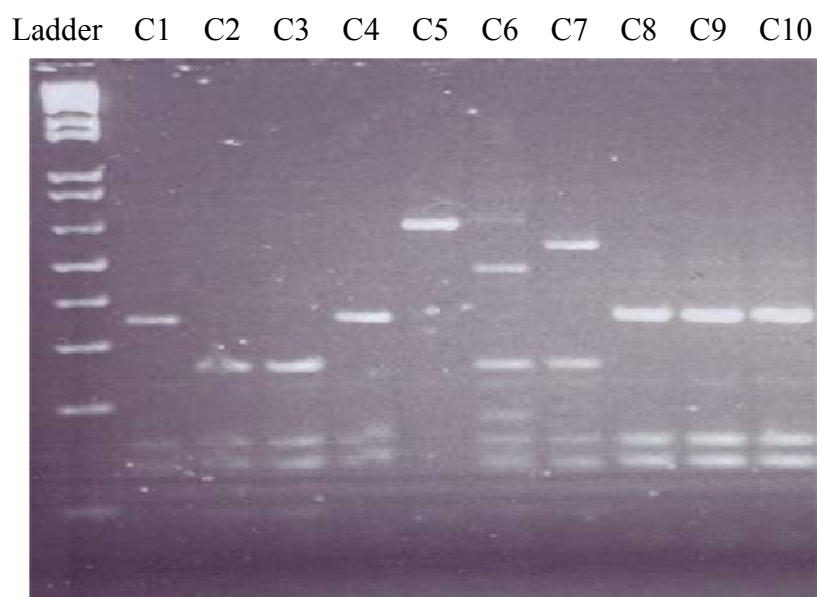
Fig. 4.12b Restriction mapping profile of 10 rabbit scFv gene inserts. Lane 1 contained 1 Kb Plus DNA molecular weight ladder (Invitrogen) and lanes 2-11 contained scFv gene inserts cut with the high-frequency cutting enzyme *Alu*I. Lanes C1-10 = clone 1-10.

4.2.2.8 Sequence alignment of eleven randomly selected rabbit anti-P2X$_3$ scFv fragments

To avoid inter-contamination of scFv colones, three of positive colones (D11, F10, F11 and H7) from step 3.2.2.6 were chosen for re-plating LB agar plates (100 g/mL carbenicillin) to obtain single colonies. After overnight incubation at 37°C, single coloines were picked to culture for sequencing.

Plasmids extracted from overnight culture of single colonies D11A-D, F10A-D, F11A-D and H7A-D were sequenced by Source BioScience. Five colonies could not be sequenced (perhaps their plasmids were not successfully extracted or purified or they were contaminated) but the remaining eleven scFv colonies gave three distinctly different sequences and one heterogeneity existed in the complementary-determining (CDR) regions. These two sequences were then applied for further experiments (F11A and H7C). All the CDR regions, linker, His-tag, HA-tag and differences among them are shown in Fig. 4.13.

Alignment (residues 1–80)

CDR-L1 | **CDR-L2**

```
              10         20         30         40         50         60         70         80
         ....|....|....|....|....|....|....|....|....|....|....|....|....|....|....|....|
D11A     VMTQTPSS ASEPVGGTVT INCQASQSVY RONYLSWFQQ KPGQPPKLLI YKASTLASGV PSRFRGSGSG TQFTLTISDVQC
D11F     VMTQTPSS ASEPVGGTVT INCQASQSVY RONYLSWFQQ KPGQPPKLLI YKASTLASGV PSRFRGSGSG TQFTLTISDVQC
F10A     VMTQTPSS ASEPVGGTVT INCQASQSVY RONYLSWFQQ KPGQPPKLLI YKASTLASGV PSRFRGSGSG TQFTLTISDVQC
F10B     VMTQTPSS ASEPVGGTVT INCQASQSVY RONYLSWFQQ KPGQPPKLLI YKASTLASGV PSRFRGSGSG TQFTLTISDVQC
F10D     VMTQTPSS ASEPVGGTVT INCQASQSVY RONYLSWFQQ KPGQPPKLLI YKASTLASGV PSRFRGSGSG TQFTLTISDVQC
F11A     DLTQTPSS ASEPVGGTVT INCQASQSVY RONYLSWFQQ KPGQPPKLLI YKASTLASGV PSRFRGSGSG TQFTLTISDVQC
F11C     DLTQTPSS ASEPVGGTVT INCQASQSVY RONYLSWFQQ KPGQPPKLLI YKASTLASGV PSRFRGSGSG TQFTLTISDVQC
F11D     DLTQTPSS ASEPVGGTVT INCQASQSVY RONYLSWFQQ KPGQPPKLLI YKASTLASGV PSRFRGSGSG TQFTLTISDVQC
F11E     DLTQTPSS ASEPVGGTVT INCQASQSVY RONYLSWFQQ KPGQPPKLLI YKASTLASGV PSRFRGSGSG TQFTLTISDVQC
H7A      VMTQTPSS ASEPVGGTVT INCQASQSVY RONYLSWFQQ KPGQPPKLLI YKASTLASGV PSRFRGSGSG TQFTLTISDVQC
H7C      VMTQTPSS ASEPVGGTVI INCQASQSVY RONYLSWFQQ KPGQPPKLLI YKASTLASGV PSRFRGSGSG TQFTLTISDVQC
Clustal Co :*:***** ********** ********** ********** ********** ********** ********** ***********
```

Alignment (residues 81–160)

CDR-L3 | **Linker** | **CDR-H1**

```
              90         100        110        120        130        140        150        160
         ....|....|....|....|....|....|....|....|....|....|....|....|....|....|....|....|
D11A     DDAATYYC AGSTGIDDHD TDFGGGTEVV VKSSGGGGSG GGGGGSSRSS QSVEBSGGRL VTPGTPLTVT CTASGFSLGFFD
D11F     DDAATYYC AGSTGIDDHD TDFGGGTEVV VKSSGGGGSG GGGGGSSRSS QSVEBSGGRL VTPGTPLTVT CTASGFSLGFFD
F10A     DDAATYYC AGSTGIDDHD TDFGGGTEVV VKSSGGGGSG GGGGGSSRSS QSVEBSGGRL VTPGTPLTVT CTASGFSLGFFD
F10B     DDAATYYC AGSTGIDDHD TDFGGGTEVV VKSSGGGGSG GGGGGSSRSS QSVEBSGGRL VTPGTPLTVT CTASGFSLGFFD
F10D     DDAATYYC AGSTGIDDHD TDFGGGTEVV VKSSGGGGSG GGGGGSSRSS QSVEBSGGRL VTPGTPLTVT CTASGFSLGFFD
F11A     DDAATYYC AGSTGIDDHD TDFGGGTEVV VKSSGGGGSG GGGGGSSRSS QSVEBSGGRL VTPGTPLTVT CTASGFSLGFFD
F11C     DDAATYYC AGSTGIDDHD TDFGGGTEVV VKSSGGGGSG GGGGGSSRSS QSVEBSGGRL VTPGTPLTVT CTASGFSLGFFD
F11D     DDAATYYC AGSTGIDDHD TDFGGGTEVV VKSSGGGGSG GGGGGSSRSS QSVEBSGGRL VTPGTPLTVT CTASGFSLGFFD
F11E     DDAATYYC AGSTGIDDHD TDFGGGTEVV VKSSGGGGSG GGGGGSSRSS QSVEBSGGRL VTPGTPLTVT CTASGFSLGFFD
H7A      DDAATYYC AGSTGIDDHD TDFGGGTEVV VKSSGGGGSG GGGGGSSRSS QSVEBSGGRL VTPGTPLTVT CTASGFSLGFFD
H7C      DDAATYYC AGSTGIDDHD TDFGGGTEVV VKSSGGGGSG GGGGGSSRSS QSVEBSGGRL VTPGTPLTVT CTASGFSLGFFD
Clustal Co ******** ********** ********** ********** ********** *:******* ********** ***********
```

Fig. 4.13 Sequence alignment of 11 rabbit anti-P2X$_3$-257 scFv antibodies. The three CDR regions for variable light (CDR-L) regions are highlighted in yellow; and variable heavy (CDR-H) regions are highlighted in gray. The glycine-serine linker, highlighted in red, fused the variable heavy and light regions together. A hexa-histidine tag (pink) and a HA epitope tag (dark green) were incorporated at the carboxyl (C) terminus of the scFv fragment for purification and characterization. Five amino acid differences (blue) were observed among these sequences and one difference exist in the CDR regions.

4.2.2.9 Anti-P2X$_3$-257 scFv F11A and H7C purification using IMAC

The two rabbit anti-P2X$_3$-257 scFv colonies (F11A and H7C) whose sequences varied in the CDR regions were expressed in large-scale and then purified by IMAC (section 2.2.3.15). Highly pure scFv fragments from both colonies were obtained after IMAC purification, with little non-specific protein contamination as indicated by few contaminating bands (Fig. 4.14).
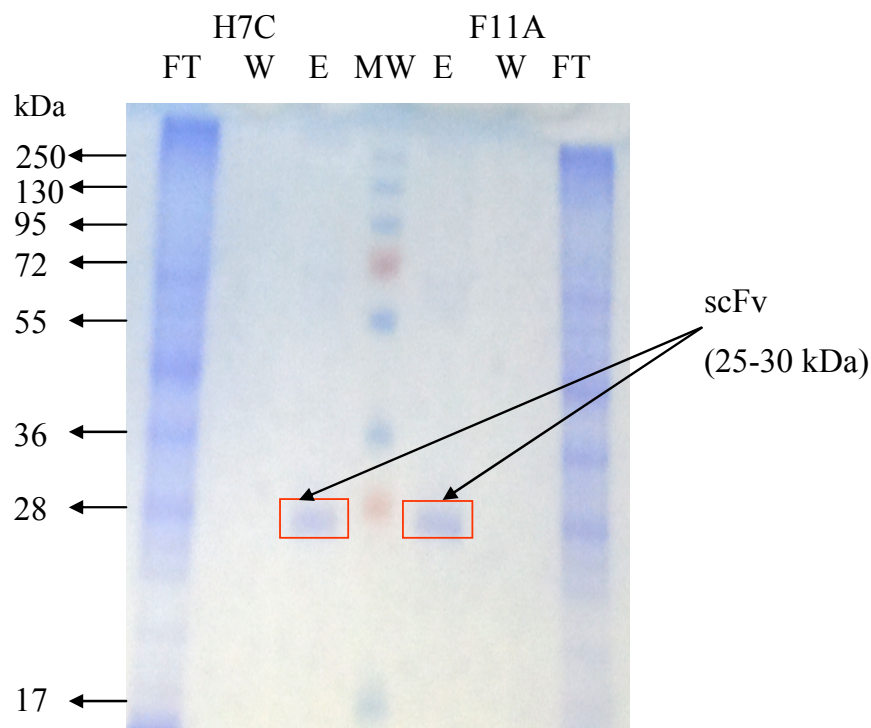
Fig. 4.14 SDS-PAGE analysis of anti-P2X$_3$-257 scFv antibody colonies (F11A and H7C) purified by IMAC. The elution fraction (E) contained bands of 25 kDa (scFv), which indicated anti-P2X$_3$-257 scFv antibody fragments were successfully extracted and purified. The presence of band around 25 kDa in lane E indicated the anti-P2X$_3$-257 scFv antibodies were extracted and purified successfully. MW = molecular weight markers; F-T = 'flow-through'; W = wash; E = elution. F11A and H7C = Rabbit anti-P2X$_3$-257 scFv clone F11A and H7C.

4.2.2.10 Titres and IC$_{50}$ of anti-P2X$_3$-257 scFvs testing via ELISA

The titres of anti-P2X$_3$-257 scFvs (H7C and F11A) were analyzed using crude lysate against P2X$_3$-257-biotin as described in section 2.2.3.16. The titre (three times greater than the background in wells containing control protein, neutravidin) for F11A was 1:100, and for H7C was 1:400 (Fig. 4.15a).

The binding affinity was evaluated by IC$_{50}$: (the concentration at which half-maximal inhibition of antibody-antigen interactions by competingantigen is achieved). With indirect competition ELISA (with competing free P2X$_3$-257 peptide), the value of IC$_{50}$ for anti-P2X$_3$-257 scFvs H7C and F11A was approximately 100 (0.04 nM) and 120 ng/mL (0.05 nM), respectively (Fig. 4.15b).
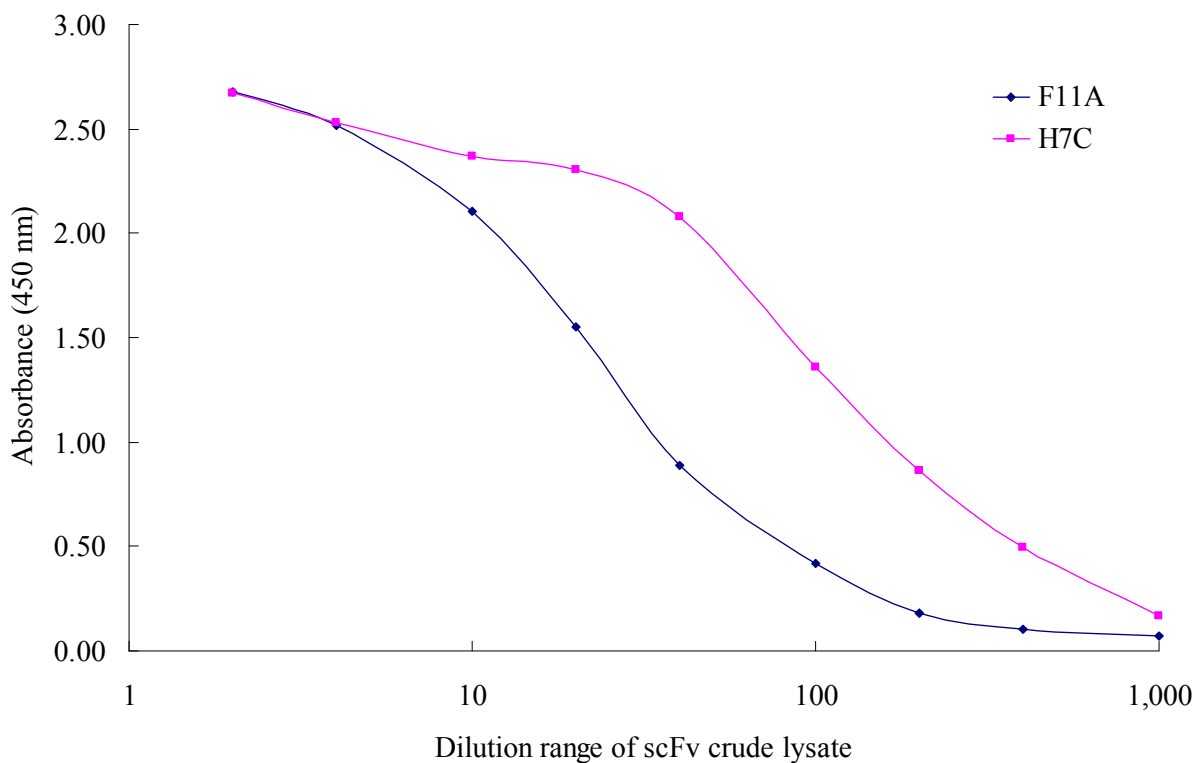
Fig. 4.15a Direct ELISA analysis of titres of anti-P2X$_3$-257 scFv antibody from colonies F11A and H7C. An ELISA plate was coated with 5 µg/mL P2X$_3$-257-biotin conjugate. A series of dilutions ranging from 1:2 to 1:1,000 of the crude lysate were diluted in 1 x PBST. HRP-labeled anti-HA antibody (1:2,000 dilution) was applied as secondary antibody. The titre was 1:100 for F11A, and 1:400 for H7C as the titres were determined as the lysate dilutionrequired to produce a signal 3 times greater than the background signal. F11A and H7C = Rabbit anti-P2X$_3$-257 scFv clone F11A and H7C.
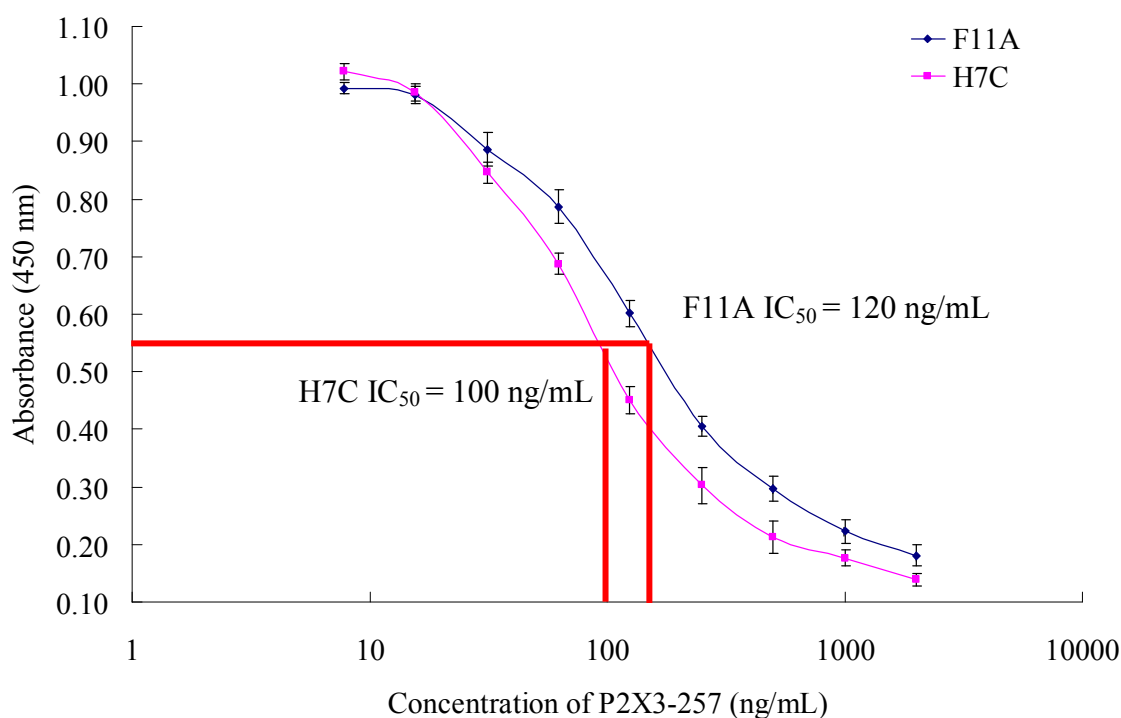
Fig. 4.15b Competitive ELISA analysis of IC_{50} of anti-P2X$_3$-257 scFv antibody colonies F11A and H7C. An ELISA plate was coated with 5 µg/mL P2X$_3$-257-biotin conjugate and blocked with 5% (w/v) milk in PBST. Various concentration of P2X$_3$-257 free peptide (2, 4, 10, 20, 40, 100, 200, 400, 1,000, 2,000 ng/mL) was added to a fixed concentration of anti-P2X$_3$-257 scFvs (H7C, 10,000 ng/mL; F11A, 20,000 ng/mL). HRP-labeled anti-HA antibody was applied as secondary antibody. The IC_{50} was 100 ng/mL (0.04 nM) for H7C and 120 ng/mL (0.05) for F11A. F11A and H7C = two different rabbit anti-P2X$_3$-257 scFv colonies. F11A and H7C = Rabbit anti-P2X$_3$-257 scFv clone F11A and H7C. The results are the mean ± standard deviation (S.D.), where n=3.

4.2.2.11 Rabbit scFv stability was analysed and compared with different storage conditions

As the H7C scFv showed a higher titre than the F11A scFv, H7C was chosen for further experiments. The purified H7C scFv stability was analysis by storage at five different conditions:

(1) In 1 volume of glycerol at 4°C.

(2) In 1% (w/v) BSA at 4°C.

(3) In 10% (v/v) protein inhibitor cocktail (p.i.c.) at 4°C.

(4) In 1% (w/v) BSA +1% (v/v) protein inhibitor cocktail at 4°C.

(5) In 1% (w/v) BSA at -80°C.

After analyzing scFv titre against $P2X_3$-biotin using ELISA (section 2.2.3.18) on day 1, day 19, day, day 30, day 60 and day 90, scFv was proved to be stable for three months in conditions (1) (2) and (5), after three months, using ELISA against $P2X_3$-biotin with a titre of around 1:100 (Fig. 4.16).
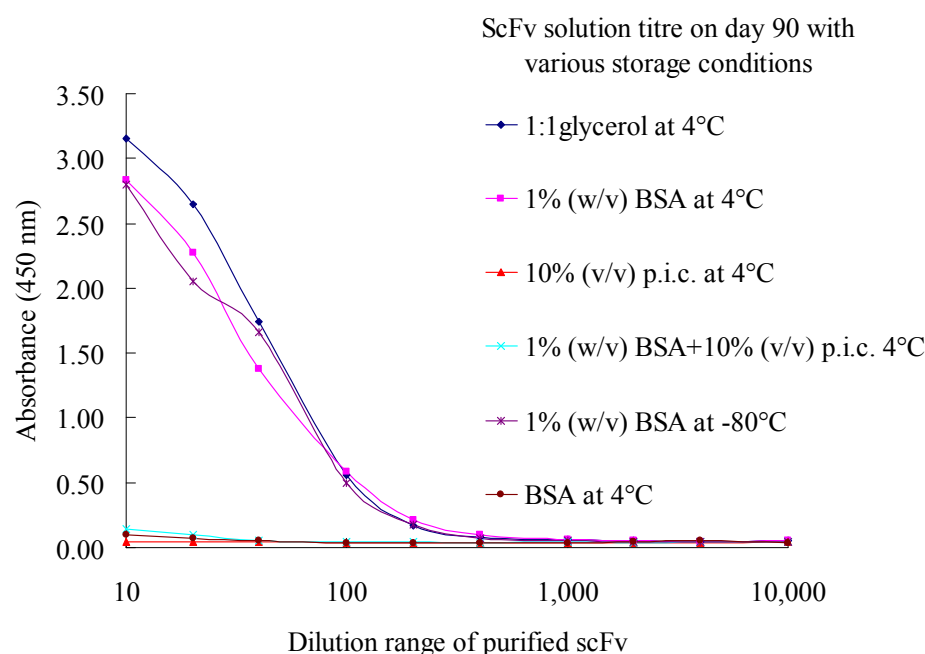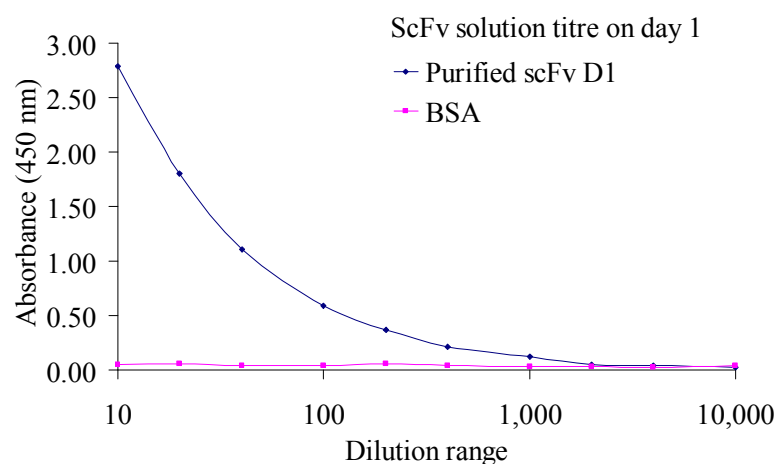
Fig. 4.16 ELISA analysis of scFv stability by titring scFv after three months. 5 μg/mL P2X$_3$-257-biotin was coated overnight at 4°C. An ELISA plate was coated with 5 μg/mL P2X$_3$-257-biotin conjugate and blocked with 5% (w/v) milk in PBST. A range of scFv dilution was performed and then applied scFv as primary antibody, followed by HRP-labelled anti-HA secondary antibody (1:2,000 dilution). H7C anti-P2X$_3$-257 scFv was stable at following three conditions after three months using ELISA against anti-P2X$_3$-biotin with titre around 1:100 [scFv: glycerol = 1: 1 (v: v) at 4°C; scFv with 1% BSA (w/v) at 4°C and scFv with 1% BSA (w/v) at -80°C].

4.2.3 Generation of mouse recombinant scFv antibodies

Mouse can generate anti-human antibody with great antibody diversity and only around 6 weeks were needed for immunization to achieve best immune response (which is about 12 weeks for rabbit). For these reasons, mice were also chosen for recombinant anti-human $P2X_3$ scFv antibodies generation.

4.2.3.1 Mouse serum antibody titre

The immunisation procedure for mice was followed as described in section 2.2.1.2. Three mice were immunised with $P2X_3$-257-BSA conjugate and another three were immunised with $P2X_3$-60-BSA conjugate. Bleeds were taken seven days after the final boost, and the serum anti-$P2X_3$ titre was performed using a direct ELISA format to detect IgG antibodies against two $P2X_3$ extracellular domains, $P2X_3$-257 and $P2X_3$-60 (section 2.1.6.1). An ELISA plate was coated with 5 µg/mL $P2X_3$-257/60-biotin conjugate. A series of dilutions ranging from 1:500 to 1:4,000,000 of the mouse sera in 1 x PBST were tested against $P2X_3$-60/257-biotin in a direct ELISA format [the sera were diluted using 1% (w/v) BSA to 'deplete' potential cross reacting antibodies]. HRP-labeled anti-mouse IgG was applied as the secondary antibody.

For mouse number 1 the sera titre (three times greater than the background in wells containing control proteins, neutravidin and BSA) against $P2X_3$-60 was 1:20,000 and for mouse number 2 and 3 was 1:20,000. The sera titre of mouse number 4 and 5 against $P2X_3$-257 was 1:400,000 (Fig. 4.17), which indicated a good immune response. This would infer production of mRNA suitable for the creation of a recombinant anti-$P2X_3$-257 antibody library. However, there was a lower level titre against $P2X_3$-60. Thus, an anti-$P2X_3$-257 scFv may be generated from mice.
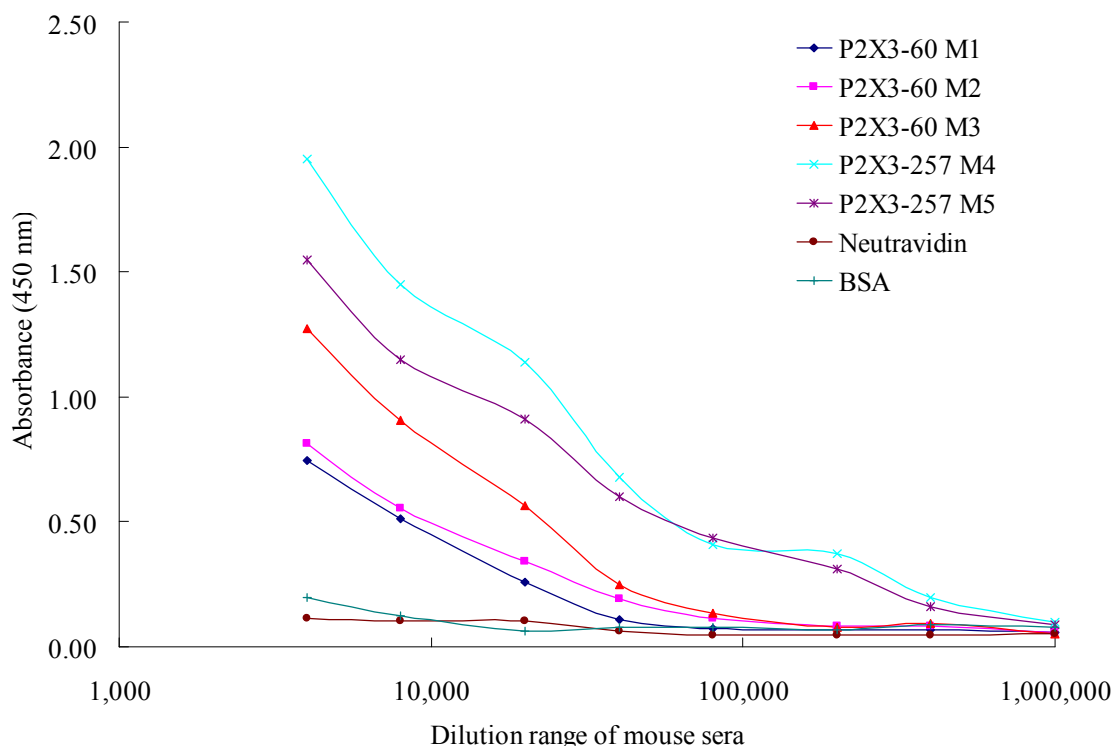
Fig. 4.17 Mouse anti-P2X$_3$-257/60 antibody titre after the 4th boost (2 μg/mL P2X$_3$-257/60-biotin was coated for screening). The titre for anti-P2X$_3$-257 Ab was 1:400,000, and the titre for anti-P2X$_3$-60 Ab was from 1:40,000 to 1:80,000. P2X$_3$-60 M1, M2 and M3 = P2X$_3$-60 immunised mouse numbers 1 to 3, P2X$_3$-257 M4 and M5 = P2X$_3$-257 immunised mouse numbers 4 and 5

4.2.3.2 Optimization of mouse variable heavy and light chain amplification

Mice were sacrificed after the fourth boost, and total RNA extracted from the spleens and then reverse transcribed to cDNA. RNA (8.4 mg) and cDNA (0.39 mg) were obtained from the P2X$_3$-257 immunised mice and 6.9 mg RNA and 0.32 mg cDNA were obtained from the P2X$_3$-60 immunised mice. RNA was stored at -80°C and cDNA stored at -20°C.

Subsequently, the amplification of the variable heavy (V$_H$) and variable light (V$_L$) genes using mice spleen cDNA as template (section 2.2.3.3.2) was performed. The V$_H$ and V$_L$ amplifications were resolved on a 1% (w/v) agarose

gel and single bands at 386-440 bp (V_H chain) and 375-402 bp (V_L chain) were observed (Fig.4.18). A large-scale PCR amplification was then performed, using the conditions described in section 2.2.3.4, for each of the variable chains in their respective buffers.
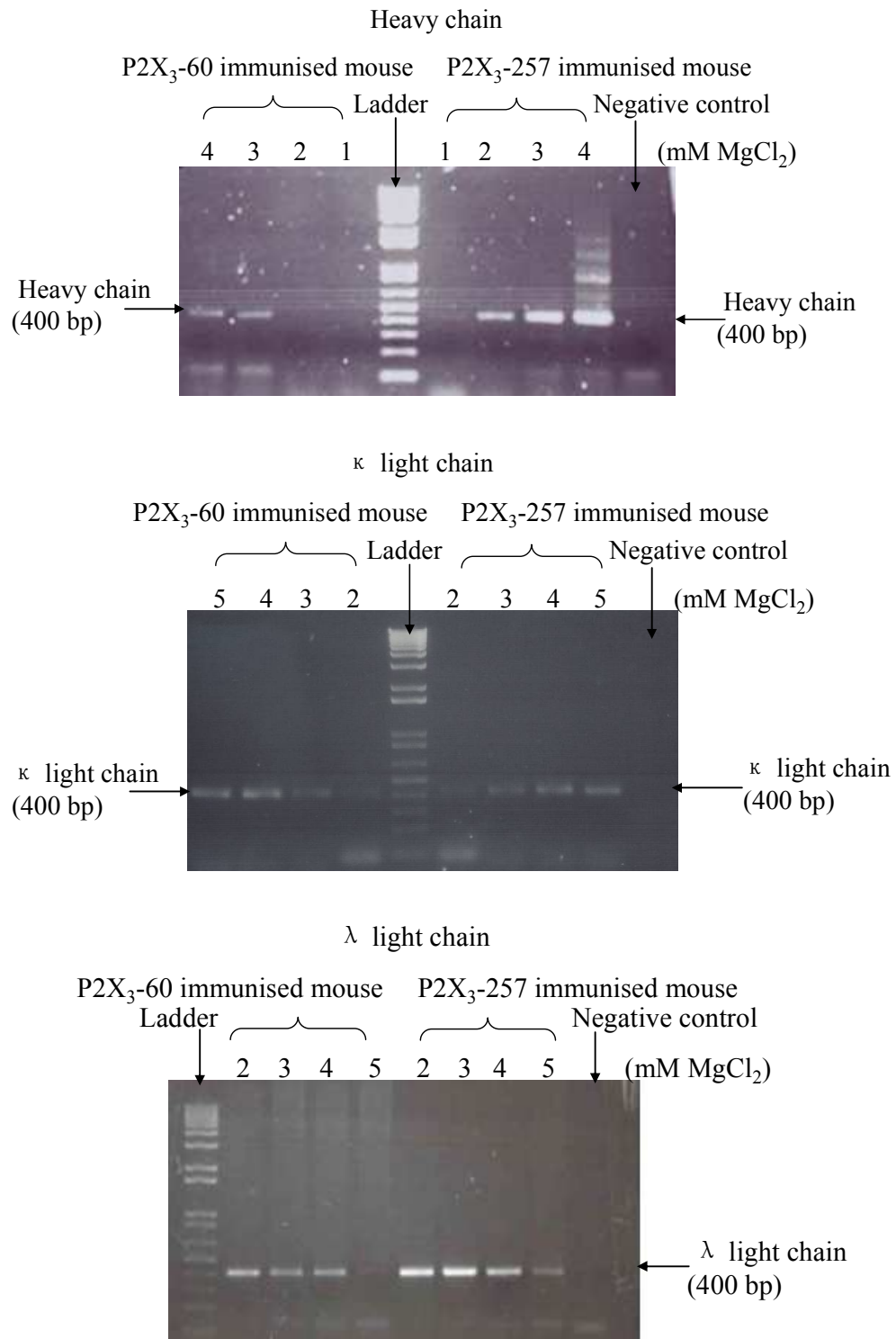
Fig. 4.18 Selection of optimal magnesium concentration for variable V_H and V_L (κ and λ light chains) gene amplification. The magnesium concentrations selected for amplification 3 mM for the variable heavy chain, 2 mM for the κ chain and 4 mM for the λ light chain. Lanes 1-5 = clones 1-5.

4.2.4 Generation of chicken polyclonal antibodies

As chickens can achieve better immune responses to human proteins than rabbit and mouse, based on their phylogenetical distance and it is more convenient to harvest large amounts of IgY from egg yolk, chickens were chosen to anti-human $P2X_3$-257/60 antibody generation.

4.2.4.1 Chicken serum titre

Four female chickens were immunised as described in section 2.2.1.3. One chicken died before any injection; another chicken was immunised with $P2X_3$-60-KLH conjugate and the other two were immunised with $P2X_3$-257-BSA conjugate. Chicken bleeds were taken seven days after the third boost and the serum anti-$P2X_3$ titre was performed using a direct ELISA format to detect IgG antibodies against the two $P2X_3$ extracellular domains, $P2X_3$-257 and $P2X_3$-60 (section 2.1.6.1).

An ELISA plate was coated with 5 µg/mL $P2X_3$-257/60-biotin conjugate. A series of dilutions ranging from 1:500 to 1:4,000,000 of the avian serum diluted in 1 x PBST were tested against $P2X_3$-60/257-biotin in a direct ELISA format [the sera were diluted using 1% (w/v) BSA or 0.1% KLH (w/v) to 'deplete' potential cross reacting antibodies]. HRP-labeled anti-chicken IgY was applied as the secondary antibody.

All the three immunized chickens gave low specific responses to $P2X_3$ after the third boost as indicated by the serum titre obtained (Fig. 4.19a-c) (titre was three times greater than the background in wells containing control proteins, BSA and KLH). Thus, neither polyclonal antibody purification nor RNA extraction was performed after the chickens were sacrificed.
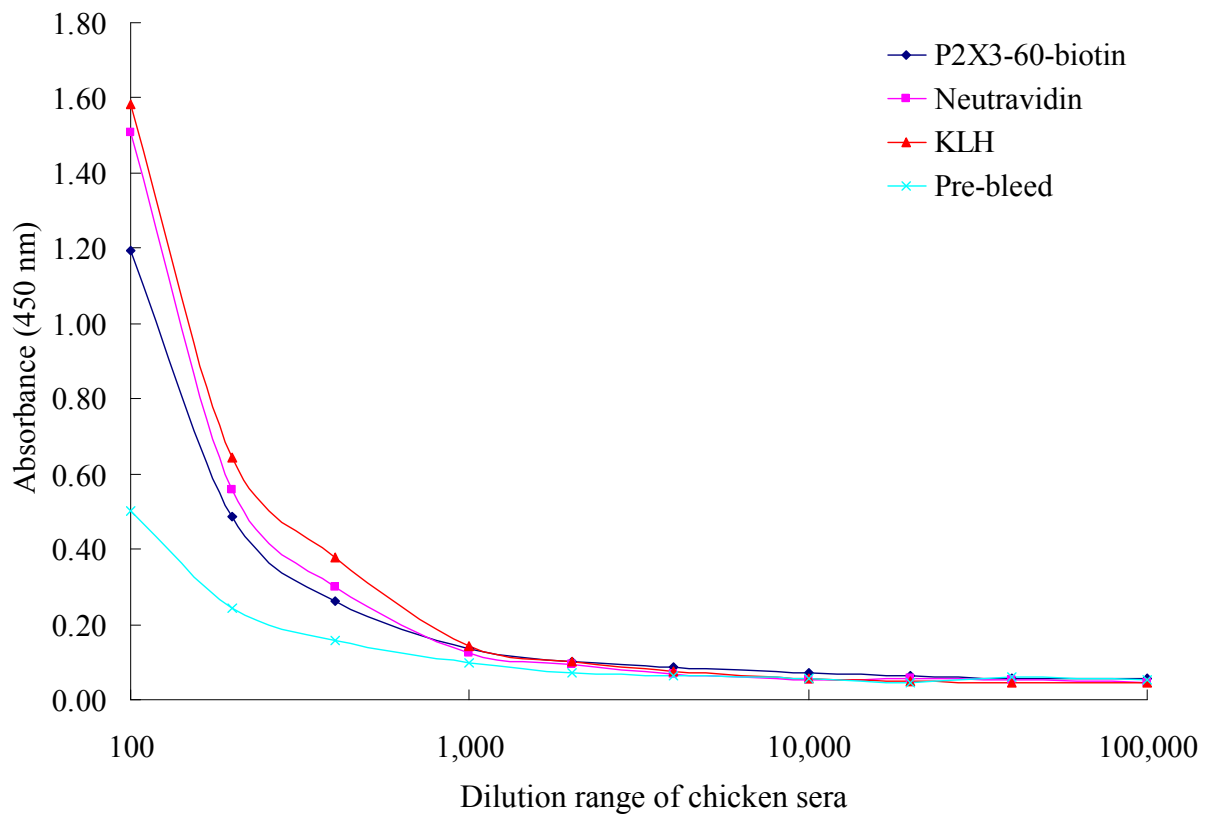
Fig. 4.19a Serum titre after the third boost of the second chicken immunised with P2X$_3$-60-KLH. No specific response to P2X$_3$-60 was detected.
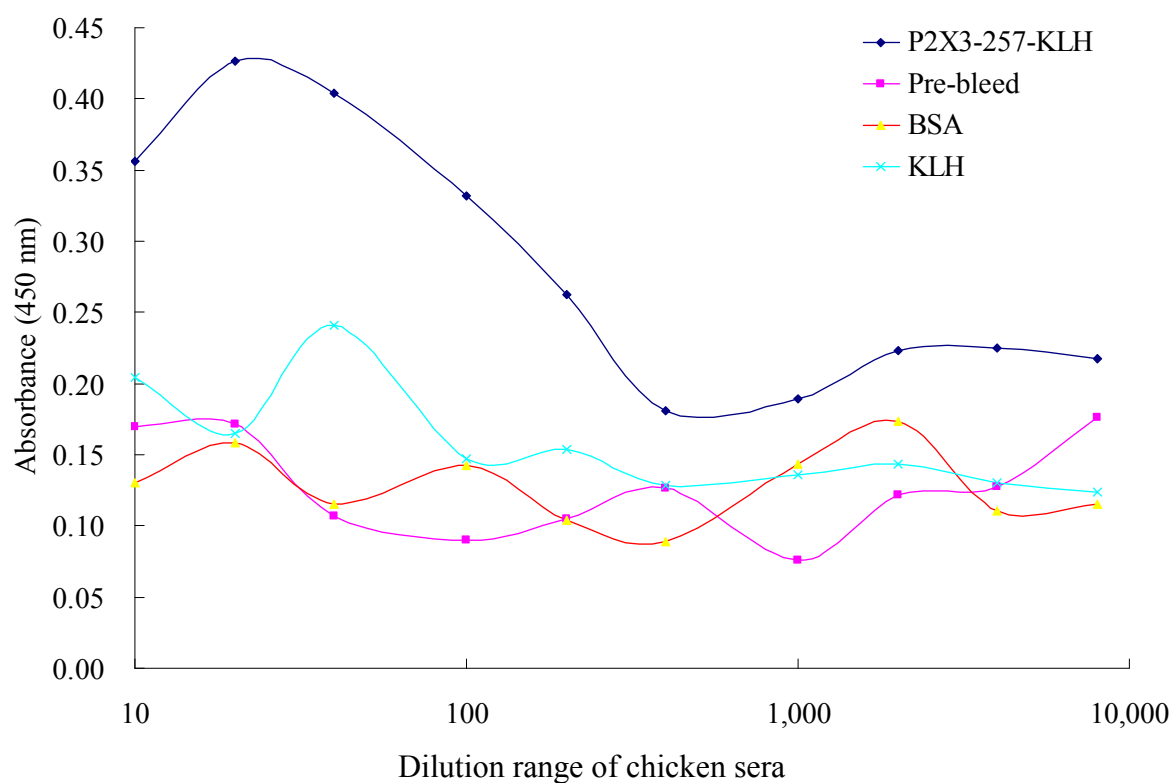
Fig. 4.19b Serum titre after the third boost of the third chicken which immunised with P2X$_3$-257-BSA. No specific response to P2X$_3$-257 was detected.
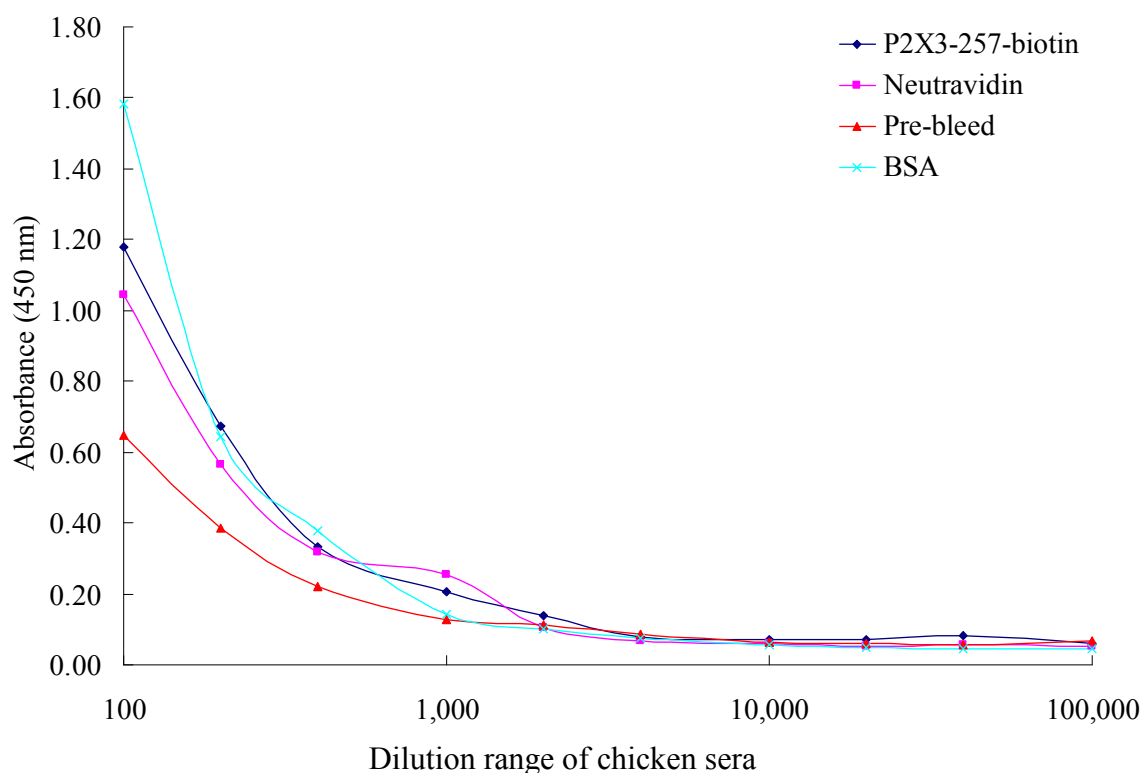
Fig. 4.19c Serum titre after the third boost of the fourth chicken which immunized with P2X$_3$-257-BSA. No specific response to P2X$_3$-257 was detected.

4.3 Discussion

Over the last twenty years, antibody genes have been cloned, genetically manipulated and expressed in *E. coli*. Antibody expression in *E. coli* has several advantages e.g. large quantities of antibody fragments can be produced quickly at low cost. Furthermore, recombinant antibody technology offers the possibility of production of anti-human protein antibodies with both high specificity and affinity for application in human disease diagnosis and therapy (de Lalla *et al.*, 1996).

It is reported that over 151 recombinant therapeutics have been approved by the FDA or by the European Medicines Agency for different clinical indications (Huang *et al.*, 2012). ScFv antibodies have been widely used as

delivery agents due to their small size and high specificity. In most cases, the scFv recombinant antibody fragment was used for targeted therapy through fusing to different proteins or genes. Wittel *et al.* (2005) reported that the scFv , sc(Fv)$_2$, is stable *in vivo* and has significant potential for diagnostic and therapeutic applications. Liu *et al.* (2009) developed a novel strategy to optimize genetically delivered immunotoxin molecular therapy for cancer, using a recombinant adenovirus vector to deliver an immunotoxin gene e23(scFv)-PE40 to the oncogene c-erbB-2 (also known as Her2/neu), which is overexpressed in mammary tumors. Schoonooghe *et al.* (2009) developed an anti-MUC1 Fab-scFv antibody with better penetration into the tumour compared with a full-size monoclonal antibody resulting in better anti-cancer therapeutics. MUC1 (a tumour-associated antigen on the surface of cells) has been used as a specific antibody target for immunotherapy of human malignancies. Chen *et al.* (2010) produced a stable anti-human CD44v6 scFv by selecting from a human phage-displayed scFv library. It can effectively and specifically target CD44v6-expressing cancer cells. Yao *et al.* (2012) successfully use a scFv for targeted intracellular delivery of small interfering RNAs (siRNAs) as anti-cancer drugs to disseminated Her2-positive breast cancer cells. These examples clearly demonstrate the capability and applicability of scFv-based targeting.

Inflammatory pain results from the activation of cascades, which mediate the inflammatory responses (involving the local vascular and immune systems and other cells at the injured site), and chemoreceptors (sensory receptors that transduce a chemical signal into an action potential) (Kidd and Urban, 2001). It is a major challenge for health providers to address this issue as pain sufferers represent ~20% of the adult population (Breivik *et al.*, 2006). There remains an unmet need for effective, non-addictive, pain treatments, as traditionally-used non-steroidal anti-inflammatory drugs are short-acting and can cause serious side effects.

The P2X purinoceptor 3 (P2X$_3$) is a member of the purinergic receptor family for adenosine 5'-triphosphate (ATP). It plays a pivotal role in processing pain signals, being highly and selectively expressed in nociceptive sensory neurons, e.g. in the dorsal root and trigeminal ganglia (North, 2004). Furthermore, several

reports have demonstrated anti-nociceptive effects of P2X$_3$ antagonists in different models of inflammatory pain, *in vivo*, consistent with the involvement of P2X$_3$ receptors in inflammatory pain (Cockayne *et al.*, 2000; Wirkner *et al.*, 2007). Knockout of the P2X$_3$ receptor results in aberrant inflammatory pain in mice, with reduced formalin-induced pain behaviour and associated enhanced thermal hyperalgesia in chronic inflammation (Souslova *et al.*, 2000). Downregulation of P2X$_3$ by antisense oligonucleotides inhibited the development of mechanical hyperalgesia in both inflammatory and neuropathic pain rat models (Barclay *et al.*, 2002). It was then suggested that an extracellular domain of the P2X$_3$ receptor could be a promising target for delivering a drug to inhibit the release of pain peptides (North, 2003).

Table 4.3 Commercial anti-P2X$_3$ antibodies (Labome, 2012).

Company	Antibody type	Antigen
Santa Cruze Biotechnology	Goat/rabbit IgG	Epitope mapping within an extracellular domain of human P2X$_3$
Abcam	Rabbit IgG	A 15 amino acid peptide corresponding to amino acids 383-397 of the C-terminus of rat P2X$_3$
Thermo Scientific Pierce Products	Rabbit IgG	A 15 amino acid peptide corresponding to amino acids 383-397 of the C-terminus of rat P2X$_3$
EMD Millipore	Rabbit/ guinea pig IgG	A 15 amino acid peptide corresponding to amino acids 383-397 of the C-terminus of rat P2X$_3$
Abnova	Rabbit IgG	A 15 amino acid peptide corresponding to amino acids 383-397 of the C-terminus of humanP2X$_3$
LifeSpan Biosciences	Rabbit IgG	A 15 amino acid peptide corresponding to amino acids 383-397 of the C-terminus of either human or rat P2X$_3$
US Biological	Rabbit/ guinea pig IgG	A 15 amino acid peptide corresponding to amino acids 383-397 of the C-terminus of either human or rat P2X$_3$
Biorbyt	Rabbit IgG	A 15 amino acid peptide corresponding to amino acids 383-397 of the C-terminus of human P2X$_3$
GeneTex	Rabbit IgG	A 15 amino acid peptide corresponding to amino acids 383-397 of the C-terminus of rat P2X$_3$

The transmembrane protein, $P2X_3$, should be bound by anti-$P2X_3$ antibodies against extracellular domains (Val_{60}-Phe_{301}). Hence a drug attached to anti-$P2X_3$ antibodies should be delivered to $P2X_3$ and then to the pain signalling pathway (Koshimizu *et al.*, 2002). To date, only Santa Cruze Biotechnology (U.S.A.) has generated polyclonal anti-$P2X_3$ antibodies against the extracellular domain (Table 4.3). However, a polyclonal antibody preparation (150 kDa) may be too large to deliver drugs like BoNT (150 kDa) effectively into cells to target the pain signalling pathway. A smaller antibody, for instance a scFv (25 kDa), should be an ideal candidate as the delivery agent for targeted treatment.

The scFv contains variable regions of antibody heavy (VH) and light chains (VL). The scFv recombinant antibody fragment is well known to have potential as a drug-delivery agent for targeted therapy through fusing with different proteins or genes.

Due to the reasons already cited previously, anti-$P2X_3$ extracellular domain scFv antibodies were generated. Two extracellular $P2X_3$ peptide conjugates ($P2X_3$-257-BSA and $P2X_3$-60-BSA/KLH) were selected to immunise rabbits, mice and chickens. Rabbits and mice showed a high immune response towards $P2X_3$-257, but a low immune response to $P2X_3$-60. Rabbit anti-$P2X_3$-257 antibody serum titre was higher than that of other rabbit polyclonal antibody generated by Yu (2000). Mouse anti-$P2X_3$-257 antibody serum titre was higher than that of the mouse polyclonal antibodies generated by Yu (2000) and Zhang (2006) (Table 3.4). The higher serum titres indicated higher and potentially more specific responses to immunised antigens which suggested higher levels of specific mRNA for the generation of recombinant antibodies.

Table 4.4 Comparison of serum titres of different antigen-immunised animals.

Animal species	Antigen	Serum titre
Rabbit	Human $P2X_3$-257	1:20,000
Rabbit	Human immunodeficiency virus type-1-PND	1:6,400-12,800 (Yu *et al.*, 2000)
Mouse	Human $P2X_3$-257	1:400,000
Mouse	Human $P2X_3$-60	1: 40,000 to 1: 80,000
Mouse	Human immunodeficiency virus type-1-PND	1:12,800-25,600 (Yu *et al.*, 2000)
Mouse	*Myxobolus rotundus*	1:8,000 to 1:16,000 (Zhang *et al.*, 2006)

After sacrificing rabbits, RNA extracted from both the spleen and bone marrow, and cDNA synthesis was performed. Rabbit cDNA was used to generate a number of scFv libraries with libraries sizes from 5×10^7 to 3.5×10^8, which was higher than that of other reported libraries , i.e. 2.0×10^6 (Gómez *et al.,* 2005) and 1.4×10^8 (Robert *et al.*, 2006). Recombinant antibody (scFv) selection against $P2X_3$-257 was successfully carried out using phage display technology. After five rounds of bio-panning, followed by a polyclonal phage ELISA, monoclonal ELISA, cross reactivity analysis, diversity analysis, DNA sequencing, scFv purification, scFv titre determination and competitive ELISAs, two anti-$P2X_3$-257 scFv clones (F11A and H7C) with good sensitivity and binding affinity were selected.

It was found that the anti-$P2X_3$-257 scFv H7C had better specificity with an IC_{50} (0.04 nM) which was 218 times lower than that of anti-$P2X_3$-257 polyclonal antibodies (IC_{50} 8.70 nM) (Fig. 3.15b). This improvement is much better than the work of Sabin *et al.* (2010). In Sabin's work, he generated an anti-human heptad repeat 1 (HK20) scFv antibody with IC_{50} values ranging from 6 to 737 nM, which was 1-2 times lower compared to anti-HK20 polyclonal antibodies (IC_{50} 7 to 1173 nM) (Table 3.5).

Table 4.5 Comparison of IC_{50} between the polyclonal antibody preparation and the scFv antibody.

Antibody	IC_{50} (Nm)	IC_{50} increased from IgG to scFv
Rabbit anti-P2X$_3$-257 polyclonal antibodies	8.70	>217 times
Anti-P2X$_3$-257 scFv (H7C)	0.04	
HK20 polyclonal antibodies	7 to 1173	1-2 times
HK20 scFv	6 to 737	

This research describes the first reports of the generation of a recombinant anti-P2X$_3$ scFv antibody, and the first recombinant antibody against an extracellular domain of P2X$_3$ (Val$_{257}$ - Asp$_{276}$), using phage display. More than 90% of commercial and published anti-P2X$_3$ antibodies are polyclonal antibodies against a fifteen-amino acid peptide sequence (Val$_{383}$-His$_{397}$) identical to the carboxyl-terminus of the P2X$_3$ receptor intracellular domain. However the anti-P2X$_3$ scFv antibodies, which can perform internalization into neuron cells through binding to the P2X$_3$ extracellular domain, are crucial for long-term targeted therapeutics. Hence, the rabbit anti-P2X$_3$-257 scFvs generated in this research, which with high specificity and affinity, provide a promising delivery agent for targeting diagnosis or therapy for inflammatory pain. The anti-P2X$_3$ scFv antibodies will be used for targeted delivery of BoNTs to nociceptive sensory neurons for targeted treatment of inflammatory pain.

Chapter 5
Optimisation and
Characterization of ScFv
Antibody *in Vitro*

5.1 Introduction

In this chapter the characterisation of the H7C scFv and its modification to improve expression are described.

After rabbit anti-P2X$_3$ scFv clones F11A and H7C were successfully selected through phage display, the specificity and affinity of these two clones were confirmed by ELISA. *In vitro* analysis was performed to select the best clone by using Western blotting and immunofluorescence staining with rat DRG cells. F11A and H7C gave similar results with Western blotting and immunofluorescence staining. Clone H7C was chosen for further characterisation as its IC$_{50}$ was slightly better than that of F11A.

The expression level of the anti-P2X$_3$ scFv increased by 3.5 fold after Cys$_{80}$ of clone H7C was mutated to Ala (MH7C). Western blotting, immunofluorescence, fluorescence-activated cell sorting (FACS) and immunohistochemical techniques were then applied for *in vitro* analysis of the specificity of the anti-P2X$_3$ scFv.

Using Western blotting, the P2X$_3$ specific band at the correct position (50-55 kDa) was successfully detected. With immunofluorescent staining, anti-P2X$_3$ scFv antibody-specific binding to P2X$_3$ was demonstrated by very good co-localisation of staining on both the DRG cell bodies and fibres with commercial anti-P2X$_3$ polyclonal antibody. In FACS analysis the scFv showed high binding-specificity to rat DRG-expressed P2X$_3$, which was indicated by a dramatically shifted peak in comparison to the negative control. Immunohistochemical analysis demonstrated that the membrane of DRG cells in rat dorsal root ganglions, rat cortical neurons and human bladder neurons were positively stained by commercial anti-P2X$_3$ antibody, rabbit-DARP polyclonal antibody and Alexa-594-labelled rabbit anti-P2X$_3$ scFv antibody.

5.2 Results

5.2.1 Western blotting and immunofluorescent staining analysis of scFv specificity to root ganglion cells (DRGs) expressed P2X$_3$

The binding specificity of anti-P2X$_3$-257 scFv antibody colonies F11A and H7C for DRGs expressing P2X$_3$ was confirmed by both Western blotting and immunofluorescent staining using the strategy described in section 2.2.3.17. Using Western blotting, the P2X$_3$-specific band was successfully detected at the expected position with a molecular weight of 50-55 kDa (Fig. 5.1a). Immunofluorescent staining showed that specific binding of anti-P2X$_3$-257 scFv antibodies to P2X$_3$ with by very good co-localisation of staining with commercial anti-P2X$_3$ polyclonal antibody staining on the surface of DRG cells (Fig. 5.1b).

Fig. 5.1a Western blot analysis of purified anti-P2X$_3$ scFv antibody specificity for P2X$_3$ expressed by rat DRGs. DRGs were isolated from postnatal day 4 rats and cultured for 2 days *in vitro* before harvesting in LDS-sample buffer and analysis by SDS-PAGE and Western blotting (160 µg/lane). The membranes were stained by purified anti-P2X$_3$ scFv, followed by HRP-labelled anti-HA secondary antibody (1:2,000 dilution). For the positive control, commercial anti-P2X$_3$ antibody (1:300 dilution) was applied, followed by HRP-labelled anti-rabbit secondary antibody (1:1,000 dilution). For the negative control, anti-goat IgG (1:1,000 dilution) was added instead of anti-P2X$_3$ antibody. MW = molecular weight markers; positive = positive control; negative = negative control; F11A and H7C = Rabbit anti-P2X$_3$-257 scFv clones F11A and H7C.

Fig. 5.1b Immunofluorescence staining of cultured rat DRGs by anti-P2X$_3$ scFv antibody. Images were viewed in an inverted microscope in epifluorescence modes (A, C, E and G) and by phase contrast (B, D, F and H). Rat DRG cells grown in 24 wells plate for 5 days *in vivo* were fixed and stained by purified anti-P2X$_3$ scFvs F11A (E and F) and H7C (G and H), then incubated with fluorescein-labelled anti-HA mAb (3F10) (2 μg/mL). For the positive control, commercial rabbit anti-P2X$_3$ Ab (1:50 dilution) was added instead of the antibody lysate (C and D). For the negative control, anti-goat IgG (1:1,000 dilution) was added instead of anti-P2X$_3$ Ab (A and B). F11A and H7C = Rabbit anti-P2X$_3$-257 scFv clone F11A and H7C. Original magnification x 20; scale bars are 50 μm.

5.2.2 Improvement of scFv expression by mutation of Cys_{80} to Ala

5.2.2.1 Mutation of Cys_{80} to Ala for anti-P2X$_3$ scFv H7C

There are four constant cysteines (Cys) in scFvs to form intrachain disulphide bridges in the variable light and variable heavy chain, respectively. However, in anti-P2X$_3$ scFv H7C, there are five cysteines. This extra cysteine may lead to non-specific disulfide bond formation and result in poor expression levels. Based on the approach of Konterman and Dübel (2010), Cys_{80} was identified to be an extra Cys. It was decided to mutate it to Ala, as Ala_{80} was found in other scFvs (Guo *et al.*, 2012).

The Cys_{80} was mutated to alanine (Ala) by reverse PCR. The PCR mutated products were then transformed into Top 10 electrocompetent cells (section 2.2.3.19). Plasmid DNA from a total of 6 clones was extracted, *Sfi*I-digested and analyzed on a 1% agarose gel (Fig. 5.2a). Positive clones were then sequenced. After the required amino acid sequence was obtained (Fig. 5.2b), the mutated anti-P2X$_3$ scFv clone and non-mutated anti-P2X$_3$ scFv clones were cultured (in 500 mL volume) and purified.
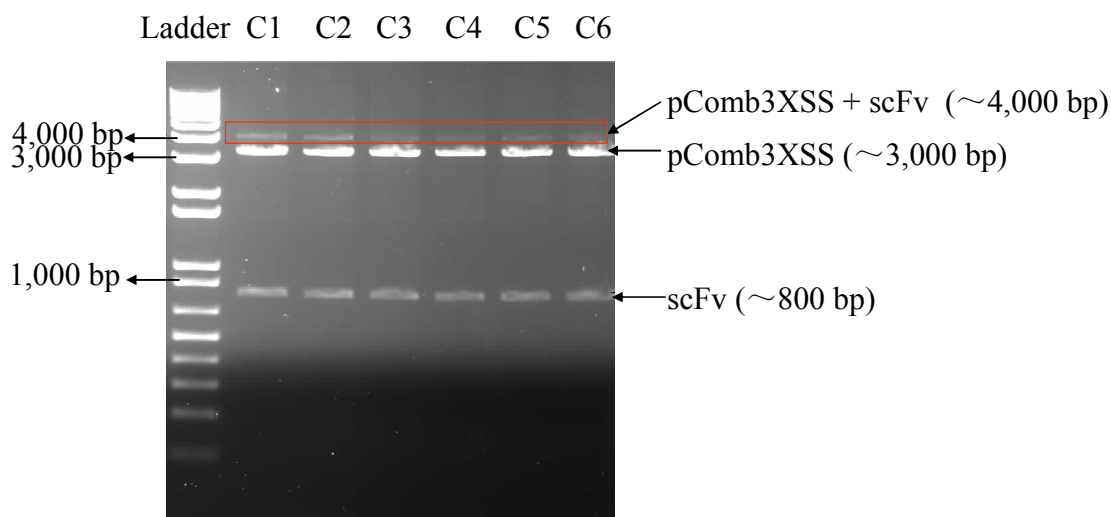
Fig. 5.2a *Sfi*I digestion of DNA from mutated scFv clone 1-6. After separation on a 1% agarose gel, all the six colonies showed to be positive indicated by correctly digested bands at 4,000 bp, for undigested pComb3xss with scFv, 3,200 bp for pComb3xss and 800 bp for the scFv. Lanes C1-C6 = clones 1-6.

```
         ....|....| ....|....| ....|....| ....|....| ....|....| ....|....| ....|....| ....|....|
              10        20        30        40        50        60        70        80
Non-mutated  DMTQTPSS ASEPVGGTVT INCQASQSVY RQNYLSWFQQ KPGQPPKLLI YKASTLASGV PSRFRGSGSG TQFTLTISDVQC
Mutated      VMTQTPSS ASEPVGGTVT INCQASQSVY RQNYLSWFQQ KPGQPPKLLI YKASTLASGV PSRFRGSGSG TQFTLTISDVQA

         ....|....| ....|....| ....|....| ....|....| ....|....| ....|....| ....|....| ....|....|
              90       100       110       120       130       140       150       160
Non-mutated  DDAATYYC AGSTGIDDHD TDFGGGTEVV VKSSGGGGSG GGGGGSSRSS QSVEESGGRL VTPGTPLTVT CTASGFSLGFFD
Mutated      DDAATYYC AGSTGIDDHD TDFGGGTEVV VKSSGGGGSG GGGGGSSRSS QSVEESGGRL VTPGTPLTVT CTASGFSLGFFD

         ....|....| ....|....| ....|....| ....|....| ....|....| ....|....| ....|....| ....|....|
             170       180       190       200       210       220       230       240
Non-mutated  MSWVRQAP GKGLEWIGTS HYDGNTYYAS WAKGRFTISK TSTTVDLTMT SLTASDTATY FCARSGYGSG LFNIWGPGTLVT
Mutated      MSWVRQAP GKGLEWIGTS HYDGNTYYAS WAKGRFTISK TSTTVDLTMT SLTASDTATY FCARSGYGSG LFNIWGPGTLVT

         ....|....| ....|.
             250
Non-mutated  VSLGQPKA PSVTS.
Mutated      VSLGQPKA PSVTS.
```

Fig. 5.2b Sequence of mutated anti-P2X$_3$ scFv. The anmino acid sequence was compared with that of non-mutated anti-P2X$_3$ scFv. The cysteine at position 80 (in red) was successfully mutated to alanine without any other mutation being made.

5.2.2.2 Comparison of anti-P2X$_3$-257 scFv expression levels before and after mutation

The scFv antibody titre against P2X$_3$-257-biotin was measured using crude bacterial lysate from a 2 L culture (section 2.2.3.16). The titre for anti-P2X$_3$-257 scFv H7C preparation before mutation was 1:100 and 1:1,000 after mutation (Fig. 5.3).

The protein concentrations after purification (section 2.2.3.15) were measured using a BCA kit (section 2.2.2.3). For the mutated anti-P2X$_3$ scFv the concentration was 978.2 µg/mL and for the non-mutated anti-P2X$_3$ scFv 277.7 µg/mL (in a total volume of 3 mL).

The expression level of mutated anti-P2X$_3$ scFv was found to be much higer than the non-mutated anti-P2X$_3$ scFv with a better antibody titre (1:1,000 vs. 1:100) and higher protein concentration (978.2 µg/mL vs. 277.7 µg/mL) (titre was three times greater than the background in wells containing control protein, neutravidin).
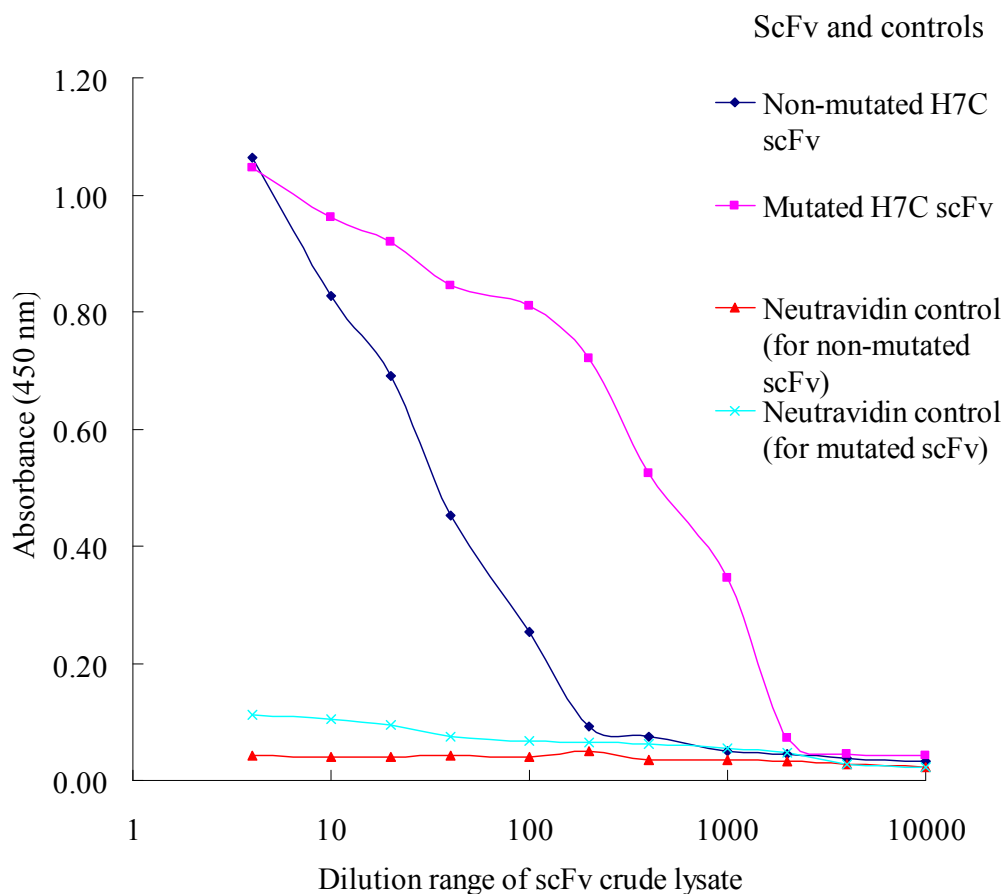
Fig. 5.3 Direct ELISA analysis of titres of the mutated and non-mutated anti-P2X$_3$ scFvs. The anti-P2X$_3$ scFv antibody titre responses (three times greater than negative control) to the P2X$_3$-257-biotin conjugate were tested before and after mutation. An ELISA plate was coated with 5 µg/mL P2X$_3$-257-biotin conjugate. A series of dilutions ranging from 1:4 to 1:4,000 of the crude lysate of the anti-P2X$_3$-257 scFv (before and after mutation) were made in 1 x PBST, followed by addition of HRP-labeled anti-HA secondary antibody. The neutravidin controls were used to detect the possible non-specific binding of scFv to neutravidin/biotin. For the neutravidin control the wells were coated with neutravidin (2.5 µg/mL) instead of the P2X$_3$-257-biotin conjugate. The lysate titre for anti-P2X$_3$-257 scFv H7C before mutation was 1:100 and 1:1,000 after mutation.

5.2.2.3 Western blotting and immunofluorescent staining analysis of mutated scFv (MH7C) specificity to rat DRGs-expressed P2X$_3$

The binding specificity of mutated anti-P2X$_3$-257 scFv antibody H7C to DRGs expressed P2X$_3$ was confirmed by both Western blotting and immunofluorescence staining, using the strategy described in section 2.2.3.17. For Western blotting, the P2X$_3$-specific band was successfully detected at the right position and molecular weight (50-55 kDa) (Fig. 5.4a). For immunofluorescent staining, specific binding of mutated anti-P2X$_3$-257 scFv antibody to P2X$_3$ was demonstrated by very good co-localisation with commercial anti-P2X$_3$ polyclonal antibody staining on the surface of DRG cells (Fig. 5.4b).
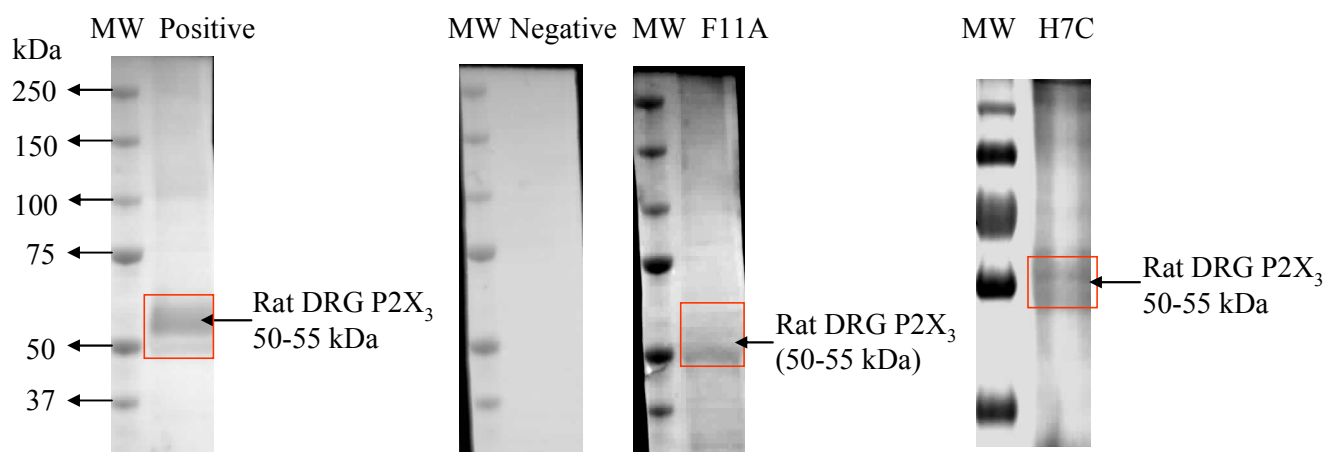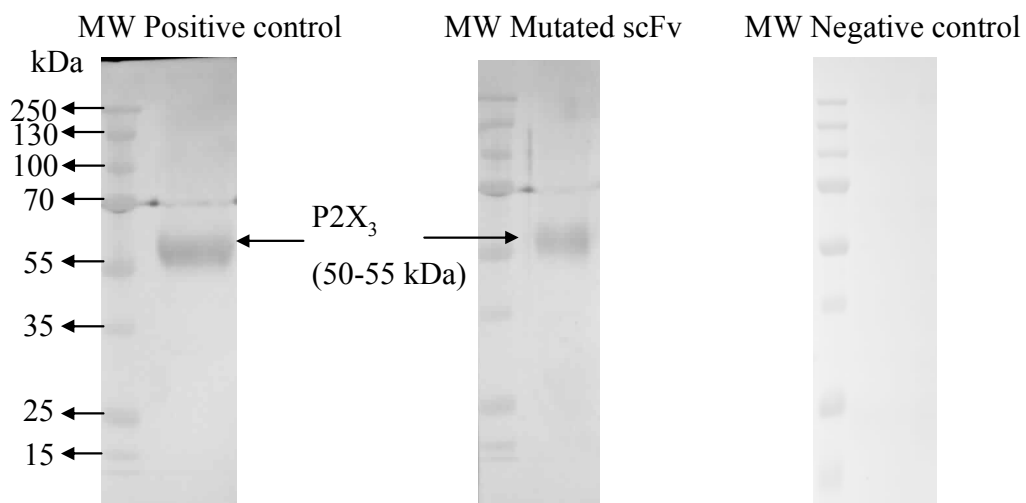
Fig. 5.4a Western blot analysis of purified mutated anti-P2X$_3$-257 scFv antibody specificity for P2X$_3$ expressed by rat DRGs. DRGs were isolated from postnatal day 4 rats and cultured 2 days *in vitro* before harvesting in SDS-sample buffer and analysis by SDS-PAGE and Western blotting (160 μg/lane). The membranes were stained by purified mutated anti-P2X$_3$-257 scFv, followed by anti-HA-HRP-labelled secondary antibody (1:2,000 dilution). For the positive control, commercial anti-P2X$_3$ polyclonal antibody (1:300 dilution) was applied, followed by HRP-labelled anti-rabbit secondary antibody (1:1,000 dilution). For the negative control, anti-goat IgG (1:1,000 dilution) was added instead of anti-P2X$_3$ antibody. MW = molecular weight markers.

Mutated
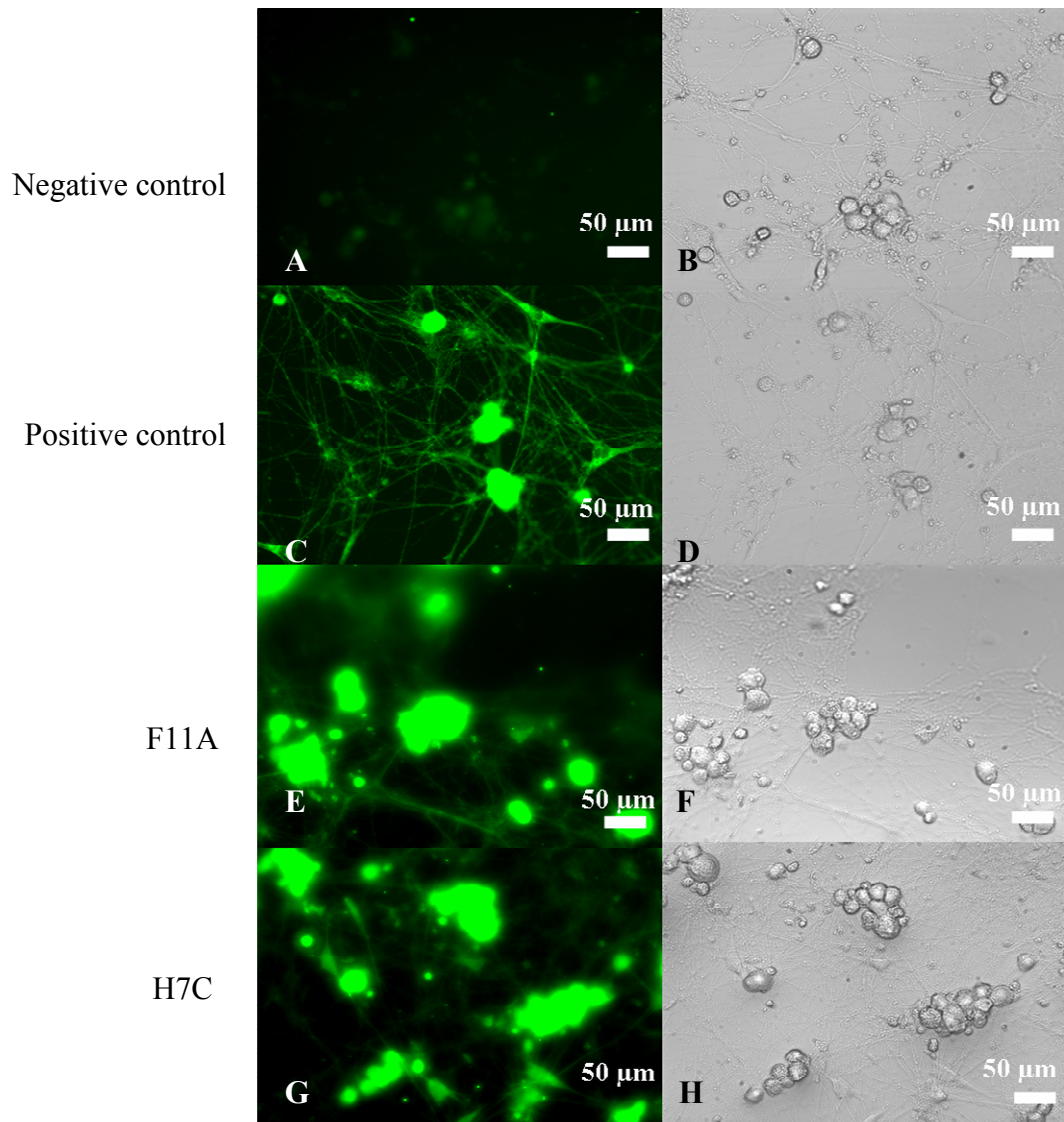anti-P2X$_3$-257
scFv

Negative
control
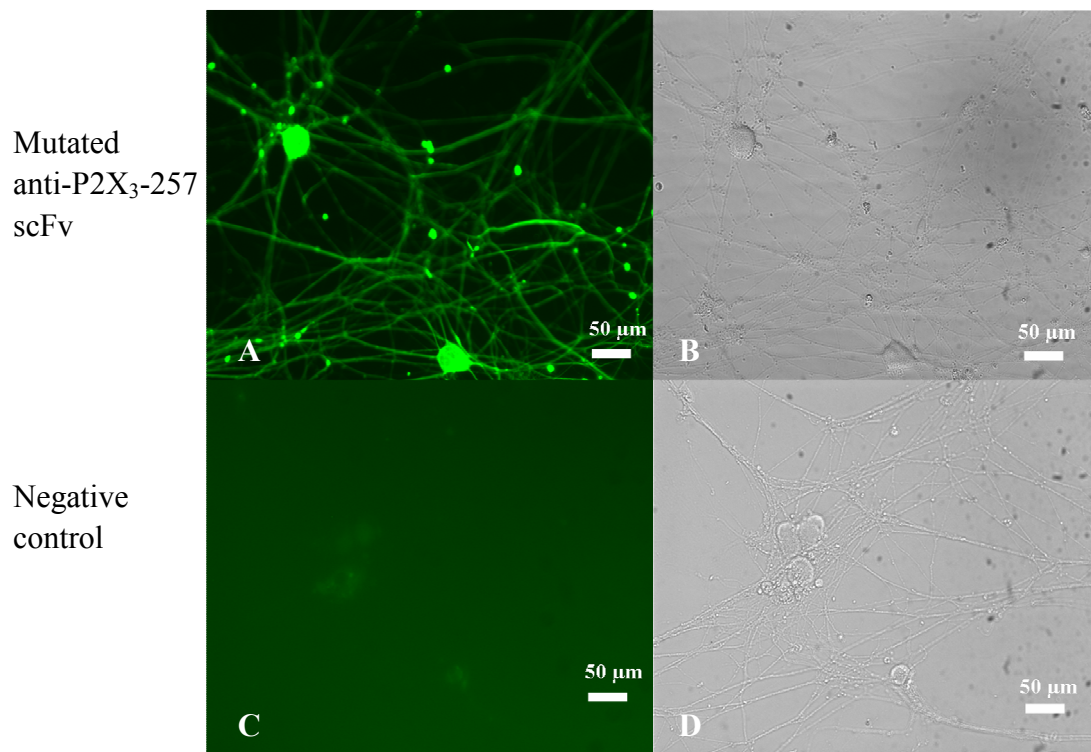
Fig. 5.4b Immunofluorescence staining of cultured rat DRGs by anti-P2X$_3$-257 scFv antibody. Images were viewed in an inverted microscope in epifluorescence modes (A and C) and by phase contrast (B and D). Rat DRG cells, grown in 24 wells plate for 5 days, *in vivo* were fixed and stained with the purified mutated anti-P2X$_3$-257 scFv, followed by incubation with fluorescein-labelled anti-HA mAb (3F10) (2 μg/mL) (A and B). For the negative control (C and D), anti-goat IgG (1:1,000 dilution) was added instead of anti-P2X$_3$ Ab. Original magnification x 20; scale bars are 50 μm.

181

5.2.3 Rabbit anti-P2X$_3$-257 antibody co-staining of rat DRGs with commercial rabbit anti-P2X$_3$ intracellular domain antibody

Confocal microscopic studies were applied to demonstrate specific binding of anti-P2X$_3$-257 scFv antibody to rat DRG neuron-expressed P2X$_3$. DRG cells cultured for 5 days were fixed and blocked, as described in section 2.2.4.5. Then Alexa-594 labelled-scFv was added, followed by permeabilisation and addition of commercial rabbit anti-P2X$_3$ intracellular domain polyclonal antibody, followed by Alexa Fluor-488-labelled goat anti-rabbit polyclonal secondary antibody (Fig. 5.5a). For Rabbit-DARP anti-P2X$_3$-257 polyclonal antibody, Alexa Fluor-576-labelled goat anti-rabbit polyclonal secondary antibody was added before permeabilisation and addition of commercial antibody (Fig. 5.5b). The specific binding of anti-P2X$_3$-257 antibodies to P2X$_3$ was demonstrated by very good co-localisation with commercial anti-P2X$_3$ polyclonal antibody staining on the surface of DRG cells and fibers.
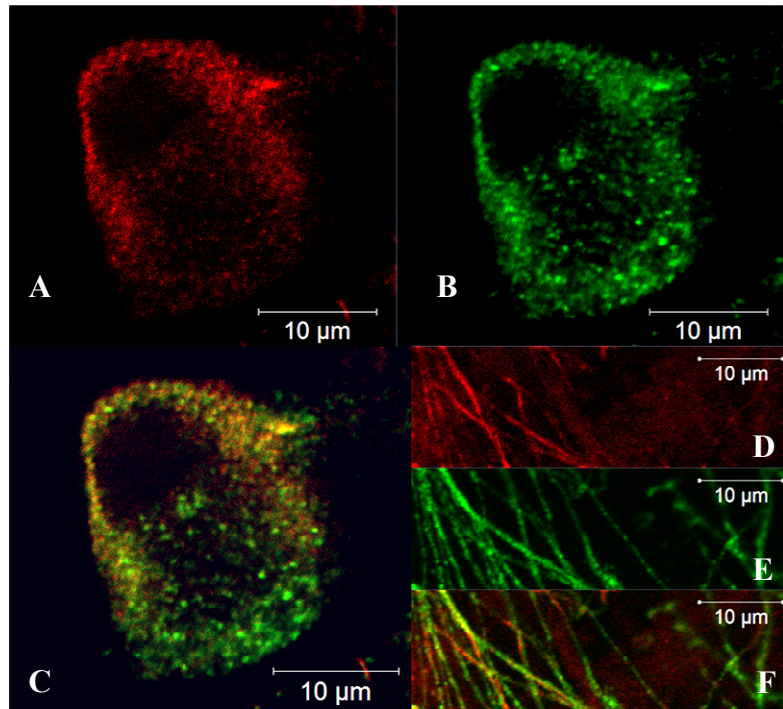
Fig. 5.5a Confocal micrographic analysis demonstrating co-localisation of staining and antibody-specific binding of rabbit-DARP anti-P2X$_3$ polyclonal antibody to P2X$_3$. Rat DRG cultures, grown in 24 wells plate for 5 days, were fixed and stained by rabbit-DARP anti-P2X$_3$-257 polyclonal antibody (A, D; red) and commercial rabbit anti-P2X$_3$ intracellular domain polyclonal antibody (B, E; green), followed by Alexa Fluor-546-labelled goat anti-rabbit secondary antibody (1:1,000 dilution) and Alexa Fluor-488-labelled goat anti-rabbit secondary antibody (1:1,000 dilution). Specific binding of scFv to P2X$_3$ expressed by rat DRG cell bodies (A-C) and fibres (D-F) was demonstrated by good co-localisation (C, F; yellow) with staining of commercial antibody. Original magnification x 40; scale bars are 10 μm.
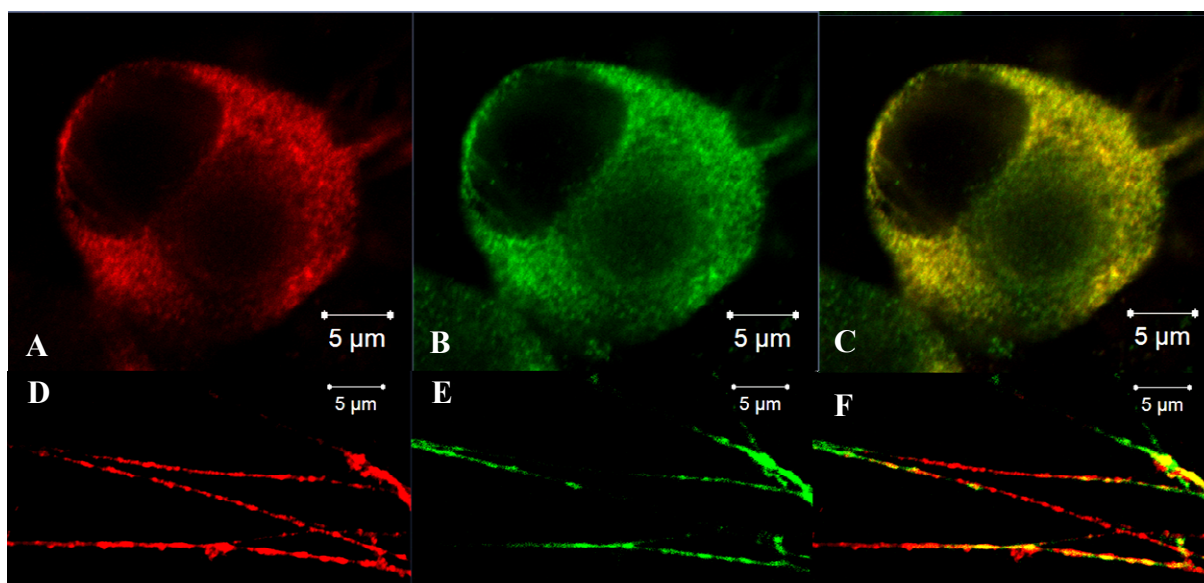
Fig. 5.5b Confocal micrographic analysis demonstrating co-localisation of staining and antibody-specific binding of anti-P2X$_3$ scFv to P2X$_3$. Rat DRG cultures, grown in 24 wells plate for 5 days, were fixed and stained by Alexa-594 labelled-scFv (A, D; red) and commercial rabbit anti-P2X$_3$ intracellular domain polyclonal antibody (B, E; green), followed by Alexa Fluor-488-labelled goat anti-rabbit secondary antibody (1:1,000 dilution). Specific binding of scFv to P2X$_3$ expressed by rat DRG cell bodies (A-C) and fibres (D-F) was demonstrated by good co-localisation (C, F; yellow) with staining of commercial antibody. Original magnification x 40; scale bars are 5 μm.

5.3.4 Analysis of binding specificity of anti-P2X3 scFv to rat DRG-expressed P2X$_3$ using flow cytometry

The specificity of scFv antibody for binding to P2X$_3$ expressed on rat DRG cell surface was analysed using FACS Calibur-based assays as described in section 2.2.3.21. It was shown that scFv (50 μM) which was labelled with Alexa-594 had high binding-specificity to rat DRG-expressed P2X$_3$ based on FACS data, which showed peaks shifted dramatically from negative control to positive control. The median fluorescence intensity of scFv (573 A.U.) was approximately 4.0 times higher than negative control (145 A.U.) and 1.2 times

higher than positive control (459 A.U.) (Fig. 3). For the negative control, DRG cells were treated with only secondary antibody, which tested for non-specific binding of secondary antibody on treated cells. For positive control, commercial rabbit anti-P2X$_3$ polyclonal antibody (50 µM) was applied instead of the scFv.
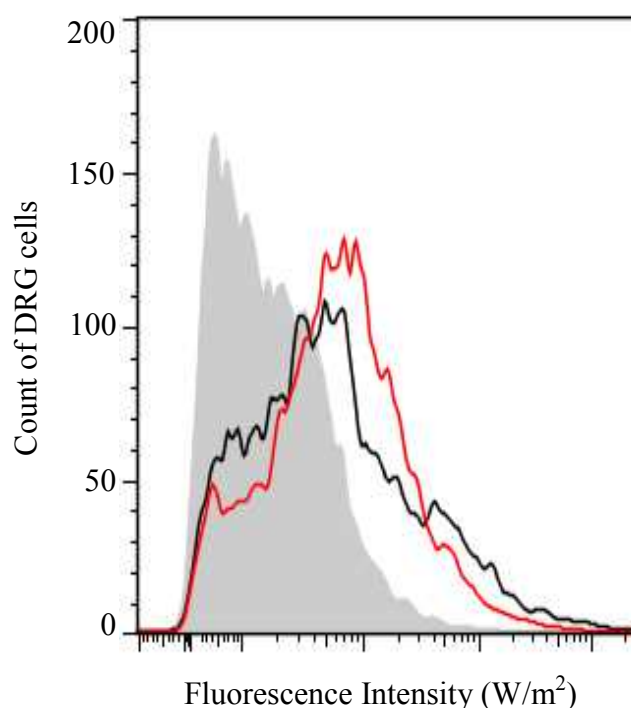
	Sample Name	Median Fluorescence Intensity (A.U.)
▬▬	Positive control	459
▬▬	Anti-P2X$_3$ scFv	573
▬▬	Negative control	145

Fig. 5.7 Flow cytometric analysis of scFv-specific binding to P2X$_3$ expressed on rat DRG cells. The x-axis represents the intensity of the fluorescence and the y-axis the number of cells. Rat DRG cells were stained with Alexa-594-labelled scFv (10 µM). For negative control, Alexa-594-labelled goat anti-rabbit antibody was added instead of Alexa-594-labelled scFv. Flow cytometric curves showed DRG cells stained by scFv (red), commercial rabbit anti-P2X$_3$ polyclonal antibody (black) and unstained (gray image).

5.3.5 Immunohistochemical analysis demonstrated anti-P2X$_3$ scFv antibody specific to sensory neurons

Tissue slides of rat (P1) DRG and rat brain (18 weeks) were immunostained with anti-P2X$_3$ antibody on an automated platform (section 2.2.8). The brown staining indicated antibody–antigen complex which was detected using a polymer-based kit with DAB, while the red fluorescence staining indicated Alexa-594-labelled scFv-P2X$_3$ complex. The membrane of DRG cells in rat dorsal root ganglion (Fig. 5.8), rat brain cortical cells (Fig. 5.9) and urothelium cells of human bladder (Fig. 5.10) were stained by commercial anti-P2X$_3$ antibody, rabbit-DARP polyclonal antibody and Alexa-594-labelled rabbit anti-P2X$_3$ scFv antibody. The Alexa-594-labelled rabbit anti-P2X$_3$ scFv antibody shared the same staining pattern with commercial anti-P2X$_3$ antibody. Therefore, it can then be concluded that this anti-P2X$_3$ scFv antibody effectively binds to sensory neurons, DRG cells and successfully detects P2X$_3$ expression in adult rat brain.

Staining of rat DRG neurons

Anti-P2X$_3$ Ab stained
rat DRG cells

Anti-P2X$_3$ Ab preincubated
with P2X$_3$ peptides

Commercial rabbit
anti-P2X$_3$ pAb

Rabbit-DARP
anti-P2X$_3$ pAb

Alexa-594-labelled
anti-P2X$_3$-257 scFv Ab
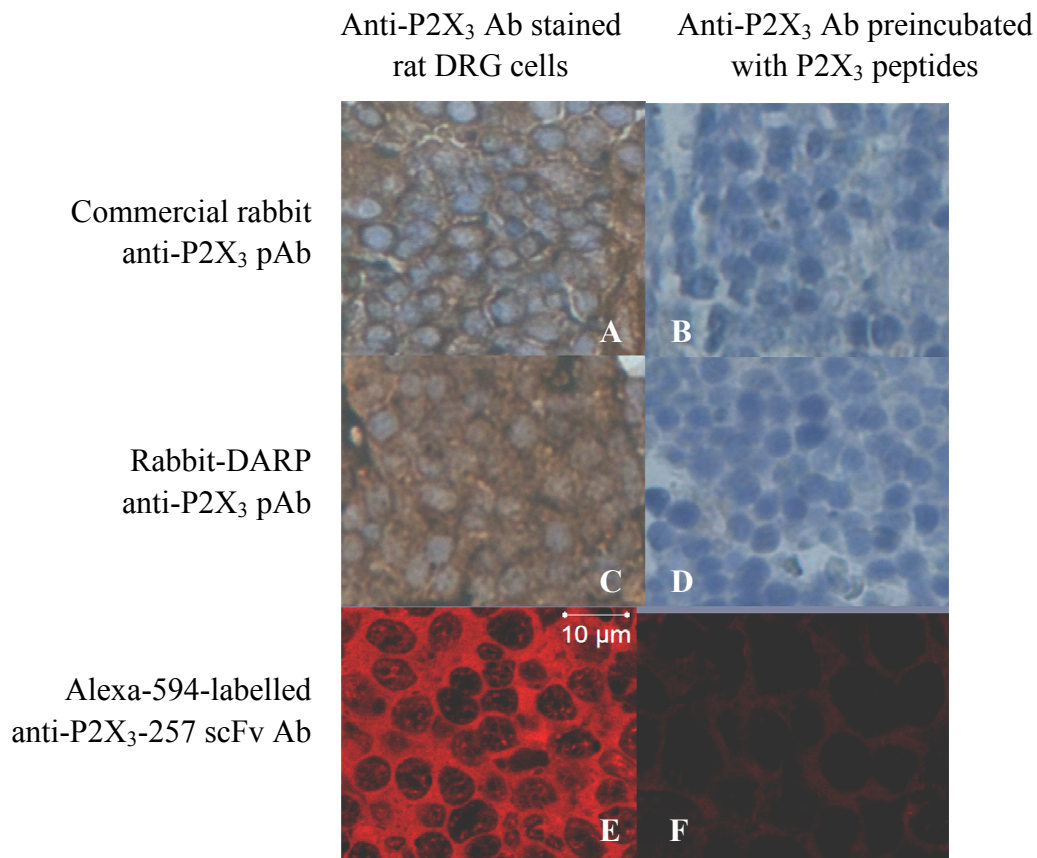
Fig. 5.8 Sections from rat DRG demonstrating MH7C scFv antibody binding specificity. Formalin-fixed, paraffin-embedded surgical specimens obtained from a 1 day old rat were immunostained with anti-P2X$_3$ antibody after antigen heat treatment. The membranes of DRG cells were positively stained by rabbit-DARP polyclonal antibody (C) and Alexa-594-labelled rabbit anti-P2X$_3$ scFv antibody (E), indicated by the same staining pattern as with commercial anti-P2X$_3$ antibody (A). This staining disappeared following preincubating antibodies with their specific antigenic P2X$_3$ peptides (B, D, F). Haematoxylin was used for nuclear staining. Original magnification x 40; scale bars are 10 μm.

Staining of rat brain cortical neurons

Anti-P2X$_3$ Ab stained
rat brain neurons

Anti-P2X$_3$ Ab preincubated
with P2X$_3$ peptides

Commercial rabbit
anti-P2X$_3$ pAb

Rabbit-DARP
anti-P2X$_3$ pAb

Alexa-594-labelled
anti-P2X$_3$-257 scFv Ab
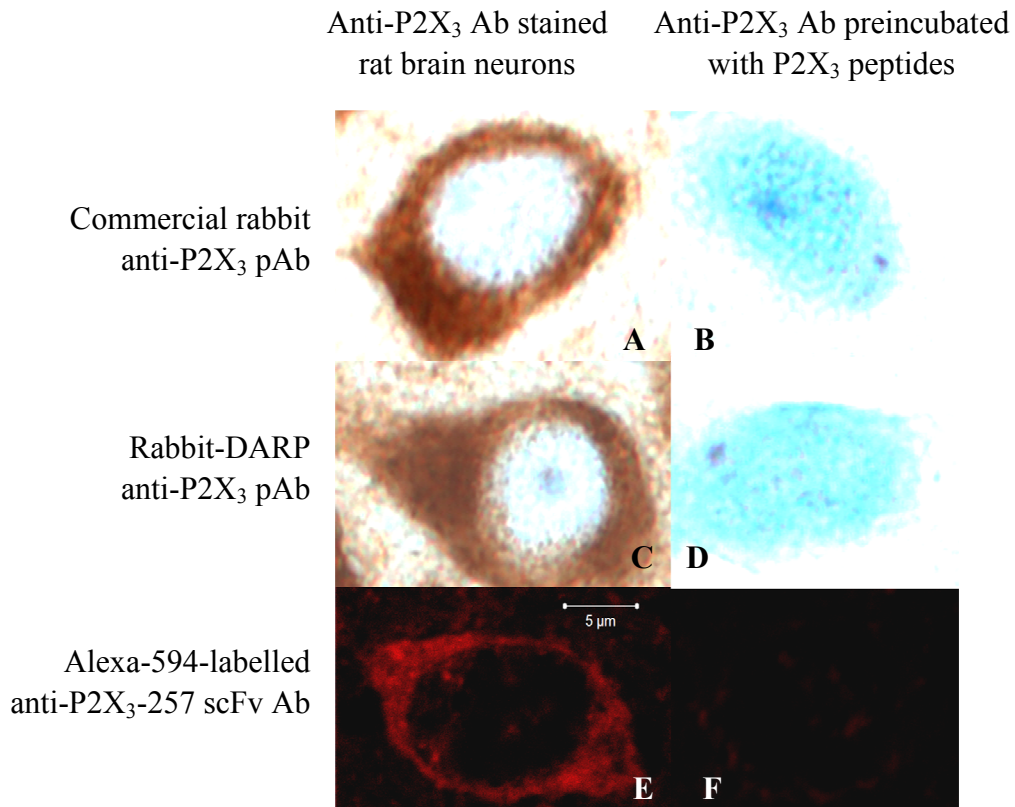
Fig. 5.9 Sections from rat brain demonstrating MH7C scFv antibody binding specificity. Formalin-fixed, paraffin-embedded surgical specimens obtained from a 18 week old rat were immunostained with anti-P2X$_3$ antibody after antigen heat treatment. The membranes of brain cortical neurons were positively stained by rabbit-DARP polyclonal antibody (C) and Alexa-594-labelled rabbit anti-P2X$_3$ scFv antibody (E), indicated by the same staining pattern as with commercial anti-P2X$_3$ antibody (A). This staining disappeared following preincubating antibodies with their specific antigenic P2X$_3$ peptides (B, D, F). Haematoxylin was used for nuclear staining. Original magnification x 40; scale bars are 5 μm.
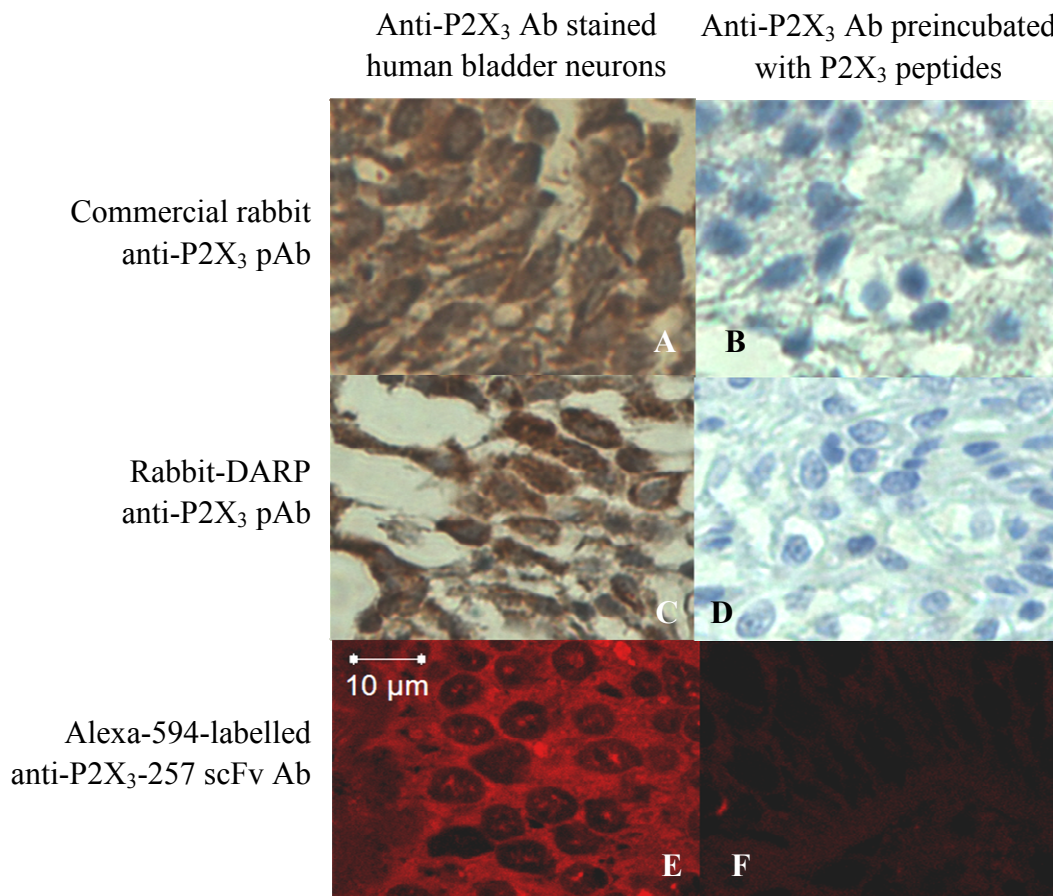
Fig. 5.10 Sections from human bladder demonstrate MH7C scFv antibody binding specificity. Formalin-fixed, paraffin-embedded surgical specimens obtained from human bladder (provided by Beaumont Hospital) were immunostained with anti-P2X$_3$ antibody after antigen heat treatment. The membranes of cells in bladder urothelium were positively stained by rabbit-DARP polyclonal antibody (C) and Alexa-594-labelled rabbit anti-P2X$_3$ scFv antibody (E), indicated by the same staining pattern as with commercial anti-P2X$_3$ antibody (A). This staining disappeared following preincubating antibodies with their specific antigenic P2X$_3$ peptides (B, D, F). Haematoxylin was used for nuclear staining. Original magnification x 40; scale bars are 10 μm.

5.3 Discussion

This chapter described successful modification of the rabbit anti-P2X$_3$-257 scFv, MH7C, for greater specificity, which was proved by Western blotting, immunofluorescence, flow cytometry and histochemical staining.

After sequencing the selected scFvs, an additional Cys (Cys$_{80}$) was discovered as part of the structure which may have lead to low expression levels, non-specific disulfide-bond formation and scFv s (Popkov *et al.*, 2003; Shen *et al.*, 2005). The Cys$_{80}$ was then mutated to Ala, as Ala$_{80}$ was reported in other rabbit scFvs (Moon *et al.*, 2011). After mutation, the crude bacterial lysate titre was 4 times higher than that of non-mutated scFv and the expression level of anti-P2X$_3$ scFv increased by 3.5 fold (from 278 µg/mL to 978 µg/mL) when compared with that of non-mutated anti-P2X$_3$ scFv. This result indicated that the Cys$_{80}$ in rabbit scFv resulted in low expression levels consistent with the results of Popkov (2003) and Shen (2005).

Usinf Western blotting, Xiang *et al.* (2008) detected P2X$_3$ in DRG protein extracts. In this chapter, the P2X$_3$-specific band was successfully detected by anti-P2X$_3$-257 scFv antibody, MH7C, at the expected position and molecular weight (50-55 kDa).

Vulchanova *et al.* (1998) successfully detected P2X$_3$ on the membrane of rat DRG cells by outlining cell bodies with strong fluorescent staining. The specific binding of anti-P2X$_3$-257 scFv antibody MH7C to rat DRG neuron-expressed P2X$_3$ was demonstrated by confocal microscopic studies by very good co-localisation with commercial anti-P2X$_3$ polyclonal antibody staining on the surface of DRG cells and fibers.

Flow cytometry is biophysical technology widely used in biomarker detection and protein engineering. Yuahasi *et al.* (2012) applied flow cytometry to detect P2X$_2$ expression. The peak of cells with high P2X$_2$ expression shifted greatly from peaks of negative controls due to increased fluorescent staining. Likewise, Alexa-594-labelled scFv had high binding-specificity to rat DRG-expressed P2X$_3$ based on flow cytometry data, which showed peaks shifted dramatically from the negative control to the positive control profiles.

190

Histochemical (IHC) staining is used by all anatomical and surgical pathologists to confirm cell types (Idikio, 2010). After formalin fixing and paraffin embedding (FFPE), the state of the proteins in a tissue sample may be altered, which may lead to non-specific binding (high background staining), and may then mask the detection of the target antigen (Marshall *et al.*, 2009). This may cause non-specific staining background in brain negative controls. However, after preincubation of antibodies with specific $P2X_3$ peptides, all of the staining on the membrane of rat (P1) DRG cells, rat (18 weeks) brain neurons and human bladder neuron cells disappeared (staining by commercial anti-P2X$_3$ antibody, rabbit-DARP polyclonal antibody and Alexa-594-labelled rabbit anti-P2X$_3$ scFv antibody). Moreover, as rabbit-DARP polyclonal antibody and Alexa-594 labelled rabbit anti-P2X$_3$ scFv antibody shared a similar staining pattern with commercial anti-P2X$_3$ antibody and published data (Pearson and Carroll, 2004; Cheung *et al.*, 2005; Liu *et al.*, 2009), it can be concluded that both rabbit-DARP polyclonal antibody and anti-P2X$_3$ scFv antibody effectively bind to both human and rat-expressed $P2X_3$.

It was reported that $P2X_3$ receptor protein was expressed in embryonic (E16) and neonatal rat brain (P7 and P14) but was not in adult rats (Kidd *et al.*, 1998). However, in this research, the cortical neuron membrane in FFPE brain tissue slides from a 18 weeks female Sprague-Dawley rat were positively stained by commercial rabbit anti-P2X$_3$ commercial polyclonal antibody, rabbit-DARP (the rabbit that was later used for scFv library construction) polyclonal antibody and rabbit anti-P2X$_3$-257 scFv antibody.

The anti-P2X$_3$ antibody used by Kidd *et al.* was rabbit polyclonal antibody against a peptide (DSGAYSIGH) corresponding to the predicted amino acids 389-397 of the rat $P2X_3$ receptor (Lewis *et al.*, 1995), generated by the Regal Group (Surrey, U.K.). The commercial antibody used in this research was a rabbit polyclonal antibody against amino acids 383-397 (VEKQSTDSGAYSIGH) of the rat $P2X_3$ receptor (Chen *et al.*, 1995), which was 6 amino acids (VEKQST) more than Kidd's antigen. Polyclonal and scFv antibodies generated in this research are from a rabbit immunised with a peptide with amino acids 257-276 of the human $P2X_3$ receptor (Koshimizu *et al.*, 2002). The homology of the chosen $P2X_3$ peptide sequence with $P2X_{1-7}$

was analysed using the Basic Local Alignment Search Tool (BLAST) and compared with rat (Roberts and Evans, 2004) and human (North, 2002) amino acid sequences. No similarity was found with amino acids 383-397 of rat $P2X_{1-7}$ receptor; and a low identity of 10% was observed in comparison to amino acids 257-276 of the human $P2X_{1-7}$ receptor. No or low identity indicated that the antibodies generated against the chosen peptides have a low possibility of cross-reactivity to $P2X_{1,2,4-7}$ receptor. The reason why Kidd's antibody cannot recognize adult rat brain may be because 6 amino acids (VEKQST) are absent and therefore not part of the binding epitope of the respective antibody. This result further provides the possibility of using anti-$P2X_3$ scFv as a target delivery agent for treatment of inflammation in the brain, which can lead to vision loss, weakness and paralysis (Aktas *et al.*, 2007).

Chapter 6

Generation of BoNT-anti-P2X$_3$ Antibody Fusion Protein

6.1 Introduction

In this chapter, proof of principle for targeting the translocation and protease domains from botulinum neurotoxin type A (or D) [LC-H_N/A or LC-H_N/D] via an anti-P2X$_3$ antibody (polyclonal antibodies and scFv antibody) to sensory neurons was provided. The targeting efficiency and selectivity of BoNT-anti-P2X$_3$ antibodies was evaluated by comparing DRGs susceptibility to BoNT/A and BoNT/D.

BoNT/A and BoNT/D inhibit inflammatory pain peptide release [calcitonion gene-related peptide (CGRP) and substance P (SP)] by cleavage of their specific intracellular SNAREs [i.e. synaptosomal-associated protein (SNAP-25) and vesicle-associated membrane protein (VAPM)] (Aoki and Guyer, 2001). BoNT/A cleaves near the C-terminus of SNAP-25 at Gln$_{197}$-Arg$_{198}$. BoNT/D cleaves the extra-vesicular loop of VAMP at Lys$_{59}$-Leu$_{60}$. The entry of BoNT/A and BoNT/D into cells is mediated by binding to synaptic vesicle protein 2 (SV2). SV2s are expressed by sensory neurons as well as cholinergic neurons, sympathetic neurons and non-neuronal cells (Dong *et al.*, 2006; Peng *et al.*, 2011), therefore, treatment with only BoNT/A or BoNT/D may result in unwanted 'off-targeting effects'. Hence, a specific targeting agent is needed.

In this study, rabbit polyclonal or scFv antibody, which recognise the extracellular domain of P2X$_3$, were utilised as targeting agents for specific delivery of LC-H_N/A or LC-H_N(-H_{CN})/D to pain-signalling DRG neurons.

Before genetically fusing rabbit anti-P2X$_3$ scFv with BoNT, the principle of this approach was proven by conjugating rabbit anti-P2X$_3$ polyclonal antibody with LC-H_N/A, to determine if the LC-H_N/A-anti-P2X$_3$ polyclonal antibody construction had the desired endopeptidase activity. Rabbit anti-P2X$_3$ polyclonal antibody was purified using both a protein A agarose and a P2X$_3$ antigen-affinity column (section 2.2.2 and section 3.2.1.2). Anti-P2X$_3$ polyclonal antibody was biotinylated using an EZ-Link sulfo-NHS-LC-biotinylation kit (section 2.2.6.1) and then conjugated to the purified botulinum toxin serotype A-core streptavidin (LC-H_N/A-CS) (section

2.2.5.1). It was shown that the anti-P2X$_3$ polyclonal antibody-LC-H$_N$/A conhugate had higher endopeptidase activity than LC-H$_N$/A alone, as shown by detection of increased cleavage of SNAP-25 in rat DRG cells, compared to LC-H$_N$/A only.

The scFv gene was then fused to LC-H$_N$/D and LC-H$_N$-H$_{CN}$/D, and expressed as a fusion protein in BL21-DE3. After purification, using immobilised metal ion affinity chromatography (IMAC), BoNT-scFv fusion constructs were incubated with cultured DRGs for 24 hours, before cleavage of their respective substrates was analysed using Western blotting. The results proved that the fused proteins did enter into sensory neuron DRGs and cleaved VAMP2 in a dose-dependent fashion, but little improvement was found when compared with control proteins, LC-H$_N$/D and LC-H$_N$-H$_{CN}$/D. This may be caused by the poor disulphide bond formation capacity of BL21-DE3, which then leads to protein dysfunction.

The MH7C scFv gene was then fused to LC-H$_N$/A and LC-H$_N$-H$_{CN}$/A, as BoNT/A-cleaved SNAP-25 was easier to quantify than VAMP2. These fusion proteins were expressed in Origami 2(DE3) in order to improve their activity, as Origami 2(DE3) was reported to enhance disulphide bond formation (Larsen *et al.*, 2008). The LC-H$_N$-H$_{CN}$/A-MH7C fusion was then purified using streptavidin-agarose resin. *In vivo* data showed this novel construct had higher endopeptidase activity than LC-H$_N$-H$_{CN}$/A control protein, as shown by detection of increased cleavage of SNAP-25 in rat DRG cells. It subsequently inhibits release of inflammatory pain peptides, SP and CGRP, from cultured rat DRG neuronal cells, and lacks cytotoxicity *in vivo* when evaluated by intraperitoneal injection of 1 µg quantities. This supports its potential safety for the use in treatment applications.

6.2 Results

6.2.1 Successful expression and purification of LC-H$_N$/A-core streptavidin (CS)

6.2.1.1 SDS-PAGE analysis of expression and purity of LC-H$_N$/A-CS

There is a Trypzean cleavage site between BoNT light and heavy chains. Before cleavage into light and heavy chains, BoNT is in a single chain (SC) form at which lacks biologically activity. After cleavage, BoNT is in a di-chain (DC) form at which in biologically activity.

Single chain LC-H$_N$/A-core streptavidin (CS5) proteins were expressed and purified using IMAC (section 2.2.5.1). The single chain form of LC-H$_N$/A-core streptavidin was then converted to the biologically active di-chain form by incubating with Trypzean (1:250 dilution) at 27°C for 40 mins. Trypsin inhibitor (100-fold concentration) was added to the solution to inactive the Trypzean. The molecular weight for the nicked protein was about 115 kDa. Intensely stained bands at the correct molecular weight positions, i.e. 115 kDa (before addition of dithiothreitol, DTT) and 65 kDa and 50 kDa (after addition of DTT to break disulfide bonds) were successfully detected) (Fig. 6.1).
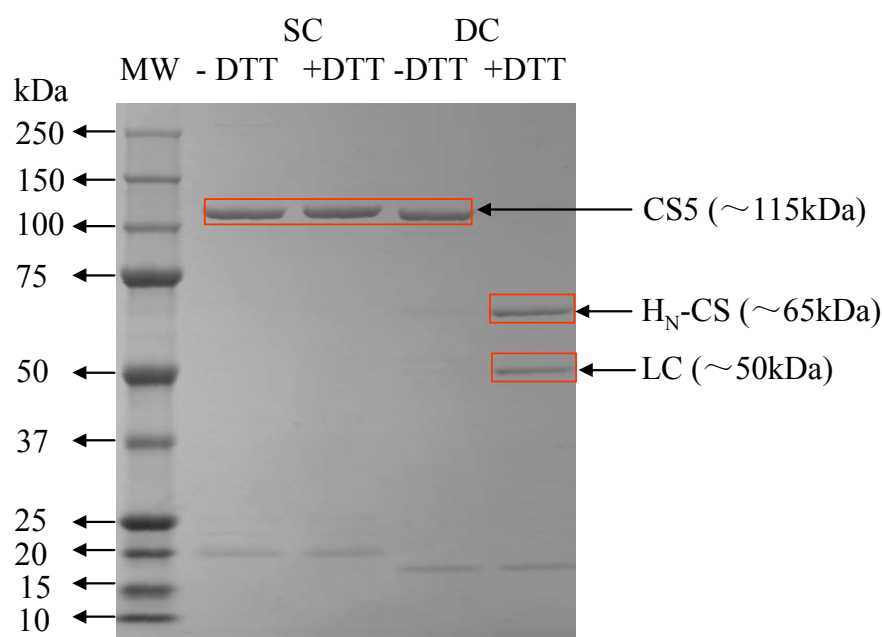
Fig. 6.1 The LC-H_N/A-core streptavidin sample were analysed by 4-12% SDS-PAGE. One µg/well of LC-H_N/A-core streptavidin preparations (before and after nicking; with or without DTT) were loaded into each lane before Coomassie staining. [SC = single chain; DC = di-chain form; DTT = dithiothreitol; MW = molecular weight markers; H_N-CS5 = core streptavidin conjugated light chain and translocation domain of botulinum toxin; LC = light chain of botulinum toxin and CS = core streptavidin.]

6.2.2 LC-H_N/A-anti-P2X$_3$ rabbit IgG conjugates

6.2.2.1 SDS-PAGE analysis of LC-H_N/A-CS-anti-P2X$_3$ rabbit IgG conjugates

After mixing biotinylated anti-P2X$_3$ rabbit polyclonal antibody (section 3.2.1.2) and LC-H_N/A-CS at 4°C for two hours in order to achieve sufficient binding (section 2.2.6.4), conjugates were detected by both SDS-PAGE and Western blotting (Fig. 5.3). The strong bands migrated to the expected position [260 kDa (LC-H_N/A-CS-anti-P2X$_3$ IgG) before addition of DTT; 65 kDa (H_N/A-CS),

197

50 kDa (antibody heavy chain and LC/A) and 25 kDa (antibody light chain) after addition of DTT] were successfully detected (Fig. 6.2).
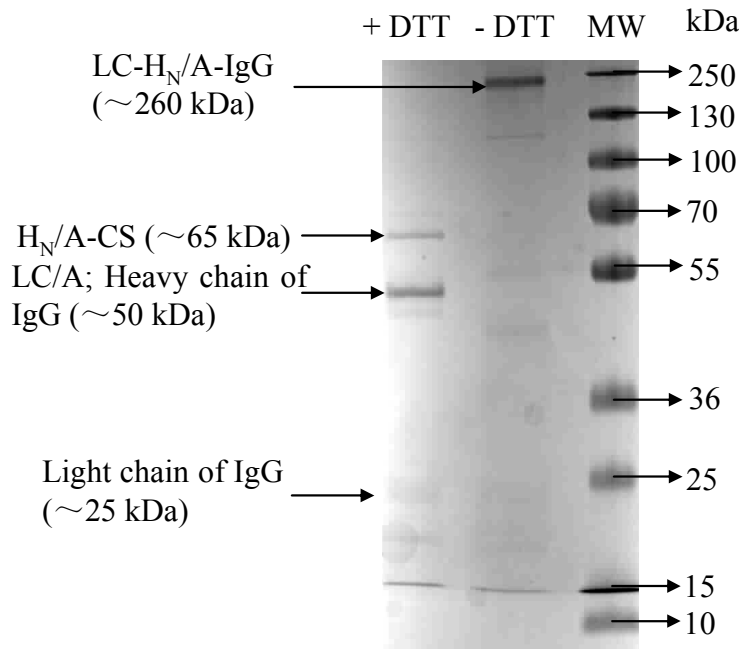
Fig. 6.2 SDS-PAGE analysis of anti-P2X$_3$-pAb-CS conjugates. The presence of a band at about 260 kDa (LC-H$_N$/A-CS-anti-P2X$_3$ IgG) before addition of DTT and three bands after addition of DTT, i.e. 65 kDa (H$_N$/A-CS), 50 kDa (antibody heavy chain and LC/A, respectively) and 25 kDa (antibody light chain). LC/A = light chain of botulinum toxin serotype A; H$_N$/A = translocation domain of botulinum toxin serotype A; CS = core streptavidin; IgG = rabbit anti-P2X$_3$ polyclonal antobody; DTT = dithiothreitol and MW = molecular weight markers.

6.2.2.2 Immunofluorescent staining analysis of LC-H$_N$/A-anti-P2X$_3$ rabbit IgG conjugates specificity targeting to DRG-expressed P2X$_3$

The specificity of LC-H$_N$/A-anti-P2X$_3$ IgG conjugates to P2X$_3$ expressed in DRGs were confirmed by immunofluorescent staining. Cultured DRGs (cultured for 5 days) were fixed, permeabilized and blocked, as described in section 2.2.6.6. The LC-H$_N$/A-anti-P2X$_3$ IgG was applied (1:50 dilution), followed by Alexa Fluor-546-labelled goat anti-rabbit secondary antibody

198

(1:200 dilution). The green fluorescence signals indicated DRG cells were positively stained by LC-H_N/A-anti-P2X$_3$ IgG conjugates (Fig. 6.3).

LC-H_N/A-anti-P2X$_3$ pAb

Negative control
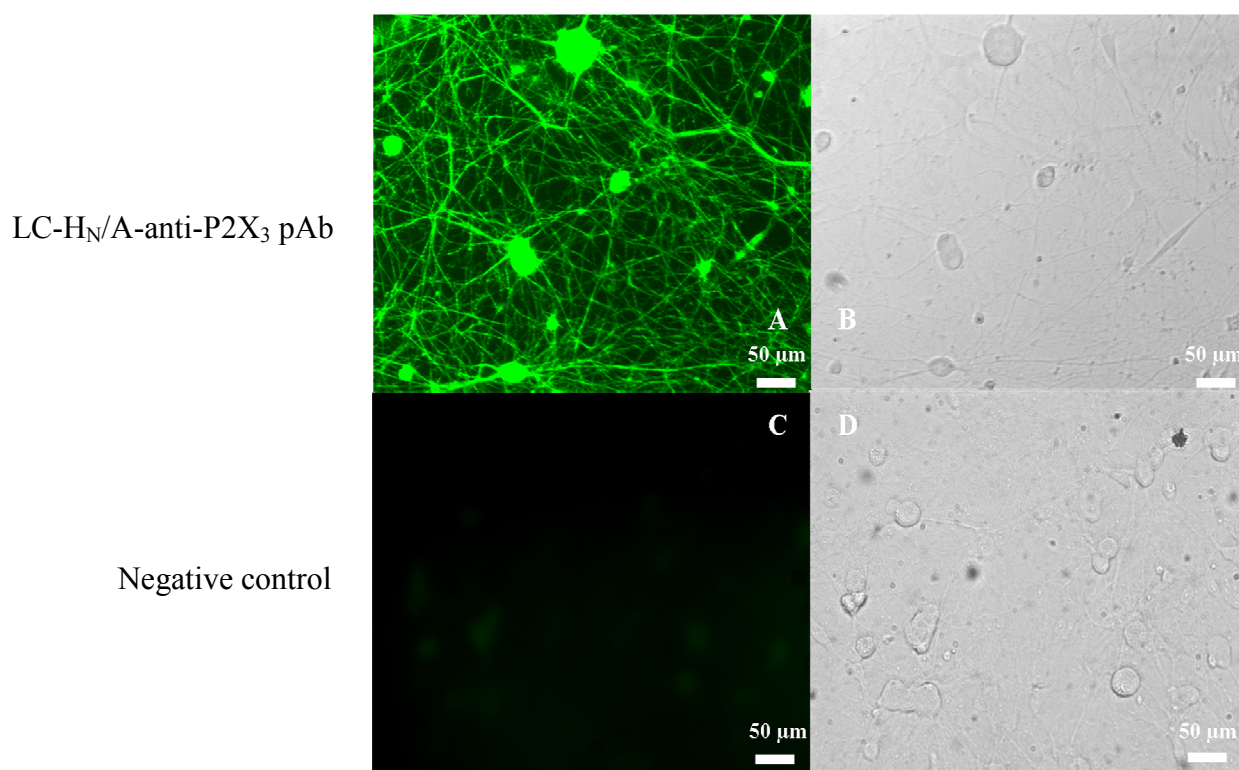
Fig. 6.3 Immunofluorescent staining of cultured DRG by LC-H_N/A-anti-P2X$_3$ rabbit IgG conjugates. Samples were viewed in an Olympus IX71 inverted microscope by phase contrast (B, D) and in fluorescence mode (A, C). Rat DRGs, grown in 24 wells plate for 5 days *in vivo* (5 DIV), were fixed and stained by LC-H_N/A-anti-P2X$_3$ IgG (1:50 dilution), followed by Alexa Fluor-546 labelled goat anti-rabbit secondary antibody (1:200 dilution). For the negative control, anti-goat IgG (1:1,000 dilution) was added instead of anti-P2X$_3$ antibody (C, D). Scale bars are 50 μm.

6.2.2.3 LC-H_N/A cleaves more SNAP-25 in cultured DRGs after conjugation to rabbit anti-P2X$_3$ IgG

A series of concentrations of LC-H_N/A-anti-P2X$_3$ IgG and LC-H_N/A-CS control (0, 10, 100 and 1,000 nM) in 250 μL were added to rat DRG cultures (P5, 6 DIV) and incubated for 24 hours at 37°C in 5% (v/v) CO_2, as described

in 2.2.6.7, in order to demonstrate the dose-dependent cleavage of SNAP-25. Observation of the cleaved form of SNAP-25 starts to occur following exposure to 100 nM of LC-H_N/A-CS, while for LC-H_N/A-anti-P2X$_3$ IgG it occurs at 10 nM. The presence of a greater amount of the cleaved form of SNAP-25 with LC-H_N/A-anti-P2X$_3$ IgG compared LC-H_N/A-CS indicates that the suspectibility of LC-H_N/A is improved by conjugation to anti-P2X$_3$ IgG. Thus, the concept that anti-P2X$_3$ IgG can target BoNT to sensory neurons for inflammatory pain treatment was successfully demonstrated *in vitro* (Fig. 6.4).
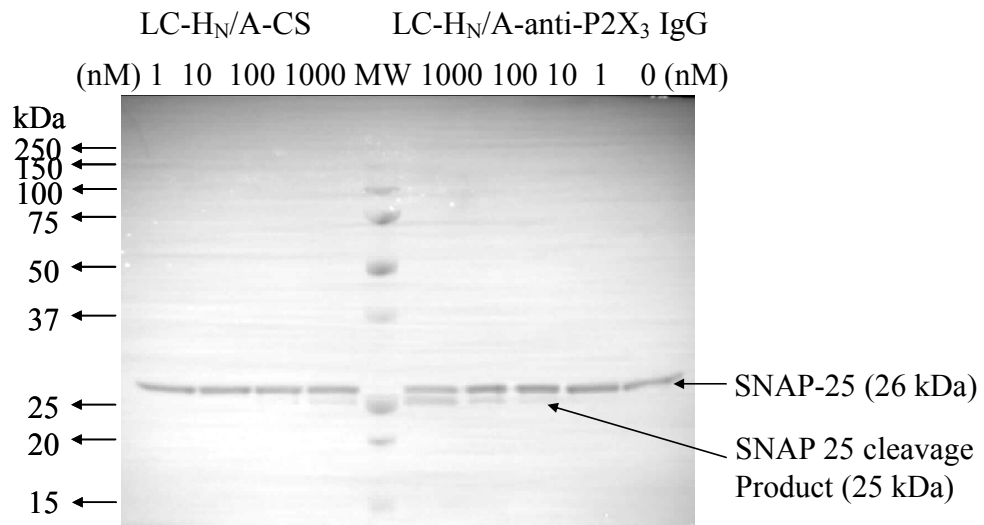
Fig. 6.4 Western blot analysis of cleavage of SNAP-25 by LC-H_N/A-anti-P2X$_3$ IgG and LC-H_N/A-CS in cultured rat DRGs. After Western blotting, the membrane was stained by mouse anti-SNAP-25 (SMI-81; 1:1,000 dilution) and mouse anti-syntaxin-1 (HPC-1; 1:1,000 dilution), followed by addition of alkaline phosphatase-conjugated anti-mouse IgG (1:5,000 dilution). Syntaxin 1 was used as an internal control. The SNAP-25 cleaved form (~ 25 kDa; lower band) was enhanced with increased concentrations of LC-H_N/A from 0 to 1,000 nM. Lanes 1-4, LC-H_N/A-CS at concentrations of 1, 10, 100 and 1,000 nM, respectively; lane 5, molecular weight markers; lanes 6-10, LC-H_N/A-anti-P2X$_3$ IgG at concentrations of 1,000, 100, 10, 1 and 0 nM, respectively. LC-H_N/A-CS = core streptavidin-conjugated light chain and translocation domain of botulinum toxin serotype A and LC-H_N/A-anti-P2X$_3$ IgG = anti-P2X$_3$ IgG-conjugated light chain and translocation domain of botulinum toxin serotype A.

200

6.2.3 Successful expression and purification of BoNT/D-scFv fusion protein with and without the N-terminal binding domain (LC-H$_N$-H$_{CN}$/D-anti-P2X$_3$ scFv and LC-H$_N$/D-anti-P2X$_3$ scFv)

6.2.3.1 Selection of positive BoNT/D-scFv clones

After genetic linkage of LC-H$_N$-H$_{CN}$/D and LC-H$_N$/D with the anti-P2X$_3$ scFv through PCR, the PCR product was extracted and purified, followed by transformation into Top 10 cells and plating on agar plates (with 30 μg/mL kanamycin) (section 2.2.7.1). Single clones were picked (6 clones for each fusion) and plasmids were extracted and purified for selection of positive clones through agarose gel electrophoresis. All the six clones of LC-H$_N$/D-scFv were shown to be positive (8 Kb), and five clones of LC-H$_N$-H$_{CN}$/D-scFv showed to be positive (9 Kb) (Fig. 6.5). Sequences of clones 6 (LC-H$_N$-H$_{CN}$/D) and clone 7 (LC-H$_N$/D) were verified by DNA sequencing and chosen for large-scale.
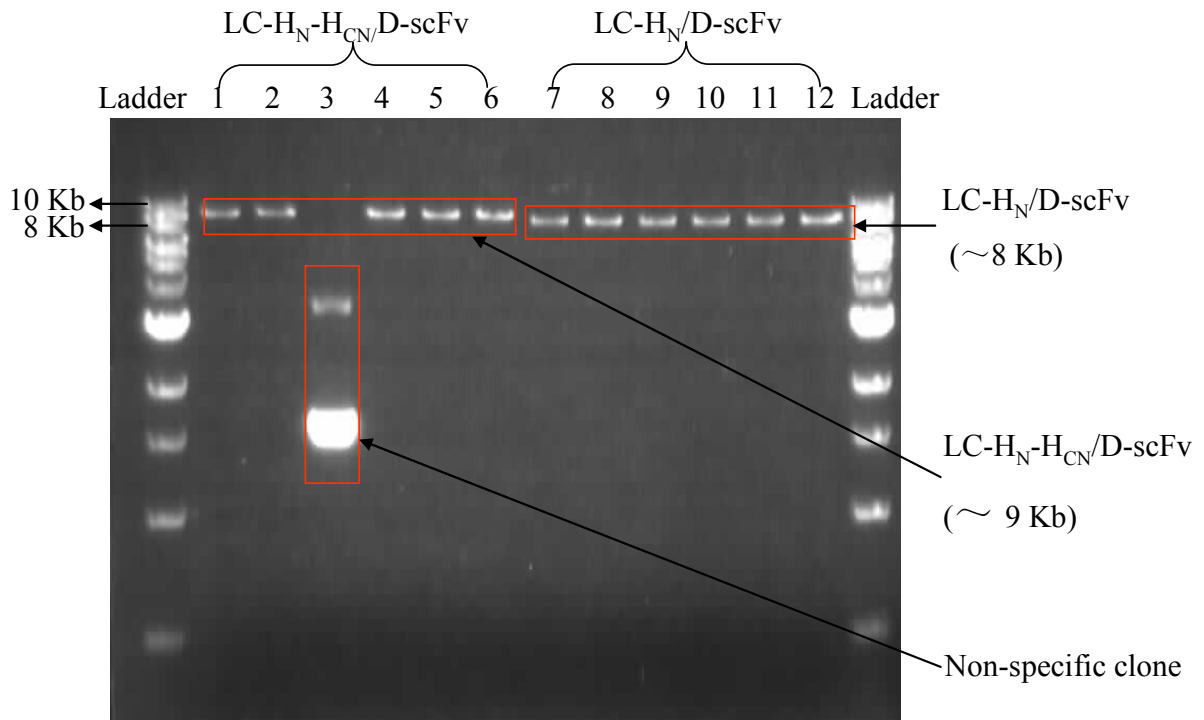
Fig. 6.5 Agarose gel analysis of positive BoNT/D scFv clones. After separation on a 1% agarose gel, all six clones of LC-H_N/D-scFv were shown to be positive, as indicated by bands at 8 Kb, while five clones of LC-H_N-H_{CN}/D-scFv showed positive expression indicated by correctly sized bands at 9 Kb. Lanes 1-12 = clones 1-12.

6.2.3.2 Western blot analysis of small-scale fusion expression

The expressing of LC-H_N-H_{CN}/A-scFv and LC-H_N/A-scFv in 1mL crude bacterial lysates was analysed using Western blotting, as described in section 2.2.7.2. Strong bands at the correct positions (150 kDa for LC-H_N-H_{CN}/A-scFv and 125 kDa for LC-H_N/A-scFv) were successfully detected (Fig. 6.6).
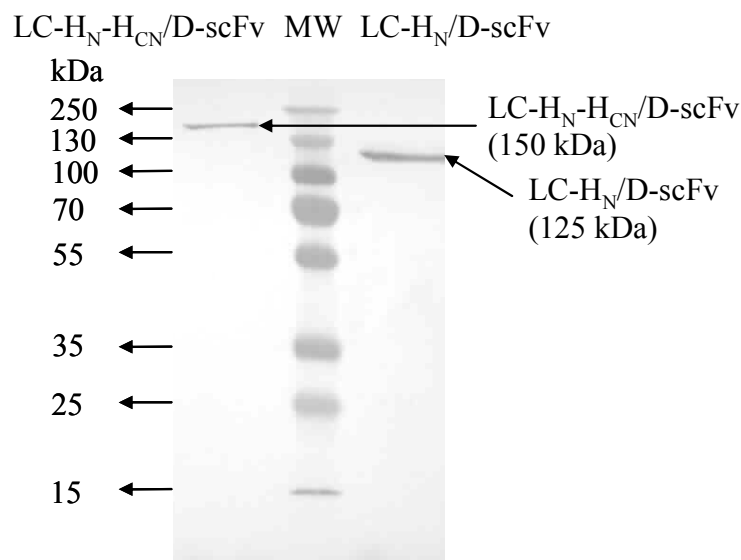
Fig. 6.6 Western blot analysis of LC-H_N-H_{CN}/D-scFv and LC-H_N/D-scFv expression. Crude bacterial lysates from LC-H_N-H_{CN}/D-scFv and LC-H_N/D-scFv culture were loaded onto SDS-PAGE. After Western blotting, the membranes were stained by HRP-labelled mouse-anti-His antibody. The presence of a band at about 150 kDa (LC-H_N-H_{CN}/D-scFv) and 125 kDa (LC-H_N/D-scFv) indicated that the LC-H_N-H_{CN}/D-scFv and LC-H_N/D-scFv fusions were successfully expressed. LC-H_N-H_{CN}/D-scFv = light chain, translocation domain and N-terminal binding domain of botulinum toxin type D; LC-H_N/D-scFv = light chain, translocation domain of botulinum toxin type D and MW = molecular weight markers.

6.2.3.3 SDS-PAGE analysis of fusion protion expression and purification

There is a Thrombin cleavage site between BoNT light and heavy chains. It was previously explained that BoNT in the single chain (SC) form has no biologically activity, whereas the di-chain (DC) from has biological activity.

The hybrid proteins LC-H_N/D-scFv and LC-H_N-H_{CN}/D-L-scFv were expressed in *E. coli* (BL21-DE3 strain) using auto-induction medium and were purified by IMAC only. The pooled samples were only partially nicked by incubation with Thrombin [1 mg intact hybrid protein/2 units Thrombin; 1/1,000 (v/v)] to convert single chain (SD) to the biologically active di-chain form (DC) (section

2.2.7.1). At the end of the incubation, APMSF was added to the reaction at a final concentration of 250 µM to inactivate Thrombin.

For LC-H_N/D-scFv, the intense bands at the correct positions [125 kDa (LC-H_N/D-scFv) before nicking; 75 kDa (H_N/D-scFv) and 50 kDa (LC) after nicking and addition of dithiothreitol (DTT) to break disulfide bonds] were detected (Fig. 6.7), which indicated successful expression and purification of these toxin-scFv conjugates.

For LC-H_N-H_{CN}/D-scFv, the intense bands at the correct position [150 kDa (LC-H_N-H_{CN}/D-scFv) before nicking; 100 kDa (H_N-H_{CN}/D-scFv) and 50 kDa (LC) after nicking and addition of dithiothreitol (DTT) to break disulfide bonds] were detected (Fig. 6.7), which indicated successful expression and purification of these toxin-scFv conjugates.
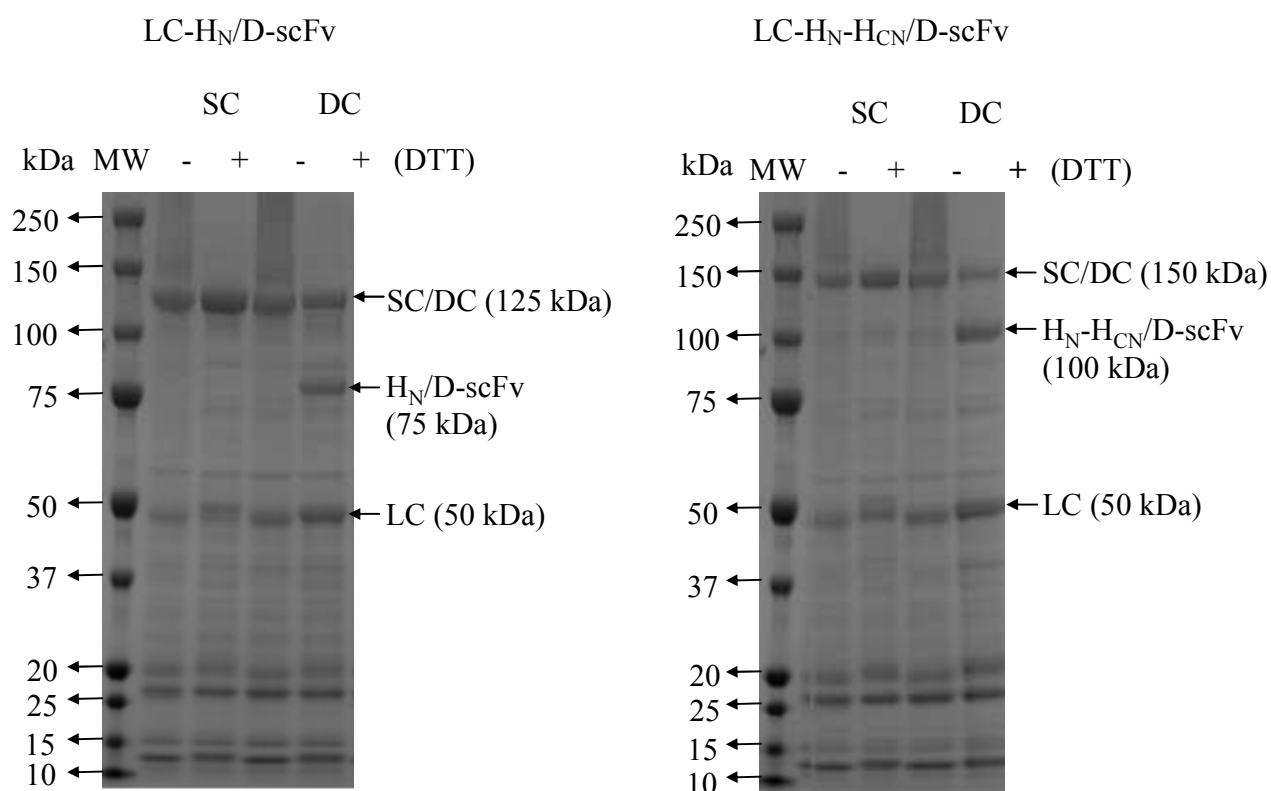
Fig. 6.7 SDS-PAGE analysis of expression and purification of hybrid proteins LC-H$_N$/D-scFv and LC-H$_N$-H$_{CN}$/D-L-scFv in *E. coli* (BL21-DE3). The protein and proteolytic fragments migrated to the expected positions. LC = light chain of botulinum toxin; H$_N$/D = translocation domain of botulinum toxin type D; H$_{CN}$/D = N-terminal binding domain of botulinum toxin type D; L = linker; DTT = dithiothreitol; SC = single chain of botulinum toxin; DC = double chain of botulinum toxin and MW = molecular weight markers.

6.2.3.4 Comparision of VAMP2 cleavage in cultured DRGs for LC-H$_N$-H$_{CN}$/D and LC-H$_N$/D before and after fusion with anti-P2X$_3$-scFv

Rat DRGs, cultured for 5 days, were incubated with different concentrations of BoNT/D-scFv fusion proteins (LC-H$_N$-H$_{CN}$/D-MH7C and LC-H$_N$/D-MH7C) and control proteins (0, 1.6, 8, 40, 200 and 1,000 nM) for 24 hours to cleave pain-related vesicle-associated membrane protein (VAMP2). Cells were then

solubilized in 2 x LDS sample buffer and subjected to SDS-PAGE and then Western blotting, as described in section 2.2.7.4.

VAMP2 cleavage (reduction of band-intensity at position of ~ 18 kDa) was detected using mouse anti-VAMP2 (V2) antibody, followed by addition of associated HRP-labelled goat anti-mouse IgG. SNARE protein, syntaxin 1 (~ 35 kDa; another inflammatory pain-related SNARE protein expressed with VAMP2 in vesicular membranes), was used as an internal control due to the lack of cleavage. The amount of VAMP2 in the loaded sample was indicated by dividing the density of VAMP2 by the density of syntaxin 1. The density of each band was analysed using ImageJ software (National Institutes of Health, U.S.A.). Syntaxin 1 was simultaneously detected by mouse anti-syntaxin-1 (HPC-1).

Fig 6.8 showed that increasing BoNT/D-scFv and BoNT/D control concentrations cleaved VAMP2, as indicated by reduction of the VAMP2 band (~ 18 kDa). Little improvement was observed after fusion with MH7C. The half-maximal effective concentration (EC_{50}) for both LC-H_N-H_{CN}/D-MH7C and LC-H_N-H_{CN}/D was around 200 nM (Fig. 6.8a) and for LC-H_N/D-MH7C and LC-H_N/D it ranged from 40 to 200 nM (Fig. 6.8b). This lack of efficacy of MH7C scFv in BoNT/D delivery may be caused by BL21-DE3 *E. coli* expression levels, as it is reported that BL21-DE3 may give rise to improper disulphide bond formation and, thus, poor stability, folding and functionality of BL21-DE3-expressed LC-H_N/D-MH7C and LC-H_N-H_{CN}/D-MH7C, which contain three functional disulphide bonds (Thangudu *et al.*, 2008). Origami 2(DE3) cells will be used for fusion protein expression since it was reported that these cells can be used to enhance disulphide bond formation (Larsen *et al.*, 2008).

(A)

L_C-HN-H_{CN}/D L_C-HN-H_{CN}/D-MH7C

(nM) 0 1.6 8 40 200 1000 MW 1000 200 40 8 1.6 0 (nM)

Syntaxin1 (~35 kDa)

VAMP2 (~18 kDa)

(B)
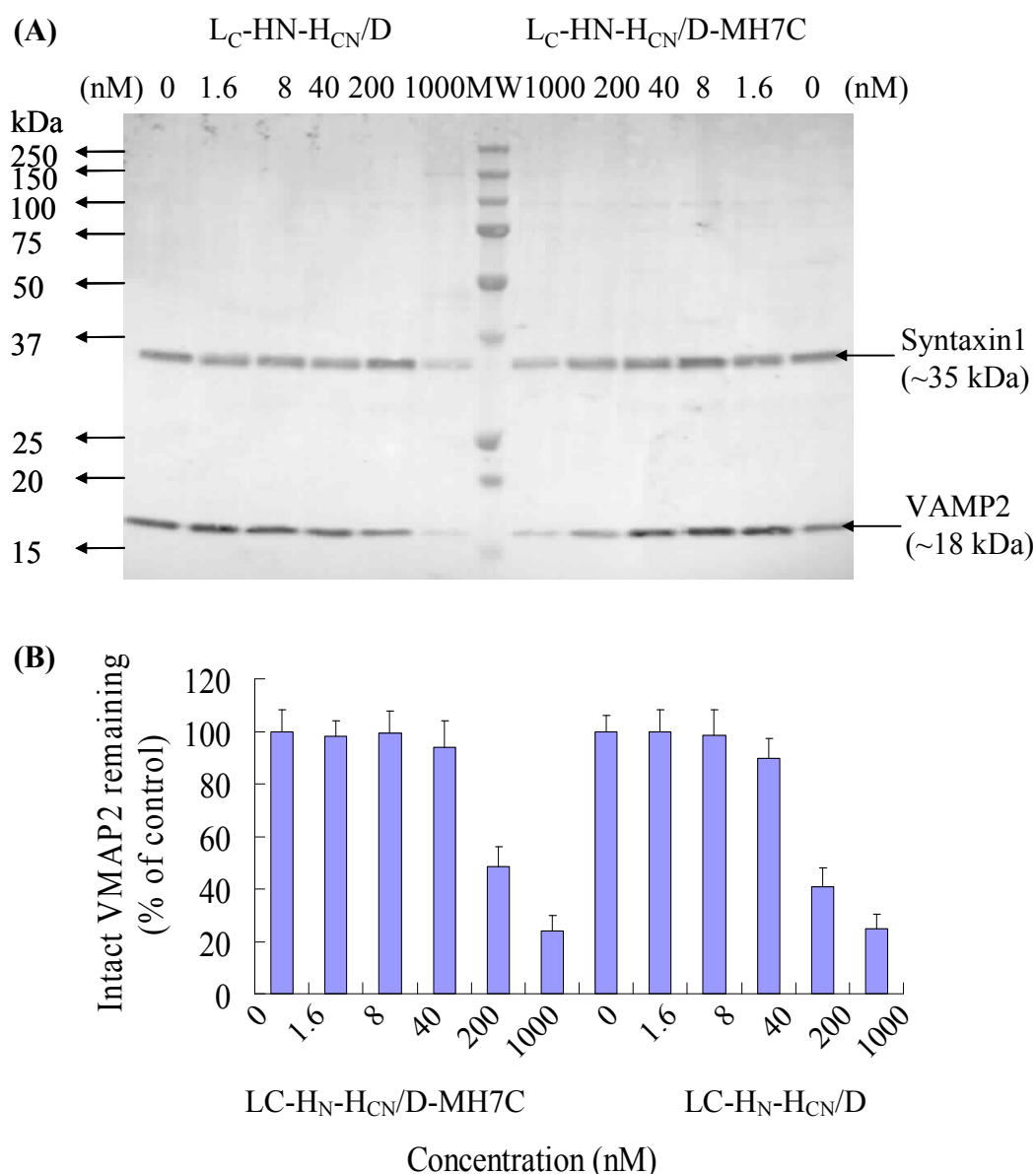
Fig. 6.8a Western blot comparison of VAMP2 cleavage by LC-H_N-H_{CN}/D-MH7C and LC-H_N-H_{CN}/D in cultured rat DRGs. Rat DRGs cultured for 5 days were exposed to different concentrations of LC-H_N-H_{CN}/D-MH7C and LC-H_N-H_{CN}/D (0, 1.6, 8, 40, 200 and 1,000 nM) for 24 hours. (A) After Western blotting, the membrane was stained with mouse anti-VAMP2 and mouse anti-syntaxin-1 antibody, followed by addition of alkaline phosphatase-conjugated anti-mouse IgG secondary antibody. (B) The EC_{50} for both LC-H_N-H_{CN}/D-MH7C and LC-H_N-H_{CN}/D was determined as being 200 nM. The results are the mean ± standard deviation (S.D.), where n = 3.
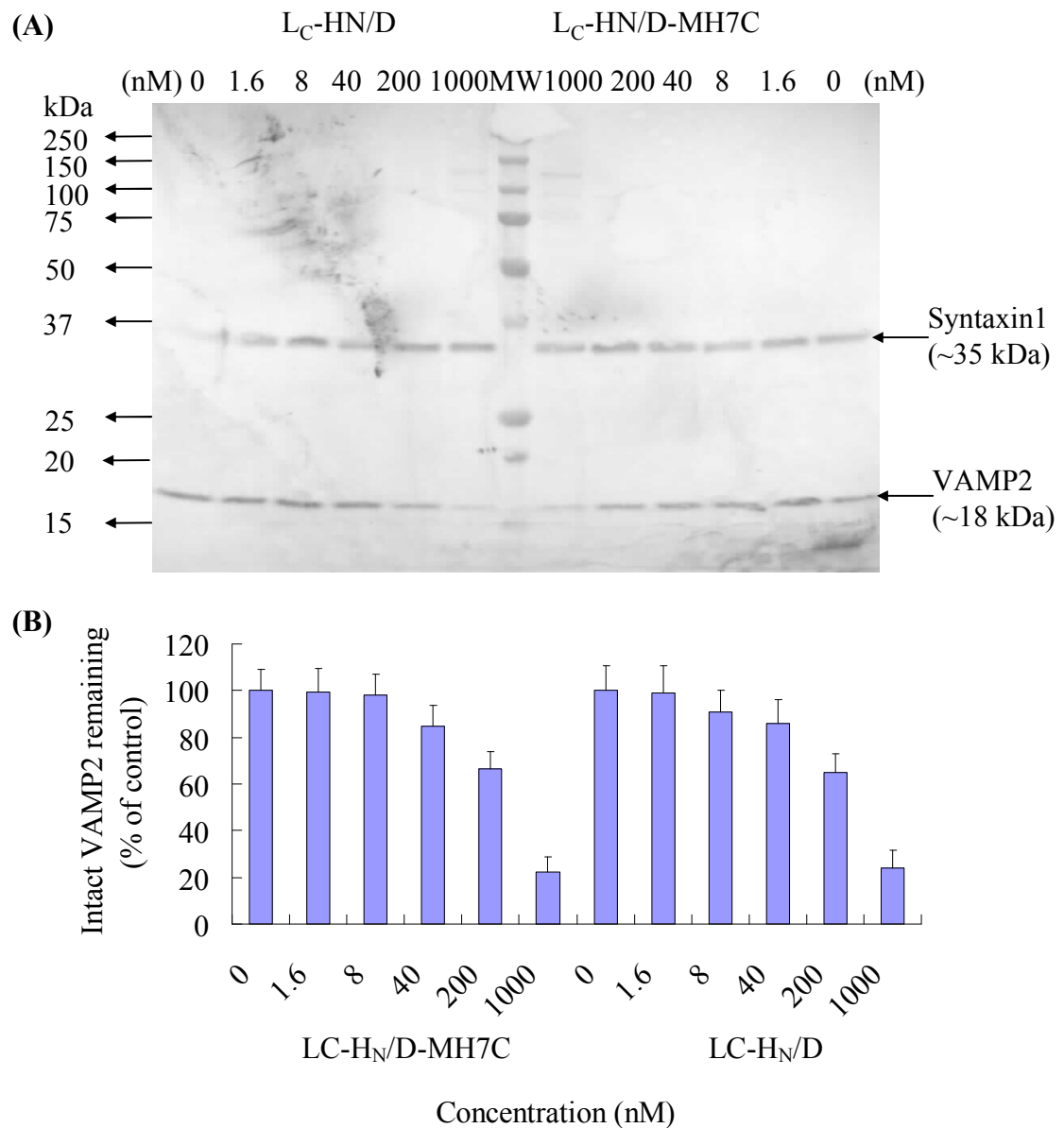
Fig. 6.8b Western blot comparison of VAMP2 cleavage by LC-H$_N$/D-MH7C and LC-H$_N$/D in cultured rat DRGs. Rat DRGs cultured for 5 days were exposed to different concentrations of LC-H$_N$/D-MH7C and LC-H$_N$/D (0, 1.6, 8, 40, 200 and 1,000 nM) for 24 hours. (A) After Western blotting, the membrane was stained with mouse anti-VAMP2 and mouse anti-syntaxin-1 antibody, followed by addition of alkaline phosphatase-conjugated anti-mouse IgG secondary antibody. (B) The EC$_{50}$ for both LC-H$_N$/D-MH7C and LC-H$_N$/D was determined as being between 200 to 1000 nM. The results are the mean ± standard deviation (S.D.), where n = 3.

6.2.4 Generation of control proteins LC-H$_N$/A and LC-H$_N$-H$_{CN}$/A

Control proteins were required for comparison of endopeptidase activity (the ability to cleave SNAREs) with the BoNT/A-scFv fusions. LC-H$_N$/A and LC-H$_N$-H$_{CN}$/A were cloned, expressed and purified as negative controls.

6.2.4.1 Western blot analysis of small-scale control protein expression

Plasmids of LC-H$_N$-H$_{CN}$/A and LC-H$_N$/A clones, in Top 10 competentant cells, were extracted, purified and sequenced. The positive clones were then transformed into BEL21-DE3. Eight clones were picked for each fusion. LC-H$_N$-H$_{CN}$/A and LC-H$_N$/A expression in 1mL crude bacterial lysates was analysed using Western blotting, as described in section 2.2.7.2. The strong bands at the correct positions (125 kDa for LC-H$_N$-H$_{CN}$/A and 100 kDa for LC-H$_N$/A) were successfully detected for all the 16 clones (Fig. 6.9). Clone 5 and 13 were then picked for large-scale expression.
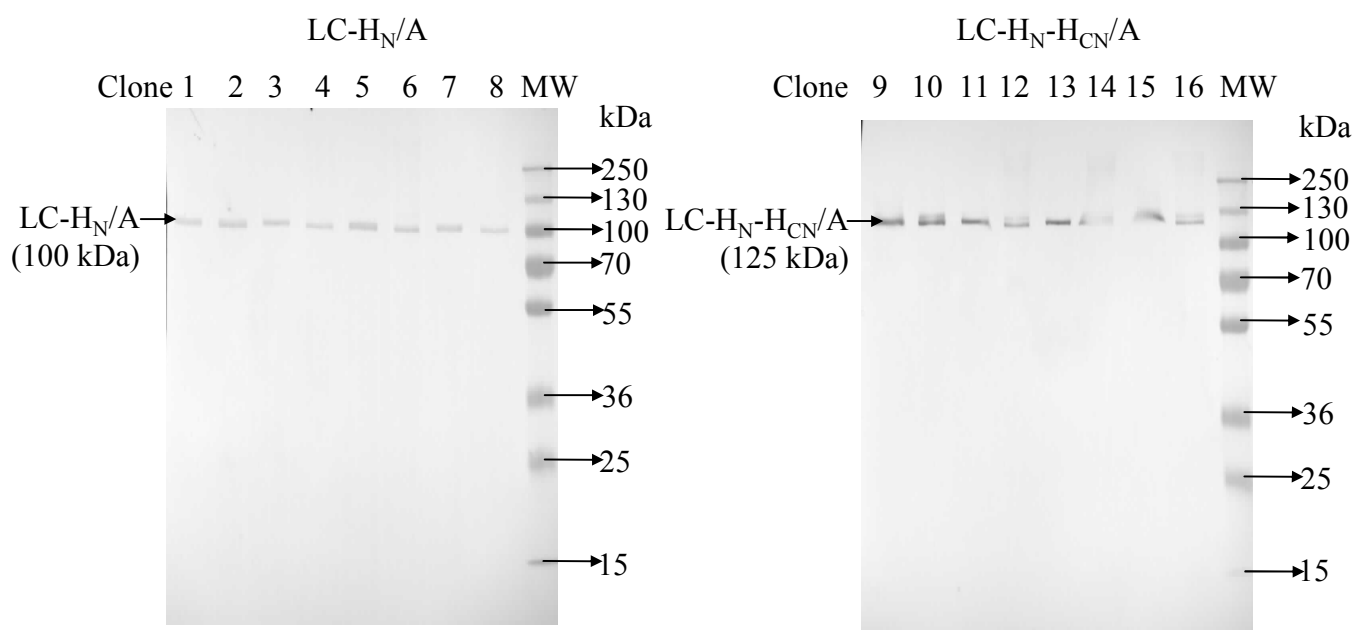
Fig. 6.9 Western blot analysis of LC-H_N-H_{CN}/A and LC-H_N/A expression. Crude bacterial lysates from LC-H_N-H_{CN}/A and LC-H_N/A cultures were loaded onto SDS-PAGE. After Western blotting, the membranes were stained by rabbit-anti-LC/A antibody. The presence of bands at about 125 kDa (LC-H_N-H_{CN}/A) and 100 kDa (LC-H_N/A) indicated that the LC-H_N-H_{CN}/A and LC-H_N/A were successfully expressed. LC-H_N-H_{CN}/A-scFv = light chain, translocation domain and N-terminal binding domain of botulinum toxin type A; LC-H_N/A-scFv = light chain, translocation domain of botulinum toxin type A; lanes 1-16 = clones 1-16 and MW = molecular weight markers.

6.2.4.2 SDS-PAGE analysis of fusion protein expression and purification

The control protein, LC-H_N-H_{CN}/A, was expressed in *E. coli* (BL21-DE3 strain) using auto-induction medium and purified by IMAC (Fig. 6.10A) and ion exchange chromatography (Fig. 6.10B). The pooled samples were only partially nicked by incubation with Thrombin to convert the single chain (SD) to the biologically active di-chain form (DC) (section 2.2.7.1). At the end of incubation, APMSF was added into the reaction, with a final concentration of 250 μM, to inactivate Thrombin. The intense bands at the correct position [125

kDa (LC-H_N-H_{CN}/A) before nicking; 75 kDa (H_N-H_{CN}/A) and 50 kDa (LC) after nicking (to break light chain and heavy chain and addition of DTT to break disulfide bonds)], respectively, were successfully detected (Fig. 6.10C), which indicated successful expression and purification of LC-H_N-H_{CN}/A.

(A) Purification with IMAC—SDS-PAGE

(B) Purification with ion exchange-SDS-PAGE
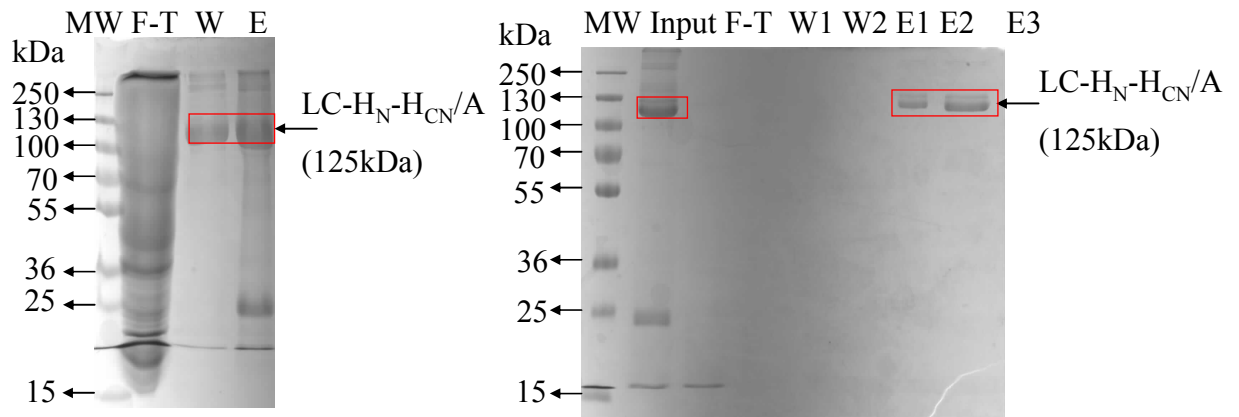
(C) LC-H_N-H_{CN}/A Control
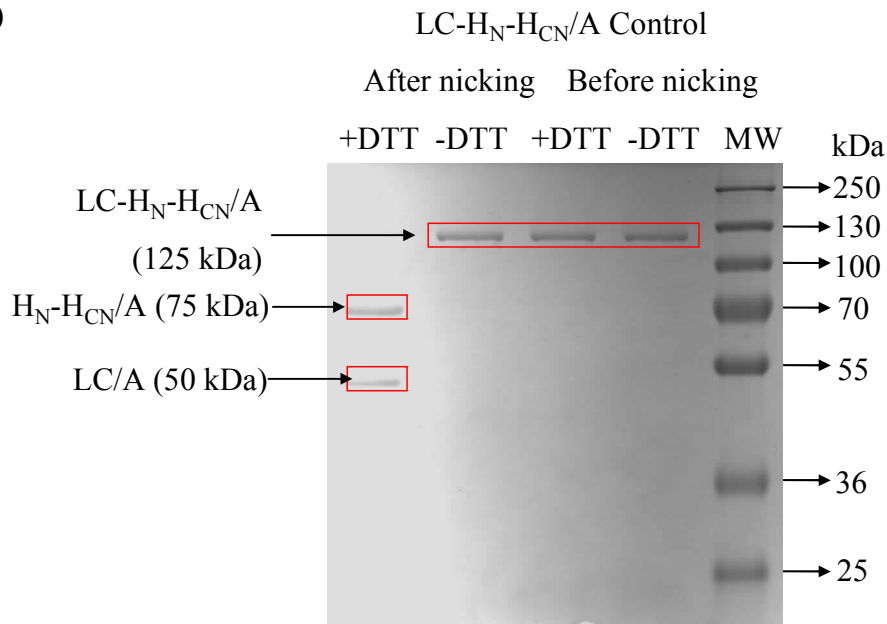
Fig. 6.10 SDS-PAGE analysis of expression and purification of control protein LC-H_N-H_{CN}/A in *E. coli* (BL21-DE3). (A) After purification by IMAC, a strong band at the expected position (125 kDa) was obtained, however, some non-specific contaminatory bands were also present. (B) A highly purified sample was obtained using ion exchange chromatography. (C) The protein and proteolytic fragments migrated to the expected positions [125 kDa (LC-H_N-H_{CN}/A) before nicking, and after nicking, without DTT; 75 kDa for H_N-H_{CN}/A and 50 kDa for LC after nicking with DTT to break disulfide bonds]. LC = light chain of botulinum toxin; H_N/A = translocation domain of botulinum toxin type A; H_{CN}/A = N-terminal binding domain of botulinum toxin type A; DTT = dithiothreitol; F-T = 'flow-through'; Lanes W1-2 = washes 1-2; Lanes E1-3 = elutions 1-3 and MW = molecular weight markers.

6.2.5 Successful expression and purification of LC-H$_N$-H$_{CN}$/A-MH7C fusion protein

6.2.5.1 Selection of positive LC-H$_N$-H$_{CN}$/A-MH7C clones

After genetic linkage of LC-H$_N$-H$_{CN}$/A and LC-H$_N$/A with the anti-P2X$_3$ scFv MH7C through PCR, the PCR product was extracted and purified, followed by transformation into *E. coli* strain, Origami™ 2(DE3) cells and plating out on agar plates (with 30 µg/mL kanamycin) (section 2.2.7.1). Five clones were picked from each fusion. After expression, plasmids were purified for selection of positive clones through agarose gel electrophoresis. All of the 5 clones of LC-H$_N$/A-scFv (8 Kb) and 4 clones of LC-H$_N$-H$_{CN}$/A-scFv (9 Kb) were shown to be positive (Fig. 6.11). The sequence of clone 7 (LC-H$_N$-H$_{CN}$/A-scFv) was verified by DNA sequencing and it was then chosen for large-scale production.
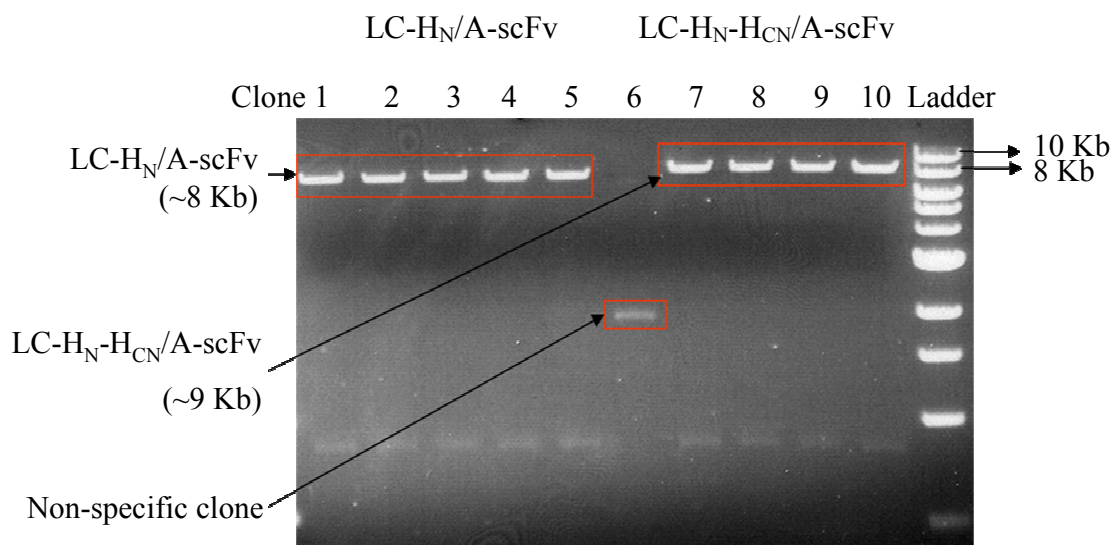
Fig. 6.11 Agarose gel analysis of positive BoNT/A scFv clones. After separation on a 1% agarose gel, all the five clones of LC-H$_N$/A-scFv were shown to be positive, as indicated by bands at 8 Kb. Four clones of LC-H$_N$-H$_{CN}$/A-scFv showed positive expression as indicated by correctly sized bands at 9 Kb. Lanes1-10 = clones 1-10.

6.2.5.2 Optimisation of fusion protein expression and purification

6.2.5.2.1 SDS-PAGE analysis of fusion expression using auto-induction medium

The hybrid protein LC-H_N-H_{CN}/A-MH7C was then expressed in *E. coli* [Origami™ 2(DE3) strain] using auto-induction medium. Fusion expression was analysed using Western blotting with 1.5 mL crude bacterial lysates from 7 picked single clones (section 2.2.7.2). The intense band at the correct position (165 kDa, LC-H_N-H_{CN}/A-MH7C) was successfully detected for all the 7 clones (Fig. 6.12). Clone 3, which gave highest expression level, was then picked for large-scale expression.
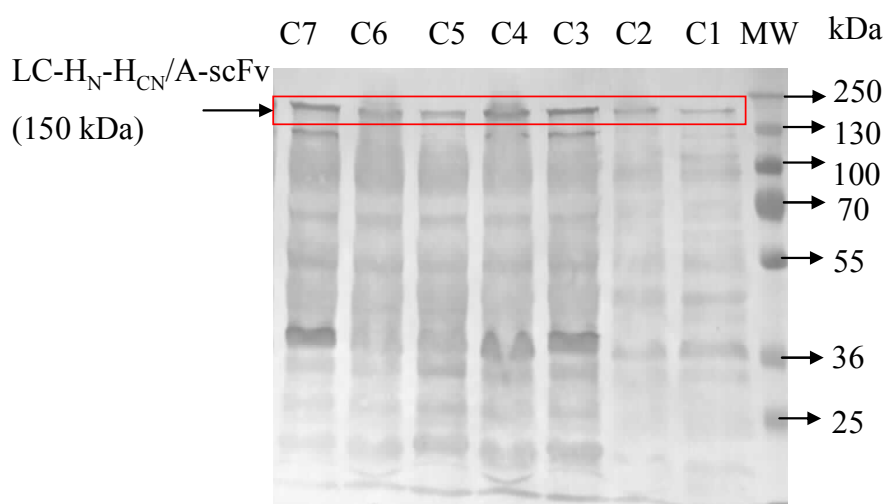
Fig. 6.12 Western blot analysis of LC-H_N-H_{CN}/A-MH7C expression. Crude bacterial lysates from 7 clones of LC-H_N-H_{CN}/A-MH7C culture were loaded onto SDS-PAGE. After Western blotting, the membranes were stained by HRP-labelled mouse anti-His antibody. The presence of bands at 165 kDa indicated that the LC-H_N-H_{CN}/A-MH7C was successfully expressed. LC = light chain of botulinum toxin; H_N/A = translocation domain of botulinum toxin type A; H_{CN}/A = N-terminal binding domain of botulinum toxin type A; Lanes C1-7 = clones 1-7 and MW = molecular weight markers.

6.2.5.2.2 Large-scale fusion expression using auto-induction medium and purification with IMAC

LC-H_N-H_{CN}/A-MH7C (clone 3) was cultured in a volume of 4 L of auto-induction medium and then purified by IMAC (section 2.2.5.1). However, no clear band was detected at the expected position of 165 kDa (Fig. 6.13). It is possible for example that the fusion protein may be degraded by certain enzymes released by *E. coli* (Origami) during expression and overnight induction. However, lower induction temperatures and shorter induction times will be considered in order to significantly reduce fusion protein degeneration by enzymes. SB medium with 0.1 mM IPTG induction will be used instead of auto-induction medium.
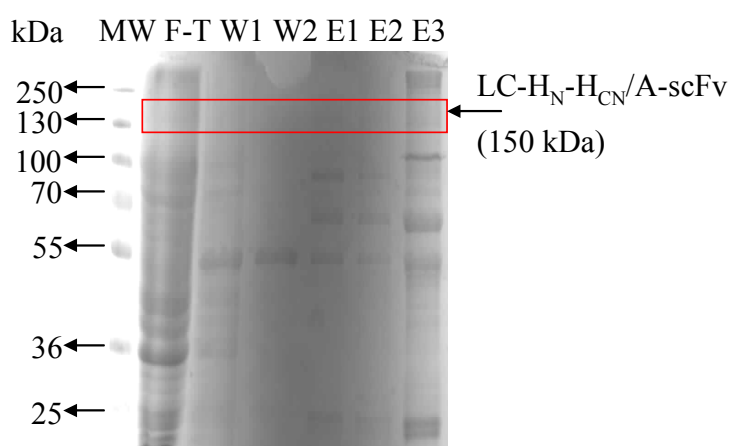
Fig. 6.13 SDS-PAGE analysis of large-scale expression and purification of hybrid proteins LC-H_N-H_{CN}/A-MH7C in *E. coli* [Origami™ 2(DE3) strain]. No protein or fragment migrated to the expected position at 165 kDa equivalent to LC-H_N-H_{CN}/A-MH7C. LC = light chain of botulinum toxin; H_N/A = translocation domain of botulinum toxin type A; H_{CN}/A = N-terminal binding domain of botulinum toxin type A; F-T = 'flow-through'; Lanes W1-2 = wash 1-2; Lanes E 1-3 = elution 1-3 and MW = molecular weight markers.

215

6.2.5.2.3 Optimisation of fusion expression in SB medium with IPTG-induction

SB medium with 0.1 mM IPTG induction was used for LC-H_N-H_{CN}/A-MH7C fusion expression instead of auto-induction medium. After OD_{600} nm reached 6.0, 0.1 mM IPTG was added for protein induction at 16°C. Five mL of culture was harvested after 1, 2, 3, 4, 5, 6, 7 and 8 hours and overnight, respectively. Both ELISA and Western blotting were then performed using crude lysates of these samples. The sample which had been induced for 4 hours, showed the best titre against P2X$_3$-257 (Fig. 6.14) and had the strongest binding at the right position (165 kDa) (Fig 6.15). Hence, a four-hour IPTG induction using SB medium was used for large-scale fusion expression.
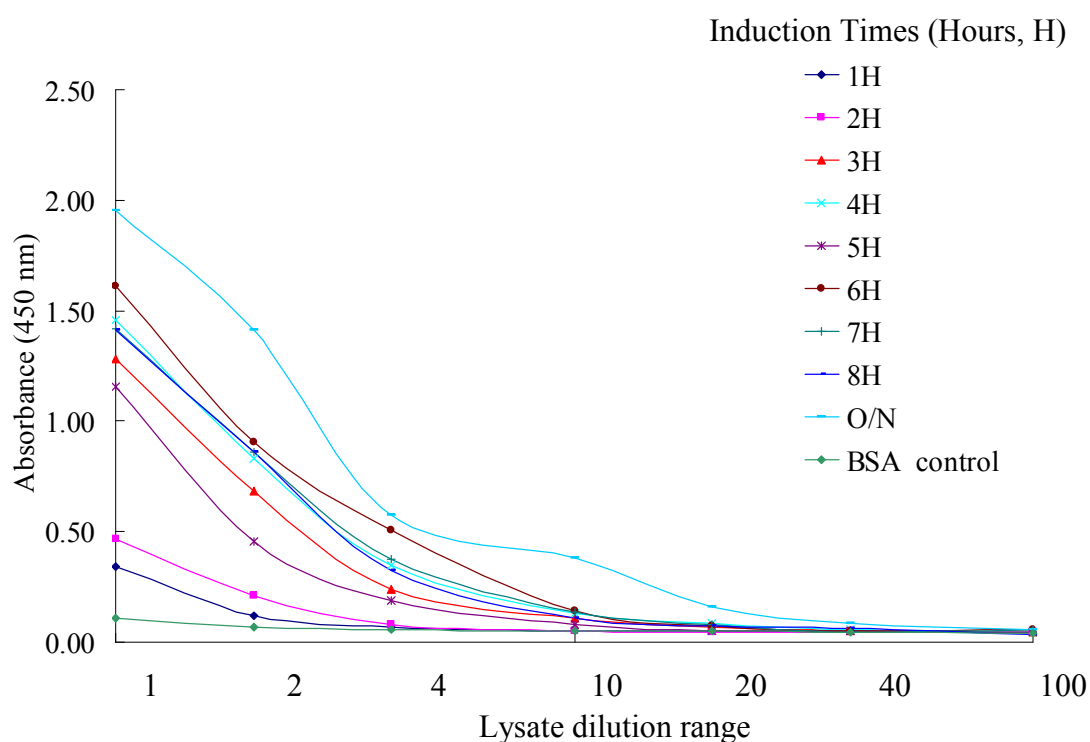
Fig. 6.14 ELISA analysis of LC-H_N-H_{CN}/A-MH7C expression by titration of crude lysates after IPTG-induction for 1-8 hours and overnight. An ELISA plate was coated with 2 µg/mL P2X$_3$-257-BSA conjugate and blocked with 5% (w/v) milk in PBST. A range of crude lysate dilutions were applied, followed by HRP-labelled mouse anti-His secondary antibody (1:1,000 dilution). Four-hour IPTG-induction gave the highest titre. Lanes 1-8H = induction times of 1-8 hours and O/N = overnight.

216
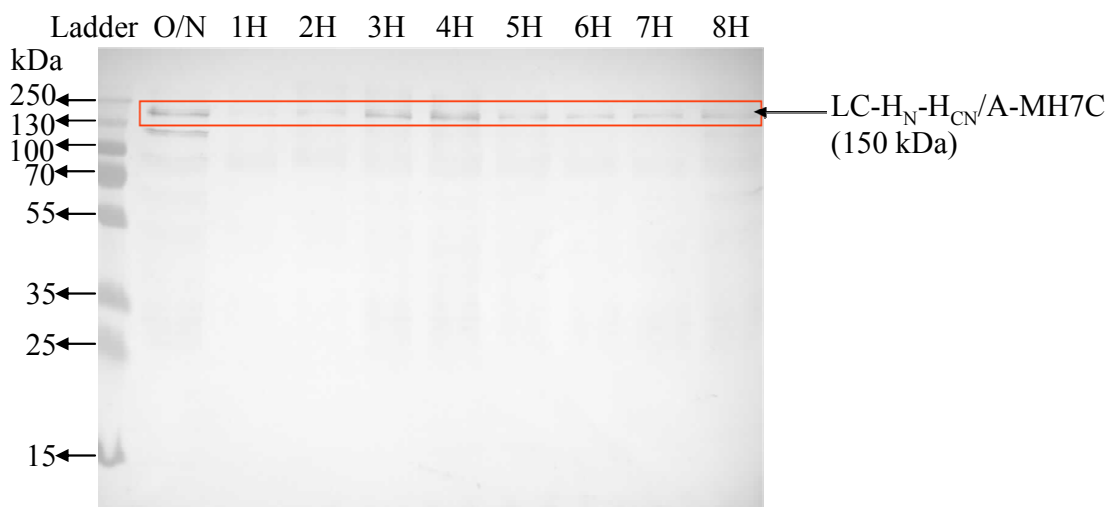
Fig. 6.15 Western blot analysis of LC-H_N-H_{CN}/A-MH7C expression with different IPTG-induction times. Crude bacterial lysates of LC-H_N-H_{CN}/A-MH7C culture, from 1-8 hours and overnight induction with 0.1 mM IPTG, were loaded onto SDS-PAGE. After Western blotting, the membranes were stained by HRP-labelled mouse anti-His antibody. The presence of bands at 165 kDa indicated that the LC-H_N-H_{CN}/A-MH7C was successfully expressed and the 4-hour induction gave the highest expression level. LC = light chain of botulinum toxin; H_N/A = translocation domain of botulinum toxin type A; H_{CN}/A = N-terminal binding domain of botulinum toxin type A; Lanes 1-8H = induction times of 1-8 hours and O/N = overnight.

6.2.5.2.4 Large-scale fusion expression with 4 hour IPTG-induction and purification using IMAC

LC-H_N-H_{CN}/A-MH7C (4 L) was expressed for 4 hours with 0.1 mM IPTG-induction and then purified by IMAC only (section 2.2.5.1). However, no clear band was detected at the right position (165 kDa) by SDS-PAGE (Fig. 6.16A). After Western blotting, the membrane was incubated with HRP-labelled mouse anti-His monoclonal antibody. The strong band of scFv at approximately 25 kDa may have resulted from the breakdown of the fusion

protein, and the other strong band above 250 kDa may be aggregated fusion protein (Fig. 6.16B). Therefore, for further optimization, the purification process will be performed in the cold room (4°C) instead of at room temperature to reduce fusion protein degeneration and aggregation, and streptavidin resin linked with biotinylated P2X$_3$-257 will be applied instead of IMAC for purification.
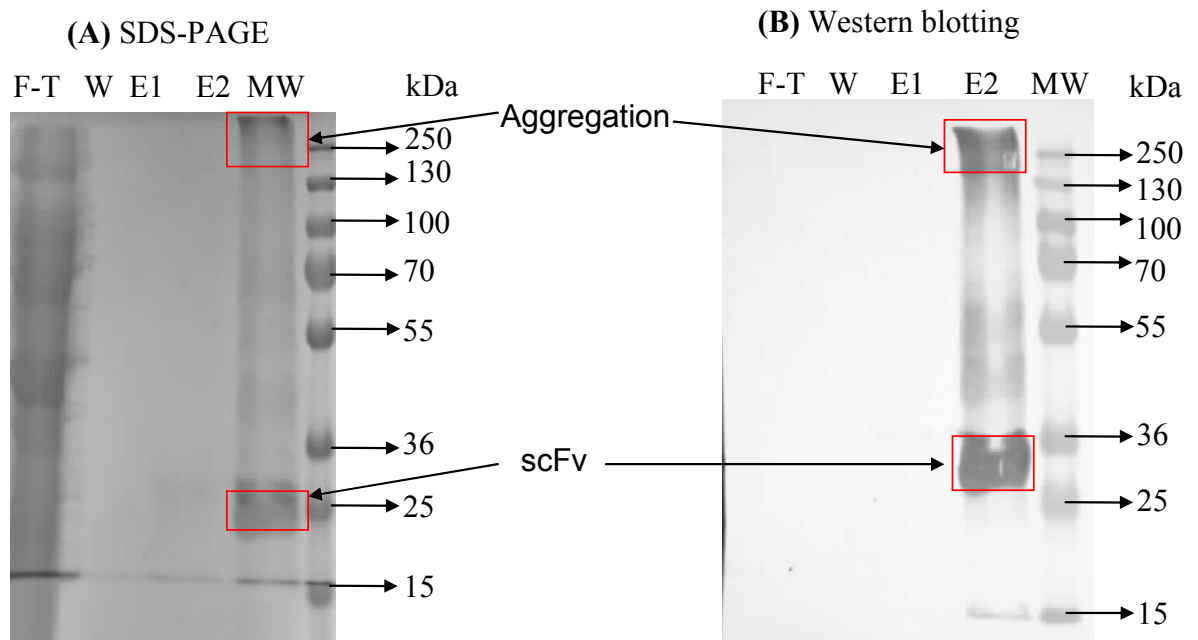
Fig. 6.16 SDS-PAGE and Western blot analysis of expression and purification of hybrid proteins LC-H$_N$-H$_{CN}$/A-MH7C in *E. coli* [Origami™ 2(DE3) strain] with 4 hours IPTG induction. (A) No band at the right position for LC-H$_N$-H$_{CN}$/A-MH7C (165 kDa) was detected. (B) After Western blotting, the membranes were stained by mouse HRP-labelled anti-His monoclonal antibody. The presence of bands above 250 kDa indicted aggregation of LC-H$_N$-H$_{CN}$/A-MH7C maybe formed. LC = light chain of botulinum toxin; H$_N$/A = translocation domain of botulinum toxin type A; H$_{CN}$/A = N-terminal binding domain of botulinum toxin type A; F-T = 'flow-through'; W = wash; E = elution and MW = molecular weight markers.

6.2.5.2.5 Fusion purification using streptavidin-agarose resin

The hybrid protein LC-H_N-H_{CN}/A-MH7C was expressed in *E. coli* [Origami™ 2(DE3) strain] using SB medium and induced with 0.1 mM IPTG. The fusion protein was then successfully purified by high affinity streptavidin resin after being linked with biotinylated P2X$_3$-257 at 4°C instead of by IMAC at room temperature (section 2.2.2.2). The intense bands at the correct position [165 kDa before addition of DTT to break disulfide bonds; 115 kDa (H_N-H_{CN}/A-MH7C) and 50 kDa (LC) after addition of DTT] were successfully detected (Fig. 6.17). This indicated successful expression and purification of these toxin-scFv conjugates.
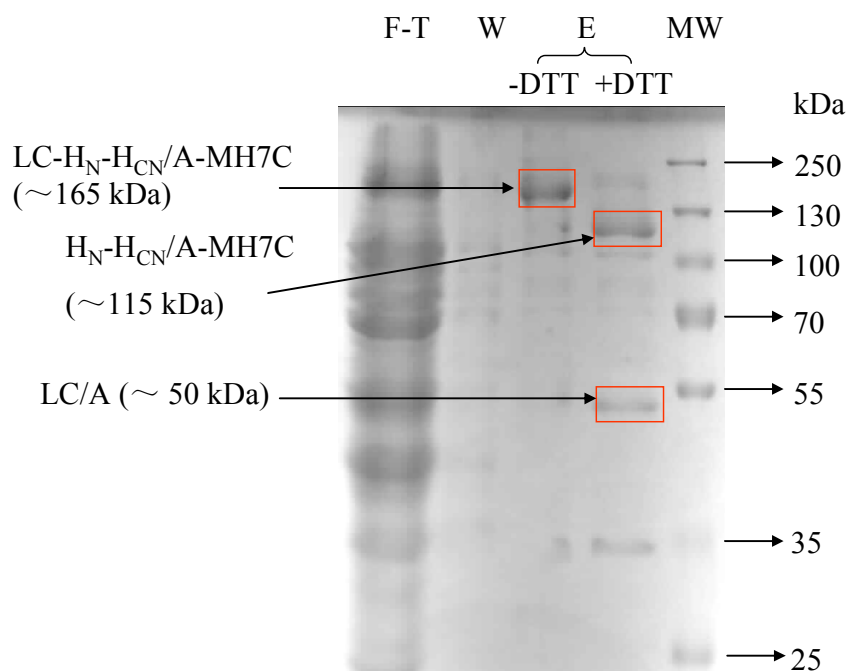
Fig. 6.17 SDS-PAGE analysis of expression and purification of hybrid proteins LC-H_N-H_{CN}/A-MH7C in *E. coli* [Origami™ 2(DE3) strain]. The protein and proteolytic fragments migrated to the expected positions [165 kDa for LC-H_N-H_{CN}/A-MH7C before addition of DTT; 50 kDa for LC and 115 kDa for H_N-H_{CN}/A-MH7C with DTT to break disulfide bonds]. LC = light chain of botulinum toxin; H_N = translocation domain; H_{CN}/A = N-terminal binding domain of botulinum toxin type A; DTT = dithiothreitol; F-T = 'flow-through'; W = wash; E = elution and MW = molecular weight markers.

6.2.5.2.6 Western blot analysis of large-scale fusion expression

Purified LC-H$_N$-H$_{CN}$/A-MH7C was identified using Western blotting, as described in section 2.2.7.2. Rabbit anti-LC/A polyclonal antibody was used as primary antibody. The strong bands at the expected positions (165 kDa for LC-H$_N$-H$_{CN}$/A-MH7Cwithout DTT; 50 kDa for LC with DTT to break disulfide bond) indicated that the LC-H$_N$-H$_{CN}$/A-MH7C was successfully expressed (Fig. 6.18).
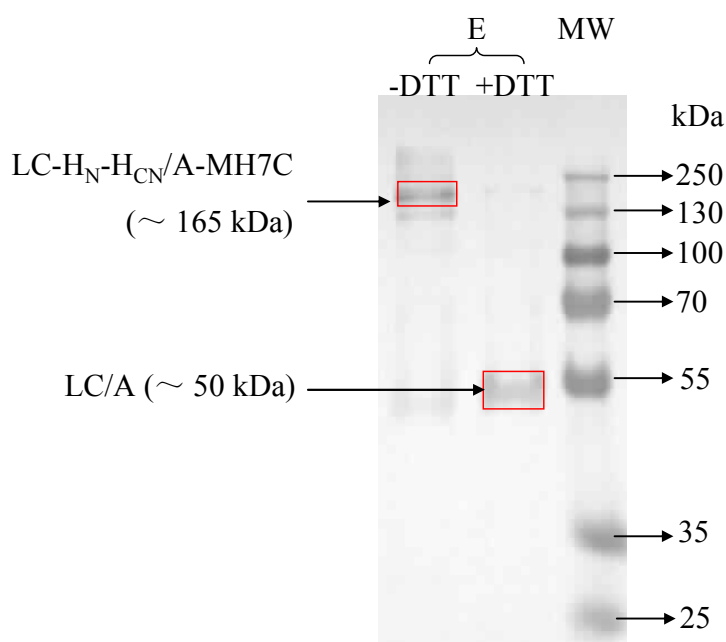
Fig. 6.18 Western blot analysis of LC-H$_N$-H$_{CN}$/A-MH7C expression. Purified LC-H$_N$-H$_{CN}$/A-MH7C was loaded onto SDS-PAGE. After Western blotting, the membranes were stained by rabbit anti-LC/A polyclonal antibody. The presence of a band at about 165 kDa (LC-H$_N$-H$_{CN}$/A-MH7C) and 50 kDa (LC/A) after addition of DTT indicated that the LC-H$_N$-H$_{CN}$/A-MH7C was successfully expressed. LC-H$_N$-H$_{CN}$/A-MH7C = light chian translocation domain and N-terminal binding domain of botulinum toxin type A fused with anti-P2X$_3$-257 scFv antibody MH7C; LC/A = light chain of botulinum toxin type A; DTT = dithiothreitol; E = elution of LC-H$_N$-H$_{CN}$/A-MH7C and MW = molecular weight markers.

6.2.5.3 *In vivo* analysis of toxicity of novel LC-HN-HCN/A -MH7C fusion via mouse lethality assay

Intraperitoneal injection of 1 µg (1 x 10^{-3} LD_{50} units/mg,) of LC-H_N-H_{CN}/A-MH7C fusion protein did not cause any mouse mortality. Therefore, LC-H_N-H_{CN}/A -MH7C had dramatically reduced toxicity compared with full length BoNT/A, which causes mouse lethality with an LD_{50} value of 5 pg (5 x 10^{-9} LD_{50} units/mg).

6.2.5.4 ELISA analysis of antigen-binding efficiency of LC-H_N-H_{CN}/A-MH7C

In order to demonstrate that MH7C scFv maintains $P2X_3$-257 binding ability on fusion to LC-H_N-H_{CN}/A, $P2X_3$-257-binding activity was analyzed using direct ELISA. An ELISA plate was coated with $P2X_3$-257-BSA conjugates, as described in section 2.2.3.13. A range of concentrations of LC-H_N-H_{CN}/A-MH7C or MH7C scFv antibody was prepared and added into individual wells, followed by the HRP-labelled mouse anti-His secondary antibody. For the negative control, BSA and LC-H_N-H_{CN} were added.

The LC-H_N-H_{CN}/A-MH7C limit of detection (LOD, three times greater than negative control) for $P2X_3$-257 antigen peptide was 60 µM, which was similar to the LOD of MH7C scFv (40 µM) (Fig. 6.19).
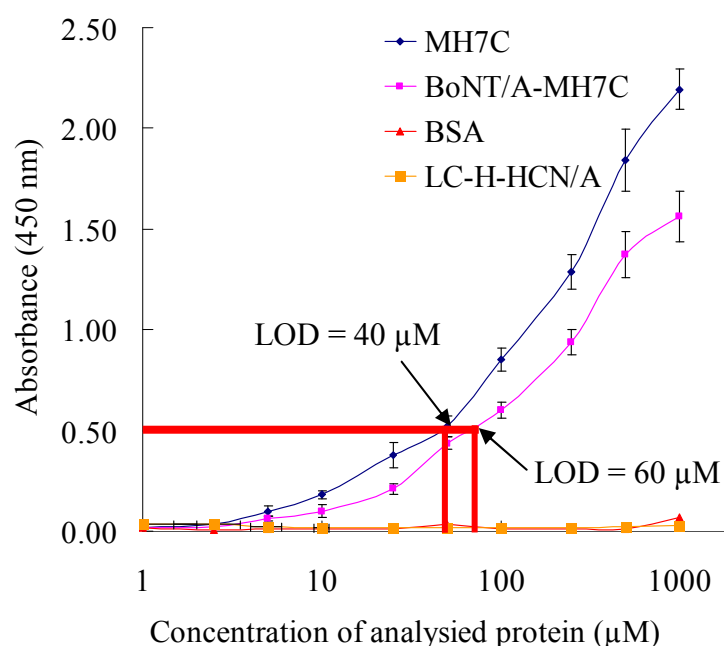
Fig. 6.19 Determination of the binding capacity for the LC-H_N-H_{CN}/A-MH7C for P2X$_3$-257. LC-H_N-H_{CN}/A-MH7C and MH7C scFv antibody gave similar binding profiles demonstrating that MH7C maintains P2X$_3$-257 binding ability after fusion with LC-H_N-H_{CN}/A. The results are the mean ± standard deviation (S.D.); where n = 3.

6.2.5.5 Cleavage of SNAP-25 in cultured DRGs for LC-H_N-H_{CN}/A before and after fusion with MH7C

A series of concentrations of LC-H_N-H_{CN}/A-MH7C and LC-H_N-H_{CN}/A control (0, 0.01, 0.1, 1, 10 and 100 nM) were added to rat DRG cultures (P5, 6 DIV) and incubated for 24 hours at 37°C in 5% (v/v) CO_2, as described in 2.2.6.7. Cells were then harvested in LDS-sample buffer and Western blotting of the cells was performed. The cleavage of SNAP-25 was detected using rabbit anti-SNAP-25 antibody which detects both cleaved SNAP-25 (~ 25 kDa) and full length SNAP-25 (~ 26 kDa). Observation of the cleaved form of SNAP-25 starts to occur following exposure to 100 nM of LC-H_N-H_{CN}/A, while for LC-H_N-H_{CN}/A-MH7C it occurs at 0.1 nM. The presence of a greater amount of the cleaved form of SNAP-25 with LC-H_N-H_{CN}/A-MH7C compared

LC-H$_N$-H$_{CN}$/A indicates that the susceptibility of LC-H$_N$-H$_{CN}$/A is improved by fusing with MH7C. Thus, the concept that recombinant rabbit anti-P2X$_3$-257 scFv antibody, MH7C, can target BoNT/A to sensory neurons for inflammatory pain treatment was verified *in vitro* (Fig. 6.20).
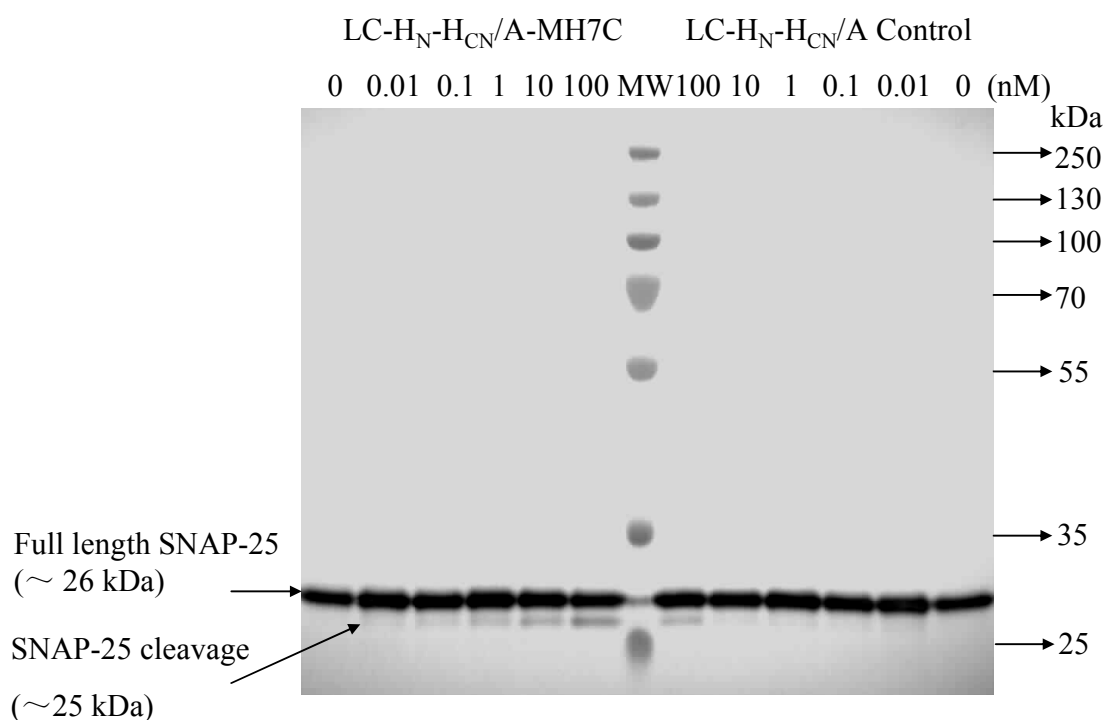
Fig. 6.20 Western blot analysis of cleavage of SNAP-25 by LC-H$_N$-H$_{CN}$-H$_{CC}$/B-scFv and LC-H$_N$-H$_{CN}$-H$_{CC}$/B in cultured rat DRGs. After Western blotting, the membrane was stained by rabbit anti-SNAP-25 (1:1,000 dilution), followed by addition of HRP-labelled anti-rabbit IgG (1:1,000 dilution). The SNAP-25 cleaved form (~ 25 kDa; lower band) was enhanced with increased concentrations of LC-H$_N$-H$_{CN}$/A-MH7C from 0 to 100 nM. LC-H$_N$-H$_{CN}$/A-MH7C = light chain, translocation domain and N-terminal binding domain of botulinum toxin type A fused with anti-P2X$_3$-257 scFv antibody MH7C and MW = molecular weight markers.

6.2.5.6 Inhibition of K$^+$-stimulated release of calcitonin gene-related peptide (CGRP) highlights the anti-nociceptive potential of the LC-H$_N$-H$_{CN}$/A-MH7C fusion protein

A range of concentrations of LC-H$_N$-H$_{CN}$/A-MH7C (0, 0.01, 0.1, 1, 10 and 100 nM) were added into rat DRGs cultures (P5, 6 DIV) and incubated for 24 hours at 37°C in 5% (v/v) CO$_2$, as described in section 2.2.7.4. K$^+$-evoked CGRP was monitored by EIA (section 2.2.7.4.2) after overnight incubation of toxins with rat DRG cultures. CGRP release was found to be significantly inhibited by 1 nM LC-H$_N$-H$_{CN}$/A-MH7C (Fig. 6.21). K$^+$-evoked CGRP release was inhibited by LC-H$_N$-H$_{CN}$/A-scFv with a concentration dependence identical to that for SNAP-25 cleavage, which demonstrated potential pain treatment value for this novel fusion construct.
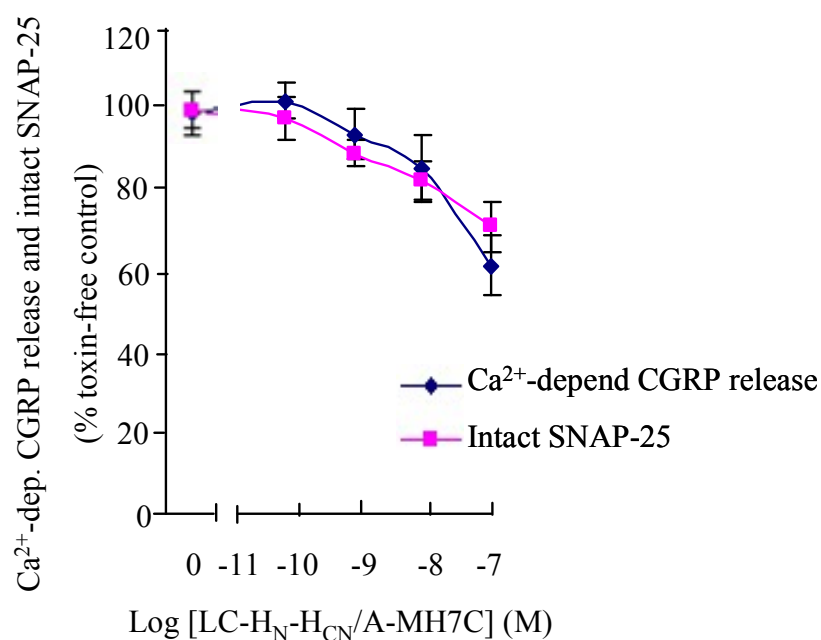
Fig. 6.21 LC-H_N-H_{CN}/A-MH7C inhibits Ca^{2+}-dependent CGRP release evoked from rat DRGs and cleaves SNAP-25. DRGs were exposed to BoNT/A and the release of CGRP was assayed over 10 minutes. The SNAP-25 cleavage ratio was calculated using digital images of the gels. An immunoblot showed cleavage of SNAP-25 by LC-H_N-H_{CN}/A-MH7C but much less was seen with the LC-H_N-H_{CN}/A control. The dose-response curve indicates BoNT/A-induced blockade of CGRP release evoked by 60 mM K^+, which correlates with the percent of remaining SNAP-25. The results are the mean ± standard deviation (S.D.); where n = 3.

6.3 Discussion

About 20% of European and United States adult populations suffer from chronic inflammatory pain, while less than 30% of these patients can be treated by current therapies. The two widely used therapies are non-medication treatments (e.g. massage, physical therapy and acupuncture) and analgesic drug treatments, for instance, nonsteroidal anti-inflammatory drugs (NSAIDs) (e.g. aspirin, ibuprofen and naproxen) and opioids. Non-medication treatments are more likely to involve physical trials, which may need long-term and frequent

225

treatment and are limited in their efficacy. NSAIDs act to reduce the production of prostaglandins (chemicals that promote inflammation, pain, and fever) and, hence, reduce inflammation and discomfort. The limitations of NSAIDs are gastrointestinal and cardiovascular harm. Opioids can relieve pain by decreasing perception of pain, decreasing reaction to pain and increasing pain tolerance. Opioids are limited in their serious side effects including sedation, respiratory depression, constipation and opioid dependence. Therefore, effective and specific therapeutics with higher efficacy and fewer side effects for chronic inflammatory pain are urgently needed (Breivik *et al.*, 2006; Röhn *et al.*, 2011). Antibody-drug conjugate, a novel type of targeted therapy, is widely used in clinical applications, and about 20 antibody conjugates are currently in clinical trials (Teicher and Chari, 2011). It consists of an antibody (or antibody fragment, for instance, scFv and Fab) linked to a drug (for instance, a toxin). The antibody enables the antibody-drug conjugates to bind to the specific protein or cells. The conjugates should then be internalized by the cell and the drug released for treatment. The side effects should be less due to antibody targeting (Chari *et al.*, 1992). Antibody-drug conjugates are widely used in cancer therapy. Many companies have put tremendous efforts into research work on antibody-drug generation and modification for better efficacy. For instance, Seattle Genetics (U.S.A.) Pfizer (U.S.A.), Abbott (U.S.A.), Roche/Genentech (U.S.A.) to optimize their therapeutic toxins and non-cleavable linkers. ImmunoGen (U.S.A.) is currently interacting with Novartis (Switzerland) and Roche/Genentech (U.S.A.) for their tumor-activated prodrug (TAP) linker technology. Many antibody-drug conjugates have been approved for clinical applications (Table 6.1), and, based on this, an antibody fragment-drug targeted therapy model was applied in this research.

It is demonstrated that P2X$_3$ plays a crucial role in inflammatory pain signalling through ATP which is released by inflamed tissue (Xu and Huang, 2002). Thus, P2X$_3$ may be exploited as a promising molecular target for pain treatment (North, 2003). In this study, a target pain treatment principle was initially proved by conjugating translocation and protease domains of BoNT/A

and BoNT/D [LC-H$_N$/A or LC-H$_N$/D] with an anti-P2X$_3$ antibody (against P2X$_3$ extracellular domain) and binding *in vitro* on rat DRG cells.

Table 6.1 Antibody-drug conjugates have been approved or are in the process of approval for clinical use.

Name of drug	Disease for treatment	Status in clinical trials
Gemtuzumab ozogamicin (Mylotarg)	Acute myelogenous leukemia	Approved in 2000 (U.S. Food and Drug Administration, 2013)
Brentuximab vedotin (Adcetris)	Relapsed and refractory hodgkin lymphoma and anaplastic large cell lymphoma	Approved in 2011 (U.S. Food and Drug Administration, 2013)
ado-Trastuzumab emtansine (T-DM1; Kadcyla)	Breast cancer	Approved in 2013 (U.S. Food and Drug Administration, 2013)
Inotuzumab ozogamicin (CMC-544)	Non-Hodgkin's lymphoma	Phase III terminated (Tuma, 2011)
Glembatumumab vedotin (CDX-011, CR011-vcMMAE)	Melanoma and metastatic breast cancer	Phase II terminated (Keir and Vahdat, 2012)
lorvotuzumab mertansine (IMGN901)	CD56 cancers (e.g. small-cell lung cancer, ovarian cancer)	Phase II terminated (Immunogen, 2013)
IMGN242 (huC242-DM4)	Can Ag- expressing gastric cancer	Phase II terminated (Qin *et al.*, 2008)
AEZS-108 (AN-152)	Ovarian cancer	Phase II terminated (Engel *et al.*, 2012)
PSMA ADC, PSMA with MMAE	Metastatic prostate cancer	Phase II terminated (Wang *et al.*, 2011)

AVE9633	Relapsed/refractory acute myeloid leukemia	Phase I terminated (Lapusan *et al.*, 2012)
SAR3419	B-cell non-Hodgkin's lymphoma (NHL)	Phase I terminated (Younes *et al.*, 2012)
Cantuzumab Mertansine (huC242-DM1)	Colorectal, pancreatic, and non-small cell lung cancer	Phase I terminated (Xie *et al.*, 2004)
CAT-8015 (anti-CD22)	Acute lymphoblastic leukemia or non-Hodgkin's lymphoma	Phase I terminated (Kreitman *et al.*, 2012)
IMGN388	Solid tumor	Phase I terminated (Immunogen, 2013)
milatuzumab-doxorubicin	Relapsed multiple myeloma	Phase I terminated (Govindan *et al.*, 2013)
SGN-75 (anti-CD70)	Non-Hodgkin's lymphoma or renal cell carcinoma	Phase I terminated (Ryan *et al.*, 2010)
AGS-16M8F	Renal cell carcinoma	Phase I terminated (Gudas *et al.*, 2010)
Anti-CD22-MCC-DM1	Leukemia	Preclinical trials initiated (Polson *et al.*, 2010)
ASG-22ME	Bladder, breast, lung and pancreatic cancers	Preclinical trials initiated (SeattleGenetics, 2013)
SGN-CD33A	Acute myeloid leukemia (AML)	Preclinical trials initiated (SeattleGenetics, 2013)

Botulinum neurotoxins (BoNTs), produced by *Clostridium botulinum*, are known to be highly potent inhibitors of regulated exocytosis of various cell mediators (Montal, 2010). There are seven serotypes of BoNTs (A - G) and

each contains three domains, a Zn^{2+}-dependent protease light chain (LC) linked by a disulphide bond to a translocation moiety (H_N) and a receptor binding domain (H_C). The C-terminal half moiety of the binding domain (H_{CC}) binds with high affinity to receptors on the pre-synaptic membrane. Little is known about the function of its N-terminal half moiety (H_{CN}). H_N forms a channel in the endosomal membrane and translocates its LC to the cytosol, after toxin binding and internalization into nerve terminals, The LC cleaves and inactivates SNAREs essential for exocytosis (Lacy and Stevens, 1998; Jin *et al.*, 2006). Toxin without H_C (termed LC-H_N) was shown to be non-toxic due to its inability to bind, whereas the replacement of the H_C with a binding moiety delivered protease to the neurons (Foster, 2004). In this study, LC/A an LC/D successfully cleaved their specific SNAREs, SNAP-25 and VAMP2. LC-H_N/A and LC-H_N/D, which was used as negative control due to lack of toxicity, showed little SNAP-25 or VAMP2 cleavage.

It was reported that BoNTs have potential value for pain treatment, including low back pain, fibromyalgia-myofascial pain, temporomandibular joint and orofacial pain. BoNT/A was proven to have potential for inflammatory pain treatment by inhibiting the release of pain-related peptides, calcitonin gene-related peptide (CGRP) and substance P (SP), through cleavage of its substrate, SNAP-25 (Datar *et al.*, 2004; Meng *et al.*, 2007). BoNT/D cleaves VAMP and then inhibits the release of substance P (SP) (Filipović *et al.*, 2012). BoNT/A and BoNT/D have been used by many researchers for pain relief (Ney and Joseph, 2007; Evidente and Adler, 2010). However, both BoNT/A and BoNT/D bind to sensory neurons as well as cholinergic neurons, sympathetic neurons and non-neuronal cells, which may give unwanted 'off-targeting effects' (Peng *et al.*, 2011). For instance, even certain types of pain (e.g. diabetic neuropathic pain, interstitial cystitis/bladder pain, visual numerical pain and inflammatory pain) can be relieved upon local injection of minute quantities of BoNT/A (Dolly *et al.*, 2011). Side effects were common and included blepharoptosis, muscle weakness, neck stiffness, parasthesia, and skin tightness (Jackson *et al.*, 2012). Therefore, targeting molecules which enable specific binding and entry into nociceptive neurons for effective relief of chronic pains

are warranted in order to reduce unwanted side effects. However, no research related to targeted BoNT for pain treatment has been reported to date.

The biotin-streptavidin interaction is known to be one of the strongest non-covalent biological interactions, with high strength and specificity (Holmberg et $al.$, 2005). Therefore, this method of linkage was chosen to join the rabbit anti-P2X$_3$ IgG and LC-H$_N$/A. Anti-P2X$_3$-IgG-LC-H$_N$/A cleaved more SNAP-25 than LC-H$_N$/A, which demonstrated that the endopeptidase activity of anti-P2X$_3$-IgG-LC-H$_N$/A was higher than that of LC-H$_N$/A (Fig. 5.4), thus, proving that anti-P2X$_3$ antibody may be a promising targeting agent for BoNT.

Anti-P2X$_3$-scFv was then applied as a delivery moiety for targeted treatment of inflammatory pain by fusing with BoNT/D, using a molecular biological approach. The non-structural linker, (GGGGS)$_3$, used to join BoNT and anti-P2X$_3$ scFv gene, can also separate BoNT and scFv in the fusion construct to prevent incorrect interactions with functional domains (Greice et $al.$, 2012). Since this is the first attempt to fuse and express botulinum toxin with a targeting antibody, no comparison can be made with another BoNT-antibody. ScFvs were previously applied for targeted therapy by fusion with other therapeutic proteins, and these fusion proteins proved to be more effective than therapeutic proteins alone, further decreasing non-specific side effects (Kreitman and Pastan, 2011; Chen et $al.$, 2012; Sheng et $al.$, 2012).

The BL21-DE3 $E.$ $coli$ can offer high-level protein expression. However, there may be a potential problem with BL21-DE3-expressed fusion proteins if those proteins possess disulphide bonds, as disulphide bonds cannot be formed in the cytoplasm of BL21-DE3 cells (Zhang et $al.$, 2010). Disulphide bonds are well known to be crucial for stability, folding and functionality of proteins and so improper formation of disulphide bonds may result in non-functional proteins (Thangudu et $al.$, 2008). For this reason, the LC-H$_N$/D-scFv and LC-H$_N$-H$_{CN}$/D-scFv (with three disulphide bonds), expressed in BL21-DE3, may have lower activity due to misfolding, which is then confirmed by comparing endopeptidase activity with LC-H$_N$/D and LC-H$_N$-H$_{CN}$/D.

Origami™ 2 host strains have mutations in both the thioredoxin reductase (trxB) and glutathione reductase (gor) genes, which greatly enhance disulfide

bond formation in cytoplasm (Larsen *et al.*, 2008). Therefore, Origami™ 2(DE3), from the Origami™ 2 strain, was used for expression of the novel fusion proteins for better disulphide bond formation. BoNT/A is also effective in treating chronic inflammatory pain and the SNAREs (SNAP-25) cleaved by BoNT/A is easier to detect than VAMP2 (Kaufman and Karceski, 2009). Hence, BoNT/A-anti-P2X$_3$ scFv (LC-H$_N$/A-MH7C and LC-H$_N$-H$_{CN}$/A-MH7C) were generated and transformed into Origami™ 2(DE3). Optimization of BoNT/A-scFv fusion protein expression and purification conditions were performed, including factors such as medium, induction temperature, induction time and purification resin. In this case, 0.1 mM IPTG-induction was proved to be better than auto-induction, as more fusion protein was obtained with less non-specific proteins. An induction temperature of 16°C gave less aggregation than 25°C (Azaman *et al.*, 2010). Purification performed at 4°C gave rise to less protein breakdown and 4 hour inductions gave the highest fusion expression levels (Yan *et al.*, 1996). Streptavidin resin, conjugated with biotinylated antigen, gave better fusion protein purification than IMAC.

In vitro data demonstrated that anti-P2X$_3$-257 antibody scFv MH7C specifically delivered the endopeptidase activity of BoNT/A to sensory neurons, as shown by the dose-dependent cleavage of SNAP-25 and the pronounced inhibition of neuropeptide release, which indicates its potential therapeutic efficacy of chronic inflammatory pain (e.g. arthritis and infections).

This report represents the first attempt to selectively target the endopeptidase activity of clostridial neurotoxins to specific cell types through the genetic fusion with an antibody. Only one paper was published by the Duggan group (2002) for a similar purpose. Their conjugated purified recombinant LC-H$_N$/A and *Erythrina cristagalli* lectin (ECL) which recognized terminal galactosyl residues at the protein level for selectively delivery of the endopeptidase activity of BoNT/A to primary nociceptive afferent neurons. Their work proved that the potent endopeptidase activity of BoNTs can be selectively retargeted to cells or pathways of interest for inhibition of neurotransmitter release, thus achieving pain treatment. However, the conjugation mixture of recombinant LC-H$_N$/A and ECL easily leads to aggregation, which makes the LC-H$_N$/A-ECL impure and

hard to quantify (Singh *et al.*, 2011). Genetic fusion can solve this problem and hence was applied in this study.

The efficacy of this therapeutic needs further *in vivo* evaluation using established capsaicin-induced or formalin-induced rat inflammatory pain models. It was reported that P2X$_3$ plays a crucial role in formalin-induced and capsaicin-induced inflammatory pain (Tsuda *et al.*, 1999; Souslova *et al.*, 2000) and both of the capsaicin receptor, VR1, and P2X$_3$ are expressed in the same group of neuronal cells (Yiangou *et al.*, 2001; Renton *et al.*, 2003). Therefore, the efficacy of LC-H$_N$-H$_{CN}$/A-MH7C can be evaluated *in vivo* in capsaicin-induced or formalin-induced inflammatory pain models.

In summary, this research represents the first attempt to conjugate botulinum toxin with a targeting anti-P2X$_3$ antibody (both polyclonal antibodies and a scFv antibody fragment, MH7C), and successfully demonstrated the principle for targeted treatment of inflammatory pain This novel approach offers improvement over existing treatments which inject BoNT/A only (Dolly *et al.*, 2011) and could protect patients from serious side effects (Jackson *et al.*, 2012), which result from nonspecific binding to cholinergic neurons, sympathetic neurons and non-neuronal cells (Peng *et al.*, 2011). Patients who suffer from low back pain, fibromyalgia-myofascial pain, temporomandibular joint and orofacial pain may benefit from this novel therapeutic.

Chapter 7

Overall Conclusions and Recommendations for Future Work

7.1 Overall conclusions

Biological techniques are widely used in medical research for understanding new diseases, in laboratory diagnostics and in drug development and immunological, cell biological, pharmacological and molecular biological approaches are applied in development of clinically applicable strategies for diagnostic and therapeutic purposes. Antibodies which target specific proteins or cells related to certain diseases play a crucial role have achieved remarkable clinical success. For over last twenty years, antibody genes have been cloned, genetically manipulated, and expressed to produce antigen-binding proteins. Recombinant antibodies (e.g. scFvs) play a crucial role in biomedical research and are often used as clinical therapeutic reagents because of their high specificity for target antigens, small size, and a lower negative response by the human immune system compared with natural antibodies (Jefferis, 2009). Antibody-drug conjugates are a relatively new form of targeted therapy and are becoming widely used in modern clinical applications (Teicher and Chari, 2011). In the research described in this thesis, a scFv antibody was linked to a drug (i.e. botulinum neurotoxins). The antibody delivers the linked drug to the target cells, followed by internalization of conjugates by the cell and, finally the drug is available for therapy. Fewer side effects should be caused or expected because of antibody-mediated targeting (Chari *et al.*, 1992).

This study presents a first attempt to generate a recombinant scFv antibody, MH7C, against a peptide sequence of the extracellular domain of $P2X_3$ (Val_{257} - Asp_{276}), using phage display. The MH7C scFv could be internalized through binding to the peptide sequence of the $P2X_3$ extracellular domain, which is crucial for targeted therapeutic delivery. Most commercial and published anti-$P2X_3$ antibodies are polyclonal antibodies against a fifteen-amino acid peptide sequence (Val_{383}-His_{397}) identical to the carboxyl-terminus of the $P2X_3$ receptor intracellular domain. The current finding also provided the first proof of principle using a scFv antibody for targeted delivery of the core BoNT/A therapeutic [LC-H_N-H_{CN}/A] to nociceptive sensory neurons. This conjugate

should have a much-improved therapeutic 'safety-window' for treatment of inflammatory pain.

BoNT/A inhibits release of pain peptides (SP and CGRP) from sensory neurons by cleavage of its specific intracellular SNAP-25 (Aoki and Guyer, 2001; Meng *et al.*, 2007; Meng *et al.*, 2009). The truncation of 9 amino acids at the C-terminus of SNAP-25 at Gln_{197}-Arg_{198} provides a long-lasting (~24 weeks) alleviation of chronic pain with reduced frequency of pain occurrence (Dodick *et al.*, 2010). The novel targeted molecule generated overcame the broad-spectrum binding of the native entire BoNT/A which binds synaptic vesicle protein 2 (SV2), that is widely expressed by cholinergic, sympathetic, sensory neurons as well as multiple non-neuronal cells (Dong *et al.*, 2006; Peng *et al.*, 2011). Therefore, treatment with BoNT/A for pain often resulted in unwanted 'off-targeting effects' (Jackson *et al.*, 2012). These could be minimised by using the specific targeting strategy reported herein.

An extracellular-domain Ile_{257}-Pro_{301} (Zemkova *et al.*, 2004), of the transmembrane protein was used to generate the anti-$P2X_3$ receptor antibodies, so that the BoNT-based therapeutic attached should be selectively delivered to $P2X_3$-expressing neurons and, hopefully, disrupt the pain signalling pathway (Koshimizu *et al.*, 2002). Genetic fusion of LC-H_N-H_{CN}/A (Fig. 7.1a) and anti-$P2X_3$ scFv antibodies against the extracellular domain of $P2X_3$ proved to be successful by monitoring cleavage of pain-related protein, SNAP-25, in sensory neurons. The scFv to $P2X_3$ was shown to bind, internalize and deliver LC/A for dose-dependent cleavage of SNAP-25 in sensory neurons (Fig. 7.1b). This binding proved to be specific, based on competition by the peptide used for antibody generation. Clearly, this would be an ideal candidate for a delivery agent for targeted treatment.

After formalin fixing and paraffin embedding (FFPE), the state of the proteins in a tissue sample may be altered, which may lead to non-specific binding (high background staining), and may then mask the detection of the target antigen (Scicchitano *et al.*, 2009). This may cause non-specific staining background in brain negative controls. However, after preincubation of antibodies with specific $P2X_3$ peptides, all of the staining on the membrane of rat (P1) DRG cells, rat (18 weeks) brain neurons and human bladder neuron

cells disappeared (stained by commercial anti-P2X$_3$ antibody, rabbit-DARP polyclonal antibody and Alexa-594-labelled rabbit anti-P2X$_3$ scFv antibody). Moreover, as rabbit-DARP polyclonal antibody and Alexa-594-labelled rabbit anti-P2X$_3$ scFv antibody shared a similar staining pattern with commercial anti-P2X$_3$ antibody and published data (Pearson and Carroll, 2004; Cheung *et al.*, 2005; Liu *et al.*, 2009), it can be concluded that both rabbit-DARP polyclonal antibody and anti-P2X$_3$ scFv antibody effectively bind to both human and rat cell-expressed P2X$_3$.
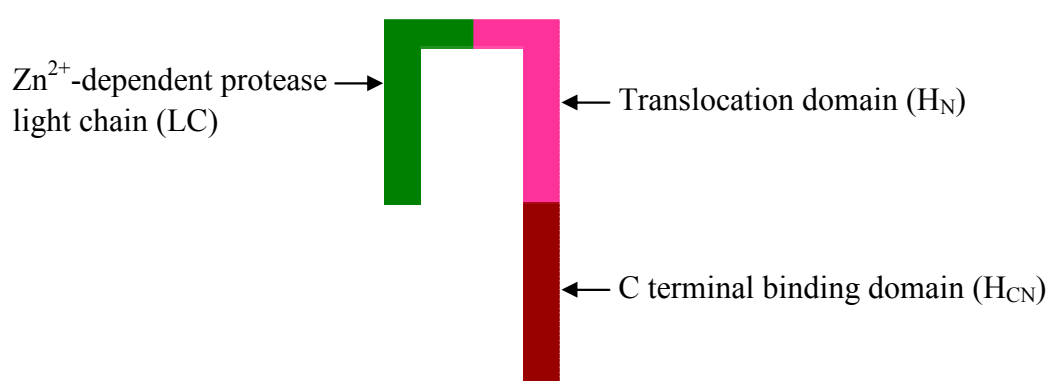
Fig. 7.1a Structure of LC-H$_N$-H$_{CN}$/A. LC-H$_N$-H$_{CN}$/A consists of one light chain (LC), one heavy chain translocation domain (H$_N$) and C terminal binding domain (H$_{CN}$).
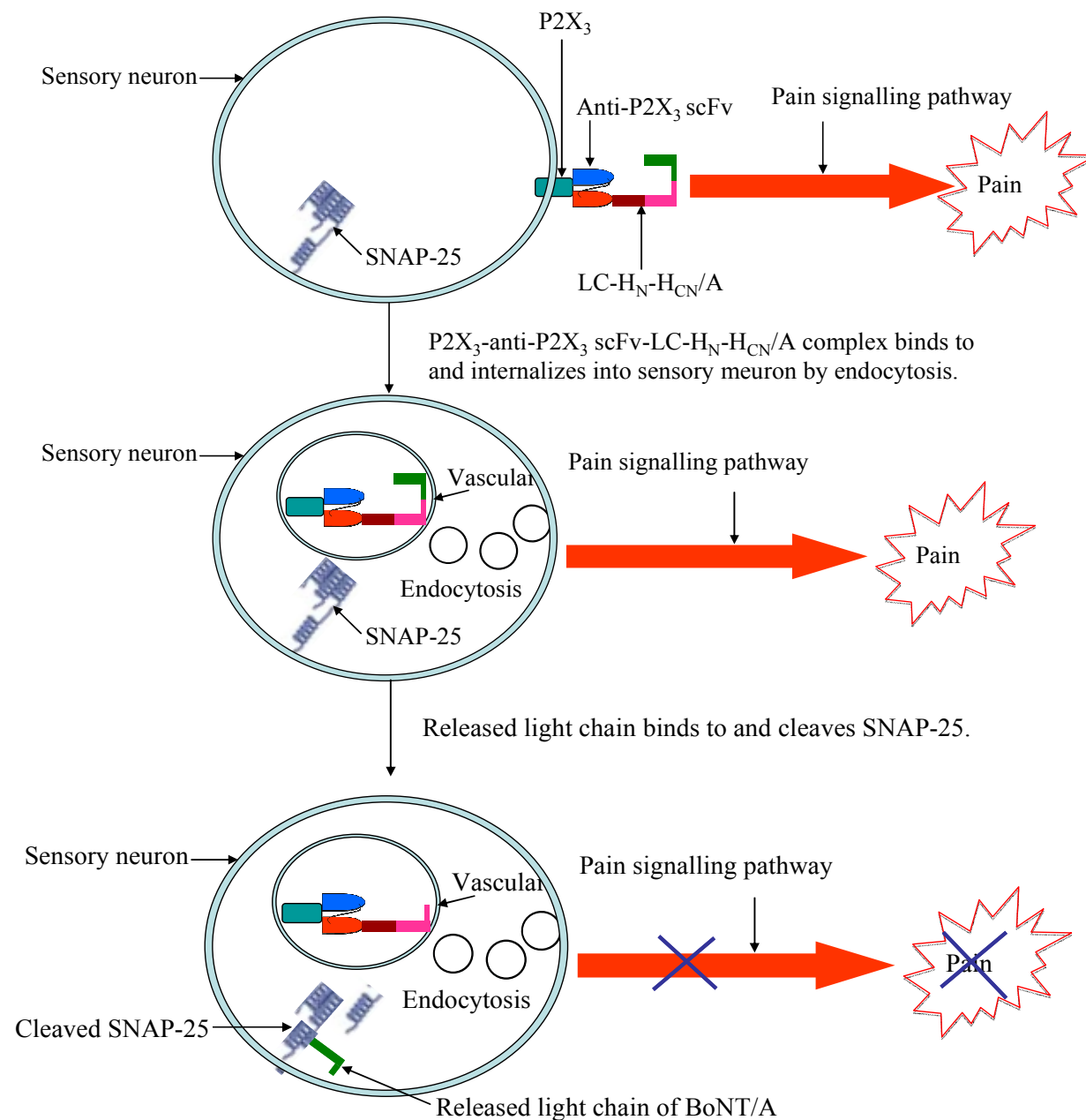
Fig 7.1b Procedure of LC-H_N-H_{CN}/A and anti-P2X$_3$ scFv fusion inhibits pain by cleavage of pain-related protein, SNAP-25. LC-H_N-H_{CN}/A delivered into sensory neuron by anti-P2X$_3$ scFv through binding of P2X$_3$ extracellulardomain, then internalizing via endocytosis. Light chain of BoNT/A is then released by heavy chain channel on vesicle, followed by binding and cleaving of SNAP-25.

In vitro data demonstrated that anti-P2X$_3$-257 antibody scFv MH7C specifically delivered the endopeptidase activity of BoNT/A to sensory neurons, as shown by the dose-dependent cleavage of a pain-related protein, SNAP-25, and the detectable inhibition of the release of a pain peptide, CGRP, which indicates its potential therapeutic efficacy, as suggested by previous studies (Meng *et al.*, 2007; Durham and Masterson, 2013). *In vivo* data showed this novel agent lacks significant cytotoxicity, which supports its safety for possible future use as an anti-nociceptive. Compared to traditional treatment which utilises injection of BoNT/A only (Dolly *et al.*, 2011), this new therapeutic provides a more specific focus as the specific delivery agent, anti-P2X$_3$-257 scFv, is fused with BoNT/A to deliver drug into the inflammatory pain signalling pathway (Jarvis *et al.*, 2002; Xu and Huang, 2002). This novel targeted treatment stops unwanted 'off-targeting effects', for instance, blepharoptosis, muscle weakness, neck stiffness, parasthesia, and skin tightness (Jackson *et al.*, 2012), which is caused by non-specific binding of cholinergic neurons, sympathetic neurons and non-neuronal cells (Peng *et al.*, 2011). The patients who suffer from diabetic neuropathic pain, chronic neuropathic pain, low back pain bladder *pain* and neck pain which can be treated using BoNT/A could benefit from this new intervention with more targeted treatment and less side effects (Jackson *et al.*, 2012).

It is the first report of selectively targeting the endopeptidase activity of clostridial neurotoxins to specific cell types through genetic fusion with an antibody. Duggan *et al*. (2002) tried to conjugate purified recombinant LC-H$_N$/A and commercial *Erythrina cristagalli* lectin (ECL) which recognized terminal galactosyl residues for selectively delivery of the endopeptidase activity of BoNT/A to primary nociceptive afferent neurons. However, as recombinant LC-H$_N$/A and a mixture of LC-H$_N$/A and ECL tend to cause heavy aggregation, the LC-H$_N$/A-ECL conjugate contained aggregates and was hard to quantify, which may be a significant negative issue for clinical analysis (Singh *et al.*, 2011). The approach used in the research undertaken in this research i.e. fusion at the gene level, may solve this problem.

Biological mechanisms may sometimes translate poorly from *in vitro* models

into clinical efficacy and effectiveness, which may relate to antibody specificity or affinity. However, this problem could be solved by scFv antibody modification, for instance, antibody light and heavy chain shuffling.

The efficacy of this therapeutic will be further evaluated in the future using established capsaicin-induced or formalin-induced rat inflammatory pain models which showed sensitivity to the delivery agent $P2X_3$ (Tsuda *et al.*, 1999; Souslova *et al.*, 2000).

The key outcomes from this study can be summarized as following four sections:

Section 1) Culture of rat DRG cells

Rat DRG cells, having a high level of $P2X_3$ expression (over 70% of the cultured DRGs stained positively for $P2X_3$ by immunofluorescence) were successfully cultured.

Cultured DRGs showed sensitivity to BoNT/A and BoNT/D, by cleavage of pain-related proteins SNAP-25 and VAMP2. Both polyclonal anti-$P2X_3$ IgG and recombinant anti-$P2X_3$ scFv antibodies demonstrated their specificity to $P2X_3$ (expressed in cultured rat DRGs) by Western blotting and immunofluorescent staining of rat DRG-expressed $P2X_3$. Thus, the cultured DRGs were proven to be a promising *in vitro* model for investigating the specificity and effect of this novel targeted therapeutic.

Section 2) Generation of rabbit anti-P2X3-scFv recombinant antibodies

Rabbit anti-$P2X_3$ extracellular domain scFv recombinant antibodies, with high specificity and affinity, were successfully generated.

Two extracellular $P2X_3$ peptide conjugates ($P2X_3$-257-BSA and $P2X_3$-60-BSA/KLH) were selected for immunization of rabbits, mice and chickens. Rabbits and mice showed a high immune response against $P2X_3$-257, but a low immune response to $P2X_3$-60, while chickens had low immune responses to both $P2X_3$-257 and $P2X_3$-60.

Rabbit polyclonal antibodies were purified using both protein A and streptavidin-agarose chromatography (bind $P2X_3$-257/60-biotin to produce $P2X_3$-257/60 column), and 8.67 mg (1.7 mg/mL) rabbit anti-$P2X_3$ Ig was generated.

A rabbit scFv library was successfully built, and phage display was used for selection of anti-$P2X_3$-257 scFv recombinant antibodies. An anti-$P2X_3$-257 scFv clone, H7C, was proven to have high specificity to $P2X_3$ using ELISA, Western blotting and immunofluorescence-based staining. The IC_{50} of the rabbit anti-$P2X_3$-257 scFv (0.17 nM) was 51 times higher than that of polyclonal anti-$P2X_3$-257 antibody (8.70 nM) (Fig. 3.15b), which indicated that a high affinity clone was isolated from this rabbit scFv library.

Section 3) H7C anti-$P2X_3$-257 scFv antibody was optimized and specificity was proved *in vitro*

After mutation of Cys_{80} to Ala, the expression level of anti-$P2X_3$ scFv was improved 3.5 fold (from 277.7 to 978.2 µg/mL) compared to the non-mutated scFv.

Specificity of rabbit anti-$P2X_3$-scFv antibody was successfully demonstrated *in vitro* by several approaches. Western blotting indicated specific binding of rabbit anti-$P2X_3$-scFv antibody by detecting the specific $P2X_3$ band at the correct position (50-55 kDa) (Fig. 5.1a). Immunofluorescence showed DRG cells staining positively with sharp green fluorescence, which was co-localised with commercial anti-$P2X_3$ polyclonal antibody staining (Fig. 5.5). In addition, flow cytometric studies showed that median fluorescence intensity is dramatically increased to 425 W/m², which is 3.6 times higher than negative control (118 W/m²) and 1.2 times higher than positive control (356 W/m²) (Fig. 5.7). Finally, immunohistochemical staining indicated that the membrane of DRG cells in rat dorsal root ganglions, rat cortical neurons and human bladder neurons were positively stained by commercial anti-$P2X_3$ antibody, rabbit-DARP polyclonal antibody and Alexa-594-labelled rabbit anti-$P2X_3$ scFv antibody (Fig. 5.8-5.10).

Section 4) Conjugation of BoNT/A(or/D) with anti-P2X$_3$ antibody

Proof of principle of targeting of BoNT/A(or/D) via anti-P2X$_3$ polyclonal and scFv antibody (against the P2X$_3$ extracellular domain) to inflammatory pain signaling pathway was shown.

Rabbit anti-P2X$_3$ IgG was conjugated with translocation and protease domains of BoNT/A (LC-H$_N$/A). The novel conjugate ((LC-H$_N$/A-anti-P2X$_3$ IgG) was shown to have higher endopeptidase activity by increasing cleavage of SNAP-25 in rat DRG cells compared to LC-H$_N$/A only.

The scFv gene was then fused to BoNT/D and cloned into the PET29a vector. Two different forms of BoNT/D-anti-P2X$_3$ scFv (LC-H$_N$/D-scFv and LC-H$_N$-H$_{CN}$/D-L scFv) were successfully expressed in BL21-DE3 and purified by IMAC (Fig. 5.6). The purified BoNT/D-anti-P2X$_3$ scFv fusion protein successfully cleaved its specific SNARE (VAMP2) on rat DRG cultures (Fig. 5.7), but little improvement was found when compared with control proteins, LC-H$_N$/D and LC-H$_N$-H$_{CN}$/D. This may be caused by poor disulphide bond formation ability of BL21-DE3, which then leads to protein dysfunction.

In order to improve fusion activity, the MH7C scFv gene was fused to LC-H$_N$/A and LC-H$_N$-H$_{CN}$/A, and then successfully expressed in Origami 2(DE3), which was reported to enhance disulphide bond formation. The LC-H$_N$-H$_{CN}$/A-MH7C fusion was successfully purified using streptavidin-agarose resin and *in vivo* data showed this novel fusion had higher endopeptidase activity than the LC-H$_N$-H$_{CN}$/A control, thus demonstrating the endopeptidase activity of this novel fusion protein and indicating potential therapeutic efficacy. Lack of cytotoxicity *in vivo* was proved by intraperitoneal injection of 1 μg of the fused protein, which supports its potential safety in treatment applications.

7.2 Recommendations for future work

For future work, modification of scFv antibody will be made for better specificity and affinity. Fresh frozen tissue samples will be used instead of formalin fixing and paraffin embedded tissue samples. Finally, the efficacy of LC-H$_N$-H$_{CN}$/A-MH7C will be evaluated *in vivo*.

Biological mechanisms may sometimes translate poorly from *in vitro* models into clinical efficacy and effectiveness. Issues that may arise may be related to antibody specificity or affinity. These could be overcome by scFv antibody modification (e.g. antibody light and heavy chain shuffling may be performed to solve such problems). Chain shuffling is an *in vitro* recombination method which is frequently used as a tool for antibody modification (Joerm, 2003; Clackson *et al.*, 2007). It was successfully and widely used on *in vitro* antibody fragment affinity maturation (Rojas *et al.*, 2004). For scFv antibody light chain shuffling, the variable heavy chain gene of MH7C would be recombined with a wide variety of rabbit light-chain variable genes (Rojas *et al.*, 2004). Otherwise, for heavy chain shuffling, the original variable light chain gene of MH7C would be recombined with a variable domain library of heavy chain genes (Kang *et al.*, 1991).

Non-specific binding (high background staining) is a common problem in formalin fixed and paraffin embedded (FFPE) tissue samples (caused by the altered state of the proteins) (Marshall *et al.*, 2009). Freshly frozen (FF) samples could be used for further optimisation of immunohistochemical staining to achieve lower background. Instead of formalin fixation and paraffin embedding, fresh tissue samples of rat brain, rat spine and human bladder could be frozen directly in OCT® or Cryomatrix®. Tissue slides would then immunostained with anti-$P2X_3$ antibody. The specific staining may be detected using a polymer-based kit with DAB (commercial anti-$P2X_3$ antibody, rabbit-DARP polyclonal antibody) or red fluorescent staining (Alexa-594-labelled rabbit anti-$P2X_3$ scFv antibody).

In vivo data showed that the novel agent, LC-H_N-H_{CN}/A-MH7C, lacked significant cytotoxicity, which supports its safety for possible future use as an anti-nociceptive. However, the efficacy of this therapeutic needs to be further evaluated using inflammatory pain models. As both of capsaicin-induced or formalin-induced inflammatory pain models were proved to be sensitive to $P2X_3$ receptor (Tsuda *et al.*, 1999; Souslova *et al.*, 2000), $P2X_3$ targeted BoNT can work on a capsaicin-sensitive and formalin-sensitive pain models. Unfortunately, these *in vivo* rat pain models have not been successfully established by our collaborators to date. In the approach envisaged injection of

capsaicin or formalin into the rat hindpaw is performed to induce the relevant pain models. and an evaluation of pain behaviour carried out (Ortega-Álvaro *et al.*, 2012) The addition of LC-H_N-H_{CN}/A-anti-P2X$_3$-scFv should result in a decrease in the number of paw licking and jumping/ lifting events (Gangadharan *et al.*, 2009).

In order to prove LC-H_N-H_{CN}/A-anti-P2X$_3$-scFv could inhibit sensory neuron sensitization selectively *in vivo* models, the rotarod test will be applied. The rotarod test is a safe and humane way to provide classical and sensitive index of motor dysfunction. In rotarod test, the animals are placed on textured drums to avoid slipping. When an animal drops onto the individual sensing platforms below, test results are recorded digitally and displayed on the front panel.

Wild type BoNTs can bind to both motor and sensory neurons, and lead to muscle paralysis. The inflammatory pain model rats will run with low speed or fall down for rotarod test.

Recombinant LC-H_N-H_{CN}/A which lack of C-terminal binding domain (H_{CC}) does not have binding ability to cells, thus can not inhibit pain. The inflammatory pain model rats which still suffer pain will perform low speed or fall down for rotarod test.

LC-H_N-H_{CN}/A-anti-P2X$_3$ antibody will bind to P2X$_3$, which specifically expressed on sensory neurons, followed by endocytosis and release of LC for inhibition of pain-related peptides, and then inhibit pain. If it is successful, the inflammatory pain model rats will not feel pain and perform normally and keep running for rotarod test. But if it is not inhibit afferent nerve sensitization selectively, but as well as motor neurons, the LC-H_N-H_{CN}/A-anti-P2X$_3$ antibody will work just as wild type BoNTs and cause muscle paralysis and lead to low speed or fall down for rotarod test.

Patients with chronic inflammatory pain, caused by arthritis, penetration wounds, fractures, burns, vasoconstriction, infections and extreme cold, could benefit from this new targeted neurotherapeutic.

Chapter 8

Biliography

Angeletti, R. (1999) Design of useful peptide antigens. J Biomol Tech., **10**: 2-10.

Ahmad, Z.A., Yeap, S.K., Ali, A.M., Ho, W.Y., Alitheen, N.B. and Hamid, M. (2012). scFv antibody: principles and clinical application. Clin. Dev. Immunol., **2012**:980250-64.

Aktas, O., Ullrich, O., Infante-Duarte, C., Nitsch, R. and Zipp, F. (2007). Neuronal damage in brain inflammation. Arch. Neurol., **64**:185-9.

Aoki, K.R. and Guyer, B. (2001). Botulinum toxin type A and other botulinum toxin serotypes: a comparative review of biochemical and pharmacological actions. Eur. J. Neurol., **8**:21-29.

Ayyar, B.V., Hearty, S. and O'Kennedy R. (2010). Highly sensitive recombinant antibodies capable of reliably differentiating heart-type fatty acid binding protein from noncardiac isoforms. Anal. Biochem., **407**:165-71.

Azaman, S.N.A., Ramanan, R.N., Tan, J.S., Rahim, R.A., Abdullah, M.P. and Ariff, A.B. (2010). Screening for the optimal induction parameters for periplasmic producing interferon-α2b in *Escherichia coli*. African J. Biotec., **9**:6345-6354.

Barbas 3rd, C.F., Burton, D.R., Scott, J.K. and Silverman, G.J. (2001). Phage Display a Laboratory Manual. Cold Spring Harbor Laboratory Press, Cold Spring Harbor, New York, U.S.A..

Barclay, J., Patel, S., Dorn, G., Wotherspoon, G., Moffatt, S., Eunson, L., Abdel'al, S., Natt. F., Hall, J., Winter, J., Bevan, S., Wishart, W., Fox, A. and Ganju, P. (2002). Functional downregulation of P2X3 receptor subunit in rat

sensory neurons reveals a significant role in chronic neuropathic and inflammatory pain. J. Neurosci., **22**:8139-47.

Beresford, G.W., Pavlinkova, G., Booth, B.J., Batra, S.K., Colcher D. (1999). Binding characteristics and tumor targeting of a covalently linked divalent CC49 single-chain antibody. Int. J. Cancer, **81**:911-917.

Berry, J.D., Rutherford, J., Silverman, G.J., Kaul, R., Elia, M., Gobuty, S., Fuller, R., Plummer, F.A. and Barbas, C.F. 3rd. (2003). Development of functional human monoclonal single-chain variable fragment antibody against HIV-1 from human cervical B cells. Hybrid Hybridomics, **22**:97-108.

Biocca, S., Ruberti, F., Tafani, M., Pierandrei-Amaldi, P. and Cattaneo, A. (1995). Redox state of single chain Fv fragments targeted to the endoplasmic reticulum, cytosol and mitochondria. Biotechnol., (N.Y.), **13**:1110-5.

Bothmann, H. and Pluckthun, A. (2000). The periplasmic *Escherichia coli* peptidylprolyl cis,trans-isomerase FkpA. I. Increased functional expression of antibody fragments with and without cis-prolines. J. Biol. Chem., **275**:17100-5.

Breivik, H., Collett, B., Ventafridda, V., Cohen, R. and Gallacher, D. (2006). Survey of chronic pain in Europe: prevalence, impact on daily life, and treatment. Eur. J. Pain, **10**:287–333.

Brown, M.C., Joaquim, T.R., Chambers, R., Onisk, D.V., Yin, F., Moriango, J.M., Xu, Y., Fancy, D.A., Crowgey, E.L., He, Y., Stave, J.W. and Lindpaintner, K. (2011). Impact of immunization technology and assay application on antibody performance--a systematic comparative evaluation. PLoS One., **6**:e28718.

Burnstock, G.. (2009). Purinergic receptors and pain. Curr. Pharm. Des., **15**:1717-35.

Burnstock, G.. (2000). P2X receptors in sensory neurones. Br. J. Anaesth., **84**:476-88.

Burnstock, G.. (1996). A unifying purinergic hypothesis for the initiation of pain. Lancet, **347**:1604-5.

BVTech Plasmid. Plasmid map of pET-29_a_(+), (2012). http://www.biovisualtech.com/bvplasmid/pET-29_a_%28+%29.htm.

Chari, R.V., Martell, B.A., Gross, J.L., Cook, S.B., Shah, S.A., Blättler, W.A., McKenzie, S.J. and Goldmacher, V.S. (1992). Immunoconjugates containing novel maytansinoids: promising anticancer drugs. Cancer Res., **52**:127-31.

Chen, C., Snedecor, B., Nishihara, J.C., Joly, J.C., McFarland, N., Andersen, D.C., Battersby, J.E. and Champion, K.M. (2004). High-level accumulation of a recombinant antibody fragment in the periplasm of *Escherichia coli* requires a triple-mutant (degP prc spr) host strain. Biotechnol. Bioeng., **85**:463-74.

Chen, C.C., Akopian, A.N., Sivilotti, L., Colquhoun, D., Burnstock, G. and Wood, J.N. (1995). A P2X purinoceptor expressed by a subset of sensory neurons. Nature (Lond.), **377**:428-431.

Chen, Y., Huang, K., Li, X., Lin, X., Zhu, Z. and Wu, Y. (2010). Generation of a stable anti-human CD44v6 scFv and analysis of its cancer-targeting ability *in vitro*. Cancer Immunol. Immunother., **59**:933-42.

Chen, H., Li, L. and Fang, J. (2012). Construction, expression and characterization of the fusion gene of super-antigen SEA and single chain Fv of the ND-1 monoclonal antibody against human colorectal cancer. Chin. J. Cell Mol. Immunol., **28**:400-3.

Cheung, K.K., Chan, W.Y. and Burnstock, G. (2005). Expression of P2X purinoceptors during rat brain development and their inhibitory role on motor axon outgrowth in neural tube explant cultures. Neuroscience, **133**:937-45.

Chuang, Y.C., Tyagi, P., Huang, C.C., Yoshimura, N., Wu, M., Kaufman, J. and Chancellor, M.B. (2009). Urodynamic and immunohistochemical evaluation of intravesical botulinum toxin A delivery using liposomes. J. Urol., **182**:786-92.

Cockayne, D.A., Hamilton, S.G., Zhu, Q.M., Dunn, P.M., Zhong, Y., Novakovic, S., Malmberg, A.B., Cain, G., Berson, A., Kassotakis, L., Hedley, L., Lachnit, W.G., Burnstock, G., McMahon, S.B. and Ford, A.P.D.W. (2000). Urinary bladder hyporeflexia and reduced pain-related behaviour in P2X3-deficient mice. Nature (Lond.), **407**:1011-1015.

Conroy, P.J., Hearty, S., Leonard, P. and O'Kennedy, R. (2009). Antibody production, design and use for biosensor-based applications. Semin. Cell Dev. Biol., **20**:10-26.

Crumling, M.A., Tong, M., Aschenbach, K.L., Liu, L.Q., Pipitone, C.M. and Duncan, R.K. (2009). P2X antagonists inhibit styryl dye entry into hair cells. Neuroscience, **161**:1144-53.

Datar, P., Srivastava, S., Coutinho, E. and Govil, G. (2004). Substance P: structure, function, and therapeutics. Current Topics in Med. Chem., **4**:75-103.

De Kruif, J. and Logtenberg, T. (1996). Leucine zipper ized bivalent and bispecific scFv antibodies from a semi-synthetic antibody phage display library. J. Biol. Chem., **271**:7630-4.

De Lalla, C., Tamborini, E., Longhi, R., Tresoldi, E., Manoni, M., Siccardi, A.G., Arosio, P. and Sidoli, A. (1996) Human recombinant antibody fragments

specific for a rye-grass pollen allergen: characterization and potential applications. Mol. Immunol., **33**:1049-58.

Devine, L., Sun, J., Barr, M.R. and Kavathas, P.B. (1999). Orientation of the Ig domains of CD8 alpha beta relative to MHC class I. J. Immunol., **162**:846-51.

Dodick, D.W., Schembri, C.T., Helmuth, M. and Aurora, S.K. (2010). Transcranial magnetic stimulation for migraine: a safety review. Headache, **50**:1153-63.

Dolly, J.O., Wang, J.F., Zurawski, T.H. and Meng, J.H. (2011). Novel therapeutics based on recombinant botulinum neurotoxins to normalize the release of transmitters and pain mediators. F.E.B.S. J., **23**:4454-66.

Dong, M., Yeh, F., Tepp, W.H., Dean, C., Johnson, E.A., Janz, R. and Chapman, E.R. (2006). SV2 is the protein receptor for botulinum neurotoxin A. Science., **312**:592-596.

Duggan, M.J., Quinn, C.P., Chaddock, J.A., Purkiss, J.R., Alexander, F.C., Doward, S., Fooks, S.J., Friis, L.M., Hall, Y.H., Kirby, E.R., Leeds, N., Moulsdale, H.J., Dickenson, A., Green, G.M., Rahman, W., Suzuki, R., Shone, C.C. and Foster, K.A. (2002). Inhibition of release of neurotransmitters from rat dorsal root ganglia by a novel conjugate of a Clostridium botulinum toxin A endopeptidase fragment and Erythrina cristagalli lectin. J. Biol. Chem., **277**:34846-52.

Durham, P.L. and Masterson, C.G. (2013). Two mechanisms involved in trigeminal CGRP release: implications for migraine treatment. Headache, **53**:67-80.

Engel, J., Emons, G., Pinski, J. and Schally, A.V. (2012). AEZS-108: a targeted cytotoxic analog of LHRH for the treatment of cancers positive for LHRH receptors. Expert. Opin. Investig. Drugs., **21**:891-9.

Evidente, V.G. and Adler, C.H. (2010). An update on the neurologic applications of botulinum toxins. Curr. Neurol. Neurosci. Rep., **10**:338-44.

Faulds, D. and Sorkin, E.M. (1994). Abciximab (c7E3 Fab). A review of its pharmacology and therapeutic potential in ischaemic heart disease. Drugs, **48**:583-98.

Filipović, B., Matak I., Rojecky, L.B. and Lacković, Z. (2012). Central action of peripherally applied botulinum toxin type A on pain and dural protein extravasation in a rat model of trigeminal neuropathy. PLoS. One., **7**:e29803.

Fischer, W., Zadori, Z., Kullnick, Y., Gröger-Arndt, H., Franke, H., Wirkner, K., Illes, P. and Mager, P.P. (2007). Conserved lysine and arginine residues in the extracellular loop of P2X3 receptors are involved in agonist binding. Eur. J. Pharmacol., **576**:7-17.

Foran, P., Mohammed, N., Lisk, G.., Nagwaney, S., Lawrence, G., Johnson, E., Smith L., Aoki, K. R. and Dolly J.O. (2003) Evaluation of the Therapeutic Usefulness of Botulinum Neurotoxin N, C1, E, and F Compared with the Long Lasting Type A. J. Biol. Chem., **278**:1363-71.

Foster, K.A. (2004). The analgesic potential of clostridial neurotoxin derivatives. Expert. Opin. Investig. Drugs., **13**:1437-43.

Gangadharan, V., Agarwal, N., Brugger, S., Tegeder, I., Bettler, B., Kuner, R. and Kurejova, M. (2009). Conditional gene deletion reveals functional redundancy of GABAB receptors in peripheral nociceptors *in vivo*. Mol. Pain, **5**:68-79.

Gao, G. and Jakobsen, B. (2000). Molecular interactions of coreceptor CD8 and MHC class I: the molecular basis for functional coordination with the T-cell receptor. Immunol. Today, **21**:630-6.

Geuijen C.A., Clijsters-van der Horst, M., Cox, F., Rood, P.M., Throsby, M., Jongeneelen, M.A., Backus, H.H., van Deventer, E., Kruisbeek, A.M., Goudsmit, J. and de Kruif, J. (2005). Affinity ranking of antibodies using flow cytometry: application in antibody phage display-based target discovery. J. Immunol. Methods, **302**:68-77.

Gómez, I., Miranda-Ríos, J., Arenas, I., Grande, R., Becerril, B., Bravo, A. and Soberón, M. (2009). Identification of scFv Molecules that Recognize Loop 3 of Domain II and Domain III of Cry1Ab Toxin from *Bacillus thuringiensis*. J. Biol. Chem., **284**:32750-57.

Govindan, S.V., Cardillo, T.M., Sharkey, R.M., Tat, F., Gold, D.V. and Goldenberg, D.M. (2013). Milatuzumab-SN-38 conjugates for the treatment of CD74+ cancers [published online ahead of print February 20 2013]. Mol. Cancer Ther., http://intl-mct.aacrjournals.org/content/early/2013/02/20/1535-7163.MCT-12-1170.full.pdf+html.

Grishin, E.V., Savchenko, G.A., Vassilevski, A.A., Korolkova, Y.V., Boychuk, Y.A., Viatchenko-Karpinski, V.Y., Nadezhdin, K.D., Arseniev, A.S., Pluzhnikov, K.A., Kulyk, V.B., Voitenko, N.V. and Krishtal, O.O. (2010). Novel peptide from spider venom inhibits P2X3 receptors and inflammatory pain. Ann. Neurol., **67**:680-3.

Gudas, J.M., Torgov, M., An, Z., Jia, X.C., Morrison, K.J., Morrison, R.K., Vincent, M., Yang, P., Kanner, S.B. and Jakobovits, A. (2010) Use of AGS-16M8F as a novel antibody drug conjugate (ADC) for treating renal cancers. J. Clin. Oncol., **28**:e15014.

Guo, Z., Bi, F., Tang, Y., Zhang, J., Yuan, D., Xia, Z. and Liu, J.N. (2006). Preparation and characterization of scFv for affinity purification of reteplase. J. Biochem. Biophys. Meth., **67**:27-36.

Hamatake, M., Komano, J., Urano, E., Maeda, F., Nagatsuka, Y. and Takekoshi, M. (2010). Inhibition of HIV replication by a CD4-reactive Fab of an IgM clone isolated from a healthy HIV-seronegative individual. Eur. J. Immunol., **40**:1504-9.

He, J., Wang, Y., Feng, J., Zhu, X., Lan, X., Iyer, A.K., Zhang, N., Seo, Y., VanBrocklin, H.F. and Liu, B. (2010). Targeting prostate cancer cells *in vivo* using a rapidly internalizing novel human single-chain antibody fragment. J. Nucl. Med., **51**:427-32.

Heitner, T., Satozawa, N., McLean, K., Vogel, D., Cobb, R.R., Liu, B., Mahmoudi, M., Finster, S., Larsen, B., Zhu, Y., Zhou, H., Müller-Tiemann, B., Monteclaro, F., Zhao, X.Y. and Light, D.R. (2006). Obligate multivalent recognition of cell surface tomoregulin following selection from a multivalent phage antibody library. J. Biomol. Screen., **11**:985-95.

Hendriksen, C. and Hau, J. (2003). Production of polyclonal and monoclonal antibodies, 391-411, In: Handbook of Laboratory Animal Science. 2nd ed., Boca Raton: CRC Press LLC, U.S.A..

Herrmann, T., Grosse-Hovest, L., Otz, T., Krammer, P.H., Rammensee, H.G. and Jung, G.. (2008). Construction of optimized bispecific antibodies for selective activation of the death receptor CD95. Cancer Res., **68**:1221-7.

Hoebe, K., Janssen, E. and Beutler, B. (2004). The interface between innate and adaptive immunity. Nature Immunol., **5**:971-4.

Holliger, P. and Hudson, P.J. (2005). Engineered antibody fragments and the rise of single domains. Nature Biotechnol., **23**:1126-36.

Holmberg, A., Blomstergren, A., Nord, O., Lukacs, M., Lundeberg, J. and Uhlén, M. (2005). The biotin-streptavidin interaction can be reversibly broken using water at elevated temperatures. Electrophoresis. **26**:501-10.

Honore, P., Mikusa., J., Bianchi, B., McDonald, H., Cartmell, J., Faltynek, C. and Jarvis, M.F. (2002). TNP-ATP, a potent P2X3 receptor antagonist, blocks acetic acid-induced abdominal constriction in mice: comparison with reference analgesics. Pain, **96**:99-105.

Huang, C.J., Lin, H. and Yang, X. (2012). Industrial production of recombinant therapeutics in *Escherichia coli* and its recent advancements. J. Ind. Microbiol. Biotechnol., **39**:383-99.

Hussain, S.F., Yang, D., Suki, D., Grimm, E. and Heimberger. A.B. (2006). Innate immune functions of microglia isolated from human glioma patients. J. Transl. Med., **4**:15-23.

Idikio, H.A. (2009). Immunohistochemistry in diagnostic surgical pathology: contributions of protein life-cycle, use of evidence-based methods and data normalization on interpretation of immunohistochemical stains. Int. J. Clin. Exp. Pathol., **3**:169-76.

Immunogen. Invester Information, (2013). http://investor.immunogen.com/releasedetail.cfm?ReleaseID=605760.

Immunogen. Product Pipeline, (2013). http://www.immunogen.com/pipeline/lorvotuzumab-mertansine/.

Jackson, J.L., Kuriyama, A. and Hayashino, Y. (2012). Botulinum toxin A for prophylactic treatment of migraine and tension headaches in adults: a meta-analysis. J.A.M.A., **307**:1736-45.

Jarvis, M.F., Burgard, E.C., McGaraughty, S., Honore, P., Lynch, K., Brennan, T.J., Subieta, A., Van Biesen, T., Cartmell, J., Bianchi, B., Niforatos, W., Kage, K., Yu, H., Mikusa., J., Wismer, C.T., Zhu, C.Z., Chu, K., Lee, C.H., Stewart, A.O., Polakowski, J., Cox, B.F., Kowaluk, E., Williams, M., Sullivan, J. and Faltynek, C. (2002). A-317491, a novel potent and selective non-nucleotide antagonist of P2X3 and P2X2/3 receptors, reduces chronic inflammatory and neuropathic pain in the rat. Proc. Natl. Acad. Sci. U.S.A., **99**:17179-84.

Jin, R., Rummel, A., Binz, T. and Brunger, A.T. (2006). Botulinum neurotoxin B recognizes its protein receptor with high affinity and specificity. Nature (Lond.), **444**:1092-5.

Kaan, T.K., Yip, P.K., Patel, S., Davies, M., Marchand, F., Cockayne, D.A., Nunn, P.A., Dickenson, A.H., Ford, A.P., Zhong, Y., Malcangio, M. and McMahon, S.B. (2010). Systemic blockade of P2X3 and P2X2/3 receptors attenuates bone cancer pain behaviour in rats. Brain, **133**:2549-64.

Kallenborn-Gerhardt, W. and Schmidtko, A. (2011). A novel signaling pathway that modulates inflammatory pain. J. Neurosci., **31**:798-800.

Kallberg, M., Wang, H., Wang, S., Peng, J., Wang, Z., Lu, H. and Xu, J. (2012) Template-based protein structure modeling using the RaptorX web server. Nature Protocols, **7**:1511-1522.

Kang, A.S., Jones, T.M. and Burton, D.R. (1991). Antibody redesign by chain shuffling from random combinatorial immunoglobulin libraries. Proc. Natl. Acad. Sci. U.S.A., 88:11120-3.

Kawate, T., Michel, J.C., Birdsong, W.T. and Gouaux, E. (2009). Crystal structure of the ATP-gated P2X(4) ion channel in the closed state. Nature (Lond.), **460**:592-8.

Keir, C.H. and Vahdat, L.T. (2012). The use of an antibody drug conjugate, glembatumumab vedotin (CDX-011), for the treatment of breast cancer. Expert. Opin. Biol. Ther., **12**:259-63.

Kidd, B.L. and Urban, L.A. (2001). Mechanisms of inflammatory pain. Br. J. Anaesth., **87**:3-11.

Kidd, E.J., Miller, K.J., Sansum, A.J. and Humphrey, P.P. (1998). Evidence for P2X3 receptors in the developing rat brain. Neuroscience, **87**:533-9.

Kim, K.J., Yoon, Y.W. and Chung, J.M. (1997) Comparison of three rodent neuropathic pain models. Exp. Brain Res., **113**:200-6.

Kimura, H., Kimura, M., Tzou, S.C., Chen, Y.C., Suzuki, K., Rose, N.R. and Caturegli, P. Expression of class II major histocompatibility complex molecules on thyrocytes does not cause spontaneous thyroiditis but mildly increases its severity after immunization. Endocrinol., **146**:1154-62.

Kontermann, R. and Dübel, S. (2010). Antibody Engineering, 2nd edition, 44-45, Springer Press, Berlin, Germany.

Koshimizu, T.A., Ueno, S., Tanoue, A., Yanagihara, N., Stojilkovic, S.S. and Tsujimoto, G..J. (2002). Heteromultimerization modulates P2X receptor functions through participating extracellular and C-terminal subdomains. J. Biol. Chem., **277**:46891-9.

Krautz-Peterson, G., Zhang, Y., Chen, K., Oyler, A.G., Feng, H. and Shoemaker, B.C. (2012). Retargeting Clostridium difficile Toxin B to Neuronal Cells as a Potential Vehicle for Cytosolic Delivery of Therapeutic Biomolecules to Treat Botulism. J. Toxicol., **2012**:760142-50.

Kreitman, R.J. and Pastan, I. (2011). Antibody fusion proteins: anti-CD22 recombinant immunotoxin moxetumomab pasudotox. Clin. Cancer Res., **17**:6398-405.

Kreitman, R.J., Tallman, M.S., Robak, T., Coutre, S., Wilson, W.H., Stetler-Stevenson, M., Fitzgerald, D.J., Lechleider, R. and Pastan, I. (2012). Phase I trial of anti-CD22 recombinant immunotoxin moxetumomab pasudotox (CAT-8015 or HA22) in patients with hairy cell leukemia. J. Clin. Oncol., **30**:1822-8.

Labome. P2X$_3$ antibody product information from all suppliers, (2012). http://www.labome.com/gene/human/P2X3-antibody.html.

Lacy, D.B., Tepp, W., Cohen, A.C., DasGupta B.R and Stevens, R.C. (1998). Crystal structure of botulinum neurotoxin type A and implications for toxicity. Nature Struct. Biol., **5**:898-902.

Lapusan, S., Vidriales, M.B., Thomas, X., de Botton, S., Vekhoff, A., Tang, R., Dumontet, C., Morariu-Zamfir, R., Lambert, J.M., Ozoux, M.L., Poncelet, P., San Miguel, J.F., Legrand, O., DeAngelo, D.J., Giles, F.J. and Marie, J.P. (2011). Phase I studies of AVE9633, an anti-CD33 antibody-maytansinoid conjugate, in adult patients with relapsed/refractory acute myeloid leukemia. Invest. New Drugs, **30**:1121-31.

Larsen, M.W., Bornscheuer, U.T. and Hult, K. (2008). Expression of *Candida antarctica* lipase B in *Pichia pastoris* and various *Escherichia coli* systems. Protein Expr. Purif., **62**:90-7.

Lattová, E., Bartusik, D., Spicer, V., Jellusova, J., Perreault, H. and Tomanek, B. (2011). Alterations in glycopeptides associated with herceptin treatment of human breast carcinoma mcf-7 and T-lymphoblastoid cells. Mol. Cell Proteomics, **10**:M111.007765.

Lavonas, E.J., Schaeffer, T.H., Kokko, J., Mlynarchek, S.L. and Bogdan, G.M. (2009). Crotaline Fab antivenom appears to be effective in cases of severe North American pit viper envenomation: an integrative review. B.M.C. Emerg. Med., **9**:13-26.

Leavenworth, J.W., Schellack, C., Kim, H.J., Lu, L., Spee, P. and Cantor, H. (2010). Analysis of the cellular mechanism underlying inhibition of EAE after treatment with anti-NKG2A F(ab')$_2$. Proc. Natl. Acad. Sci. U.S.A., **107**:2562-7.

Lewis, C., Neidhart, S., Holy, C., North, R.A., Buell, G. and Surprenant, A. (1995). Coexpression of P2X2 and P2X3 receptor subunits can account for ATP-gated currents in sensory neurons. Nature (Lond.), **377**:432-435.

Liu, J., Li, J.D., Lu, J., Xing, J. and Li, J.T. (2011). Contribution of nerve growth factor to upregulation of P2X$_3$ expression in DRG neurons of rats with femoral artery occlusion. Am. J. Physiol. Heart Circ. Physiol., **301**:H1070-9.

Liu, X., Wu, J., Zhang, S., Li, C., and Huang, Q. (2009). Novel strategies to augment genetically delivered immunotoxin molecular therapy for cancer therapy. Cancer Gene Ther., **16**:861-72.

Lu, D., Jimenez, X., Zhang, H., Bohlen, P., Witte, L. and Zhu, Z. (2002). Fab-scFv fusion protein: an efficient approach to production of bispecific antibody fragments. J. Immunol. Methods, **267**:213-26.

Macdonald, G.C., Rasamoelisolo, M., Entwistle, J., Cizeau, J., Bosc, D., Cuthbert, W., Kowalski, M., Spearman, M. and Glover, N. (2009). A phase I clinical study of VB4-845: Weekly intratumoral administration of an anti-EpCAM recombinant fusion protein in patients with squamous cell carcinoma of the head and neck. Drug Des. Devel. Ther., **2**:105-14.

Mahowald, ML, Krug, HE, Singh, JA and Dykstra, D. (2009). Intra-articular botulinum toxin type A: A new approach to treat arthritis joint pain. Toxicon., **54**:658-67.

Malin, S.A., Davis, B.M. and Molliver, D.C. (2007). Production of dissociated sensory neuron cultures and considerations for their use in studying neuronal function and plasticity. Nature Protoc., **2**:152-60.

Mao, Y., Zhang, D.W., Wen, J., Cao, Q., Chen, R.J., Zhu, J. and Feng, Z.Q. (2012). A Novel LMP1 Antibody Synergizes with Mitomycin C to Inhibit Nasopharyngeal Carcinoma Growth *in Vivo* Through Inducing Apoptosis and Downregulating Vascular Endothelial Growth Factor. Int. J. Mol. Sci., **13**:2208-18.

Mauskop, A. (2002). The Use of Botulinum Toxin in the Treatment of Headaches. Current Pain and Headache Reports, **6**:320-323.

McCafferty, J., Griffiths, A.D., Winter, G. and Chiswell, D.J. (1990). Phage antibodies: filamentous phage displaying antibody variable domains. Nature (Lond.), **348**:552-4.

Mendez, M., Gross, W.K., Glenn, T.S., Garvin, L.J. and Carretero, A.O. (2011). Vesicle-associated Membrane Protein-2 (VAMP2) Mediates cAMP-stimulated Renin Release in Mouse Juxtaglomerular Cells. J. Biol. Chem., **286**:28608-18.

Meng, J.H., Ovsepian, S.V., Wang, J.F., Pickering, M., Sasse, A., Aoki, K.R., Lawrence, G.W. and Dolly, J.O. (2009). Activation of TRPV1 mediates calcitonin gene-related peptide release, which excites trigeminal sensory neurons and is attenuated by a retargeted botulinum toxin with anti-nociceptive potential. J. Neurosci., **29**:4981-92.

Meng, J.H., Wang J.F, Lawrence, G. and Dolly, J.O. (2007). Synaptobrevin I mediates exocytosis of CGRP from sensory neurons and inhibition by

botulinum toxins reflects their anti-nociceptive potential. J. Cell Sci., **120**:2864-74.

Milner, C.M. and Campbell, R.D. (2001). Genetic organization of the human MHC class III region. Front. Bioscience, **6**:914-26.

Montal, M. (2010). Botulinum neurotoxin: a marvel of protein design. Annu. Rev. Biochem., **79**:591-617.

Moon, S.A., Ki, M.K., Lee, S., Hong, M.L., Kim, M., Kim, S., Chung, J., Rhee, S.G. and Shim, H. (2011). Antibodies against non-immunizing antigens derived from a large immune scFv library. Mol. Cells, **31**:509-13.

Morenilla-Palao, C., Planells-Cases, R., García-Sanz, N. and Ferrer-Montiel, A. (2004). Regulated exocytosis contributes to protein kinase C potentiation of vanilloid receptor activity. J. Biol. Chem., **279**:25665-72.

Morris, J.L., Jobling, P. and Gibbins, I.L. (2002). Botulinum neurotoxin A attenuates release of norepinephrine but not NPY from vasoconstrictor neurons. Am. J. Physiol. Heart Circ. Physiol., **283**:H2627-35.

Ney, J.P. and Joseph, K.R. (2007). Neurologic uses of botulinum neurotoxin type A. Neuropsychiatr. Dis. Treat., **3**:785-798.

North, R.A. (2003). The $P2X_3$ subunit: a molecular target in pain therapeutics. Curr. Opin. Investig. Drugs, **4**:833-40.

North, R.A. (2004). $P2X_3$ receptors and peripheral pain mechanisms. J. Physiol., **554**:301-8.

Nunez., R. (2001). Flow cytometry: principles and instrumentation. Curr. Issues Mol. Biol., **3**:39-45.

Ortega-Álvaro, A., Berrocoso, E., Rey-Brea, R., Leza, J.C. and Mico, J.A. (2012). Comparison of the antinociceptive effects of ibuprofen arginate and ibuprofen in rat models of inflammatory and neuropathic pain. Life Sci., **90**:13-20.

Pavlinkova, G., Beresford, G., Booth, B.J., Batra, S.K., Colcher, D.G., Pavlinkova, G., Beresford, B.J., Booth, S.K. and Batra, D.C. (1999). Charge-modified single chain antibody constructs of monoclonal antibody CC49: generation, characterization, pharmacokinetics, and biodistribution analysis. Nucl. Med. Biol., **26**:27-34.

Pearson, R.J. and Carroll, S.L. (2004). ErbB transmembrane tyrosine kinase receptors are expressed by sensory and motor neurons projecting into sciatic nerve. J. Histochem. Cytochem., **52**:1299-311.

Peng, L., Tepp, W.H., Johnson, E.A. and Dong, M. (2011). Botulinum neurotoxin D uses synaptic vesicle protein SV2 and gangliosides as receptors, PLoS. Pathog. **7**:e1002008.

Polson, A.G., Williams, M., Gray, A.M., Fuji, R.N., Poon, K.A., McBride, J., Raab, H., Januario, T., Go, M., Lau, J., Yu, S.F., Du, C., Fuh, F., Tan, C., Wu, Y., Liang, W.C., Prabhu, S., Stephan, J.P., Hongo, J.A., Dere, R.C., Deng, R., Cullen, M., de Tute, R., Bennett, F., Rawstron, A., Jack, A. and Ebens, A. (2010). Anti-CD22-MCC-DM1: an antibody-drug conjugate with a stable linker for the treatment of non-Hodgkin's lymphoma. Leukemia, 24:1566-73.

Popkov, M., Mage, R.G., Alexander, C.B., Thundivalappil, S., Barbas, C.F. 3rd and Rader, C. (2003). Rabbit immune repertoires as sources for therapeutic monoclonal antibodies: the impact of kappa allotype-correlated variation in cysteine content on antibody libraries selected by phage display. J. Mol. Biol., **325**:325-35.

Qin, A., Watermill, J., Mastico, R.A., Lutz, R.J., O'Keeffe, J., Zildjian, S., Mita, A.C., Phan, A.T. and Tolcher, A.W. (2008). The pharmacokinetics and pharmacodynamics of IMGN242 (huC242-DM4) in patients with CanAg-expressing solid tumors. A.S.C.O. Meet Abstr., **26**:3066.

Radford, K.M., Virginio, C., Surprenant, A., North, R.A. and Kawashima, E. (1997). Baculovirus expression provides direct evidence for heteromeric assembly of P2X2 and P2X3 receptors. J. Neurosci., **17**:6529-33.

Renton, T., Yiangou, Y., Baecker, P.A., Ford, A.P. and Anand, P. (2003). Capsaicin receptor VR1 and ATP purinoceptor P2X3 in painful and nonpainful human tooth pulp. J. Orofac. Pain, **17**:245-50.

Roberts, J.A. and Evans, R.J. (2004). ATP binding at human P2X1 receptors. Contribution of aromatic and basic amino acids revealed using mutagenesis and partial agonists. J. Biol. Chem., **279**:9043-55.

Robert, R., Jacobin-Valat, M.J., Daret, D., Miraux, S., Nurden, A.T., Franconi, J.M. and Clofent-Sanchez, G. (2006). Identification of human scFvs targeting atherosclerotic lesions: selection by single round *in vivo* phage display. J. Biol. Chem., **281**:40135-43.

Rodenko, B., Toebes, M., Celie, P.H., Perrakis, A., Schumacher, T.N. and Ovaa, H. (2009). Class I major histocompatibility complexes loaded by a periodate trigger. J. Am. Chem. Soc., **131**:12305-13.

Rojas, G., Talavera, A., Munoz, Y., Rengifo, E., Krengel, U., Angström, J., Gavilondo, J. and Moreno, E. (2004). Light-chain shuffling results in successful phage display selection of functional prokaryotic-expressed antibody fragments to N-glycolyl GM3 ganglioside. J. Immunol. Methods., **293**:71-83.

Ruan, H.Z, Moules, E. and Burnstock, G.. (2004). Changes in P2X3 purinoceptors in sensory ganglia of the mouse during embryonic and postnatal development. Histochem. Cell Biol., **122**:539-51.

Ryan, M.C., Kostner, H., Gordon, K.A., Duniho, S., Sutherland, M.K., Yu, C., Kim, K.M., Nesterova, A., Anderson, M., McEarchern, J.A., Law, C.L. and Smith, L.M. (2010). Targeting pancreatic and ovarian carcinomas using the auristatin-based anti-CD70 antibody-drug conjugate SGN-75. Br. J. Cancer, **103**:676-84.

Sabin, C., Corti, D., Buzon, V., Seaman, M.S., Lutje, H.D., Hinz, A., Vanzetta, F., Agatic, G., Silacci, C., Mainetti, L., Scarlatti, G., Sallusto, F., Weiss, R., Lanzavecchia, A. and Weissenhorn, W. (2010). Crystal structure and size-dependent neutralization properties of HK20, a human monoclonal antibody binding to the highly conserved heptad repeat 1 of gp41. PLoS. Pathog., **6**:e1001195.

Sacha, A.M., Brian, M.D. and Derek, C.M. (2007). Production of dissociated sensory neuron cultures and considerations for their use in studying neuronal function and plasticity. Nature Protocols, **2**:152-160.

Sandström, K., Haylock, A.K., Spiegelberg, D., Qvarnström, F., Wester, K. and Nestor, M. (2012). A novel CD44v6 targeting antibody fragment with improved tumor-to-blood ratio. Int. J. Oncol., **40**:1525-32.

Schoonjans, R., Willems, A., Schoonooghe, S., Leoen, J., Grooten, J. and Mertens, N. (2001). A new model for intermediate molecular weight recombinant bispecific and trispecific antibodies by efficient heteroization of single chain variable domains through fusion to a Fab-chain. Biomol. Eng., **17**:193-202.

Schoonjans, R., Willems, A., Schoonooghe, S., Fiers, W., Grooten, J. and Mertens, N. (2000). Fab chains as an efficient heteroization scaffold for the

production of recombinant bispecific and trispecific antibody derivatives. J. Immunol., **165**:7050-57.

Schoonooghe, S., Kaigorodov, V., Zawisza, M., Dumolyn, C., Haustraete, J., Grooten, J. and Mertens, N. (2009). Efficient production of human bivalent and trivalent anti-MUC1 Fab-scFv antibodies in *Pichia pastoris*. B.M.C. Biotechnol., **11**:70-83.

Scicchitano, M.S., Dalmas, D.A., Boyce, R.W., Thomas, H.C. and Frazier, K.S. (2009). Protein extraction of formalin-fixed, paraffin-embedded tissue enables robust proteomic profiles by mass spectrometry. J. Histochem. Cytochem., **57**:49-860.

SeattleGenetics. Pipeline, (2013). http://www.seattlegenetics.com/SGN-CD33A.

SeattleGenetics. Pipeline, (2013). http://www.seattlegenetics.com/asg22me.

Shen, Z., Stryker, A.G., Mernaugh, L.R., Yu, L., Yan, H. and Zeng, X. (2005). Single-Chain Fragment Variable Antibody Piezoimmunosensors. Anal. Chem., **77**:797-805.

Sheng, W., Shang, Y., Miao, Q., Li, Y. and Zhen, Y. (2012). Anti-tumor efficacy of the scFv-based fusion protein and its enediyne-energized analogue directed against epidermal growth factor receptor. Anticancer Drugs, **23**:406-16.

Sokolova, E., Skorinkin, A., Fabbretti, E., Masten, L., Nistri, A. and Giniatullin, R. (2004). Agonist-dependence of recovery from desensitization of P2X3 receptors provides a novel and sensitive approach for their rapid up or downregulation. Br. J. Pharmacol., **141**:1048-58.

Souslova, V., Cesare, P., Ding, Y., Akopian, A.N., Stanfa, L., Suzuki, R., Carpenter, K., Dickenson, A., Boyce, S., Hill, R., Nebenuis-Oosthuizen, D., Smith, A.J., Kidd, E.J. and Wood, J.N. (2000). Warm-coding deficits and aberrant inflammatory pain in mice lacking P2X3 receptors. Nature (Lond.), **407**:1015-7.

Singh, P., Singh, M.K., Chauhan, V., Gupta, P. and Dhaked, R.K. (2011). Prevention of aggregation and autocatalysis for sustaining biological activity of recombinant BoNT/A-LC upon long-term storage. Protein Pept. Lett., **18**:1177-87.

Smith, G.P. (1985). Filamentous fusion phage: novel expression vectors that display cloned antigens on the virion surface. Science, **228**:1315-7.

Spector, D.L. (2003). The dynamics of chromosome organization and gene regulation. Annu. Rev. Biochem., **72**:573-608.

Strome, S.E., Sausville, E.A. and Mann, D. (2007). A mechanistic perspective of monoclonal antibodies in cancer therapy beyond target-related effects. Oncologist, **12**:1084-95.

Sundukova, M., Vilotti, S., Abbate, R., Fabbretti, E. and Nistri, A. (2012). Functional differences between ATP-gated human and rat $P2X_3$ receptors are caused by critical residues of the intracellular C-terminal domain. J. Neurochem., **122**:557-67.

Teicher, B.A. and Chari, R.V. (2011). Antibody conjugate therapeutics: challenges and potential. Clin. Cancer Res., **17**:6389-97.

Thangudu, R.R., Manoharan, M., Srinivasan, N., Cadet, F., Sowdhamini, R. and Offmann, B. (2008). Analysis on conservation of disulphide bonds and their structural features in homologous protein domain families. BMC Struct. Biol., **8**:55-76.

The Merk Manual. Components of the Immune System, (2012). http://www.merckmanuals.com/professional/immunology_allergic_disorders/biology_of_the_immune_system/components_of_the_immune_system.html.

Townsend, S., Finlay, W.J.J., Hearty, S. and O'Kennedy R. (2006) Optimizing recombinant antibody function in SPR immunosensing. The influence of antibody structural format and chip surface chemistry on assay sensitivity. Biosens. Bioelectron., **22**:268-74.

Tsuda, M., Ueno, S. and Inoue, K. (1999). Evidence for the involvement of spinal endogenous ATP and P2X receptors in nociceptive responses caused by formalin and capsaicin in mice. Br J Pharmacol. **128**:1497-504.

Tuma, R.S. (2011). Enthusiasm for antibody-drug conjugates. J. Natl. Cancer Inst., **103**:1493-4.

Vulchanova, L., Riedl, M.S., Shuster, S.J., Stone, L.S., Hargreaves, K.M., Buell, G., Surprenant, A., North, R.A. and Elde, R. (1998). $P2X_3$ is expressed by DRG neurons that terminate in inner lamina II. Eur. J. Neurosci., **10**:3470-8.

Wang, J.F., Meng, J.H., Lawrence, G.W., Zurawski, T.H., Sasse, A., Bodeker, M.O., Gilmore, M.A., Fernández-Salas, E., Francis, J., Steward, L.E., Aoki, K.R. and Dolly, J.O. (2008). Novel chimeras of botulinum neurotoxins A and E unveil contributions from the binding, translocation, and protease domains to their functional characteristics. J. Biol. Chem., **283**:16993-7002.

Wang, J., Zurawski, T.H., Meng, J., Lawrence, G., Olango, W.M., Finn, D.P., Wheeler, L. and Dolly, J.O. (2011). A dileucine in the protease of botulinum toxin A underlies its long-lived neuroparalysis: transfer of longevity to a novel potential therapeutic. J. Biol. Chem., **286**:6375-85.

Wang, X., Ma, D., Olson, W.C. and Heston, W.D. (2011). *In vitro* and *in vivo* responses of advanced prostate tumors to PSMA ADC, an auristatin-conjugated antibody to prostate-specific membrane antigen. Mol. Cancer Ther., **10**:1728-39.

Wirkner, K., Sperlagh, B. and Illes, P. (2007). P2X$_3$ receptor involvement in pain states. Mol. Neurobiol., **36**:165-83.

Wittel, U.A., Jain, M., Goel, A., Baranowska-Kortylewicz, J., Kurizaki, T., Chauhan, S.C., Agrawal, D.K., Colcher, D. and Batra, S.K. (2005). Engineering and characterization of a divalent single-chain Fv angiotensin II fusion construct of the monoclonal antibody CC49. Biochem. Biophys. Res. Commun., **329**:168-76.

Wu, Y.T. (2009). The co-receptor signaling model of HIV-1 pathogenesis in peripheral CD4 T cells. Retrovirology, **6**:41-6.

Xiang, Z., Xiong, Y., Yan, N., Li, X., Mao, Y., Ni, X., He, C., LaMotte, R.H., Burnstock, G. and Sun, J. (2008). Functional up-regulation of P2X$_3$ receptors in the chronically compressed dorsal root ganglion. Pain. **140**:23-34.

Xie, H., Audette, C., Hoffee, M., Lambert, J.M. and Blättler, W.A. (2004). Pharmacokinetics and biodistribution of the antitumor immunoconjugate, cantuzumab mertansine (huC242-DM1), and its two components in mice. J. Pharmacol. Exp. Ther., **308**:1073-82.

Xiong, H., Li, L., Liang, Q.C., Bian, H.J., Tang, J., Zhang, Q., Mi, L. and Chen, Z.N. (2006). Recombinant chimeric antibody hCAb as a novel anti-human colorectal carcinoma agent. Mol. Med., **12**:229-36.

Xu, G.Y. and Huang, L.Y. (2002). Peripheral inflammation sensitizes P2X receptor-mediated responses in rat dorsal root ganglion neurons. J. Neurosci., **22**:93-102.

Yan, S.Z., Hahn, D., Huang, Z.H.and Tang, W.J. (1996). Two cytoplasmic domains of mammalian adenylyl cyclase form a Gs alpha- and forskolin-activated enzyme *in vitro*. J. Biol. Chem., **271**:10941-5.

Yao, Y.D., Sun, T.M., Huang, S.Y., Dou, S., Lin, L., Chen, J.N., Ruan, J.B., Mao, C.Q., Yu, F.Y., Zeng, M.S., Zang, J.Y., Liu, Q., Su, F.X., Zhang, P., Lieberman, J., Wang, J. and Song, E. (2012). Targeted delivery of PLK1-siRNA by ScFv suppresses Her2$^+$ breast cancer growth and metastasis. Sci. Transl. Med., **4**:130ra48.

Yiangou, Y., Facer, P., Ford, A., Brady, C., Wiseman, O., Fowler, C.J. and Anand, P. (2001). Capsaicin receptor VR1 and ATP-gated ion channel P2X3 in human urinary bladder. B.J.U. Int., **87**:774-9.

Younes, A., Kim, S., Romaguera, J., Copeland, A., Farial Sde, C., Kwak, L.W., Fayad, L., Hagemeister, F., Fanale, M., Neelapu, S., Lambert, J.M., Morariu-Zamfir, R., Payrard, S. and Gordon, L.I. (2012). Phase I multidose-escalation study of the anti-CD19 maytansinoid immunoconjugate SAR3419 administered by intravenous infusion every 3 weeks to patients with relapsed/refractory B-cell lymphoma. J. Clin. Oncol., **30**:2776-82.

Yu, T., Bai, Y., Dierich, M.P. and Chen, Y.H. (2000). Induction of high levels of epitope-specific antibodies by epitope/peptide candidate vaccines against human immunodeficiency virus type-1 (HIV-1). Microbiol. Immunol., **44**:105-10.

Yuahasi, K.K., Demasi, M.A., Tamajusuku, A.S., Lenz, G., Sogayar, M.C., Fornazari, M., Lameu, C., Nascimento, I.C., Glaser, T., Schwindt, T.T., Negraes, P.D. and Ulrich, H. (2012). Regulation of neurogenesis and gliogenesis of retinoic acid-induced P19 embryonal carcinoma cells by P2X$_2$ and P2X$_7$ receptors studied by RNA interference. Int. J. Dev. Neurosci., **30**:91-7.

Zemkova, H., He, M.L., Koshimizu, T.A. and Stojilkovic, S.S. (2004). Identification of ectodomain regions contributing to gating, deactivation, and resensitization of purinergic P2X receptors. J. Neurosci., **24**:6968-78.

Zhang, J.Y., Wang, J.G., Wu, Y.S., Li, M., Li, A.H. and Gong, X.L. (2006). A combined phage display scFv library against *Myxobolus rotundus* infecting crucian carp, *Carassius auratus auratus* (L.), in China. J. Fish Dis., **29**:1-7.

Zhang, L., Moo-Young, M. and Chou, P.C. (2010). Effect of aberrant disulfide bond formation on protein conformation and molecular property of recombinant therapeutics. Pure Appl. Chem., **82**:149-159.

Zhang, Z., Li, Z.H., Wang, F., Fang, M., Yin, C.C., Zhou, Z.Y. and Lin, Q. and Huang H.L. (2002). Overexpression of DsbC and DsbG markedly improves soluble and functional expression of single-chain Fv antibodies in *Escherichia coli*. Protein Expr. Purif., **26**:218-28.

Zhong, G., Zhang, S., Li, Y., Liu, X., Gao, R., Miao, Q. and Zhen, Y. (2010). A tandem scFv-based fusion protein and its enediyne-energized analogue show intensified therapeutic efficacy against lung carcinoma xenograft in athymic mice. Cancer Lett., **295**:124-33.